UNIVERSITÀ DI SIENA 1240

Dipartimento di Scienze fisiche, della Terra e dell'ambiente

Dottorato in Scienze e tecnologie ambientali, geologiche e polari

33° Ciclo

Coordinatore: Prof. Simone Bastianoni

Palynology and Paleobotany of Permo-Triassic Beacon Supergroup at Allan Hills, South Victoria Land, Antarctica: stratigraphical and paleoenvironmental change implications.

Settore scientifico disciplinare: GEO/02

Candidata

Corti Valentina

Università di Siena

Tutori

Prof. Franco Maria Talarico

Università di Siena

Prof. Gianluca Cornamusini

Università di Siena

Co-tutori

Prof.ssa Amalia Spina

Università di Perugia

Prof. Erik Gulbranson

Gustavus Adolphus College (MN-USA)

Anno accademico di conseguimento del titolo di Dottore di ricerca

2019/20

Università degli Studi di Siena

Dottorato in Scienze e tecnologie ambientali, geologiche e polari

33° Ciclo

Data dell'esame finale: 29/03/2021

Commissione giudicatrice:

Prof.ssa Simonetta Cirilli, Università di Perugia

Prof.ssa Cecilia Viti, Università di Siena

Prof.ssa Monica Ghirotti, Università di Ferrara

Supplente:

Prof. Pier Lorenzo Fantozzi, Università di Siena

In Memoriam Professor Franco Maria Talarico

Table of contents

Abstract

Nowadays the Antarctic continent is almost entirely covered by ice (around 98% of the total land surface) and the conditions are inhospitable for vegetation, apart from very few species such as mosses and lichens.

During the geological time however, conditions were very different and the Phanerozoic fossil record documents several occurrences of vegetation remains also indicating the presence of wide high latitude forests. The life of plants in the continent was obviously strictly influenced by the evolving paleogeography and paleoenvironmental conditions and their mutual interactions during each time age of vegetation record.

The thesis project has been finalized to define, constrain and discuss with new field and laboratory data the most likely Late Permian and Triassic paleoenvironmental reconstructions for the Victoria Land region in Antarctica, on the basis of a new set of paleobotany and palynological investigations of the unique fossiliferous strata recently found in the Beacon Supergroup of Allan Hills (South Victoria Land).

The study was developed following a broad multidisciplinary and multi-analytical methodology in which paleobotany (including innovative approaches), palynology and palynostratigraphy methods and techniques play a key role in the reconstruction of the paleoenvironmental conditions and their changes through the time.

In the palynostratigraphic sequence of Allan Hills were recovered the EPE, a strata horizon with long-shaped inertinite probably referred to a paleo-fire, situated in the last level of coal of the Permian sequence; going up in the sequence the paleoflora is affected by deeply change, as an adaptation to the new environmental condition up to the PTB, were the major samples were completely inert, due to a poor presence of flora and a changing of the sedimentary condition. After the PTB the first palynomorphs recovered are associated to an intensive fungal and algae activity, and just at the end of the Early Triassic, the flora came back to be flourishing, even if with a quite completely new association of pollen and spores, where is dominant the genus of *Alisporites* in the whole Middle and Late Triassic. The genus of *Alisporites* is probably linked to the *Dicroidium* macroflora, playing a central role during the Triassic time, replacing the *Glossopteris* flora which, on the other hand, dominated the Permian landscape. The *Dicroidium*, together with other genera, were recovered in great abundance in the Middle Triassic deposits of the Lashly Formation in Allan Hills, particularly within a horizon containing a so-called "Allan Hills Fossil Forest", even if the term "forest " is not strictly pertinent, as a way the trunks were deposited and transported by a massive flow, and no more in the growth-position.

With an innovative technique was possible to reconstruct the main differences between the trunks there deposited and some other Permian fossil trunks outcropping in other areas of South Victoria Land. From this study, after a completely reconstruction of 237 years, that is the longest life-time never done for so old samples, were possible to note that the amplitude of the rings is probably linked to the amount of hours of sunlight during the years, so they are linked to the latitude to which the land was at time life-time of the trees.

The last topic analysed about the "*Allan Hills fossil forest*" is the peculiar kind of fossilization, with a multianalytic approach were in fact possible to reconstruct modalities of coalification/charcoalification and multi-phase fossilization.

The PAHs analysis highlights the presence of a high percentage of PAHs >4 ringed polynuclear aromatic hydrocarbons, that are typical attribute to pyrogenetic materials as fluoranthene, 9,10-dimethylanthracene and Pyrene, moreover also the $\delta^{13}C$ measured on the growth tree rings shows a shifting of the curve in the more external rings, as an enrichment of ^{13}C due to a partial combustion.

After a first phase where the trunks were partially burned due to paleofires, they were transported through massive water flows. Subsequently, they were buried, deformed and petrified by a massive silica gel, probably occurred mainly during the Jurassic sill intrusion. The last step of the fossilization is the precipitation of calcite in a rounded shape occurred for some samples.

Taken together the results of the study provide new important constraints and implications for reconstructing the history of sedimentary processes and coupled changing of the paleo-flora during a transition of deeply transformation of the biodiversity linked to the onset of greenhouse conditions, which occurred after the Permo-Triassic boundary, particularly during the Early Triassic.

1. Introduction

The Permian-Triassic Victoria Group in south Victoria Land represents a typical Gondawanan Succession, where the Carboniferous-Lower Permian glacial beds are overlain by fluvial sandstones and mudstones with numerous levels of coal, defining an articulate succession, characterized by changing in environment and climate continental conditions.

Due to the nature of the sedimentary environment, in these deposits were recovered numerous traces of the past life. The first paleobotanical observations date back to 1903 from the British Discovery Expedition, while the first sampling of some paleobotany samples were done during the famous Scott Expedition in 1912 and were collected the first samples of *Glossopteris* from the Central Transantarctic Mountains.

Since then on numerous discovered were done about the geology, the stratigraphy and the reconstruction of the paleoenvironment that dominated the Beacon Sandstones of the Transantarctic Mountains. Nowadays is known that the Victoria Group exposed in Allan Hills, a nunatack located in South Victoria Land, was deposited during Permian and Triassic times. During the Permian time the environmental condition underwent an abrupt change, passing from a glacial time at the beginning, showed by the deposition of tillite in many areas of the Gondwana Land, to a warmer climate condition, with a consequent blooming of the life. At the boundary between the Permian and Triassic (252 Ma) occurred the bigger mass extinction in the history of the Earth (Erwin et al.,1990; Hudson et al., 2003) with a massive loss of genera and species. The biotic crisis lasted until Early Triassic, while during the Middle Triassic time there was a recovery and the life returned to be luxuriant, also in high latitude areas.

In the reconstruction of the paleoenvironmental changing trough time, palynology and paleobotany studies play a fundamental rule. From this kind of study is, in fact, possible to recognize different associations of pollen and/or plants that characterized the paleoenvironments through times.

Starting from the Middle Permian, at the end of the Late Paleozoic Ice Age (LPIA), the *Glossopteris* flora started to colonize more and more lands widespread in all the Gondwana, until this time the *Glossopteris* still existed, but they were located only in lower latitudes, where the climatic conditions were more favourable. With the end of the glaciation and a general global increasing of the temperature the *Glossopteris* colonized various area of the Gondwana reaching higher latitudes (Figure 1). During the colonization of the land, the genus *Glossopteris* occurred in a great variety of growth forms, due to different areas and/or different times. This is testified in the different shape of leaf, on the base of the morphological aspect as the size, the ratio between long and short axes of the leaves and the venation; a common feature is indeed the presence, in

the fossil trunk of marked and wide growth rings. The higher number of *Glossopteris* in the paleobotanical fossil assemblages recovered, created the name "Glossopteris Flora".

The *Glossopteris Flora* is the typical assemblage of Permian Flora composed, not only from various species of *Glossopteris*, but also from *Gangamopteris* and other *Pteridospermophyta,* ferns and other genus of plants. As regards the palynoassemblage during the middle and late Permian, the palynofacies were dominated by striate and taeniate bisaccate pollen grain, with the strongly dominance of *Protohaploxypinus* spp., commonly related to the *Glossopteris Flora.*
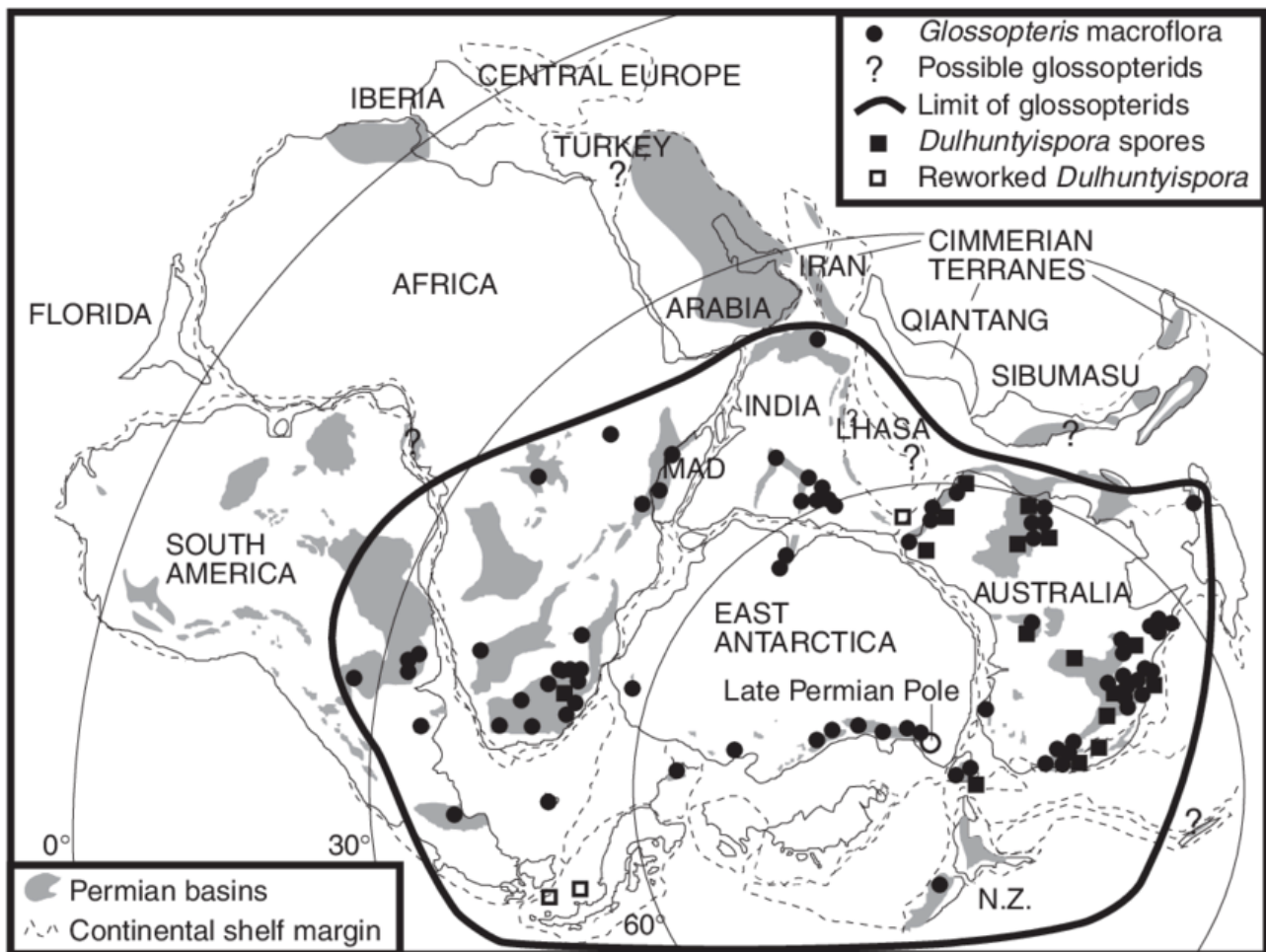
Figure 1 Gondwana map and distribution of Glossopteris Flora, from Mcloughlin 2011

The presence of this plants is witnessed mega- and micro- fossil as by fossil trunk, compression/impression of leaf and pollen grain, but also from the thick and frequent deposit of coal that dominate the Late Permian Gondawanian succession.

The Permo-Triassic transition is testified by a strongly changing in the sedimentary basins, both the fluvial style and the micro and macro botanical remains. Here the typical *Glossopteris Flora* was quite entirely

destroyed and was replaced, after a time dominated only from algae/fungal spores, from a Triassic Flora mainly composed from *Dicroidium*. At the same time the sedimentary basin had a deep changing, witnessed with the early Triassic coal gap. In this part of the succession (Fleming Member and Feather Sandstone in South Victoria Land), there is the complete loss of coal deposit and the deposition of coarse sandstone, with only less level of mudstone/limestone.

Only from Middle Triassic the land of Antarctica became again abundant in plant life, high latitude fossil forest was recovered widespread across the TAM, as impression/compression of leaf and coal deposits rich in sporomorphs. The most common group in the Triassic Flora are *Lycopsids*, *Equisetaleans*, Ferns, Seen Ferns, *Ginkoaleans* and conifers, while the sporomorphs are dominated by various species of *Alisporites*. The abundant and differentiate amount of flora is due to a warmer global condition during the Triassic and at the shift of the Antarctica to a lower latitude, reaching a minimum of around 65° South during the Late Triassic. In this environmental setting were deposited the fossil forest of Allan Hills, in this area were recovered more than 300 fossil trunks imbedded in a massive fluvial sandstone of the Middle Triassic age.

In Allan Hills are exposed a complete Permian-Triassic succession, with the Permian Weller Coal Measures Formation and the Triassic Feather Sandstone and Lashly Fm. The palynology study was done on 96 samples (Figure 2) of the entire succession for a high-definition reconstruction of the palynostratigraphy zonation and for the reconstruction of the environmental changes through the end-Permian extinction event.

The paleobotany studies are furtherly focused for the samples of the Allan Hills Fossil forest (differently by the numerous recovery of Permian and Triassic fossil trunks in Victoria Land, this geo-site is interesting for the remarkable number of trunks recovered and for the well-preserved conditions of them, besides their relationships with the sandstone sedimentary flow structures.
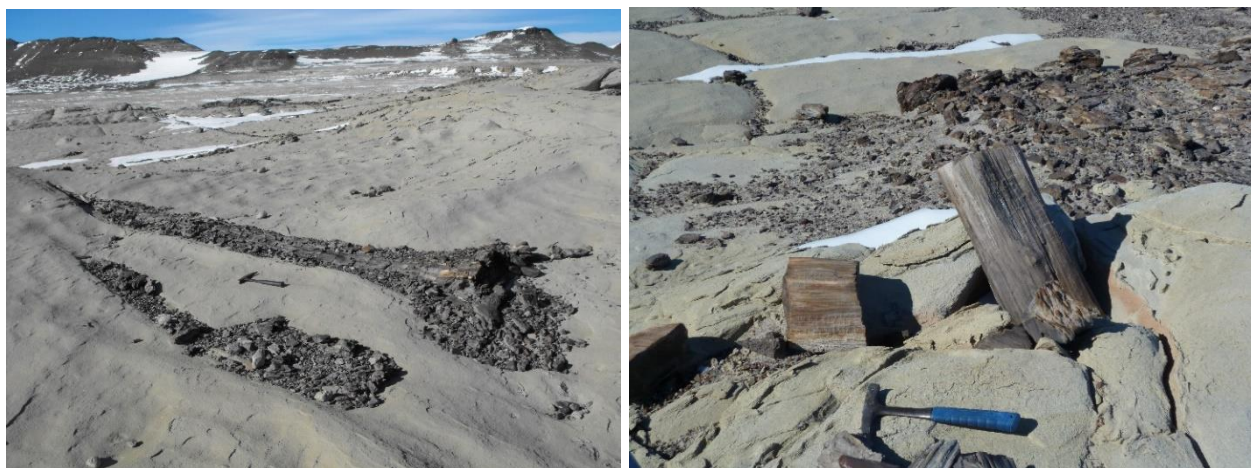

Figure 2 Fossil trunks of Allan Hills drifted fossil forest

In that area the fossil trunks were deposited in three different stratigraphic levels, due to different massive hydraulic flows, associated with pieces of peat and leaves (recognizable as impression/compression) of *Dicroidium* and *Heidiphyllum elongatum*.

The Allan Hills Fossil Forest has been recovered in the Member B of the Lashly Formation (see Cox et al., 2012). This member was analysed for the palynological content and a high percentage of non- taeniate bisaccate, with a good amount of various species of *Alisporites* made to attribute that to the Middle Triassic.

The fossil trunks reach 15 meters of maximum length and 60 cm in diameter, with preserved growth rings and, occasionally, pith and/or root system, while all the samples are devoid of bark. The prevalent colour is grey, shifting to a red/brow-red in the exposed parts due to the weathering and, in some case are characterized by a side with intense black colour and peculiar superficial features.

Samples of fossil trunks have been analysed with a multidisciplinary approach, from the classical paleobotanical methods (reflectance, dendrology, SEM and carbon isotope analyses), to innovative techniques, as the application of the dendrochronology technique at fossil samples for a detailed paleoenvironmental reconstruction or the study of the different concentration of Polycyclic Aromatic Hydrocarbon (PAHs) in fossil coal and charcoal, useful for to testify the eventual occurrence of paleowildfires.

This work, focused on Allan Hills, is therefore subdivided in two macro fields: palynology and paleobotany (classical and experimental) for a wide reconstruction of the Permo-Triassic environments and the deep changes occurred through the biggest mass life extinction of the PTB.

2. Geological Setting

The Transantartic Mountains (TAM) cross the Antarctic continent for 3800 Km from the Weddel Sea to the Ross Sea and divide the continent in two area: a stable craton of East Antarctica and a more tectonically active area of West Antarctica.

The Victoria Land is situated between the Ross Sea and the Wilkes Land and represents the extreme N-E part of the TAM, where the chain forms the western shoulder of the Meso-Cenozoic West Antarctic Rift System. The Victoria Land is divided in a North part and a South part (Figure 3), in both these areas, a thick sedimentary sequence (Beacon Supergroup) unconformably overlain a Precambrian Basement consisting of granitoids and metasediments. (Collinson et al., 1986).
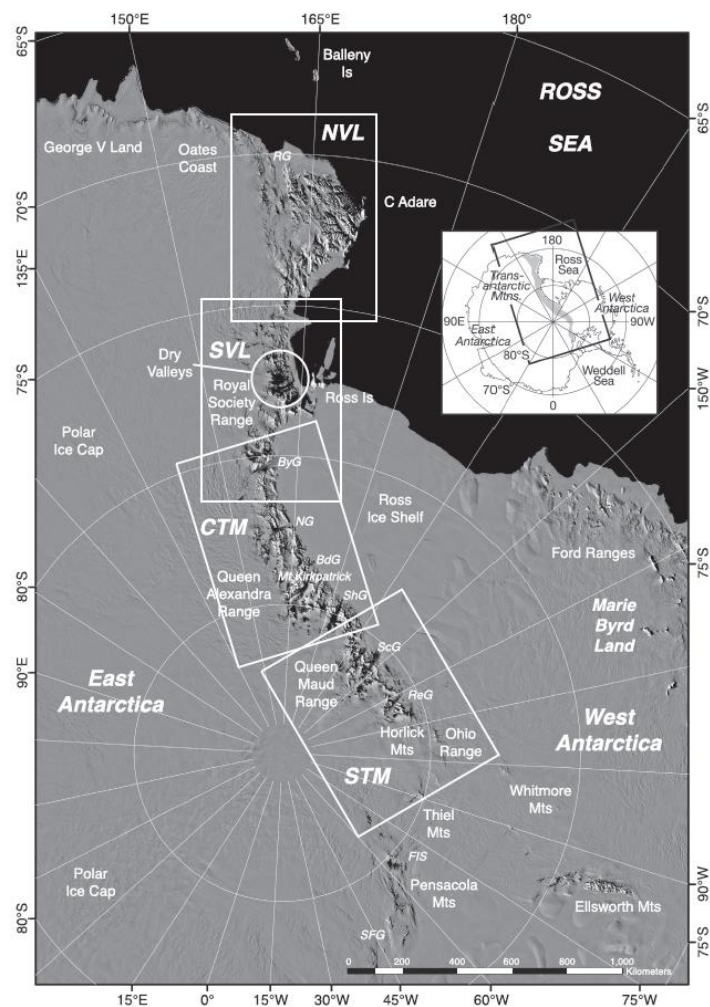

Figure 3 Subdivision of Transantarctic Mountains: North Victoria Land (NVL), South Victoria Land (SVL), Central Transantarctic Mountains (CTM) and South Transantarctic Mountains (STM); From Goodge 2020

The uplift and exhumation of the Transantartic Mountains (TAM) in the Victoria Land began in the Early Cretaceous and developed through three main tectonic phases (Fitzgerald, 2002; Olivetti et al., 2018), but this mountain range shows a longer history. The basement is formed by metamorphic rock of the Upper Proterozoic (Beardmore orogen) overlain by sedimentary series metamorphosed during the PanAfrican Orogenesis. At the end of this orogenesis the area became more stable and was affected by a deep erosion that created the Kukri erosion surface (Barrett, 1991; Goodge, 2020).
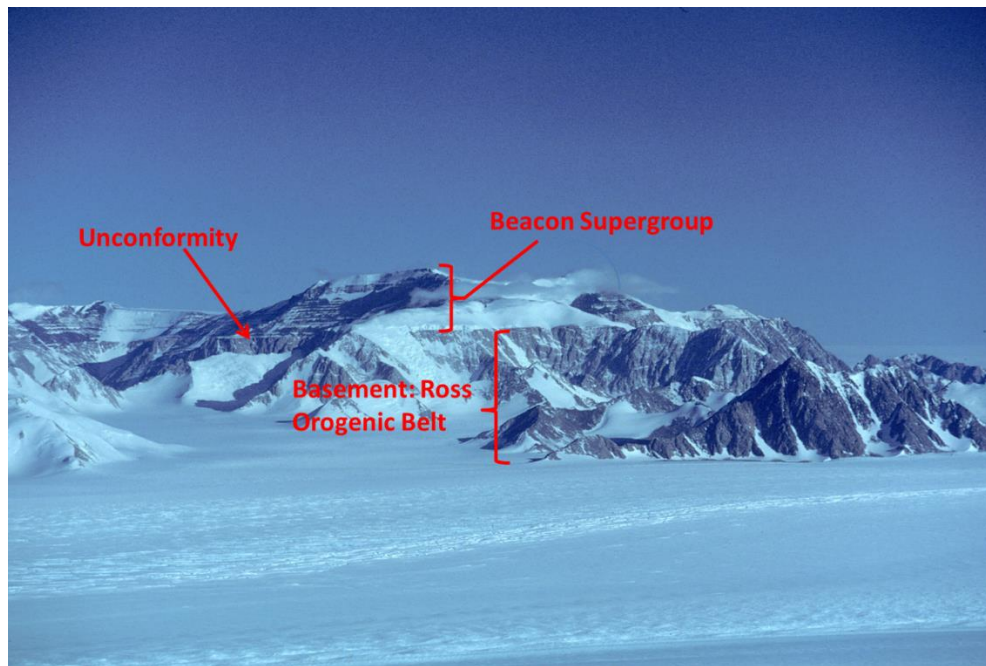
Figure 4 Beacon Supergroup in Victoria Land

To follow, from Devonian to Late Triassic-Early Jurassic, there was the deposition of sediments within various continental environments (fluvial, lacustrine, glacio-lacustrine and eolic) and in marine shallow water environments, characterizing coeval foredeep, epicratonic and protorifting basins (Goodge, 2020).

This sedimentary succession is called Beacon Supergroup (Fig. 4) in the whole, whereas it is divided in two units, respectively the Taylor Group the lower and the Victoria Group the upper, by a regional unconformity surface and a glacial phase deposit (Barrett, 1981; 1991). During the Permo-Carboniferous the Gondwana, and the Antarctica in particular, was covered by extensive ice-cups or ice-sheets linked with the Late Paleozoic Ice Age (Barrett, 1981; 1991; Isbell et al., 2012). They are also recordedr in Victoria Land where formed tillite deposits (Collinson et al., 1983; Isbell et al., Cornamusini et al., 2017).

At the end of the LPIA the temperature growth up with a global warming and climate amelioration favouring the growth of the vegetation (*Glossopteris flora*- flora assemblage mainly composed by various species of

Glossopteris but also by *Gangamopteris* and other genera), contemporaneously in the South Victoria Land (SVL) extensive swamp systems were formed, then developing thick coal seams.

The transition between Permian and Triassic marked another abrupt global challenge, with the end Permian mass extinction, and the consequent catastrophic events, as the starting of a general greenhouse during the early Triassic, with the progressive climate improvement during the middle and late Triassic, with the appearance and development of new species (Vaijda et al., 2020; Fielding et al., 2020).

In fact, following the Permo-Triassic boundary, the Early Triassic represented for the Gondwana, a phase characterized by aridity (diffuse red sandstones), the Glossopteris flora was extinct at the PTB or probably just before (Vajida et al., 2020; Fielding et al., 2020) and replaced since the Middle Triassic, by a rich vegetation mainly characterized by Dicroidium, ferns and other genera. In the Middle-Late Triassic the environment came back to be more temperate and this produced new coal horizons, particularly diffused during the Late Triassic.
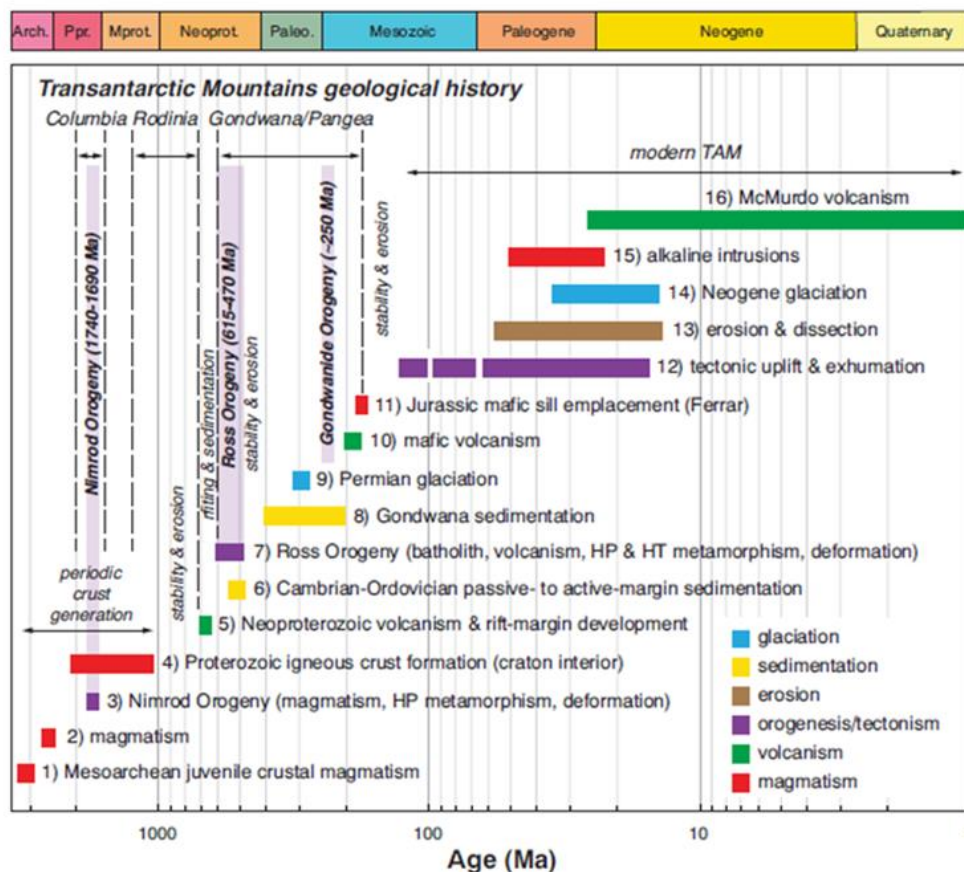
Figure 5 Timeline showing major geologic and tectonic events during development of the Transantarctic Mountains (TAM); From Goodge 2020

The sedimentary succession of the Beacon Supergroup (Fig. 5 and Fig. 6) has its uppermost term of early Jurassic age, accompanying the beginning of the break-up of the Gondwana, characterized by interlayering of alluvial siliciclastic and volcanoclastic deposits. During this time basaltic flow and sill were emplaced up and into the sedimentary succession.
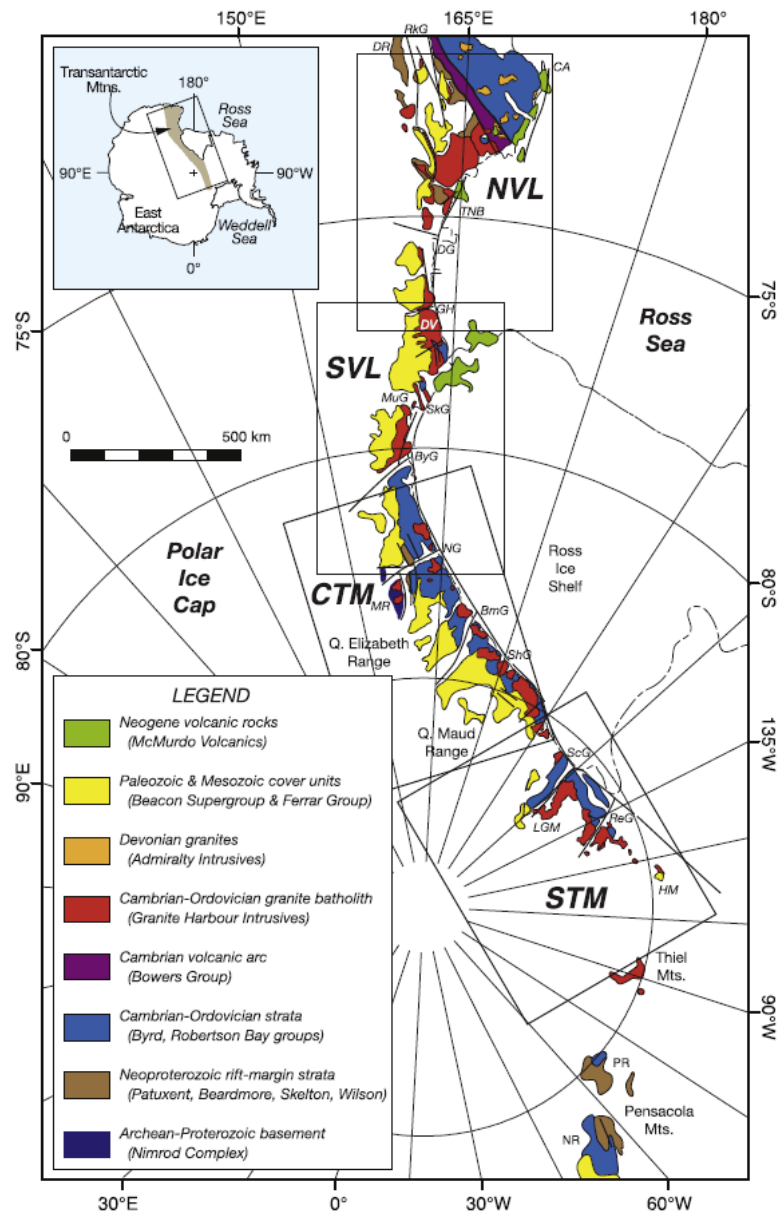
Figure 6: Simplified geological scheme for the Transantarctic Mountains From Goodge 2020

2.1 BASEMENT

The basement in Victoria Land (Fig. 7) could be subdivided between the north and the south parts. As regards the North Victoria Land three different units or terranes as follow:

- **Wilson Terrane** with a various grade from low to high; it is a metamorphic complex that crops out in the East Wilson Hills (Matusevich Glacier); it is mainly formed by metasedimentary rocks and igneous rocks with a mainly granitoid composition. The emplacement of the Granite Harbour Intrusive at approximately 480 Ma represents the major part of the igneous rocks. The Wilson Terrane is characterised by metamorphic rocks generated in a facies of high temperature and low pressure (Roland et al., 2004)and it could be divided in:

  - Rennick Schist, fine grained schists and gneiss whit a minor level of calc-silicates. The diagnostic metamorphic minerals are garnet, andalusite, sillimanite, cordierite, diopside and amphibol; these show a amphibolitic metamorphic facies.
  - Wilson Gneiss mainly formed by ortho-gneiss, but it is also present a facies characterised by biotite-quartz-feldspar.

- **Robertson Bay Terrane** mainly constituted by phyllites of low grade; crops out in many localities of NVL, this is very continuous except for some granitoid intrusion, moreover some outcrops were also found in some areas of the Rennick Glacier. The Robertson Bay Terrane is also formed of turbiditic sequences, consisting of alternations of greywackes and shales. In the east area of the NVL (from the Robertson Bay to the Mirabito Range), the metamorphism that affected the Robertson Bay Terrane was of low grade; while on the western part (west of the Little Glacier) the metamorphic grade is higher.

- **Bowers Terrane** consists of a metasedimentary and volcanic complex; it is constituted by rocks from Middle Cambrian to Lower Ordovician in age (Stump 1995) and the maximum metamorphic deformation reaches the greenschist facies (Roland et al., 2004). It is formed by sequences of sedimentary and volcanic deposits and rocks.

The first two groups are distributed in a range of age from Late Pre-Cambrian to Cambrian, while the Bowers Terrane contains fossils of the Cambrian but reach the Ordovician in the upper terms.

Regarding the South Victoria Land, in these areas the basement is formed by the **Skelton and the Koettlitz Groups,** a different grade metamorphic complex with depositional Neoproterozoic age.

The **Skelton Group**, so called by (Gunn and Warren, 1962) is dominated by greenschist to upper-amphibolite facies calcsilicate schist, marble, and amphibolite, with minor mafic, quartzo-feldspathic and shale rocks firstly mapped in the Skelton Glacier area, where the metamorphic grade is of greenschist facies. In the northern area, exactly in the eastern Dry Valleys, higher grade of metamorphic rocks, amphibolite facies, were firstly described by (Grindley and Warren 1964) and called Koettlitz Group, but this division in two different groups, is most recently less common and some authors (Cook and Craw,2001) (Wysoczanski and Allibone 2004) used the name Skelton Group indiscriminately for both groups.

Rocks of the Skelton Group are exposed on Teall Island, on both sides of the Skelton Glacier, and near Mt. Cocks between the Skelton and the Koettlitz glaciers (Faure and Mensing 2010).

The primary sedimentary and stratigraphic framework of the rocks forming the Skelton Group were mostly destroyed and deformed by intensive metamorphic events, even if it is possible to reconstruct the depositional marine environment, Laird (1981)

The Skelton Group deposited during a rifting phase of the supercontinent Rodinia (Goodge et al.,1993) (Goodge, et al.,2004) (Cook and Craw 2002) in a continental margin with some smaller marginal marine basins Cook (2007). Various evidences show a depositional age of Neoproterozoic, after 650 Ma for the Skelton group (Cox et al., 2012).

After the deposition, a different grade of metamorphism affected the Skelton Group. North of the Shear Zone, the metamorphic grade is entirely upper amphibolite facies, with significant migmatization (Allibone and Norris 1992). (Talarico et al., 2005) proposed two phases of metamorphism in the area between the Shear Zone and the Ferrar Glacier: a first one of medium pressure followed by a second event of lower pressure and higher temperature, associated to the granitic intrusion.

(Gunn and Warren 1962) divided the rocks of the Skelton Group into the upper Teall Formation and the underlying Anthill Formation, but after Skinner (1982) the Teall Formation, was renamed as Cocks Formation.

The Anthill Formation is about 3,300 m thick Stump (1995) and consists of well-bedded white to grey limestones interbedded with lesser amounts of mudstone, siltstone, and quartzite. The limestone appears to be unfossiliferous. The metamorphic grade of the Anthill Formation increases from the greenschist facies on the south side of the Skelton Glacier to the amphibolite facies farther north between the Skelton and the Koettlitz glaciers.

The Cocks Formation contains a porphyritic pillow lava that was dated by (Rowell et al., 1993) by means of the samarium-neodymium (Sm-Nd) method and revealed an age of 700–800 Ma, which indicates that the

flow was extruded during the Neoproterozoic. The metamorphic grade of the Cocks Formation also increases northernwards.

These three units were intruded during different time, by two different granitoid groups; during the Ross Orogen in many areas of the TAM, including the NVL, the Granite Harbour Intrusive Complex (Cambrian to Ordovician) occurs. Moreover, also a second stage of granitic intrusion was emplaced, just in NVL, from Devonian to Carboniferous and this is called Admiralty Intrusive:

- **Granite Harbour Intrusive** (just in the Wilson Terrane) of Cambrian Ordovician age (530-480 Ma, with the maximum at 500 Ma) is interpreted as a sin and post- tectonic remain of the magmatic arc of the Ross Orogen (Ghezzo et al., 1987). This is formed by granite and granitoid rocks containing anhedral zircon, tourmaline and ilmenite; the K-feldspar is abundant unlike the plagioclase that is rare and usually contain An<25. The Granite Harbour Intrusive Complex is mainly composed by S-I granitoid with an alkaline growth to the west areas.

- **Admiralty Intrusives** (this group intruded the Roberson Bay Terrane) from Devonian to Carboniferous. It is formed by plutonic rocks crops that cross the Bowers Terrane and the Robertson Bay Terrane and sometimes the eastern part of the Wilson Terrane. The major component is the monzo-granite followed by tonalite and diorite; most of these monzo-granites are classified as I-kind and are composed by feldspar, biotite and hornblend (and as accessories zircon, apatite and opaque minerals). Across the Admiralty Intrusive Complex, the petrography is quite uniform, with just a little growth of crustal material go to north/north-east.
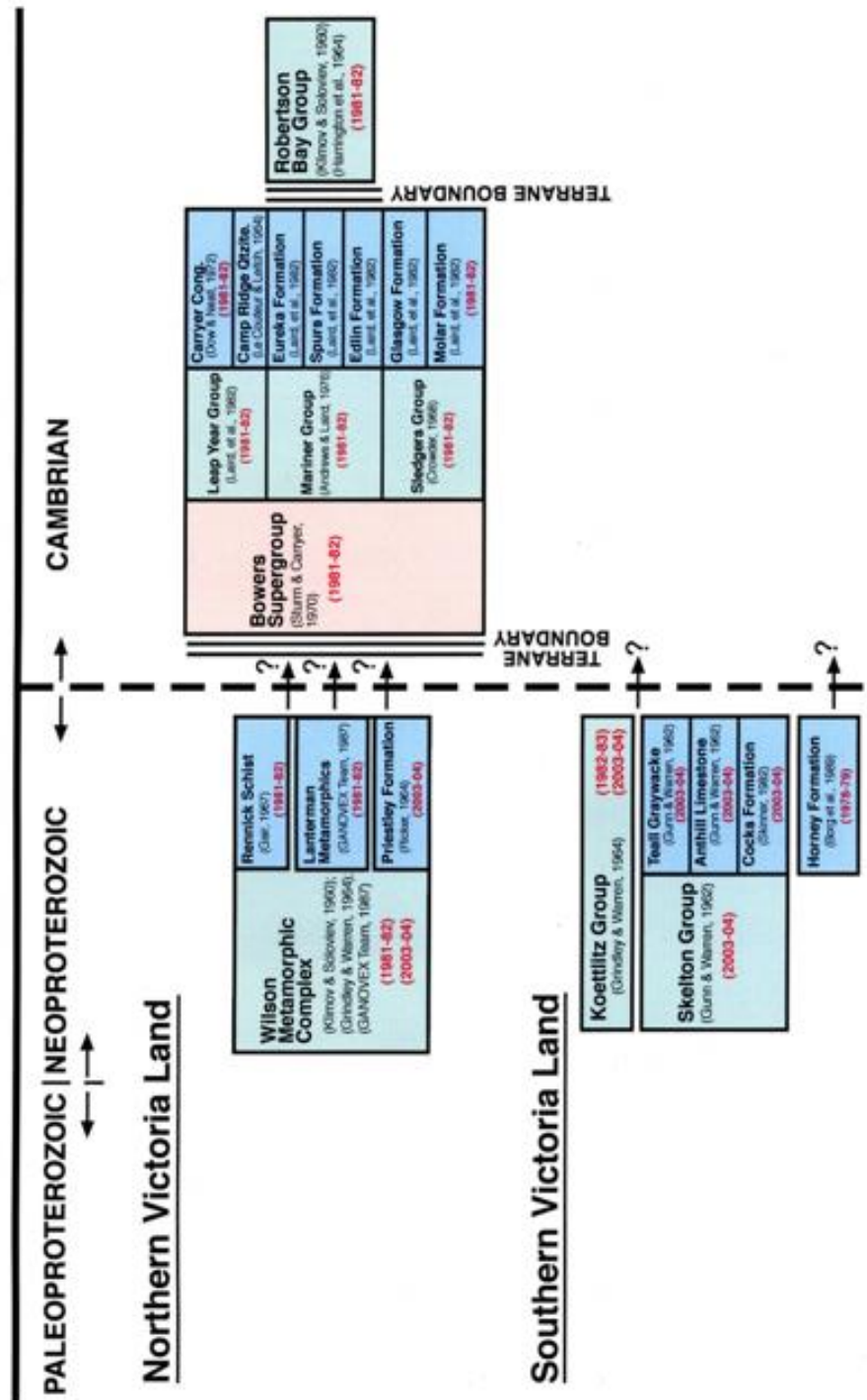
Figure 7: Basement in Victoria Land: Differentiation between basement in North Victoria Land and South Victoria Land

2.2 SEDIMENTARY SEQUENCE: The Beacon Supergroup

The Victoria Land is characterized by the occurrence of a "Gondwanan" sedimentary siliciclastic cover, called Beacon Supergroup, which rests through a marked unconformity on Ross's crystalline basement (Barrett, 1991). The Beacon Supergroup (Fig. 8) has an overall age between the Devonian and the late Triassic / early Jurassic for the Central TAM and the SVL (Barrett, 1991; Elliot, 2016), while in the Northern Victoria Land, here are only the stratigraphic terms distributed by the Permian to early Jurassic (Collinson et al., 1983). This highlights a marked lateral variability of the Beacon stratigraphy along the Victoria Land and the Transantarctic Mountains, linked to the presence of more sedimentary basins or sub-basins, articulated by the presence of morpho-structural highs and lows (Collinson et al., 1986; Barrett 1991).
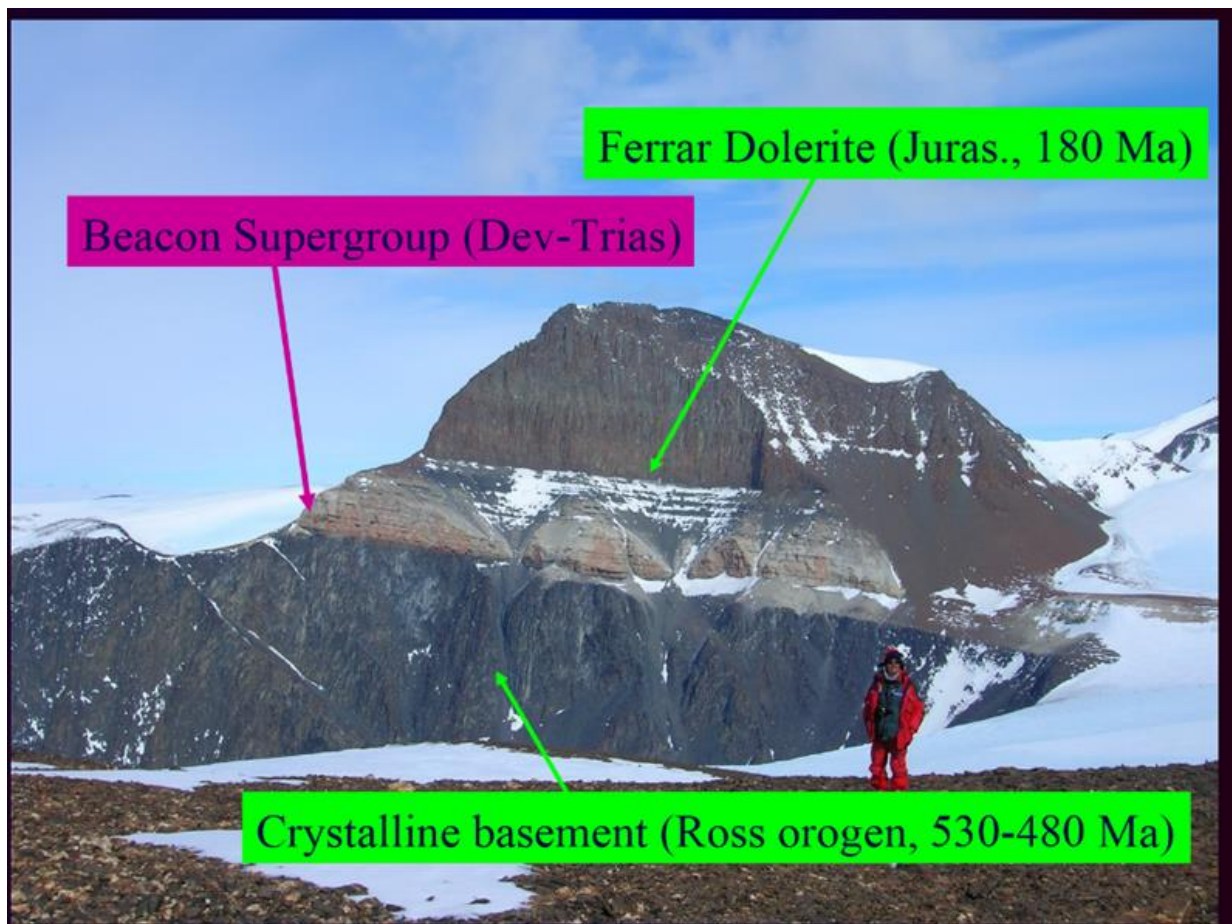
Figure 8 Beacon Supergroup exposure in Victoria Land. The Beacon sandstone overlain the crystalline basement and it's intruded by a dolerite sill of the Jurassic Ferrar group

In Southern Victoria Land, the Beacon Supergroup is divided into two groups, the Devonian Taylor Group, which rests on the base through a marked erosion surface that determines the so-called Kukri Peneplain, and separated from the Victoria Group (?Late Carboniferous – early Jurassic in age) from another erosional or unconformity surface, which is the Maya disconformity, on which rests a glaciogenic succession, the Metschel Tillite, which in turn passes upwards to the typical arenaceous succession of Beacon through a further erosional surface, the Pyramid disconformity (Collinson et al., 1986).

The stratigraphic units of the Beacon Supergroup (Fig. 9), as well as the basement, present doleritic intrusions in the form of dykes and sills forming part of the Ferrar Group of early-middle Jurassic age (Collinson et al., 1986), while they are overlain at the top by the basaltic layers of the Kirkpatrick Basalt of Middle Jurassic age.
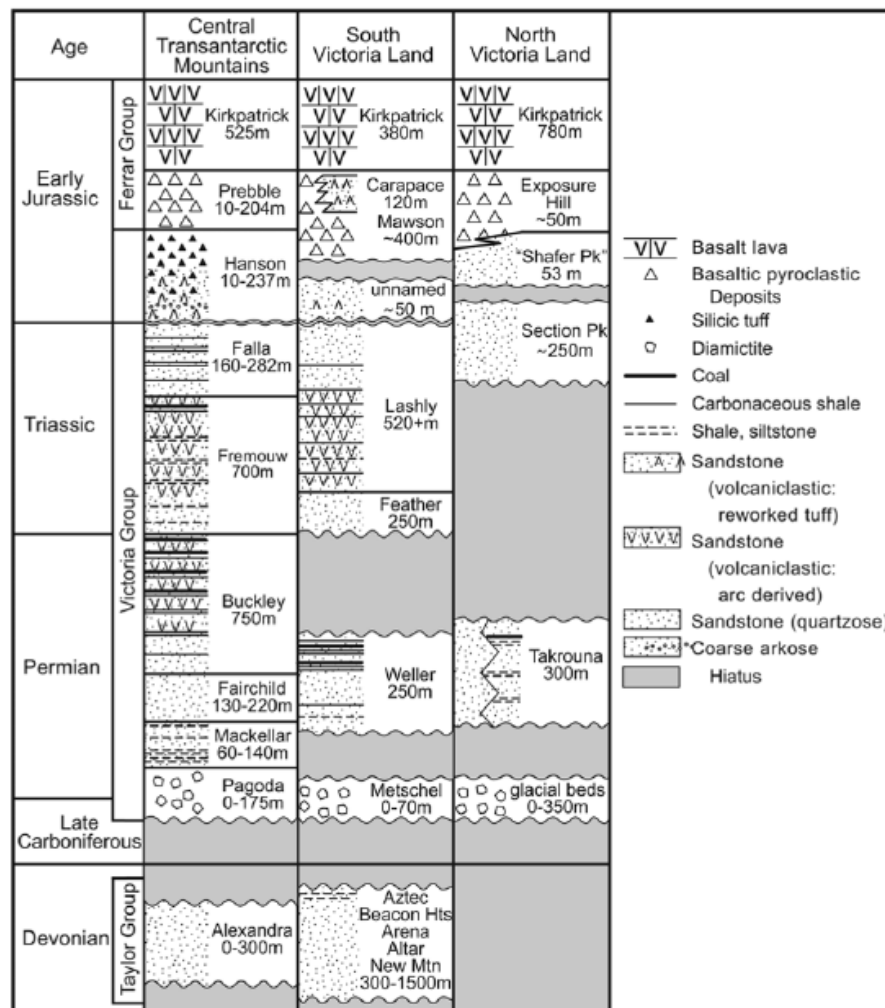

Figure 9: Sedimentary Sequences in Victoria Land, From Elliot 2013

2.2.1 Beacon Supergroup in North Victoria Land

In the NVL the sedimentary succession of the Beacon Supergroup shows an average thickness of about 250-300 m and overlain the basement, through a marked unconformity surface. The Beacon is there composed by four litho-stratigraphy units, following recent revision of the regional lithostratigraphy by Schoner et al. (2011) and Schoner and John (2014):

- The Lanterman Tillite (early Permian)

- The Takrouna Formation (Permian)

- The Section Peak Formation (late Triassic)

- The Shafer Peak Formation (late Triassic- early Jurassic)

In the NVL the stratigraphy correlation between the various units is complicated due to the absence of stratigraphic connections, indeed, the Section Peak Fm. overlain directly the basement in the southern part of the NVL (Eisenhower Range), lacking of the Permian unit below, whereas in the northern part of the NVL (Rennick Glacier) the Permian deposits formed by glacigenic deposits below and the Takrouna Fm. above, lay unconformably on the basement (Cornamusini et al., 2017) and lack of the Triassic unit at the top. To this regard, Bomfleur et al. (2014) showed Permian deposits underlying the Section Peak Fm. also for the Eisenhower Range.

2.2.1.1 LANTERMAN TILLITE

The Lanterman Tillite is the most representative tillite in the NVL, but some tillite outcrops occur in all the NVL with a not clear stratigraphy correlation with the upper Takrouna Formation. The depositional age of this unit is early Permian (Cornamusini et al., 2017), during a glacial age.

The type-section of the Lanterman Tillite is recovered at the western edge of the Lanterman Range, at the boundary with the Rennick Glacier, more precisely close to the Orr Glacier. The Lanterman Tillite is characterized by tectonic deformational structure, forming syncline and overlaining directly the basement. The Lanterman Tillite is thick around 150 m, and with the overlain sandstones the section reaches 350 m.

Vertical relationships with the Takrouna Fm. can be hypothesized, because the tillite succession passes upward to a sandstone succession, totally recalling the above formation.

The Lanterman Tillite (Figure 10) consists of a diamictite glacial portion, including mudstone with lonestones and an upper postglacial succession formed by mudstone and conglomerate (Laird and Bradshaw, 1981; Cornamusini et al., 2017).

Other basal diamictite or rudite units occurring in the NVL are at DeGoes Cliff and showing a thickness of at least 56 m at Neall Massif, where the passage at the top of Takrouna Fm is quite clear (Collinson et al., 1986; Woo et al., in prep.). In this specific case, however, the glacigenic character of the diamictite portion is in question, since both Collinson et al. (1986), John (2014) and Schöner & John (2014) assert that at least partially it is not glacigenic, but referable to glaciofluvial or fluvial debris flows processes.
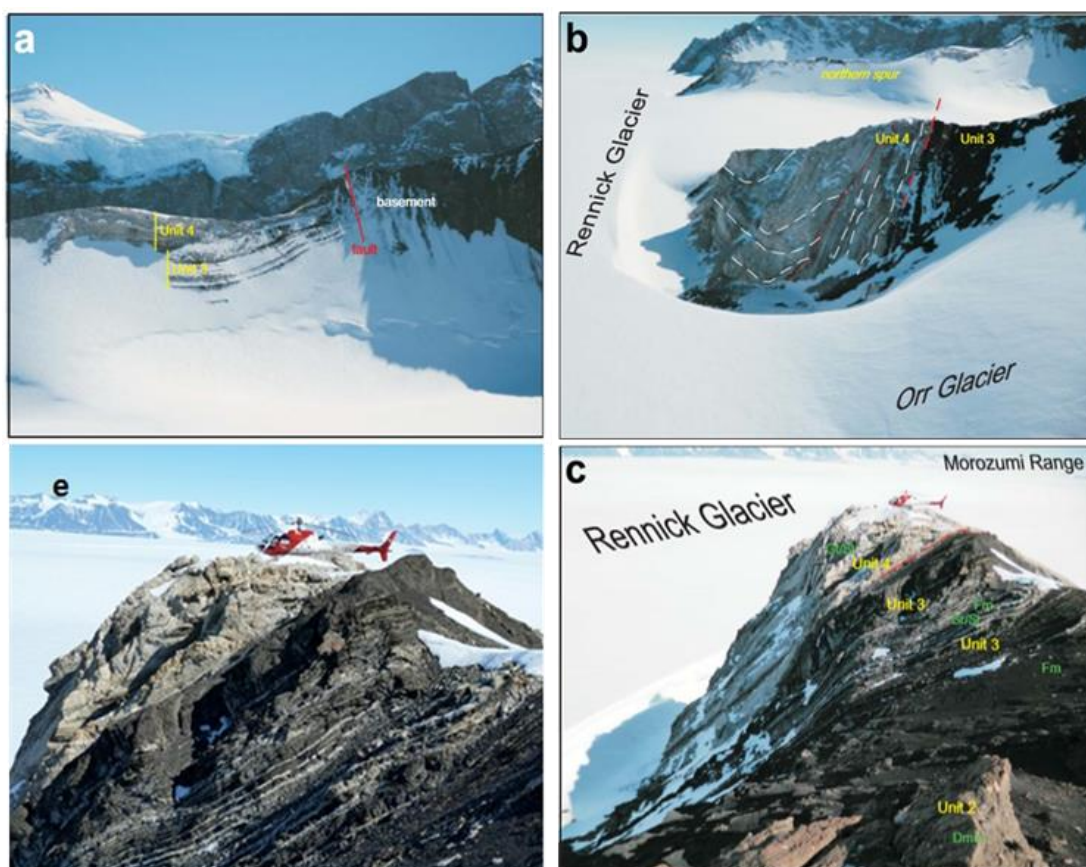
Figure 10 Lanterman Tillite outcrop pictures.

Two other minor diamictite outcrops occur in the Eisenhower Range (Zurli et al., in press), one at the western end of Thern Promontory (Casnedi et al., 2012; Pertusati et al., 2012; Cornamusini et al., 2013), where diamictite lies unconformably on to granitoid rocks of the basement, while it passes upwards to a conglomerate lithofacies of the Section Peak Fm. The other outcrops are along the

eastern flank of Mt. Nansen, where it passes upwards to a conglomeratic-arenaceous lithofacies always belonging to the Section Peak Fm. (Schöner et al., 2011; Cornamusini et al., 2013). To this regard, Bomfleur et al. (2014) showed that in this last area, the sandstone portion directly overlaining the diamictite has an age referable to the Permian and not to the Triassic, and therefore time-equivalent with the Takrouna Fm, representing the first record of such formation for the Eisenhower Range.

The typical outcrop of the Lanterman Tillite consists of two correlatable sections about 1 km apart, which, as highlighted in Cornamusini et al. (2017) are subdivided into two portions, one lower in contact with the base, relating to a phase and a glacial continental and glacial-lacustrine environments with repeated advances and withdrawals of the glacier front, while the upper portion, which then passes to the sandstones comparable with the Takrouna Fm., it is related to a post-glacial phase of lake environment, which then passes to fluvial environment. Still the same authors, based on palynological analyses on samples of lacustrine carbonates, attributed the succession to the Asselian (Early Permian).

Samples dating back to the Permo-Carboniferous in this area are located immediately below the Takrouna Formation, which contains a flora characterized by *Glossopteris* and *Gangamopteris*, which allow a dating at least to the Permian and above all can be correlated with other tillites that are in the same stratigraphic position, but located in other areas of Antarctica or Tasmania, which was adjacent to the NVL, following the reconstructions of Gondwana (Isbell et al., 2008).

2.2.1.2   TAKROUNA FORMATION

The Takrouna Formation was thus named by Dow and Neall in 1974, to indicate a thick succession up to 300 m of sandstone and carbonaceous rocks well outcropping at Takrouna Bluff and in the North Alamein Range.

Although the basis of this formation is not exposed in this locality, the section seems to represent the lowest part of the formation. This formation has an age referable to the Permian, determined thanks to paleobotanical associations, above all for the abundance of flora dominated by *Glossopteris* and *Gangamopteris.* The formation consists of a succession mainly formed of quartz and quartz-feldspatich sandstones, characterized by crossbedding, with the presence of siltites, sometimes carbonaceous.

Sturm & Carryer (1970) suggested that the maximum thickness of the Beacon sequences in NVL was about 300 m. Walker (1983) suggested dividing the formation into two members: one with a fine grain size and one with a coarse grain size, but was unable to demonstrate the vertical relationships between

these two members: Member A includes only the northern part of the area and some remaining locations, while member B is more extensive.

Collinson and Kemp (1983) attributed this granulometric variation to changes in lateral facies. They noted that overall the sandstones of the formation passed from a finer grain size and a greater abundance of carbon content proceeding westward with respect to Neall Massif towards Morozumi Range and the Helliwell Hills. Comparing the outcrop of Monte Cassino with that of Mohawango Nèvè it seems that in the Fryberg Mountains the first 200 m of section are richer in carbonaceous material than the rest of the formation. This observation generally agrees with the lithological reports in the 290 m section analyzed by Walker (1983) in the Northern Alamein Range.

The sequence at the Neall Massif is composed mainly of coarse-grained quartz-feldspathic sandstone beds and beds of conglomerate with granite-like pebbles and low-grade metamorphic rocks mainly, indicating a location closer to the clastic source area.

These places, close to the eastern edge of the Beacon outcrop in Northern Victoria Land can be interpreted as close to the margin of the depositional basin. The succession of the more western outcrops, along the edge of the Polar Plateau, from Roberts Butte to Vantage Hills, are less thick and consist of coarse quartz-feldspathic sandstone beds with dominant facies characterized by cross-stratification. In several locations the Takrouna Formation rests unconformably on a pre-paleozoic metamorphic or granite basement. In some places such as in the Lanterman Range, Morozumi Range and in the area of the Neall Massif, between the basement and the Takrouna Formation, the diamictitic succession is interposed, which at least for some outcrops can be traced to the Lanterman Tillite (see the previous paragraph). The top contact of the Takrouna Fm. it is not observable with other sedimentary units, as the passage to the younger Section Peak Fm. it has never been observed, while the contact with the Jurassic dolerites of the Ferrar Group is observed.

Dow & Neall (1971) described the paleo-floristic content of the formation, mostly given by: *Gangamopteris cyclopteroide*, *Glossopteris*, *Paracalamites*, and *Vertebraria*. The presence of *Gangamopteris* in association with *Glossopteris* is probably indicative of an age referable to the early Permian.

The sedimentary sequence with the typical facies of the Takrouna Formation is shown in Figure 11: The succession is dominated by facies with medium to coarse-grained sandstone, with cross-stratification mainly of through type and subordinately of tabular type. Amalgamation and basal erosion surfaces, while graded beds are rare.
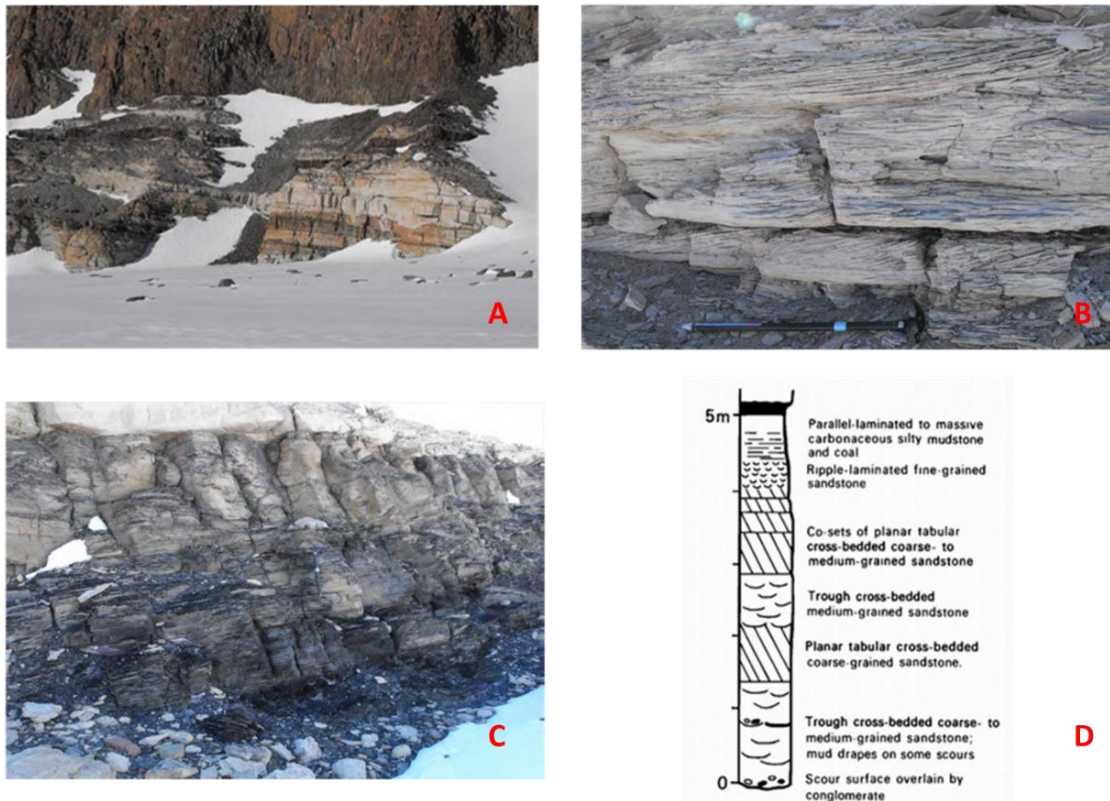
Figure 11 Images of the Takrouna Formation_A) Section at Takrouna Bluff; B) and C) carbonaceous laminated sandstones at Monte Cassino; D) Example of an ideal sedimentary cycle of Takrouna Formation.

2.2.1.3   SECTION PEAK FORMATION

The Section Peak Formation (Figure 12) is widely spreaded in the NVL (from the Eisenhower Range to the Mesa, including the Priestley and Campbell glaciers). The thickness is variable from 10 meters to more than 200m. In some locality the base of the formation is not exposed, while in other (as Mt. Nansen, Mt. Archambault., Folk Ridge, Section Peak and Stewart Heights) this overlain directly the granitoid basement.

The majority of the succession is composed by sandstone, whit layer of high grained cross bedding sandstone-rich in quartz-feldspar. Beds of carbonaceous sandstone and sometimes fragment of fossilized wood occur diffusely across the sections. This formation is assigned to a Triassic age due to the presence of a flora with the abundance of *Dicroidium*, but for the moment are not well know the age at the top and at base; some authors (Pertusati et al., 2006) suggest an early Jurassic age for the top of the formation close to the volcanic strata of the Ferrar Group.

Figure 12 Section Peak Formation_A) cross-bedded sandstones at Thern Promontory, B) and D) cross-bedded sandstones at Skinner Ridge; C) cross-bedded sandstones and pebbly sandstones at Timber Peak.

2.2.1.4   SHAFER PEAK FORMATION

The Shafer Peak Formation is the uppermost unit of the sedimentary succession, outcropping just in few localities (i.e. Mt. Carson, Shafer Peak and Deep Freeze Range) (Schoner et al., 2007; 2011). The mainly representative section is at Shafer Peak (up to 3200 m); this section is formed by cross bedded sandstones rich in volcaniclastites, from fine to coarse grained, reaching a maximum thickness of 53 m. Here there is also a mafic sill emplaced at around 28 m from the base. Remains of vegetal material are bad preserved and less abundance than in the other formation, but they suggest a replacing of the *Dicroidium* due to *Cycadophytes* and *Dipterid*.

2.2.1.5   SILLS

The mafic dykes and sills belonging to the Ferrar Group intruded within the Beacon sedimentary successions as well within the basement, with a cumulative thickness exceeding 300 m (Schoner et al., 2011; (Vierek-Goette et al., 2007). These intrusions can be divided into two groups of different generations: a first generation with a more massive structure, joined vertically, with constant levels of intrusion at the kilometric scale, these often have alteration crusts dominated by red-coloured oxides and a second generation characterized by a dark gray to black color, partially discordant with the sedimentary succession and with non-constant horizons within the succession itself.

2.2.2 BEACON SUPERGROUP In South Victoria Land

The geology of the South Victoria Land (SVL) has been widely discussed by many authors, i.e. Elliot (2014), Barrett (1991) (Collinson et al., 1994) for some reviews, with of particular importance are the regional review by Cox et al. (2012) with a geological map covering the whole SVL, Stump (1995) and Goodge (2020) due its regional and updated synthesis.

The basement rocks, referable to the Ross Orogen, occurring in the SVL are the Precambrian metasediments and metavolcanics of the Skelton Group and the Upper Precambrian-Lower Ordovician granitoids and gneisses of the Granite Harbour Intrusive Complex.
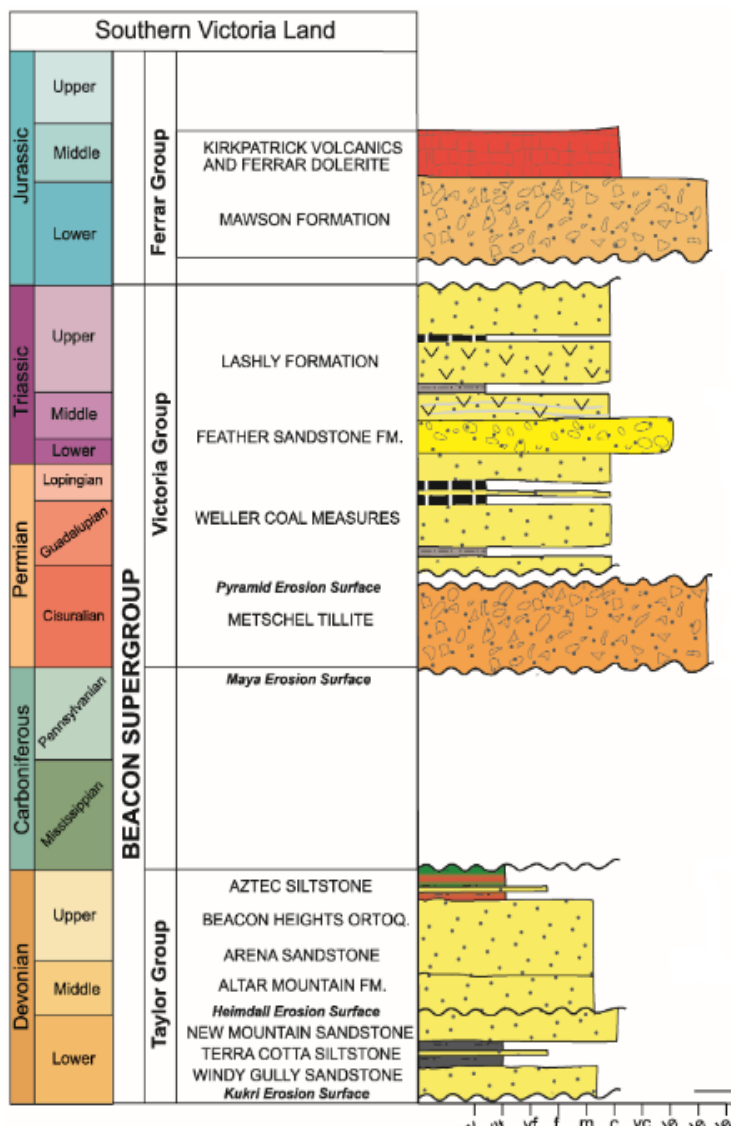

Figure 13 Stratigraphy Section of Beacon Supergroup in South Victoria Land

The oldest Skelton Group was deposited in a Neoproterozoic rift system (around 650 Ma) and was subsequently strongly deformed and intruded by a variety of plutons: the Granite Harbour Intrusive Complex (Gunn and Warren, 1962). Episodic deformation and magmatism at the active paleo-Pacific continental margin of Gondwana continued at least until Early Ordovician time (Ross Orogen) (Cox et al., 2012).

The uplift caused by the Ross Orogen was followed by a deep erosion during the Devonian time (c. 414 Ma) which generated the Kukri Erosion Surface. This erosional surface is overlying through a marked angular unconformity and nonconformity, by the Beacon Supergroup, a thick (up to 2,5 Km) sedimentary succession deposited from Devonian to early Jurassic time.

One more important erosional event is registered within the Beacon Supergroup, dividing it in two lithostratigraphic groups. This event is marked by the Maya Erosion Surface (that represent a non-depositional and/or erosional stage of 86-109 million Years, equivalent to the Carboniferous period and possibly longer) (Cox et al., 2012); this one divided the Beacon Supergroup in two different group: Taylor Group (Devonian) and Victoria Group (?Carboniferous/Permian to early Jurassic). The Beacon Supergroup as well as the basement have been then intruded by dykes and sills of the Ferrar Group, Jurassic in age.

The Beacon Supergroup outcropping extensively in SVL and with its correlative series along the whole TAM for about 2500 km, is a Devonian to Lower Jurassic clastic mainly non-marine succession (Barrett, 1981; 1991). In SVL, it forms a gently monocline west dipping (to be sealed by the East Antarctica Ice Sheet), with local sectors with more tectonic deformation (e.g. western side of the Lanterman Range or the Pensacola Mountains). The Beacon Supergroup, lying on to the Ross basement through the Kukri erosional surface, is subdivided in two groups on the base of unconformities, lithological differences and the occurrence of deposits related with an important glacial phase. They are the Devonian Taylor Group and the (?Carboniferous) Permian-Lower Jurassic Victoria Group, divided by the regional extent Maya erosional surface, recording a wide time-gap, at least inclusive of late Devonian to late Carboniferous (Barrett, 1991; Collinson et al., 1994). The Victoria Group, object of the present research, is thick about 400 meters in Allan Hills, with significant lateral changes and thickness for the whole SVL, due to the irregular paleo-depositional surface. In the Southern Victoria Land (SVL), it is represented by glacial deposits of the Metschel Tillite Fm. at the base, ?late Carboniferous – Early Permian in age, passing upwards through a minor regional disconformity that locally become a conformable surface (Pyramid erosional surface), to the Weller Coal Measures Fm., Permian in age. This last is formed by sandstones interlayered with coals and mudstones of fluvial to alluvial plain environment (Isbell and Cuneo, 1996). This passes upwards to the Feather Conglomerate Fm. of a not well-constrained age, probably Early Triassic. Nevertheless, lacking constraining chronostratigraphic data, this contact has not yet well defined in characterization. In fact, it has been defined

as disconformable for the Allan Hills section, recording a lacuna (Isbell and Cuneo, 1996, according to Collinson et al., 1994), whilst recently Liberato et al. (2017) reported for a conformable and gradual boundary, based on the strata attitude and field observations, on agree with paleosols stratigraphy and sedimentology dataset performed by Retallack and Krull (1999). The Feather Conglomerates Fm., except for its upper member (Mt. Fleming Mb.), is formed of pebbly sandstones and coarse sandstones, lacking mudstones, with interbedded paleosols horizons (Retallack and Krull, 1999). The Mt. Fleming Mb. differs from the latter, mainly on the base of a lower sand/mud ratio, with frequent mudstone interlayers and a smaller grain size of the sandstones, which are medium to coarse. It passes conformably upwards to the fluvial to alluvial plain environment Triassic Lashly Fm., which is so internally articulated, to be subdivided in four lithostratigraphic members A, B, C and D, in (Barrett and Webb 1973), particularly on the base of sand/mud ratio, stacking pattern, sandstone grain size and occurrence of coal levels. To follow, the Lashly Fm. passes upwards to a volcanoclastic formation, which is the Mawson Fm., Early Jurassic in age, that in Allan Hills as in the most of SVL is expressed by a significant unconformity with erosional surface. The whole succession is intruded by Jurassic dykes and sills of the Ferrar Supergroup.

Along the TAM, particularly SVL, such succession forms a westward gently dipping monocline, determining the outcropping of the lower and older formations of the Taylor Group, as well as the basal boundary with the basement, mainly in the eastern-central side of the SVL (as the Dry Valleys, Beacon Heights and the Royal Society Range), whereas the formations of the Victoria Group crop out mainly in the western side close to the East Antarctica Plateau (e.g. Allan Hills, Lashly Mts., Warren Range, Boomerang Range).

Lithologically, the Beacon Supergroup in general consists of conglomerate, sandstone, mudstone and coal strata, deposited in articulated continental paleoenvironment settings of the Gondwanian Antarctica alluvial basins (with the exception of few portions of the Devonian Taylor Group, showing probable tidal-marine influence, see in (Bradshaw, 1981) and some of the lower Permian glaciomarine tillites, see in Isbell et al., 2008).

The study area of Allan Hills is in SVL, at the edge of the East Antarctica Ice Plateau. Spectacular extensive exposures of some hundreds of meters thick fluvial rock successions of the Permian to Lower Jurassic Beacon Supergroup occur. These alluvial sequences exposed at Allan Hills, consist of flat-lying sandstone-dominated successions comprised into the Victoria Group. In general, along the SVL, this is characterised by tillites, coal measures, carbonaceous mudstones, conglomerates and quartzose, arkosic and feldspathic sandstones. A thickness variability for the Beacon Supergroup also within the SVL has been emphasized (Barrett, 1991; Collinson et al., 1994).

To follow, some features of each major lithostratigraphic unit has been shown.

2.2.2.1   TAYLOR GROUP

The lower part of Beacon Supergroup is represented by the Taylor Group (just in the SVL because it doesn't occur in the NVL, to represent the most important difference between the basins in SVL and NVL). The most complete succession crops out close to McMourdo Sound, where a 1400 m thick sequence from Early to Late Devonian is exposed. The Taylor Group is divided in 8 lithostratigraphic formations, lying on to the Kukri Erosional Surface (Cox et al., 2012).

The lithostratigraphic units are as follow, starting from the bottom of the succession:

- **Windy Gully Sandstone** a thin discontinues basal conglomerate with clast of quartz and basement rock from angular to subrounded and mainly siliciclastic quartzose sandstones.

- **Terra Cotta Siltstone** is an alternation of dark siltstones and claystones and thinly bedded, fine grained sandstones.

- **New Mountain Sandstone** is formed by medium to coarse-grained sandstones with abundant trace fossils that conformably overlain the Terracotta Siltstone.

- **Altar Mountain Formation** overlays the New Mountain Sandstone through a minor and discontinuous erosional surface called Heimdal erosional surface. This formation is built by cross-bedded quartzose sandstones with subordinate siltstones and shales; at the basal part is recognized the Odin Arkose Member, a feldspatic sandstone and conglomerate lithological association.

- **Arena Sandstone** is formed by planar and cross-bedded medium to fine grained sandstones with siltstone and shale beds, many trace fossils have been described, including *Skolithos*-type and *Beaconites*; on the upper part of the formation is recognized the Pivot Member.

- **Beacon Heights Orthoquarzite** this formation is mainly formed of well-sorted quartz sandstones with few feldspar clasts, to be defined as quartzarenites. It could be divided in two part: the lower part of medium grained quartzose sandstones, with tabular to trough crossbedding, while the upper part shows interbeds of dark mudstones within the sandstones; *Lycopod* stems indicate a Middle Devonian age.

- **Aztec Siltstone** conformably overlays the Beacon Heights Orthoquartzite, and it is formed by cross-bedded and rippled sandstones with interlayers of red and green mudstone, with nonmarine fish fossil remains. (first collected at Mackay Glacier, also recovered at Allan Hills)

The Taylor group is erosionally truncated by the Maya Erosion Surface, a glacial originated unconformity, and overlain by the Victoria Group, the lower units of which are Early Permian (or Late Carboniferous?) in age.

2.2.2.2 VICTORIA GROUP

The Victoria Group is separated from the Taylor Group by the Maya Erosional Surface, this is a typical Gondwana Sequence with glaciogenic deposits at the base and fluvial/alluvial deposits above. The total thickness of the group is about 1 Km and the age is from Early Permian (or Late Carboniferous) to Late Triassic (or early Jurassic). The Victoria Group crops out in the South Victoria Land, whereas, differently by the Taylor Group, deposits correlatable with them occur also in the North Victoria Land (Collinson et al., 1994)

In the South Victoria Land, the Victoria Group is divided in four formations, from the bottom: The Metschel Tillite, The Weller Coal Measures, The Feather Conglomerate, The Lashly Formation, The Mawson Formation.

2.2.2.2.1. THE METSCHEL TILLITE

The **Metschel Tillite** is a matrix-supported pebble-cobble diamictite, in some localities (as Slump Mountain) this tillite is disrupted by folding and faulting structures due to subglacial deformation processes (Isbell et al., 2010). Equivalents of the Metschel Tillite elsewhere in Antarctica (i.e. Pagoda Formation in Central TAM) are ascribed, through palynomorphs, to the Early Permian (or Late Carboniferous) Elliot (2014), but the Metschel Tillite for the moment is never been directly dated in SVL.

2.2.2.2.2 THE WELLER COAL MEASURES

The **Weller Coal Measures** stay on the Metschel Tillite, but the boundary shows differences depending by the area, in fact, at Beacon Heights it shows an erosional surface which is the Pyramid Erosion Surface, while at Mt Fleming is exposed a gradational contact. The basal unit of this formation, occurring only locally, is called Maya Arkose Member, formed of conglomerates, arkosic coarse-grained sandstones; while the upper part is formed by cross-bedded and massive pebbly sandstone grading up into carbonaceous, fine-grained sandstones and siltstones. The Weller Coal Measures were deposited in an alluvial plain, braided river, lacustrine and meandering river setting system; plant fragments are more common with also some fossil trunk (some of them in position of growth). The age of this formation, on the base of macroflora and palynomorphs has been ascribed to the Permian for the Central TAM, whereas the age has been restricted at the Early-Middle Permian for the SVL, in that the late Permian seems to lack, emphasizing a time gap with the Triassic above formation (Kyle and Schopf, 1982) (Isbell and Askin, 1999). Differently, other authors, on the base of non-direct evidences, consider the Weller Coal Measures of SVL ranging for the whole Permian, including also its upper part, so to record the Permian-Triassic Boundary (Retallack et al., 1998) Retallack G.J. (1999) (Retallack et al., 2005) (Retallack et al., 2006), even if recently Awatar et al. (2014) recognized late Permian palynomorphs at Allan Hills.

2.2.2.2.3 THE FEATHER CONGLOMERATE

The **Feather Conglomerate** comprises granular and pebbly quartzo-feldspathic sandstones, with lesser quartz pebble conglomerates, and very rare mudstones, except for some muddy paleosols; furthermore, it is characterized by its unfossiliferous feature, lacking any animal and floral character. The upper portion of the formation, due its occurrence of finer sandstone and mudstone beds, has been defined as Mt. Fleming Member (see in Cox et al., 2012). The Feather Conglomerate was deposited in an alluvial plain characterized by braided river systems. The age of the Feather Sandstone is not known, due its total lacking fossil age constraints, so it is indirectly ascribed to the at the Early Triassic, even if few authors think it as late Permian.

2.2.2.2.4 THE LASHLY FORMATION

The **Lashly Formation** is an articulated lithological unit subdivided in four lithostratigraphic members on the base of different sand/mud ratios (Barrett, 1981). It is mainly formed of carbonaceous sandstones, siltstones and mudstones, rich in vegetal fossil fragments as leaves, roots and tree stumps with logs up to 15 meters long. The formation was deposited in alluvial plain characterized by meandering to braided rivers and ephemeral lake and palustrine environments. The bottom contact of the Lashly Formation shows conformable relationships with the Feather Conglomerate Fm., while in the top of the formation is erosional truncated by the, volcanoclastic overlaying Mawson Formation. The Lashly Formation is divided into four members (A-D) on the base of lithostratigraphy. The age of the formation has been defined on the base of plant macrofossils and palynomorphs to the Triassic (Kyle, 1977; Kyle and Schopf, 1983; Retallack et al., 1998).

2.3   FERRAR GROUP

The Ferrar Group large igneous province rocks are exposed in a belt that extends for c. 3500Km along the TAM, in southern Victoria Land the Ferrar province includes volcanic and volcaniclastic rocks, dykes and sills of the Ferrar Dolerite and of the Kirckpatrick Basalt. The Ferrar sills and their effusive equivalents were emplaced and erupted in a short period of magmatic activity over a few million years or less in the Late Jurassic time (Cox et al., 2012).

The rocks of the Ferrar Group consist of dykes and sills of the Ferrar Dolerite, of the flows of the Kirkpatrick Basalt, and the phreatomagmatic volcanic breccias that underlie the basal plateau. These rocks formed in a short interval of time during the Middle Jurassic in a setting of extensional tectonic. The basal magmas originated at depth in the subcrustal mantle and intruded the basement of the Transantarctic Mountains and the overlying sedimentary rocks of the Beacon Supergroup by means of deep crustal rifts that started the ultimate break-up of Gondwana (Faure and Mensing, 2010)

2.4 Lithostratigraphy of Allan Hills

The stratigraphy of Allan Hills (map in Fig. 14) was early discussed by (Balance, 1977), Gunn and Warren (1962) and other authors.
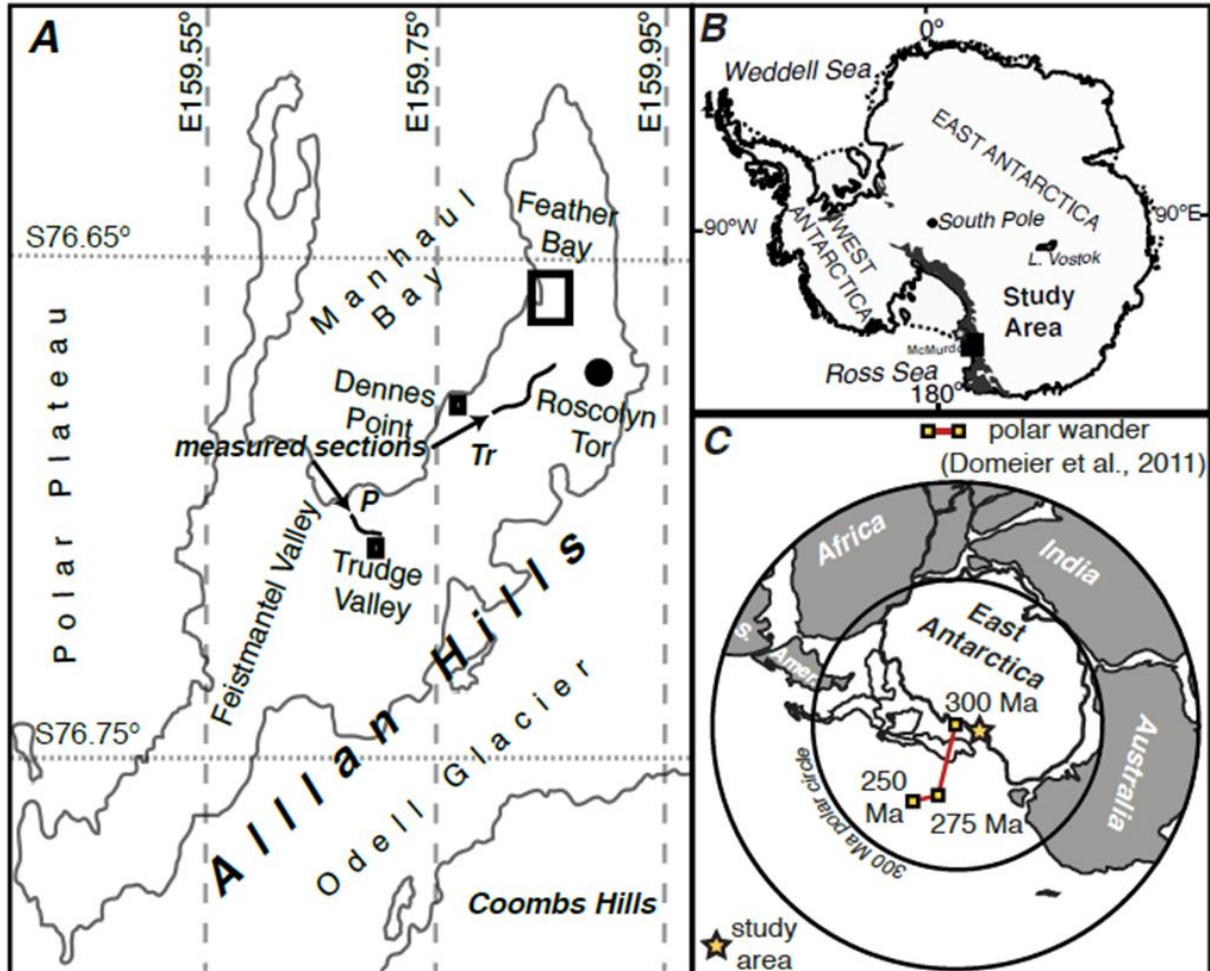
Figure 14 : A) Map of the location; B) localization in Antarctica; C) Migration of the area of Allan Hills trough the time (from Gulbranson et al., 2020)

Three lithostratigraphic units of the Beacon Supergroup (Fig. 15 and 17), all belonging to the Victoria Group, crop out widely, to form a gently NNE dipping monocline (max 10° of inclination), almost sub horizontal in the Halle Flat where we measured several sections: the Weller Coal Measures Fm (Permian), the Feather Sandstone Fm (Early Triassic) and the Lashly Fm (Middle-Late Triassic) (Barrett, 1991; Gulbranson et al., 2020).
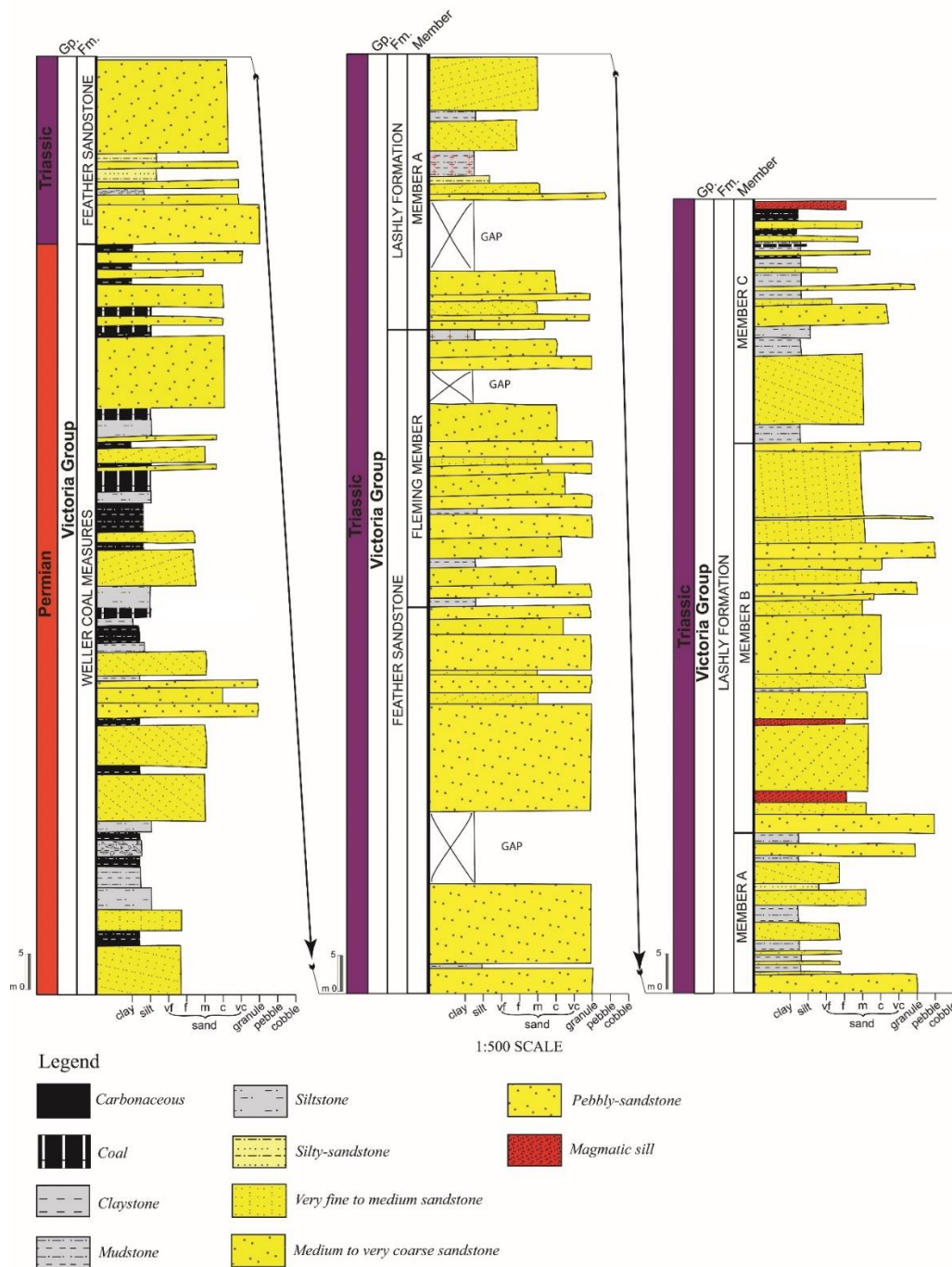
Figure 15 Lithostratigraphy of Allan Hills from Liberato et al 2017

The Weller Coal Measures Fm. is divided in some members, but we indagated only the uppermost one. The upper part of the Feather Sandstone Fm. has been identified as Fleming Member. The Lashly Fm. has been further subdivided in four members following Barrett and Kohn (1975), but the uppermost Member D crops out in a minor way in Allan Hills (Tewari et al., 2015). In general, in SVL the Weller Coal Measures Fm lies unconformably onto the ?Late Carboniferous-Early Permian Metschel Tillite (which does not crop out in Allan

30

Hills) separated through the Pyramid erosional surface. The Lashly Fm. is unconformably overlain by the Jurassic volcaniclastic Mawson Fm., with the Kirkpatrick Basalt on top (Ballance and Watters, 1971). All the formations are intruded by dolerite dykes and sills of the Ferrar Group, Early-Middle Jurassic in age.

The magmatic dykes, mainly N-S and NW-SE oriented, form a wide belt located in the Trudge Valley-Odell Glacier up to the Dennes Point and the Shimmering Icefield, get more complicated the relationships between the lithostratigraphic units. Other minor dykes and sills occur widespread in the area, intruding the sedimentary units. No evidences of tectonic dislocation are evident between them, except for few dykes placed south of Roscollyn Tor, displacing the boundaries in between the Lashly Fm. and the Feather Sst. Fm. The Mawson Fm. is well exposed on the top of the Roscollynn Tor and along its NE prolonging ridge up to Maiden Castle.
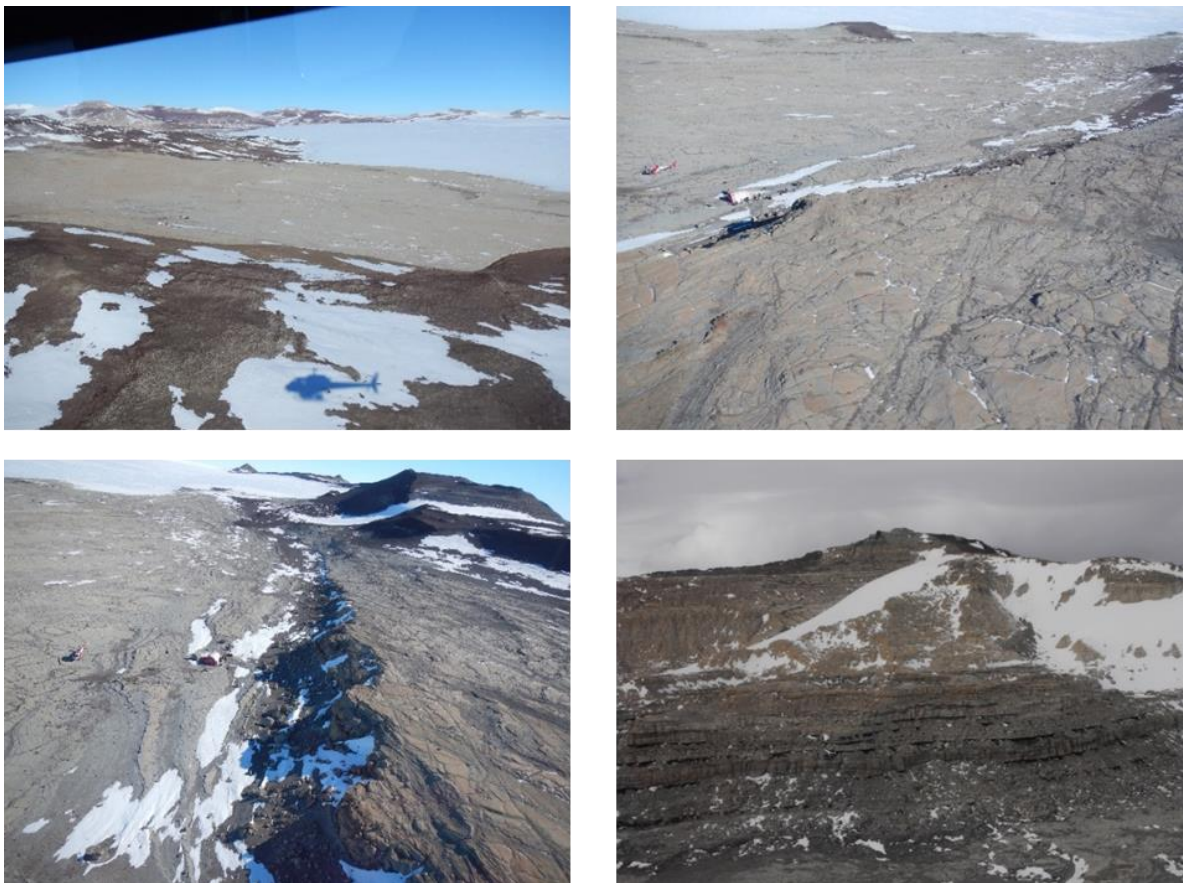
Figure 16 Allan Hills field images: Lashly Formation member A-B and C

The age of the different formations through PTB (respectively Weller Coal Measures and Feather Sandstone Fm.) is mainly based on plant fossils of the *Glossopteris* and *Dicroidium* flora, indicating respectively Permian and Triassic age (Townrow, 1967). Furthermore, palynomorph assemblage documented the Early-Middle Permian (middle Artinskian to early Roadian, in Kyle, 1977; Kyle and Schopf, 1982; Farabee et al., 1990; Askin, 1995; Isbell and Cuneo, 1996) for the middle-upper part of the former, while more recent age-dating suggests

a Late Permian age for its uppermost part (Awatar et al., 2014) according to paleosol and paleoflora data by Retallack et al. (2005). The above Feather Sandstone Fm. does not reveal any form useful to the age-dating, but should be restricted to the Early Triassic, whereas the Lashly Fm. was assigned on the base of palynomorphs, to the Early Triassic-earliest Middle Triassic for the Member A, and to the Middle Triassic for the members B and Late Triassic for member C (Kyle and Schopf, 1982).
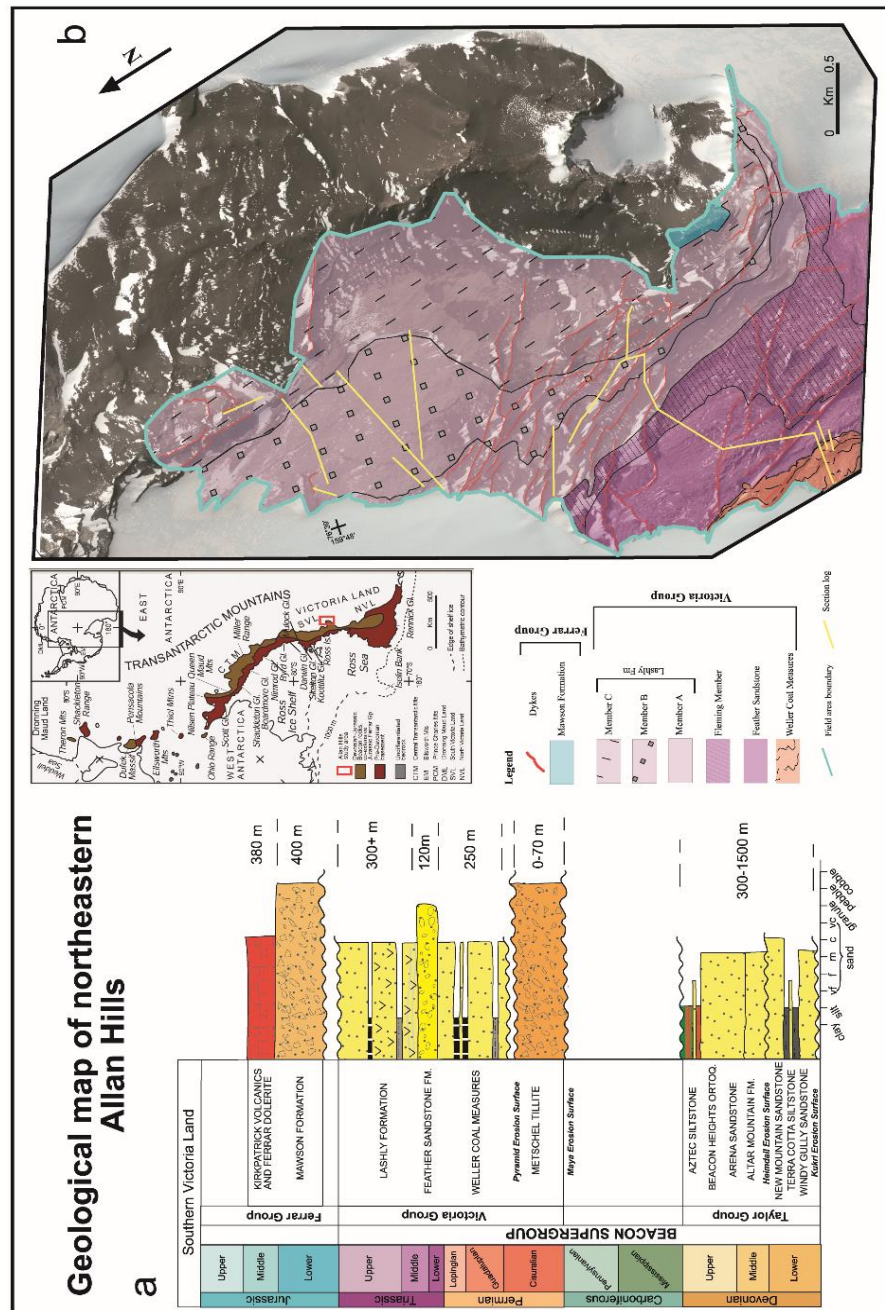

Figure 17 Geological map and lithostratigraphy of Allan Hills (from Liberato et al., 2017).

Part I: PALYNOLOGY

1.Introduction

The palynological reconstruction of the Permian and Triassic deposits in Gondwana Land is a fundamental key, not only for the chronostratigraphic calibration of the deposits, but also for the paleoenvironmental and paleogeographic reconstruction across the Permo-Triassic Boundary in such paleocontinent.

The Permo-Triassic mass extinction (about 252 Ma) represents the most impacted extinction recorded in the history of the Earth (Erwin, 1990; Hudson, 2003). During this event were lost over than 80% of marine species (Erwin, 2015; Stanley, 2016) and a total of 57% of biological families and 83% of genera.

The causes of this big mass extinction are still a source of debate, even if the prevailing hypotheses are related to the massive eruption of the Siberian Traps, or due to a meteorite impact, or also to the combination of these two causes (Erwin, 2002, 2015; Bond and Grasby, 2017). Otherwise, leaving aside the causes that generated the mass extinction, that they will be not discussed in this thesis, the fact is that during the transition between Permian and Triassic, an extreme greenhouse and anoxic condition were manifested all around the Earth (Retallack et al., 2011). Within the Lower Triassic deposits of Gondwana Land there is a diffused loss of coal, very common in the Permian ones; moreover a deep change through the paleoflora and the fluvial styles, indicates a dramatic change in the paleo-environmental conditions between the Permian and the Triassic times.

As regards the paleoflora reconstruction (Archangelsky, 1991; Taylor and Taylor, 2012), it well known that the *Glossopteris* flora dominated the paleoenvironment during the Permian time, and it was replaced with a total different flora assemblage, mainly represented by *Dicroidium*, but also by Lycopsids, Equisetaleans, Ferns, Seen Ferns, Ginkoaleans and Conifers (Escapa et al., 2011).

The deep change in the paleoflora associations, emphasized by several findings of fossil trunks, roots and impression-compression of leaves in many areas of Gondwana, is reflected- obviously- in a deep change about the palynological assemblages: the *Protohaploxypinus*, a striate bisaccate pollen grain, that dominated the palynoassemblage of the Permian deposits, is in good amount replaced by various species of *Alisporites*, a non taeniate bisaccate, in the Triassic deposits (Kyle, 1977). Moreover, also many species-and genus- of other bisaccate, monosaccate and spore suffered from

this crisis time, with the complete extinction and replacement of some genera or an evident loss in the abundance of these.

This thesis aims to define the paleoenvironmental setting derived from palynological inferences, of Permian to Middle Triassic fluvial deposits of Allan Hills (South Victoria Land, Antarctica). In the SVL, the Permo-Triassic sequences, represented by the Victoria Group (upper part of the Beacon Supergroup), are characterized by glacial beds in the basal part, passing upwards to alluvial/fluvial deposits. This group is separated from the underlying Devonian Taylor Group, by the Maya Erosional Surface and it is divided into four formations (from bottom to top): Metschel Tillite, Weller Coal Measures, Feather Conglomerate, Lashly Formation. The whole succession is extensively intruded by Jurassic dolerite sills. The present study is focused on the Triassic Lashly Formation. This formation is a sandstone, siltstone and mudstone bed alternation, carbonaceous-rich, with land plants fragments as leaves, roots and *in situ* and transported permineralized tree stumps. The Lashly Formation is in turn divided in four members (A-D), mainly on the base of the sand/mud ratio, where the Member D is not occurring in the study area. The Member A is characterized by sandstone and mudstone alternances, with the former characterized by trough cross-bedding forming sandy bedforms as downstream accretion forms; the Member B shows a high increase in the sandstone content, with lowering mudstone and concentrations of fossil trunk and peat rafts in particular stratigraphic sandy horizons; the Member C shows an increase in the mudstone and siltstone content, with the occurrence of thin carbonaceous and coal levels. The paleoenvironment inferred by literature, based on sedimentological data, has been defined as relative to floodplain/fluvial channel of changing meandering to sandy braided streams (see in Liberato et al., 2017; Gulbranson et al., 2020).

Permian-Triassic strata of the Beacon Supergroup, particularly the Victoria Group, representing a thick sedimentary cover lying on to the Ross Orogen terranes, have been defined in age through palynological studies in the past (i.e. Kyle, 1977; Kyle and Schopf, 1983), through the whole Transantarctic Mountains, giving rise to stratigraphic assessments both in age and paleoenvironment. The detailed stratigraphic definition of such deposits is very important, due to their significance within the whole southern Gondwana depositional framework across the Permian to Triassic. In fact, the Victoria Group represents the expression of the fluvial to alluvial sedimentation during such time, within the South Victoria Land Basin, to be correlated with other

basins of the Antarctica (Barrett, 1981, 1990; Collinson et al., 1986) and to be related in a more extended way with systems of Tasmania, Australia, India, South Africa, for to reconstruct the "gondwanian" depositional sequences and basins (Elliott, 1996 with references therein). Furthermore, the importance of these sequences also lies in the record of the Permian-Triassic transition (PTT), although for continental successions.

However, despite numerous palynological and paleobotanical studies (Kyle, 1977; Bomfleur et al., 2011; Gulbranson et al., 2014; Cornamusini et al., 2017), several open problems remain, particularly concerning the definition of gap in sedimentation and the stratigraphic relationships among the depositional units, also due to the complex architectural pattern linked with the mainly fluvial paleoenvironment. With the aim to refine the stratigraphic setting of such deposits, we have performed palynological and palynofacies analyses of one of the more complete and better exposed Permian-Triassic series of South Victoria Land, which crop out in Allan Hills. Here a thick succession occurs, where main sandstones and pebbly sandstones are interlayered with mudstone and coal beds, with different ratios along the vertical stacking pattern, depending by sand/mud ratio, here represented through a lithostratigraphic subdivision.

In the present work, we studied palynological assemblages from the upper part of the Weller Coal Measures and the Lashly Formation of Allan Hills, to review their ages in the light of new biostratigraphic advances for the Transantarctic Mountains, through the analysis of a conspicuous series of new data.

Many of the processed samples contain organic matter, even if affected by high thermal maturity, but in a good amount of these were still preserved several recognizable palynomorphs. The reconstruction of the depositional environments is discussed using an integrated approach based on facies, microfacies and palynofacies analysis.

1.2   Palynological background

Townrow (1967) described macroflora leave assemblages from Allan Hills, indicating a Permian age for the Weller Coal Measures and the Middle to Late Triassic age for the Lashly Fm.

The stratigraphically lowest depositional unit investigated in this thesis is represented by the upper part of the Weller Coal Measures Fm. It and correlatable formations crop out for a wide area in SVL and along the TAM (Fairchild Fm. and Buckley Fm. for the Beardmore Glacier area, as the lower part of the Glossopteris Fm. for the Ohio Range, the Takrouna Fm. for the Northern Victoria Land) and ascribed to the early Permian (Barrett, 1991) (Barrett, 1981). The leaves of *Glossopteris* and the plant remains indicate a generic Permian age for this formation (Askin and Fasola, 1997). (Rigby and Schopf, 1969), on the base of the *Glossopteris* flora pointed to a middle-late Permian for the formation of the whole SVL, without excluding the early Permian for the lowermost part of the formation. Differently (Kyle, 1977) based on *Glossopteris* plant macrofossils, defined that the formation in SVL was only Early Permian in age, excluding the late Permian.

Also (Collinson, 1994) determined an early Permian age for the Weller Coal Measures in SVL accompanied by a lacuna up to the lower Triassic deposits, while it comprises also the late Permian for the Central Transantarctic Mountains (CTAM, particularly the Beardmore Glacier and the Ohio Range). Furthermore, coal deposits containing a flora association of *Gangamopteris-Glossopteris* in SVL allowed to establish an age up to the early Late Permian age (Artinskian – Kungurian) (Collinson et al., 1994). Differently, the Central TAM showed microflora assemblages referable to the Eastern Australia Stage 5 of the Late Permian (Kyle and Schopf, 1982; Farabee, et al., 1991), which seems to lack in Victoria Land, so to emphasize an important lacuna. In particular Kyle (1977, 1982) ascribe the Weller Coal Measures Fm. to the *Protohaploxypinus* Zone, correlatable with the Australian Stage 4, of early Permian age for the members B and C of the same formation, whereas the Stage 5 of late Permian would be lacking in SVL; the middle Permian age for the upper part of the formation has been confirmed on the base of stratigraphic and paleontological data by (Cuneo et al.,1993) and (Isbell and Askin, 1999).

Askin (1995; 1997) revisited some Permian outcrops of South Victoria Land (Allan Hills and Mount Crean) and confirmed the data of Kyle and Schopf (1982), but, despite the poor and bad preserved palynomorph assemblages, without clearly exclude the possibility to record the Late Permian,

particularly for the outcrop of Mount Crean, due to the possible recognition of the *Praelcopatites* Zone established by Playford (1990) for the uppermost part of the formation. More recently, Awatar, et al. (2014), although based on only one sample, recorded a palynomorph assemblage referred to the *Densipollenites magnicorpus* palynozone (comparable with the western Australian Upper Stage 5) of late Permian (Lopingian) age for the Weller Coal Measures of Allan Hills. The possibility to have a short or none lacuna between the Weller Coal Measures and the Feather Conglomerate Fm. in Allan Hills, has been suggested also by Retallack and Krull (1999) on the base of stratigraphic paleosol analysis and of the recovery of a macroflora assemblage with *Glossopteris*, *Gangamopteris*, *Vertebraria* and particularly *Phylloteca australis* few meters below the lithostratigraphic boundary; this last specie indicating possibly the late Permian Retallack et al., (2005, 2006).

The late Permian age for the upper part of the Weller Coal Measures has been inferred also by a few authors (Retallack et al., 2005; Tewari et al., 2015), on the base of *Glossopteris* flora assemblage. It is worth to note that (Retallack et al., 2005) placed the Permian Triassic boundary in Allan Hills, ten meters below the lithostratigraphic contact between the Weller Coal Measures and the Feather Conglomerate Fm., based on the distribution of different paleosols.

The above lying formation of the Feather Conglomerate, due to its dominance of pebbly sandstones with rare or absent mudstone layer, has been considered barren of microfossils. However, Barrett and Kohn (1973) believed that it is late Permian in age on the base of sedimentological data, while Kyle et al., (1982) determined an although rare microflora assemblage of Early Triassic age for the uppermost part of the formation (top of the Mt. Fleming Member). Moreover, Kumar et al., (2011; 2013) reported the occurrence of wildfire-induced micro charcoal from the Lashly Fm. of Allan Hills. Lower Triassic deposits occurring in the CTAM, belonging to the lower member of the Fremouw Fm., contain a rich *Lystrosaurus* Zone fauna (Collinson J.W., 1994). They record the same palynological assemblages of the above lying Lashly Fm., in particular of the lower-middle part of its Member A (correlated with the middle member of the Fremouw Fm.), indicating the subzone A of the *Alisporites* Zone of the upper part of the Early Triassic (Kyle, 1977) (Kyle et al., 1982), on agree with macroflora assemblage data (Gabites, 1985) (Isbell et al., 1999) (Retallack et al., 2005).

The upper part of the Member A and the lower-middle part of the Member B of the Lashly Fm. have been ascribed by (Kyle, 1977) and (Kyle and Schopf, 1982) to the subzone B of the *Alisporites* Zone, referred to the Middle Triassic, while the upper part of the Member B and the Member C has been ascribed to the subzone C, of Late Triassic age (Carnian). The Member D has been ascribed by the same authors to the subzone D, Late Triassic in age (Norian-Rhaetian). (Awatar et al., 2014) recognized the subzones A and B of the *Alisporites* Zone for one sample from the Member C of the Lashly Fm. of Allan Hills, indicating an Early to Middle Triassic age (Induan to Anisian). Several authors (Taylor et al., 1994; Bomfleur et al. 2011; Gulbranson et al., 2020) recognized macroflora assemblages dominated by *Dicroidium* within mud beds of the Lashly Fm., so to attribute the members A (including its base) and B in Allan Hills to the Middle Triassic (late Anisian to Ladinian) of the *Dicroidium odontopteroides* Zone of (Retallack, 1977), as confirmed by (Gabites, 1985) and (Taylor et al., 1990). Macroflora content allowed also the attribution of the Member C of Allan Hills to the Late Triassic (Taylor et al., 1990). (Helby and McElroy, 1968) recorded a pollen assemblage of late Middle Triassic age for the Lashly Fm. outcropping at Kennar Valley in SVL.

Triassic succession has been barren of vertebrates, instead occurring in Central TAM (Retallack and Alonso-Zarza, 1998).

2. Materials and Methods

A total of 95 samples, collected during the XXVIII-XXX-XXI Antarctica Italian Expedition, were worked at the University of Siena, at the "Marleni Marques Toigo Palynology Laboratory" – UFRGS Porto Alegre, at the laboratory of palynology of the University of Perugia.

The processing of the samples has followed the standard laboratory methods and steps reported below and in fig. 18.

For each sample were taken 20 gr crushed portions with a grained between 3-5 mm. These were tested with HCl 37%; just the 10% of the samples had a reaction. These were put in 100 ml of HCl 37% for two hours. After that was added 1 l H_2O for rinse; a total of 3 rinse has been made at 8 hours distance at least.

After that all the samples were placed in HF 40% for 24 hours, then three rinses again with 1 liter of filtered water each time.

When the samples have a pH neutral, were put in HCl 37% for 2 hours then three rinses again as before.

The samples after that were sieved for to take a granulometry between 20 μm and 250μm.

For each sample was taken just the organic part and tried to let in the sieve the mineral part rounding the sieve.

Just a little part of the organic part was put on the cover glass and let dry for 5 minutes at 50°C, after that it was added a little bit of glue and the glass slide and cover with the cover glass where there are the organic matter.

For each sample were mounted 2 slides and on each slide were counted 300 points, for the palynofacies analysis, dividing that in four main organic components, as to follow:

Vitrinite is one of the primary components of coal and most sedimentary kerogens. Chemically It is composed of polymers, cellulose and lignin. Vitrinite may have a shiny appearance, vitreous (like a glass). It is derived from cell-wall material or woody tissue of the plants.

PM1- Brown to dark brown, equidimensional or lath-shaped particles, with or without structures, they most include material derived from partial oxidation of cortex, stem and roots tissue.

PM2- More translucent phytoclasts consisting of brown to orange, usually structured particles. They are composed of leaf, stem, cortex, and roots tissues. Here the original cellular structures are visible, different of PM1.

Cutinite (PM3) is generally translucent-yellow to brown. It is formed by cuticles (leaf epidermal tissue), that are extra-cellular layers covering the epidermis of higher land plants, characterized by unalerted cellular structure and by the presence of stomata or palisade parenchyma, with visible structures. Leaf debris can be altered and degraded very fast during transportation so it cannot be found in a distal environment.

Inertinite (PM4) is oxidized organic material or fossilized charcoal. It could represent a record of paleo wildfires or indicate oxidation due to atmospheric exposure or fungal decomposition during deposition. Inertinite is a common maceral in most type of coal. Inertinite is a maceral group that comprises maceral group reflectance in low and medium rank coals; inertinite is also characterised by absence or lower fluorescence. These last two types have different hydrodynamic behaviour: The lath-shaped PM4 can be transported for long distance.

Sporomorphs with the subdivision of spores and pollen, and the pollen in mono and bisaccate (the last one was furtherly subdivided in striate and non-striate).

Amorphous organic matter (AOM) The major portion of organic matter in source rock sediments is in the form of amorphous kerogen (amorphinite). Characterization of amorphous organic matter (AOM) is a fundamental factor in source rock evaluation trough the microscope, and in the reconstruction of the conditions of sedimentation. The high values of the AOM point to reducing (dysoxic and anoxic) environments with high preservation potential of organic matter.
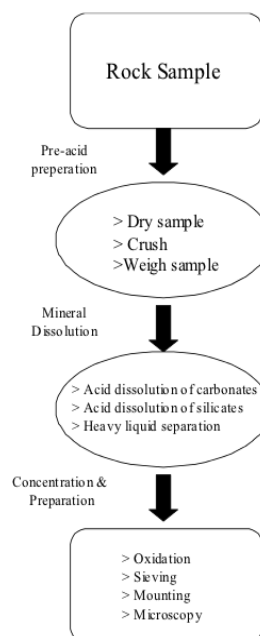
Figure 18 Classic Lab-Technique for palynology sample process

Experimental method

Some of the samples have been processed twice or more times for testing different procedures for the preparing of the slides, so to obtain the best preparation of the samples, compatibly with time savings and simple and well replicable procedure.

In all the different procedures, the solvents were still HF and HCl, but differed timing.

After lots of experimental attempts, the best process has been tested with reduction of timing and number or rinses.

Following this process, the utilization of the centrifuge has been removed, and a reduction to the minimal number of rinses has been obtained, avoiding alterations of the occurring palynomorphs. After numerous experimental attempts, it has been estimated that this procedure increases the productivity of the samples of 20-30%, reaching 70% in some samples.

Here is exposed step by step the lab procedure performed for this study:

- Taken 20 gr. crushed with a grained between 3-5 mm in a plastic Becker
- Add slowly HF, as little as possible, since to the ending of the reaction
- Repeat the same procedure with HCl
- Wait for the ending of the reaction (1-2 hours, depending on the composition of the samples)
- Add water in the becker and wait 8 hours for the deposition, rise and do it again for a total of three times
- Check for the neutral pH of the solution, if it isn't rise it again
- Sieve the solution, under the water. The wide of the sieve depending from the sample, in this case 20-250 μm.
- Take from the sieve only the organic-rich part (darker than the mineral portion) by rotating the sieve
- Take a little portion of the solution for the slide.

3. Results

A total of 95 samples were processed from the Permo-Triassic Victoria Group in Allan Hills, of these 22 result barren, while the other 73 were suitable for the analysis. For each sample were defined the percentages of inertinite, vitrinite, cutinite, amorphous organic matter (AOM), spores, pollen monosaccate and pollen bisaccate (with the subdivision, where possible, in striate and non-striate). The results are then reported for each lithostratigraphic unit, starting from the lowest Permian one.

3.1 Weller Coal Measures Formation

From the Weller Coal Measures Formation were treated 39 samples, of these 10 result barren, while the other 29 were counted for to define the association percentage.

Through the Diagram 1 is clear that from bottom to top of the stratigraphic log, 4 different main associations of palynofacies are recognizable, here summarized.

1- A first association could be described from sample 26-12-15_C22 to sample 26-12-15_C6; this assemblage shows the mayor role defined by the inertinite, with a good amount of sporomorphs and well preserved cutinite (Weller Coal 1- WC1).

2- From sample 26-12-15_C5 to sample 28-1-15_C19, the palynofacies is totally different, quite entirely composed by inertinite, AOM and barren of sporomorphs. Moreover, the inertinite founded here, differently by the WC1, is totally long-shaped (WC2).

3- From 28-1-15_C20 to 24-1-15_C3 a few palynomorphs are recognizable, even if in poor quantity (WC3).

4- From 28-1-15_C26 to the top of the Weller Coal Measures Formation all the samples are barren or composed by inertinite (not log-shaped) an/or AOM. None palynomorphs are recognizable here (WC4).

This palynofacies stratigraphic differentiation and distribution suggest us important insights to understand the event that affecting the depositional environments and their change through time.

Each palynomorphs association of the Weller Coal Measures Formation is described as follow, from bottom to top of the stratigraphic succession.
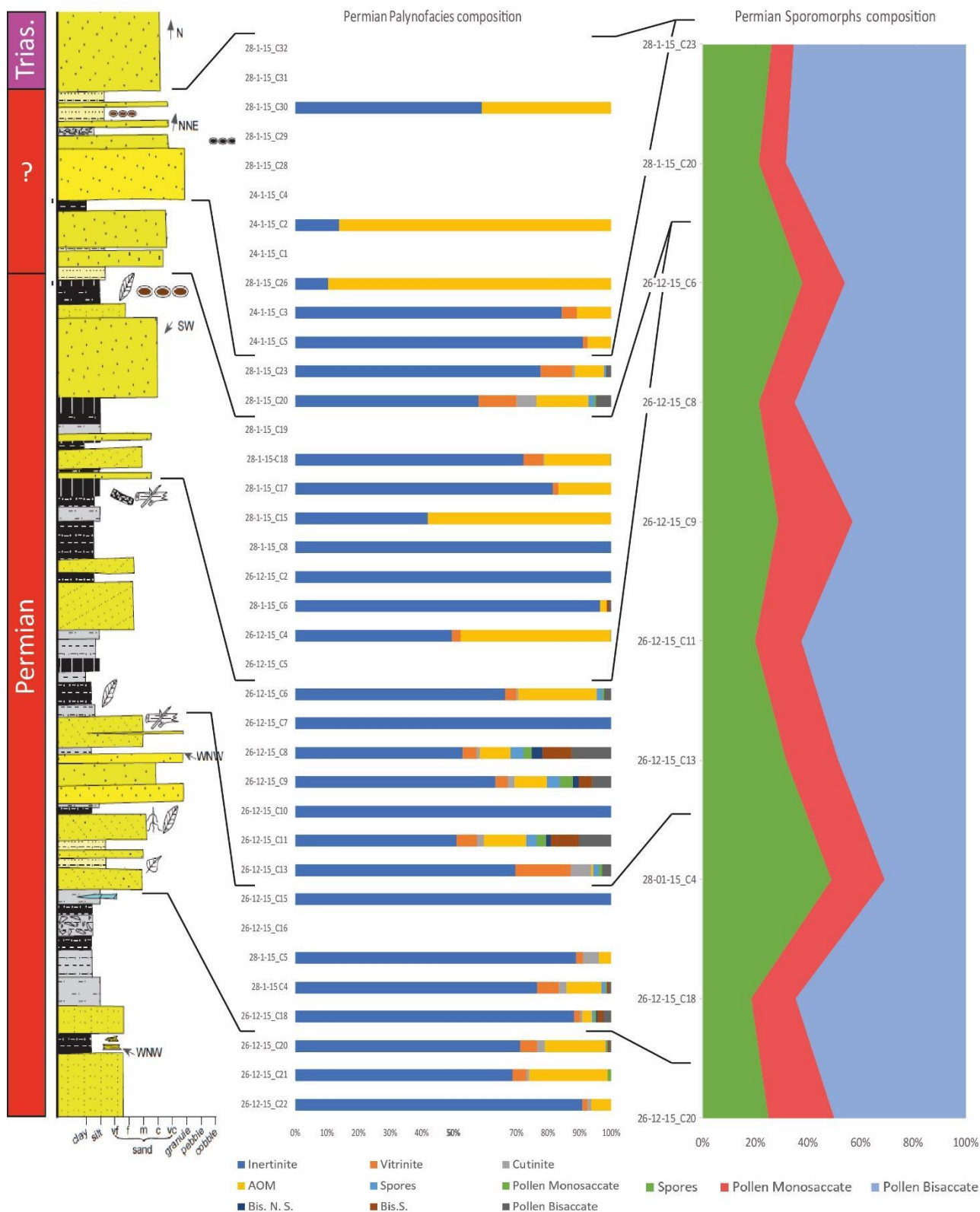
Diagram 1 Palynostratigraphy and sporomorphs composition in Permian Weller Coal Measures Formation of Allan Hills. The stratigraphic log is composite, assembled by several detailed stratigraphic-sedimentological logs (see in Liberato et al., 2016).

3.1.1. Weller Coal 1 (WC1)

The lowermost analysed sample is 26-12-15_C22, with very fine grain size (claystone) and the colour is dark; this sample is a piece of peat, with fragment of coalified wood.

The palynofacies is mainly characterized by inertinite (90,8%), followed by AOM (6,5%), in the order of 1% are also recovered vitrinite and cutinite.

In the sample 22-12-15_C21, the main part of palynomorphs are undeterminable at the genus level due to the poorly preservation; the bisaccate pollen grains are mostly striate-taeniate forms. The inertinite dominates this palynofacies: 68,9% inertinite, 25% AOM, 4,2% vitrinite, 1,1 % sporomorphs and 0,8% cutinite. The only recognizable sporomorphs are: *Polycingulatisporites ?dejerseyi, Protohaploxypinus* sp*., Scheuringipollenites* sp., *Striatipodocarpites fusus.*

The sample 26-12-15_C20 is a very fine sandstone. The palynofacies is composed of: inertinite 71,6 %, AOM 19,3%, vitrinite 5,4%, cutinite 2,4 %, sporomorphs 1,3 %, here are recognizable various species of *Protohaploxypinus* spp.

The sample 26-12-15_C18 came from a coal level with evidence of roots. The palynofacies is dominated by inertinite 90,5% and minor: sporomorphs 3,8%, AOM 3,1%, vitrinite 2,1%, cutinite 0,5%. The sample 26-12-15_C16 and 26-12-15_C15 are barren.

The sample 26-12-15_C13 came from a level of coal. The palynofacies consist of abundant inertinite 70%; followed by: vitrinite 17,3%, cutinite 6,3%, sporomorphs 5,7%, AOM 0,7%

The sporomorphs here occurring are: *Alisporites opii, Cycadopites cimbatus, Cyclogranisporites* sp., *Densoisporites* sp., *Lunatisporites* sp., *Playfordiaspora* sp., *Protohaploxypinus* sp., *Protohaploxypinus suchonensis, Punctatisporites* sp., *Quadrisporites horridus, Reticutalisporites fabaginus, Scheuringipollenites* sp., *Striatipodocarpites* sp..
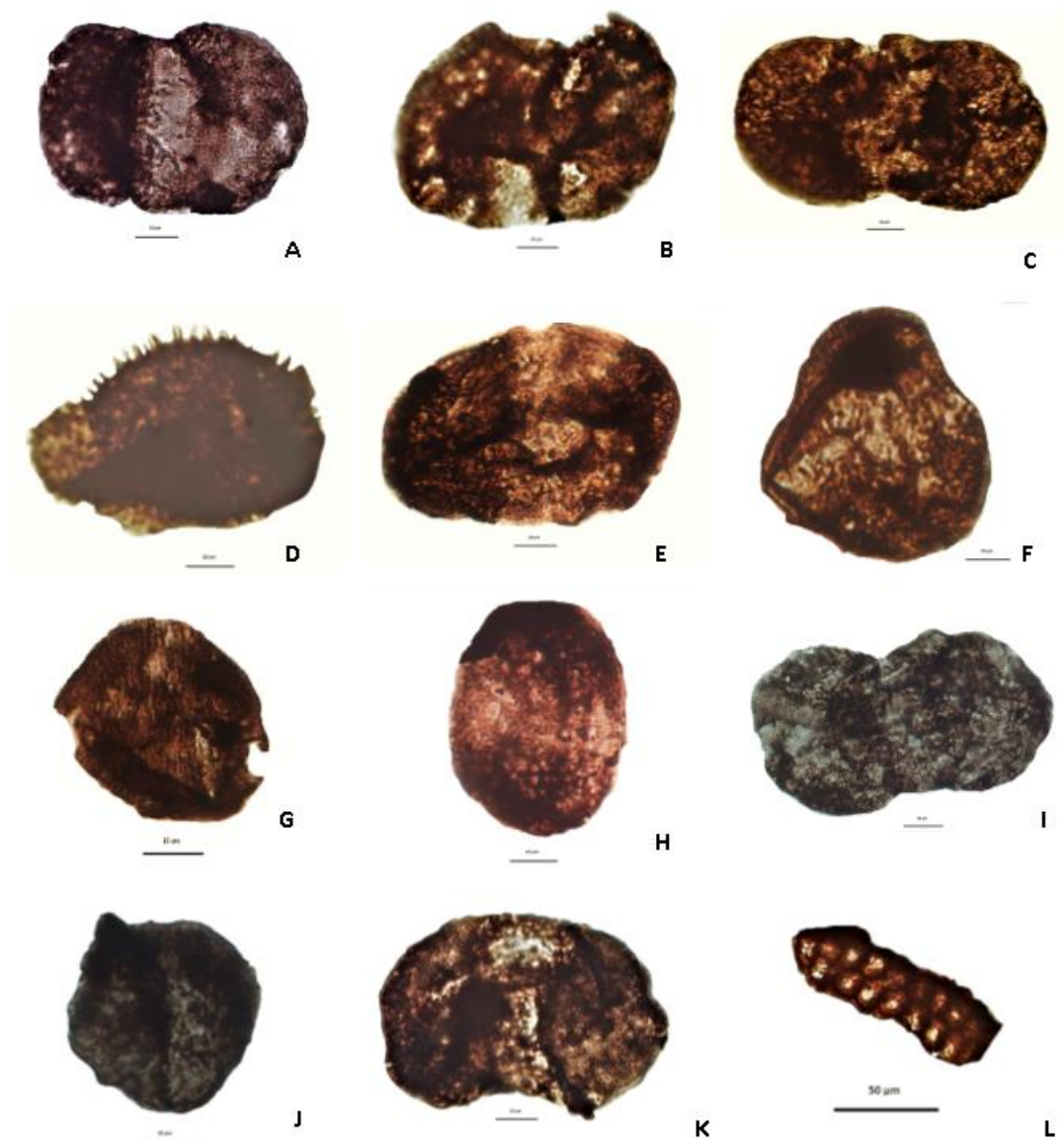
*Plate 1 **Sample 26-12-15_C11 A**: A-G22-3 Alisporites australis; **B**: A-H33-2 Indeterminated monosaccate; **C**: A-H41-1 Alisporites tenuicorpus; **D**: A-V32-3 Carboniferous reworking; **E**: B-F36-2 Lunatisporites sp. cf. pellucidus; **F**: B-J27-2 Aberrant Striomonosaccites ovatus; **G**: B-J27-2b Crucisaccites variosulcatus; **H**: B-N41-4 Lunatisporites sp.; **I**: B-Q34-3 Striatopodocarpites canellatus; **J**: B-Q37-1 Indeterminated monosaccate; **K**: B-R35-1 Lunatisporites sp.; **L**: B-S40-2 Fragment of metaxylem tracheids.*

The sample 26-12-15_C11 is a mudstone contain a good amount of well-preserved palynomorphs; the palynofacies is composed by 61% inertinite, 16,5 % sporomorphs (3,3% spores, 2,9% monosaccate, 10,3% bisaccate), 13,8 % AOM, 6,6% vitrinite and 2,1% cutinite. The recorder sporomorphs are: *Alisporites australis, A. tenuicorpus, Crucisaccites variosulcatus, Lunatisporites* sp.*, Lunatisporites pellucidus, Striatopodocarpites canellatus,* moreover, in this sample an aberrant forms of *Striomonosaccites ovatus* occurs, as well as some reworked sporomorphs (probably of Carboniferous age).
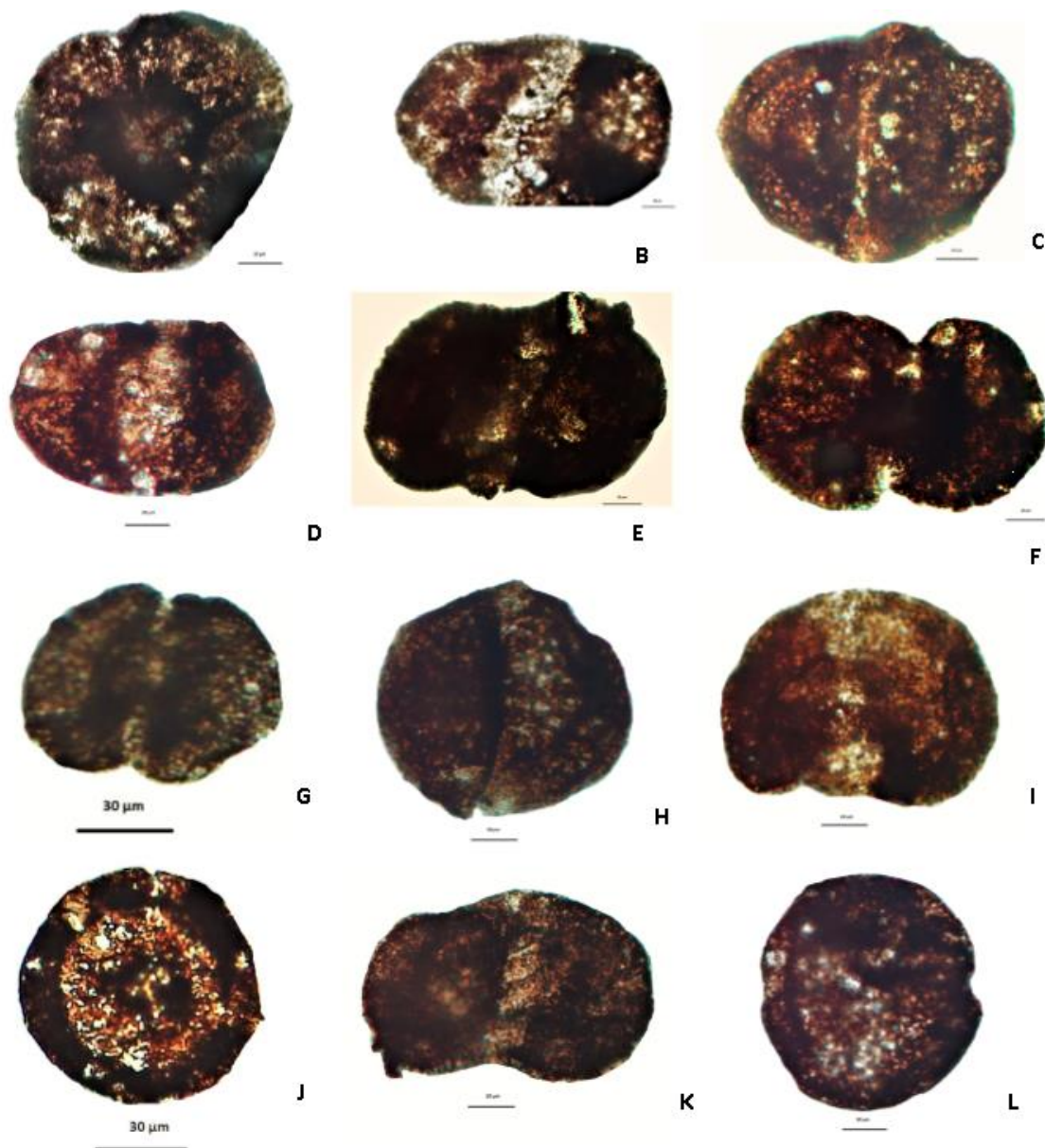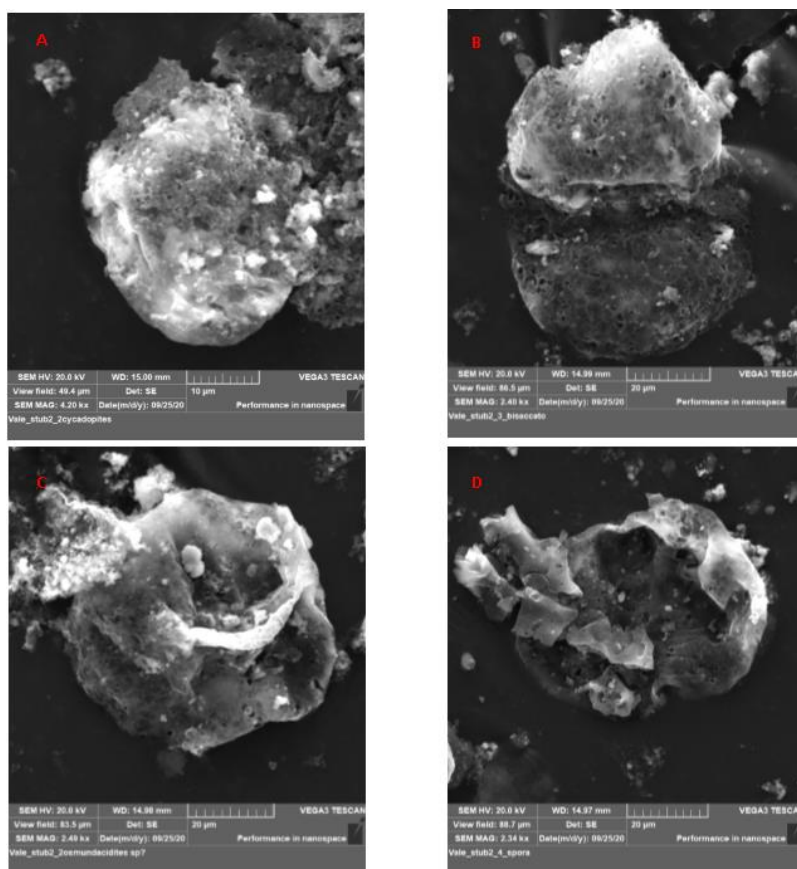
*Plate 2 **Sample 26-12-15_C8**: **A**: A-G 40 Florinites sp.; **B**: A-J33-1 Protohaploxypinus sp. Cf. limpidus; **C**: A-L33-3 Sulcatisporites ovatus; **D**: A-O27-1 Protohaploxypinus microcorpus; **E**: A-O37-4 Indeterminate bisaccate pollen grain; **F**: A-R36 Striatopodocarpites fusus; **G**: A-T34-1 Striatopodocarpites fusus; **H**: A-U46-1 Alisporites sp.; **I**: B-L29 Lunatisporites pellucidus; **J**: B-Q36-1 Barakarites rotates; **K**: B-S27-4 a Lunatisporites noviaulensis; **L**: B-S27-4b Barakarites sp..*

The sample 26-12-15_C10 is a coal and it is composed only by inertinite, while the sample 26 -12-15_C9 is composed by 67,4% inertinite, 11% AOM, 15% sporomorphs (4,3% spores, 4,2% moosaccate, 6,5% bisaccate), 4,4% vitrinite, 2,2 % cutinite. The sample 26-12-15_C8 is a grey mudstone, lying 13 m above the previous one (between them there are a level of sandstone and a level of coal). The palynofacies is composed by: 60,7% inertinite, 21% sporomorphs (14,4 bisaccate, 4,7 spores, 3% monosaccate), 11% AOM, 4,8% vitrinite, 1,3% cutinite. The sporomorphs here recovered are:

Alisporites sp*., Barakarites* sp*., Barakarites rotates, Florinites* sp*., Lunatisporites noviaulensis, Lunatisporites pellucidus, Protohaploxypinus limpidus, Protohaploxypinus microcorpus, Striatopodocarpites fusus, Sulcatisporites ovatus.* Sample 26-12-15_C7 is from a level of coal composed only by inertinite, while sample 26-12-15_C6 is from a very dark mudstone, composed by: 67,8% inertinite, 24% AOM, 4% sporomorphs (2,1% bisaccate, 1,8% spores, 0,7% monosaccate) 3,7% vitrinite, 0,5% cutinite; the identification of the sporomorphs in this samples isn't possible due to the high level of alteration, but it could be notable that the major part of the bisaccate pollens are striate.

Plate 3 SEM image of sample 26-12-15_C8: A: Cycadopites sp*.; B: Indeterminate bisaccate; C: Osmundacidites* spp*.; D: Fragment of spore;*

3.1.2 Weller Coal 2 (WC2)

From the sample 26-12-15_C5 to the sample 28-1-15_C19, the preservation of sporomorphs is very poor, many samples are sterile (but the major part of them are from coarse sandstone), while only in few samples, the organic material is recognizable, often as inertinite. None of these samples are suitable for a palynomorph compositional analysis, although it is performable the analysis of palynofacies.

Sample 28-1-15_C5, that came from a level of coal, is composed by inertinite (88,8%), and subordinately by cutinite 5%, AOM 4% and vitrinite 2,2%; the cutinite and the fragments of metaxylem tracheid here recovered is very well preserved (Fig. 19).

Figure 19: Fragments of metaxylem tracheid in sample 28-1-15_C5

The samples 28-1-15_C6 and 28-1-15_C8 show assemblages dominated by inertinite; the major part of that is long shape inertinite (Fig. 20).
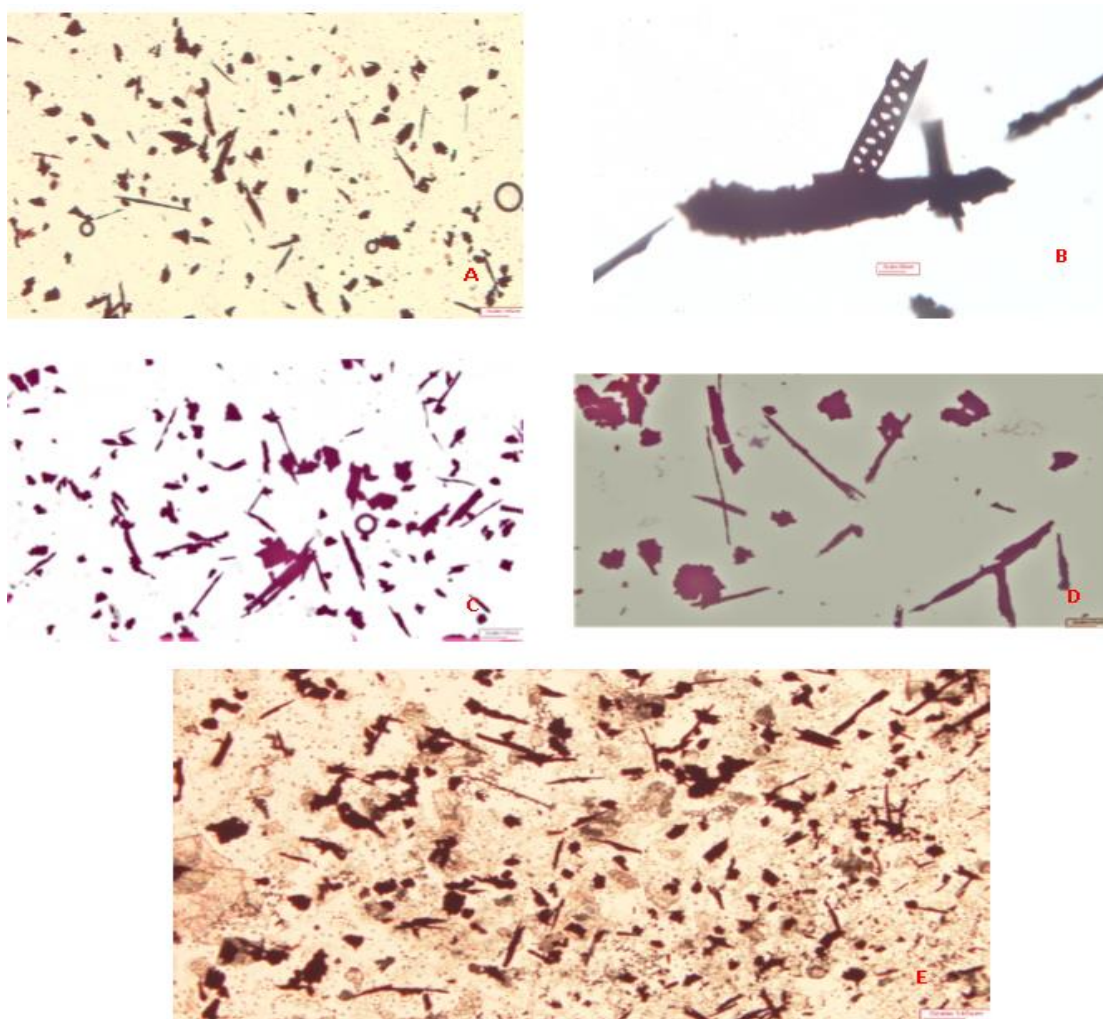
Figure 20: Palynofacies mostly dominated by long shape inertinite, with the presence of equidimensional inertinite– A-B-C Sample n. 28-1-15_C8, D) E) sample n. 28-1-15_C6

3.1.2 Weller Coal 3 (WC3)

The WC3 is characterized by only two samples: 28-1-15_C20 and 28-1-15_C23. The general composition of the palynofacies is close to WC1, but here the *Protohaploxypinus microcorpus* is the most abundant *taxa*.

Sample 28-1-15_C20 is from fine sandstone, mainly composed by inertinite (58%), followed by AOM (16,8%), vitrinite (12%), sporomorphs 7% (bisaccate 4,8%, spores 1,5%, monosaccate 0,7%), cutinite 6,2%, while the sample 28-1-15_C23 is composed by 77,7% inertinite, 10% vitrinite, 9,3% AOM,2,3% sporomorphs, 0,7% cutinite. The sporomorphs here recovered are: *Cycadopites* sp*., Lunatisporites* sp., *Osmundacidites* sp*., Protohaploxypinus* sp*., Protohaploxypinus microcorpus, Scheuringipollenites* sp*., Striatopodocarpites* sp*..*

3.1.2 Weller Coal 4 (WC4)

The WC4 is composed by samples from 28-1-15_C26 to the top of the Weller Coal Measures Formation, and by the samples 24-1-15_C1 to 24-1-15_C5. All the samples overlaining the WC3 are totally sterile, only in some cases, inertinite or AOM are preserved. The major part of these samples are fine to coarse sandstone; this could play a crucial role in the absence of preservation of these samples.

3.2 Feather Sandstone Formation

From the Feather Sandstone Formation and from its upper Fleming Member only 3 samples have been analysed, due to the absence of mudstone/siltstone beds suitable for palynological analysis. Nevertheless, all the 3 samples are lacking of organic material.

The sample 28-a-15_C38, located 17 meters above the sample 28-1-15_C32 is completely sterile; it is from the only recorded fine (mud) level in this formation.

The sample 22-12-15_C15 is located at the boundary with the Fleming Member, and it is also totally sterile.

The only one where is preserved a little portion of organic matter is the sample 22-12-15_C12. It is from dark-grey mudstone with yellow/orange colour alteration. This is from the uppermost mudstone bed of the Mt. Fleming Member, close to the Member A of the Lashly Formation.

This sample is mainly composed by inertinite (95%), followed by vitrinite (2,1%), sporomorphs (2,3%) and AOM (0,6%). In this sample there are just inertinite (the major part of that came from palynomorph, but they are not recognizable).

3.3 Lashly Formation

The Lashly Formation, differently by the uppermost part of the Weller Coal Measures and the Feather Sandstone Fm., shows several samples suitable for palynological analysis. Also in the Lashly Formation, as in the Weller Coal Measures Fm. were possible to establish different palynofacies and sporomorphs assemblage (Diagram 2). In the Lashly Fm. has been recognized five palynofacies named: LF1-LF2-LF3-LF4-LF5.
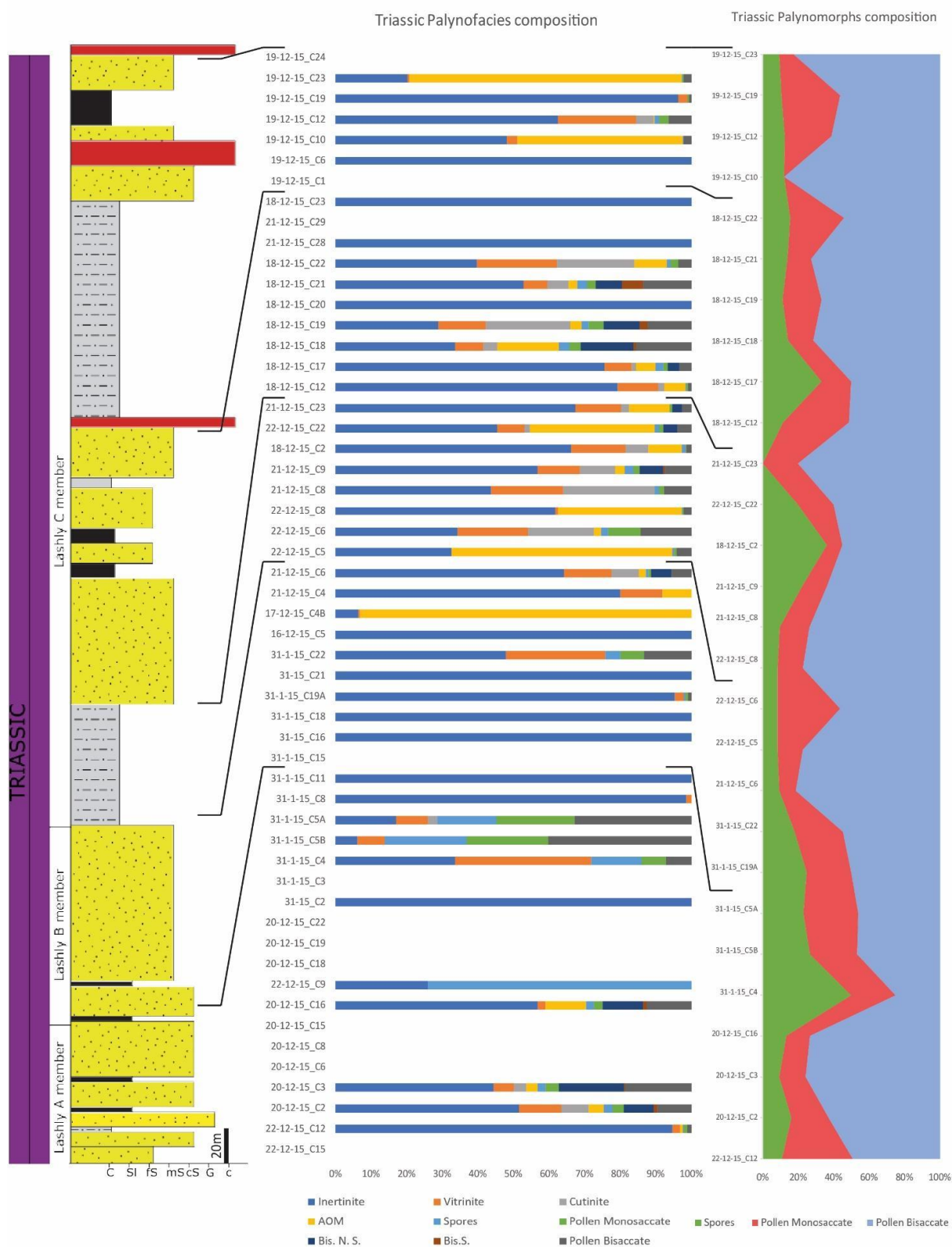
Diagram 2 Palynostratigraphy and sporomorphs distribution in the Triassic Lashly Fm. of Allan Hills. The stratigraphic log is composite, assembled by several detailed stratigraphic-sedimentological logs (see in Liberato et al., 2016).

3.3.1 Lashly Formation 1 (LF1)

The lower part of the Member A of the Lashly Formation reveals two samples, with good fossil content: sample 20-12-15_C2 and sample 20-12-15_ C3. There, the percentages of sporomorphs in the palynofacies are, respectively, 27,3% and 53%. The two samples are both very fine in grain size (claystone). Even if the percentage of spores, monosaccate and bisaccate pollen are variable in the samples, the major part of the assemblage is composed by bisaccate pollen grains (of which mostly not taeniate, not striate), with minor pollen monosaccate and spores. The sample 20-12-15_C2 shows the following palynological composition: 57%inertinite, 17%sporomoprhs (10,5% bisaccate, 3,5% monosaccate and 3% spores), 13% vitrinite, 8,6% cutinite and 4,4 % AOM; while the sample 20-12-15_C3 has the following composition: inertinite 55%, sporomorphs 30% (23% bisaccate, 4,5% monosaccate, 2,5% spores), vitrinite 6,7%, cutiite 4,4%, AOM 3,9%.The assemblages of the two samples are characterized by: *Alisporites (A. australis, A. nuthallensis, A. splendens), Bascanisporites undosus, Playfordiaspora crenulata, Quadrisporites* sp, *Striatopodocarpites* sp*., Vesicaspora wilsonii.* Moreover, these two samples revealed a good amount of cutinite fragments, sometimes well preserved.
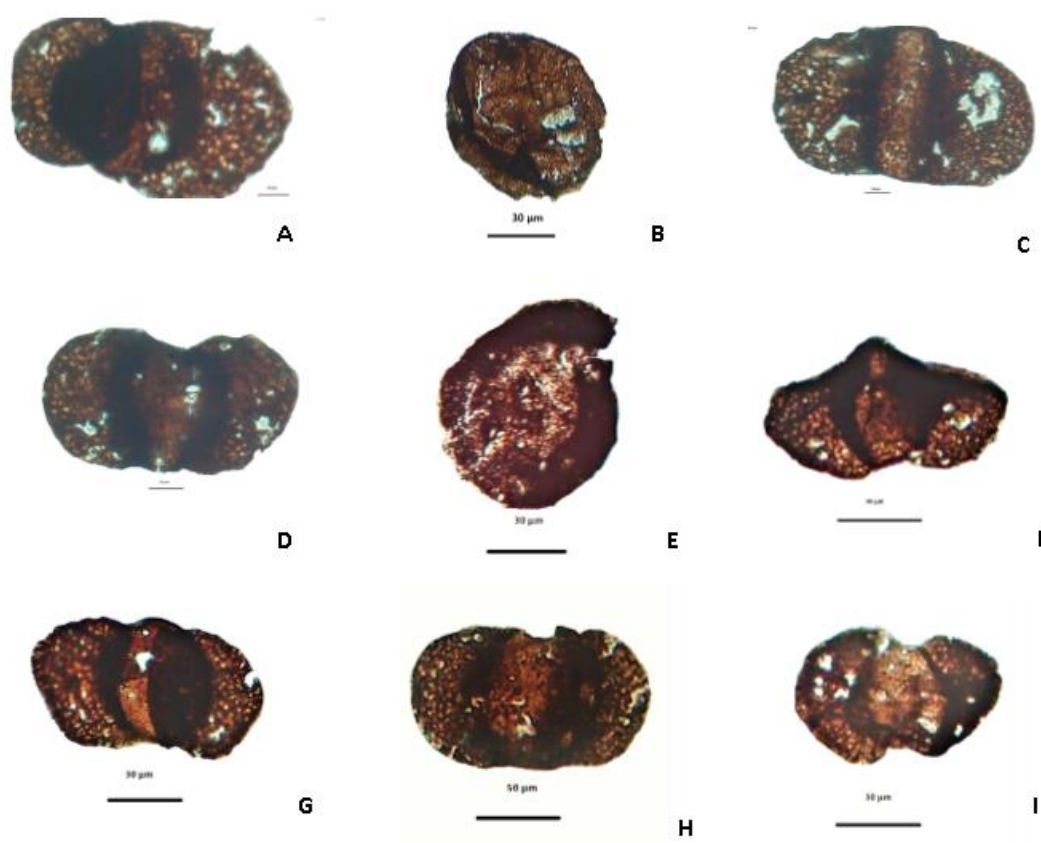

*Plate 4 Sample **20-12-15_C2** A, C, D, F, G, H, I: Alisporites spp.; B. sp. Ind.; E.? Barakarites rotatus.*
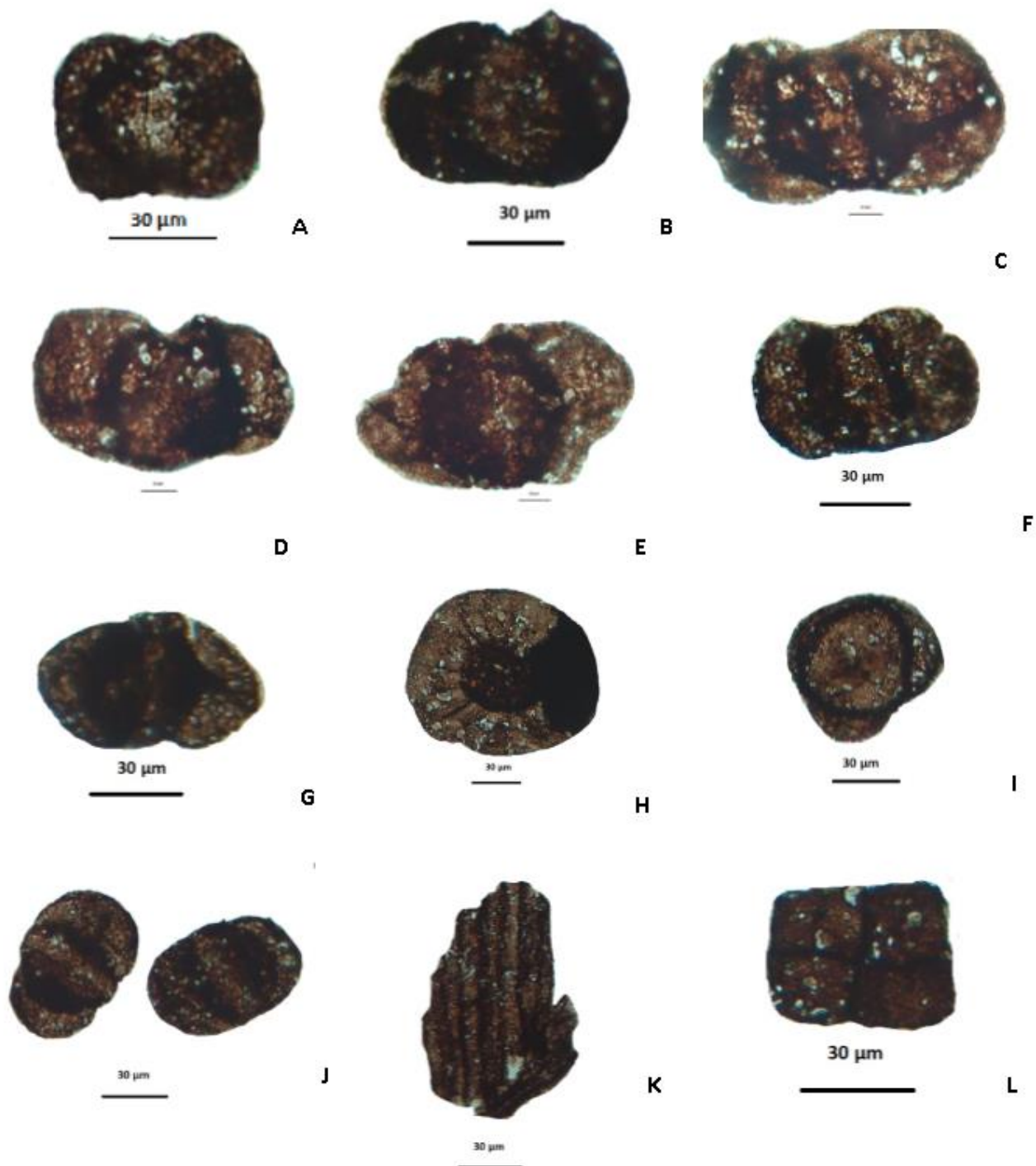
*Plate 5 **Sample 20-12-15_C3: A**: Striatopodocarpites sp.? (A-M45-1); **B**: Alisporites nuthallensis (A-R29-2); **C**: Alisporites australis (A-R30-2); **D**: Alisporites nuthallensis (A-T31-3); **E**: Vesicaspora wilsonii (A-T36-2); **F**: Alisporites splendens (A-T40-2); **G**: Alisporites australis (B-X33-2); **H**: Playfordiaspora crenulata (B-R30); **I**: Bascanisporites undosus (B-N42-1); **J**: Alisporites spp.; **K**: Cutinite fragment; **L**: Quadrisporites sp.?.*

3.3.2 Lashly Formation 2 (LF2)

The samples from the middle-upper part of the Member A of the Lashly Formation are sterile or poor in organic material. Particularly, the sample 22-12-15_C9, from the middle part of the Member A, is only composed by inertinite (26%), AOM (73%) and fungal/algae spores (1%). This kind of spores are uncommon, and they probably derived from hypogeum fungal (although the uncommon forms, the organic nature of these is confirmed by the chemical composition analysed by SEM-EDS, excluding a non-organic origin). The different forms of the spores are probably related to different maturity stage of the same species.
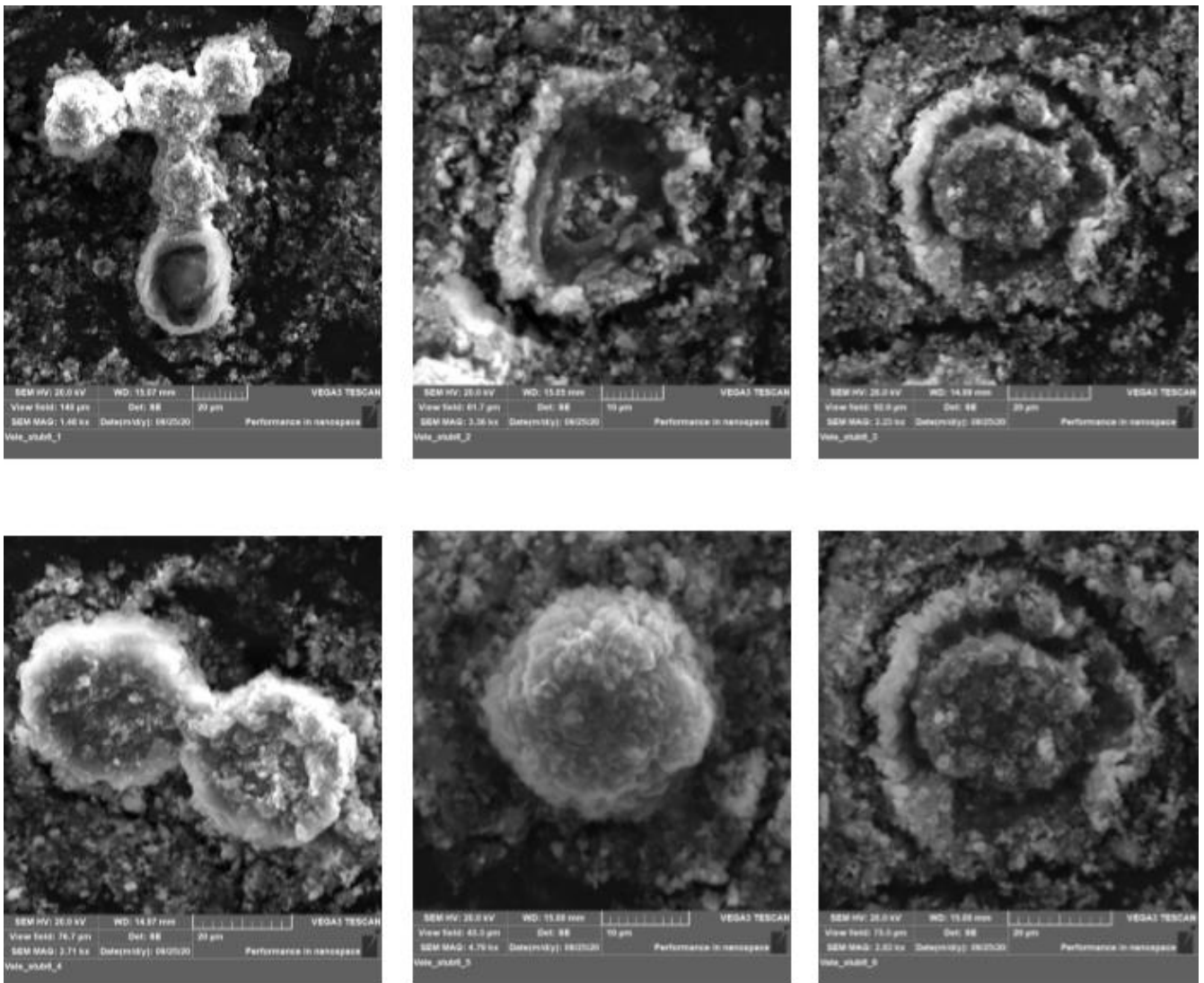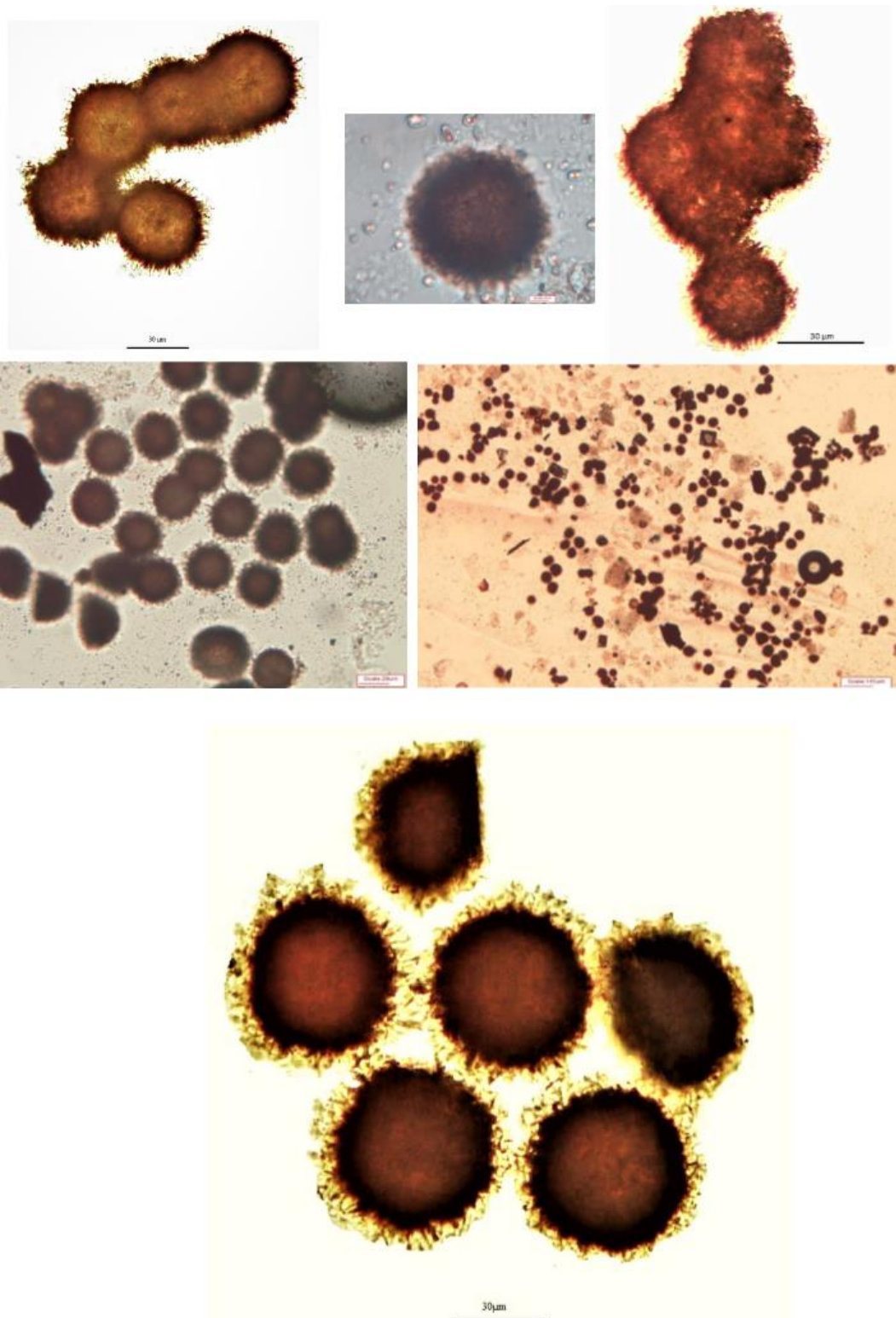

Plate 6 SEM images of spores in the sample 22-12-15_C9

Plate 7 Fungal spores from the sample 22-12-15_C9

3.3.3 Lashly Formation 3 (LF3)

At the boundary between the Member A and the Member B of the Lashly Formation the samples 31-1-15_C5 and b show a good fossil content. These samples are from grey mudstone of Lashly Formation Member A., is divided in two different samples: A and B.

The sample 31-1-15_C5A shows the following composition: 33,7% inertinite, 38,1% vitrinite, AOM 14,1%, sporomorphs 14,1% (7% spores and 7,1% bisaccate)

The sample 31-1-15_C5B has a much higher sporomorphs content that reach 63,3% (with the bisaccate 40,3% and spores 23%), followed by AOM (23%), vitrinite (7,6%) and inertinite (6,1%).
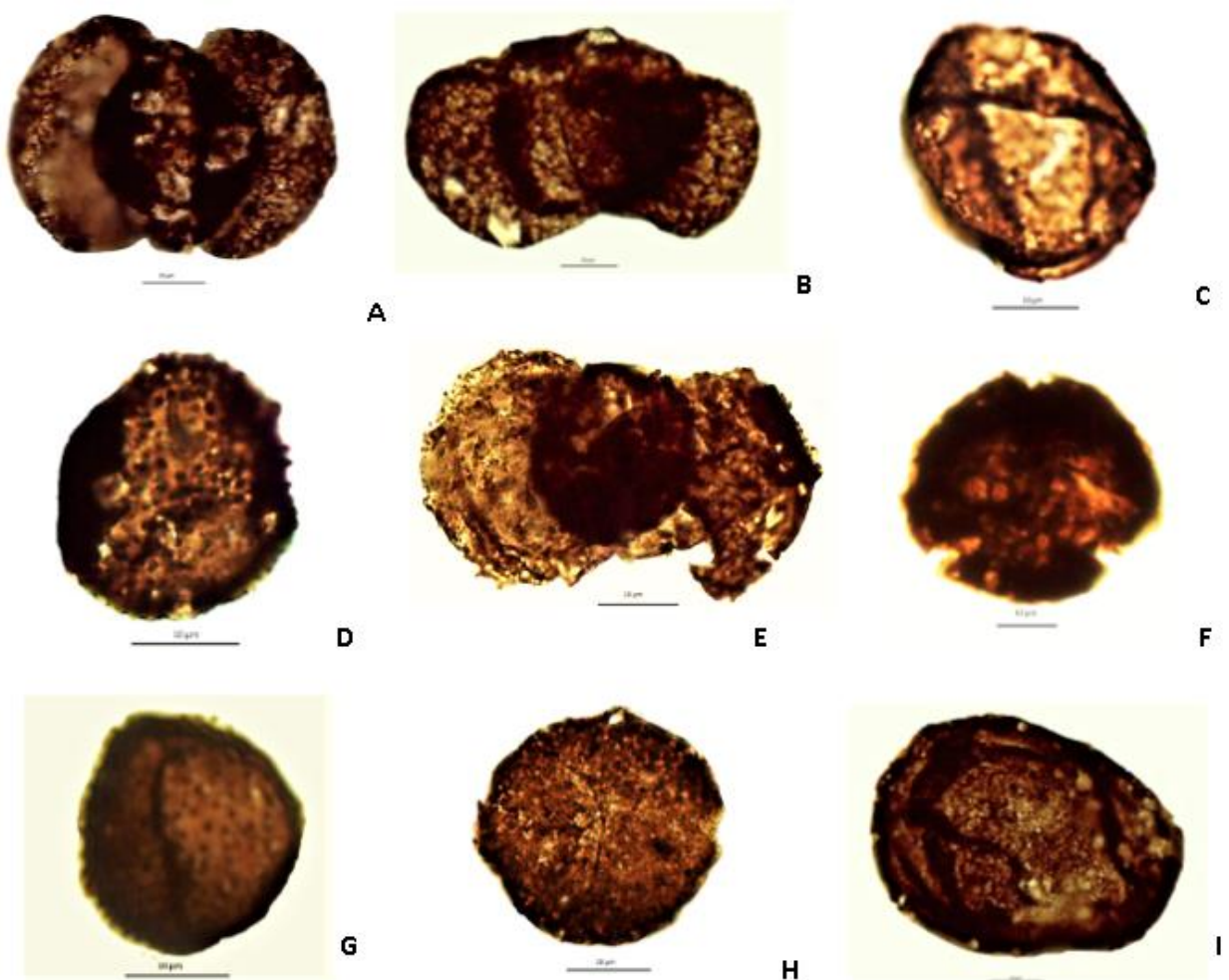
Plate 8: Sample 31-1-15_A, E: Striatopodocarpites sp.; B: Alisporites sp.; H: Alisporites ovatus; C, D, F, G, I: indeterminate forms.
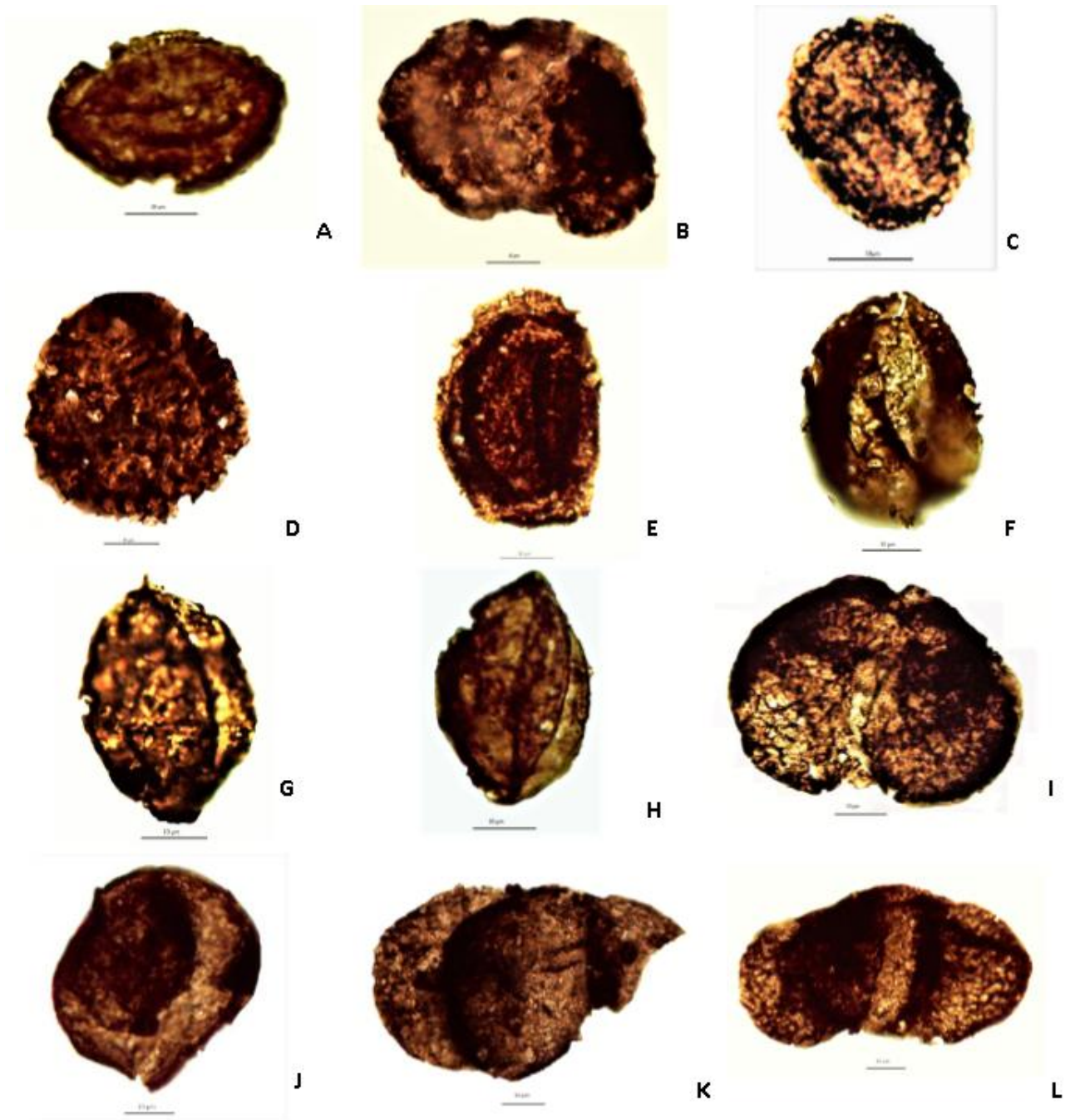
*Plate 9 **Sample 31-1-15_C5b:** **A**: Aratisporites sp. (92-5/38); **B**: Alisporites landianus (93-5/28); **C**: Lunbladispora sp. (93-5/36); **D**: Kraeuselisporites apiculatus (94-1/36); **E**: Aratisporites sp. (94-4/33); **F**: Guttatisporites sp. (94-8/36); **G**: Ephedripites sp.(94-6/33); **H**: Ephedripites sp. (94-36/5); **I**: Alisporites australis (95-3/32); **J**: indeterminate (95-35/8); **K**: Alisporites sp. (96-6/31); **L**: Alisporites nuthallensis (96-5/25).*

Many samples from the Member B of the Lashly Fm. are sterile or with poor preserved organic material, also due to the high sand/mud ratio and the scarcity of mudstone/siltstone beds. However, the sample 19-12-15_C29, from the lower part of the Member B of the Lashly Fm., shows some preserved sporomorphs, as *Alisporites* sp. and *Cycadopites* sp., as well as some associations of spores.
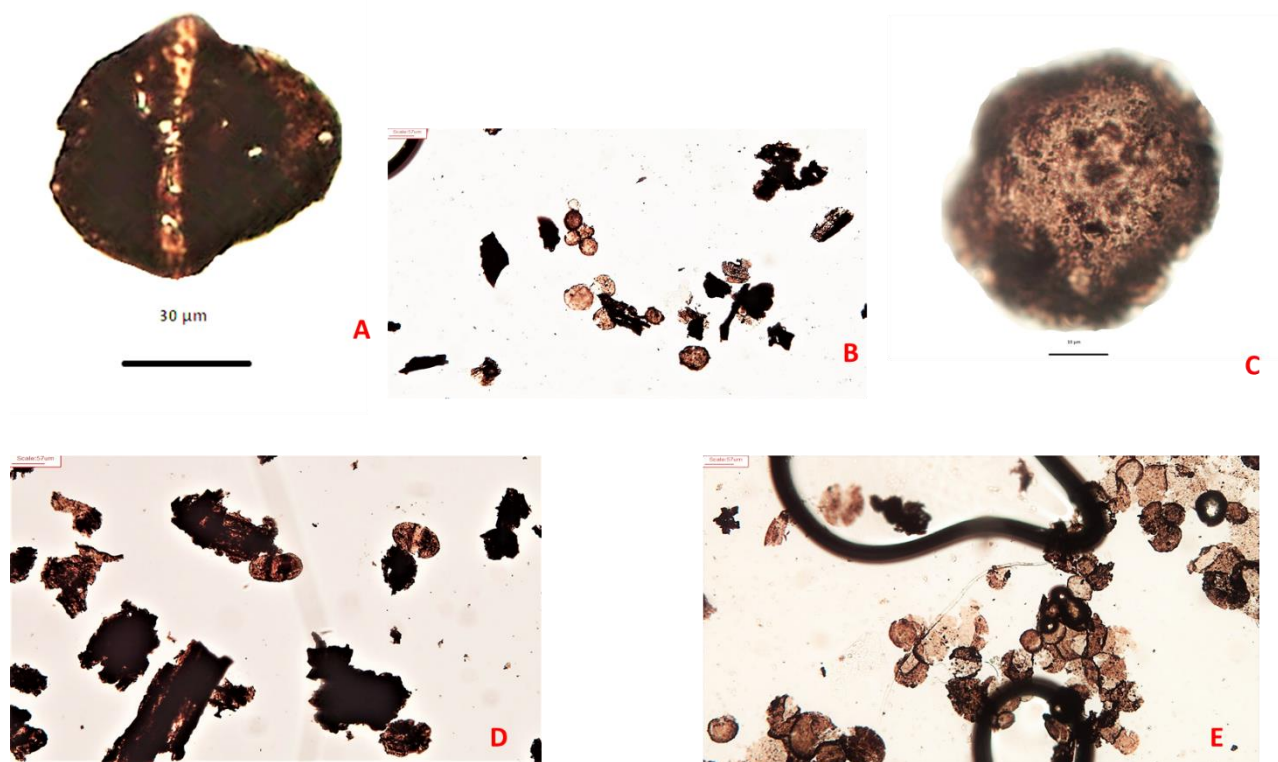
Figure 20 Palynofacies association of sample 19-12-15_C29; presence of Alisporites spp. (A-D) and spores associations (B-C-E)

The sample 31-1-15_C22 shows preserved sporomorphs as *Cycadopites* spp. and *Alisporites* spp..

The sample 21-12-15_C6, from the top part of the Member B, is mainly composed of inertinite (68,2%), vitrinite (13,9%), cutinite (8,1%), sporomorphs (7,4%), of which bisaccate (6%), monosaccate (0,7%), spores (0,7%), AOM 2,4% with the major part of bisaccate sporomorphs referred to *Alisporites* spp.

3.2.4 Lashly Formation 4 (LF4)

The deposits of the Member C of the Lashly Formation show an average of the grain size less than the deposits of the belowlying Member B, due to the occurrence of frequent alternances of mudstone and siltstone, coal-rich mudstone and sandstone and the organic material and sporomorphs are more preserved.

From the base of the Member C, the sample 22-12-15_C5, from carbonaceous mudstone with impression and compression of leaves (*Heidiphyllum elongatum)*, provides well-preserved sporomorphs and it shows a not well-identifiable structure, probably to be referred as a fructiferous organ.

The palynofacies is composed by: AOM (62,2%), inertinite (32,5%), sporomorphs 5,3% (bisaccate 4,1 %, monosaccate 0,7 and spores 0,5%). The palynofacies of this sample is characterized by a general dark colour, indeed of that, abound palynomorph are preserved. The percentage of sporomorphs is absolutely dominated by non-taeniate bisaccate pollen grains, the majority referred to *Alisporites* genus, as follow: *Alisporites* spp., *A.australis,* A*. indicus, A. nuthallensis, A. opii, A. ovatus, Apiculatisporites* sp*., Cycadopites cymbatus, Pityosporites* sp. *Protohaploxypinus* sp..
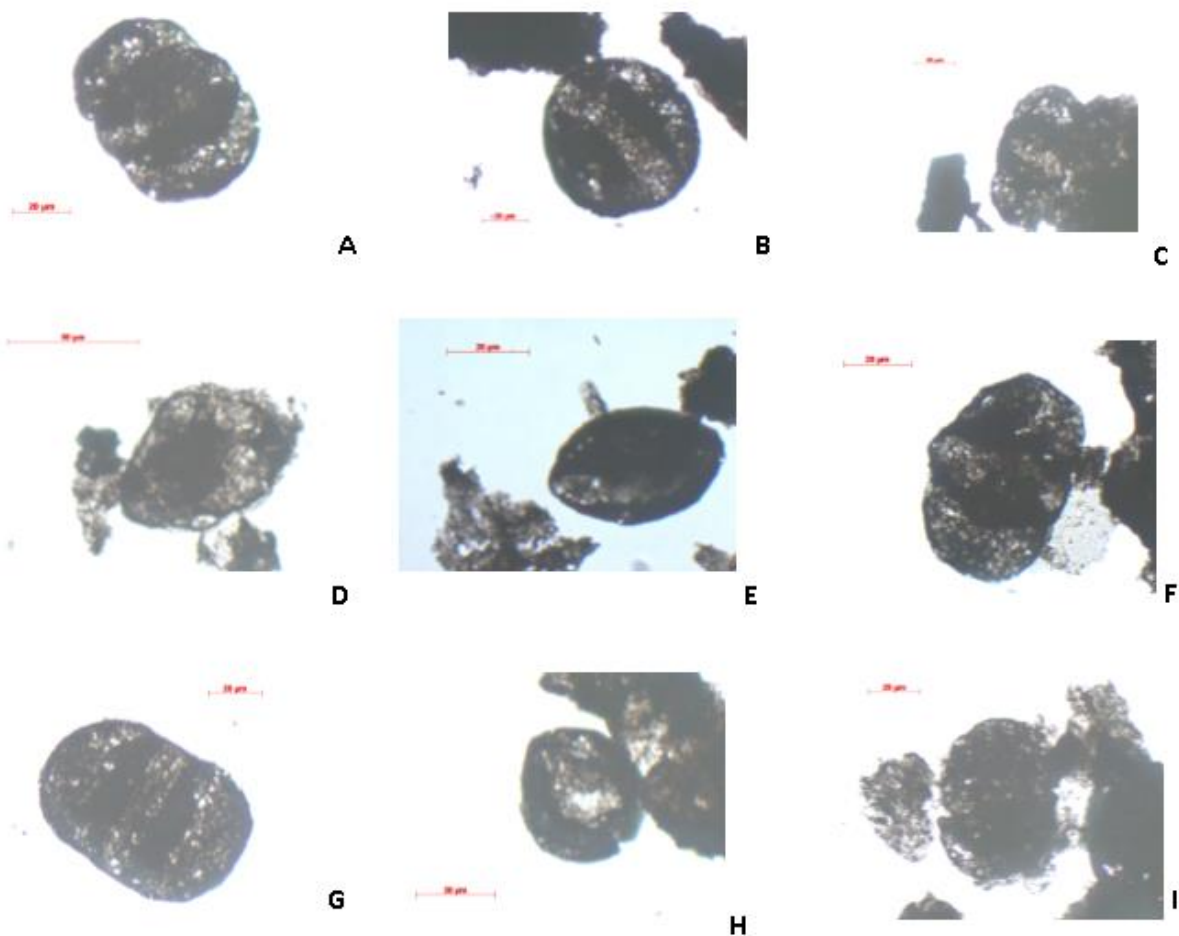
*Plate 10 Sample 22-12-15_C5: **A**: Alisporites indicus (14408-F43); **B**: Alisporites opii (14408-G35-2); **C**: Alisporites australis (14408-L40-4); **D**: Florinites sp. (14408- M43-3); **E**: Cycadopites cymbatus (14408-P23-3); **F**: Alisporites sp. (14408-T45); **G**: Alisporites sp. (14408-V36-1); **H**: Apiculatisporites sp. (14408-V36-1); **I**: Scheuringipollenites sp. (14408-V36-1).*
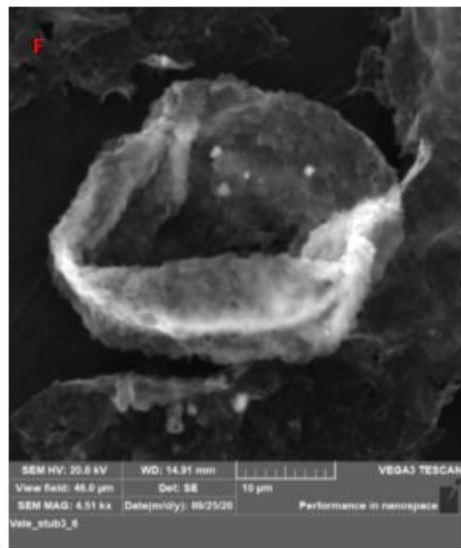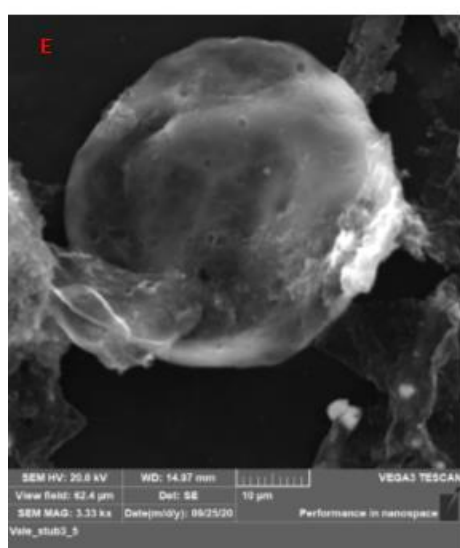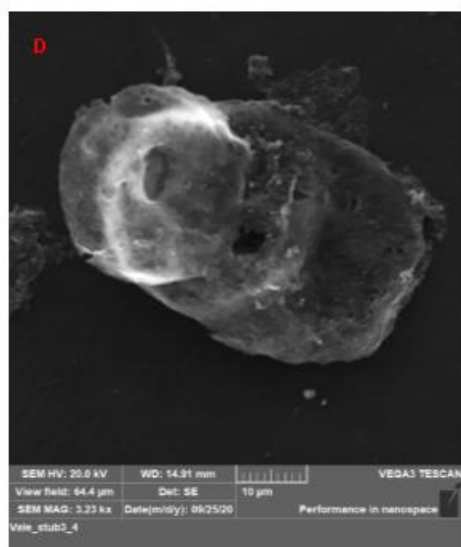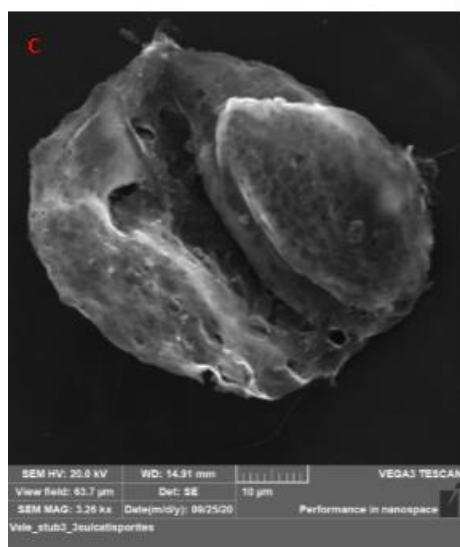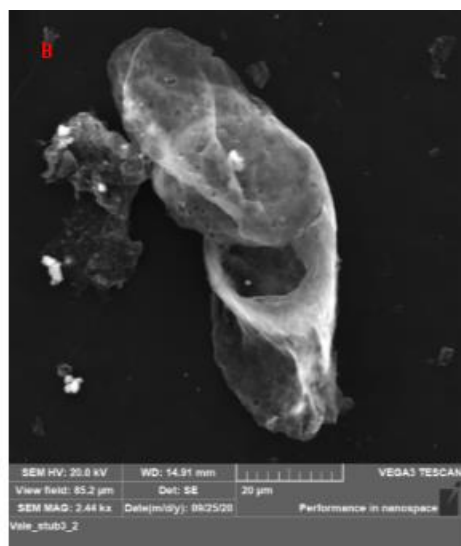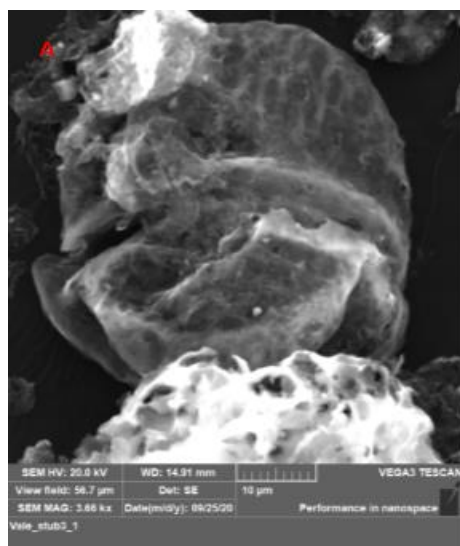
Plate 11 SEM images of Sample 22-12-15_C5
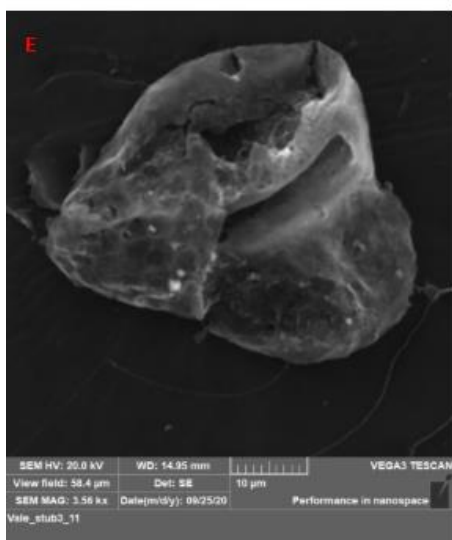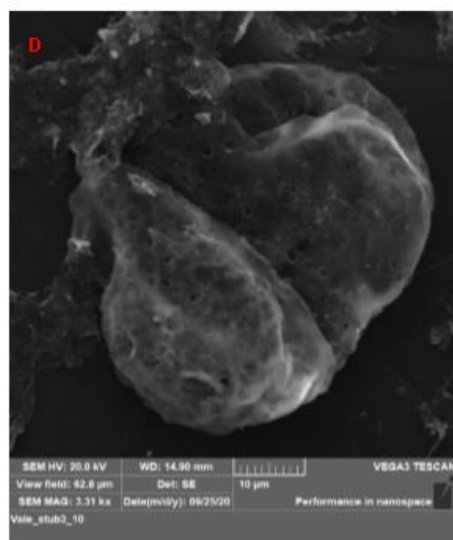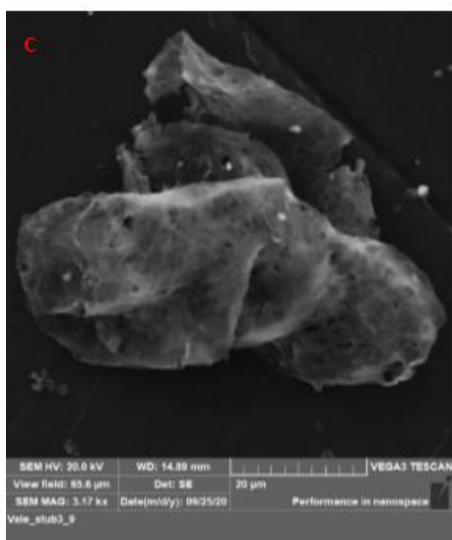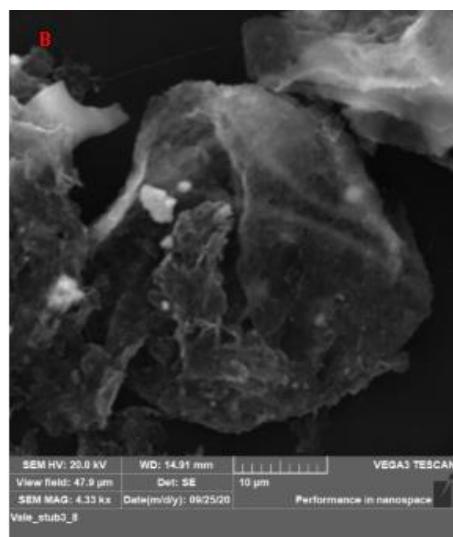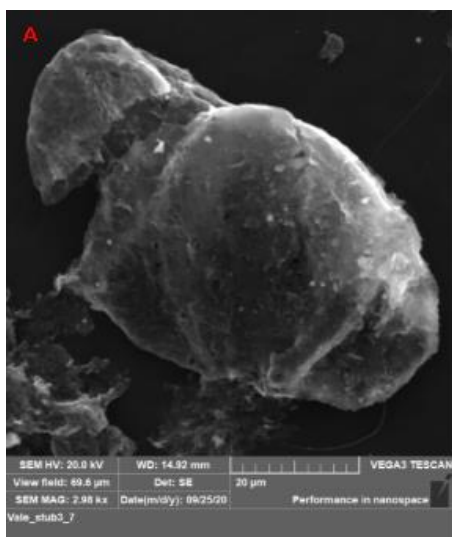
Plate 12 SEM images of sample 22-12-15_C5
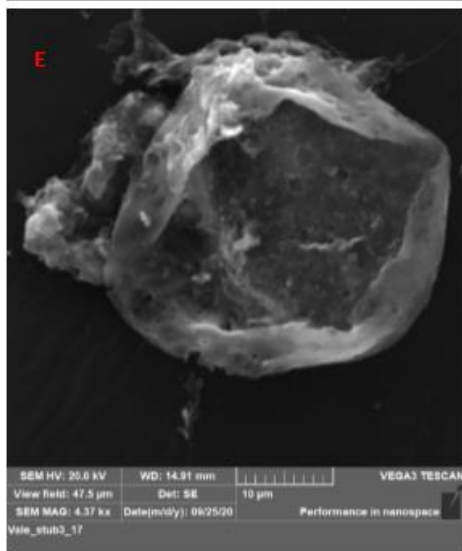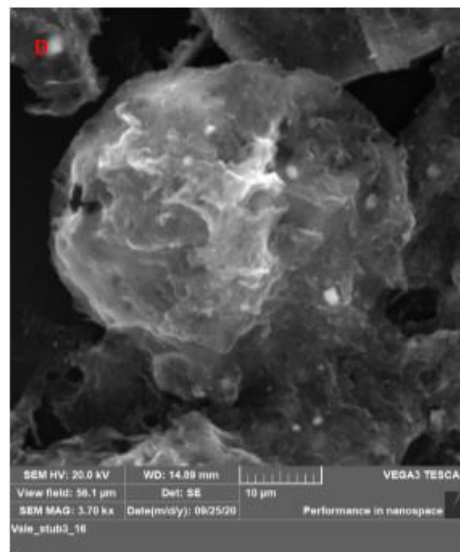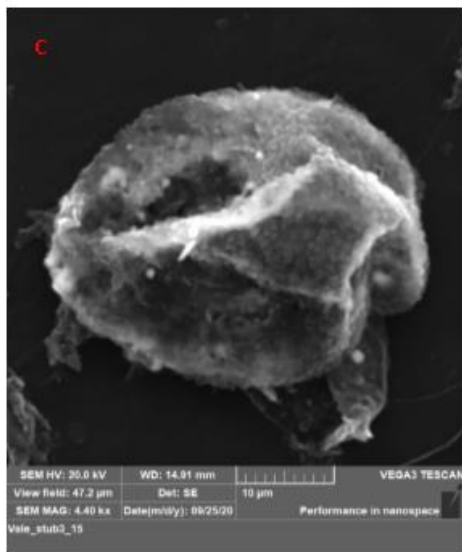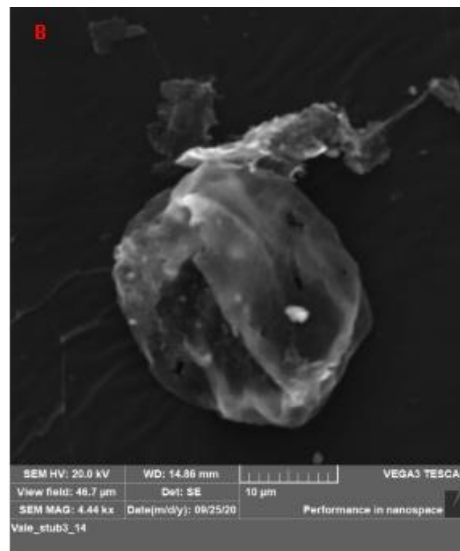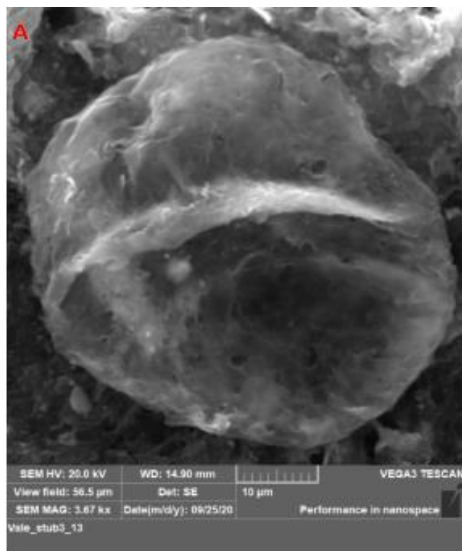
Plate 11: A) Bisaccate, Alisporites sp.;

B) indeterminate; C) Sulcatisporites spp;

D) Monosaccate pollen grain;

E) Polycyngulatisporites spp.

Plate 12: A) Bisaccate; B) Spore with evident mark

trilete; C) Bisaccate; D) Spore; E) Bisaccate;

F) Monosaccate.

Plate 13: Indeterminate pollen grains

Plate 13: SEM images of sample 22-12-15_C5

The sample 22-12-15_C6, located 10 meters above the previous sample (22-12-15_C5), consisting of mudstone with impression-compression of fossil leaf- *Dicroidium*, shows abundant material, with 34% inertinite, 25,5% of sporomorphs (14,3 bisaccate, 9% monosaccate and 2,2% spores), and 19,7 vitrinite, 18,7% cutinite and 2,1% AOM.

The microscopic observation, with polarized light, shows that the colour of this sample is completely different with respect the sample 22-12-15_C5. In fact, the light brown colour indicates a very good preservation, and the sporomorphs can be recognized very well. Instead of the good preservation, a lot of palynomorph are broken, probably due to the transport process (the saccus or the other parts of pollen grains are broken even if well preserved). The major part of the pollen grains is constituted by non-taeniate, non-striate bisaccate (the majority haploxynoid). The sporomorphs here recovered are: *Brevitriletes* sp*., Cycadopites cymbatus, Densoisporites* sp*., Falcisporites* sp*., Marsupipollenites* sp*., Marupipollenites triradiatus, Miscroblasculispora villosa, Osmundacidites* sp*., Playfordispora crenulata, Protohaploxypinus noviaulensis* (probably reworked due to the darker colour), *Straurosaccites* sp*..*

The above sample 21-12-15_C8, mainly composed by inertinite (43,8%), shows a good amount of sporomorphs (10,2% mainly composed by bisaccate 7,5%),
cutinite (25,6%) and vitrinite (20,4%); the main sporomorphs recovered are: *Alisporites* spp., *Horriditriletes* sp. and *Leuckosporites* sp.

The sample 21-12-15_C9 shows a good amount of sporomorphs, that reach 12,4 % (7,9% bisaccate), the inertinite is 61,5%, vitrinite 12,8% and cutinite 10,0%. The sporomorphs here recovered are: *Alisporites* spp., *Alisporites splendens, Calamospora* sp*., Scheuringipollenites ovatus.*

The sample 18-12-15_C2 is characterized by abundant inertinite fragments (also cutinite and vitrinite). But there are also some recognizable palynomorphs, mainly constituted by *Alisporites* spp., but there are also *Marsupipollenites striatus, Marsupipollenites* sp., *Horriditriletes* sp., *Osmundacidite*s sp., *Protohaploxypinus* sp.

The sample 21-12-15_C23 is composed by 70,5% inertinite, 13% vitrinite, 11% AOM, 3,5% sporomorphs (2,7% bisaccate) and 2% cutinite. The sporomorphs here recovered
are: *Alisporites* (*A. nuthallensis,* A. *splendens, A.* spp*.), Distriatites* sp.? and some indeterminate monosaccate

forms; while sample 18-12-15_C17 is mainly composed by inertinite (78%), the sporomorphs are 6,9% (3,5 bisaccate), 8% vitrinite, 7,1% AOM.
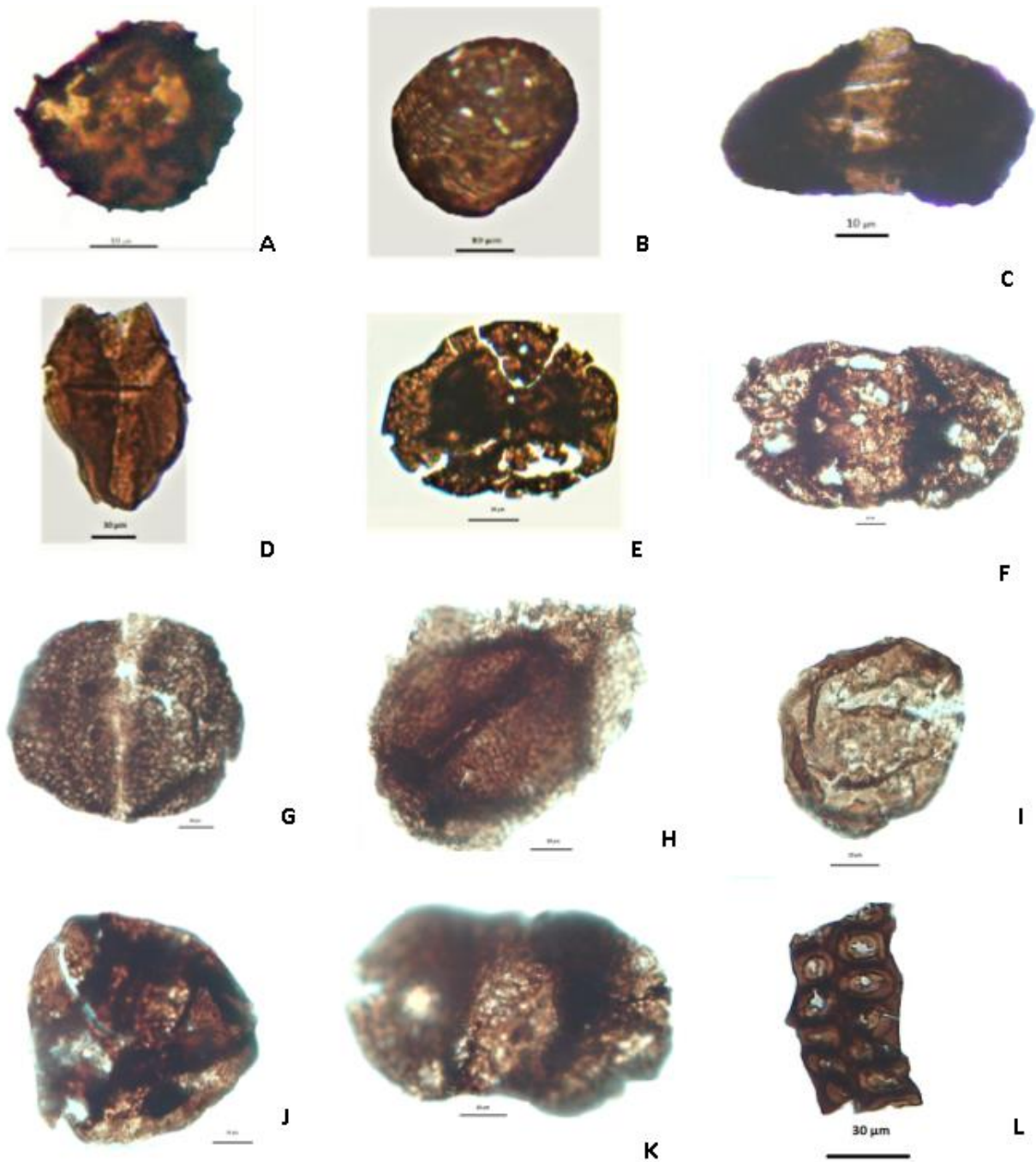
*Plate 14 **A**: Horriditriletes sp. (18-12-15_C2/14424/D25); **B**: Osmundacidites sp. (18-12-15_C2/14424/D25); **C**: Protohaploxypinus sp. (18-12-15_C2/14424/D25); **D**: Marsupipollenits sp. (18-12-15_C2/14424/M29); **E**: Klassopollis meyerianus (18-12-15_C22/14429/K35); **F**: Alisporites splendens (A_V45-2)/21-12-15_C9; **G**: Scheuringipollenites ovatus (B_G41-1)/21-12-15_C9; **H**: Aratisporites sp. (B_L29-3)/21-12-15_C9; **I**: Calamospora sp. (B_Q31)/21-12-15_C9; **J**: indeterminate (B_Q35)/21-12-15_C9; **K**: Alisporites sp. ? (B_Q39-3)/21-12-15_C9; **L**: fragment of metaxylem tracheid 21-12-15_C9.*

The sample 18-12-15_C18 is from a carbonaceous coal and contain 25% sporomorphs (18% bisaccate), 39% inertinite, 22% AOM, 10% vitrinite and 4% cutinite.
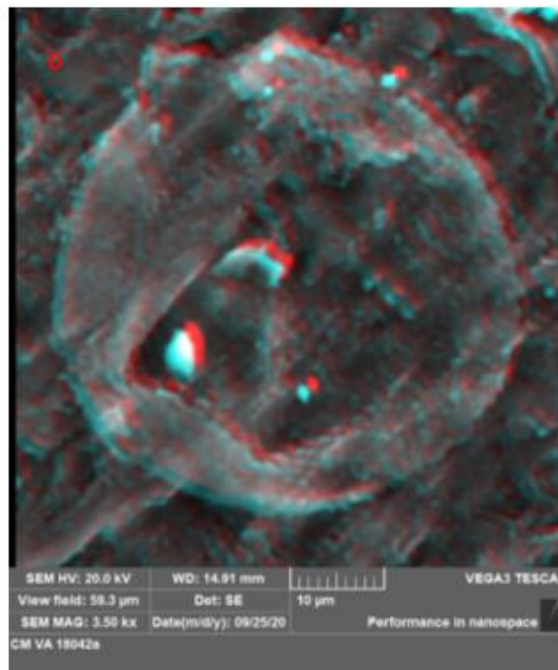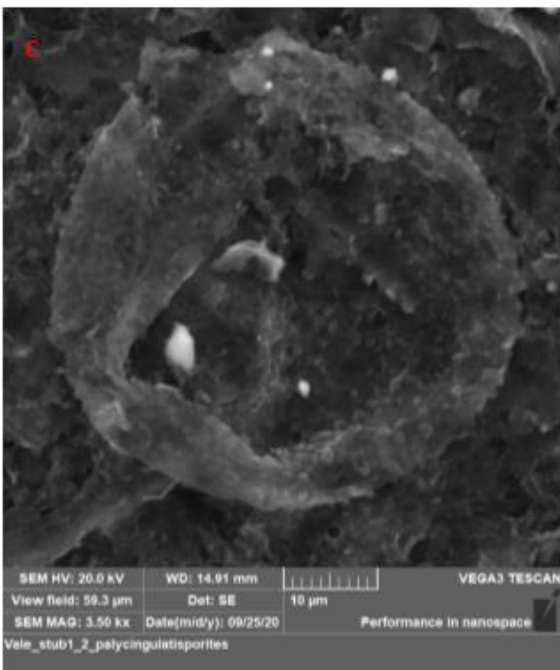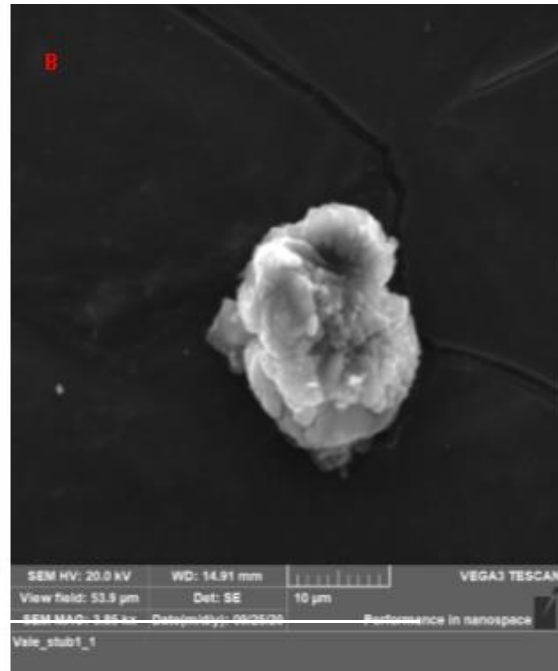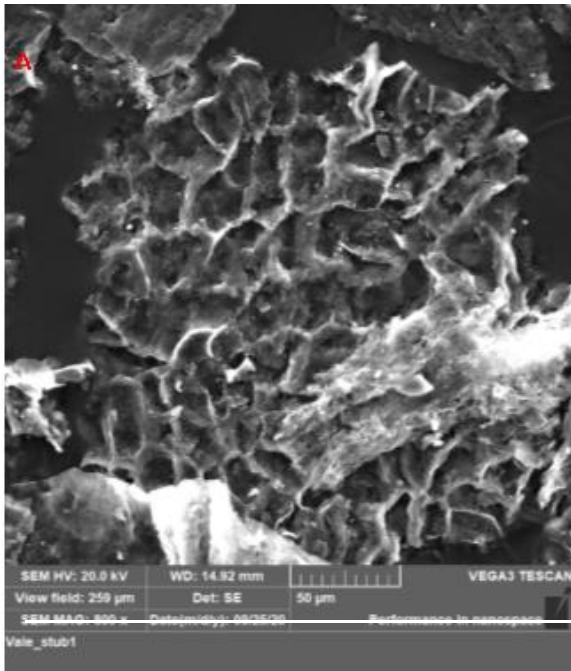
*Plate 15 SEM image of sample 18-12-15_C19: A) cutinite fragment, B) undefined; C) Polycingulatisporites* sp*. D) Polycingulatisporites* sp*., D) 3D image of the form in C.*

In sample 18-12-15_C21 the sporomorphs are abundant (reach 21%), moreover in the sample are preserved some leaves as impression/compression.
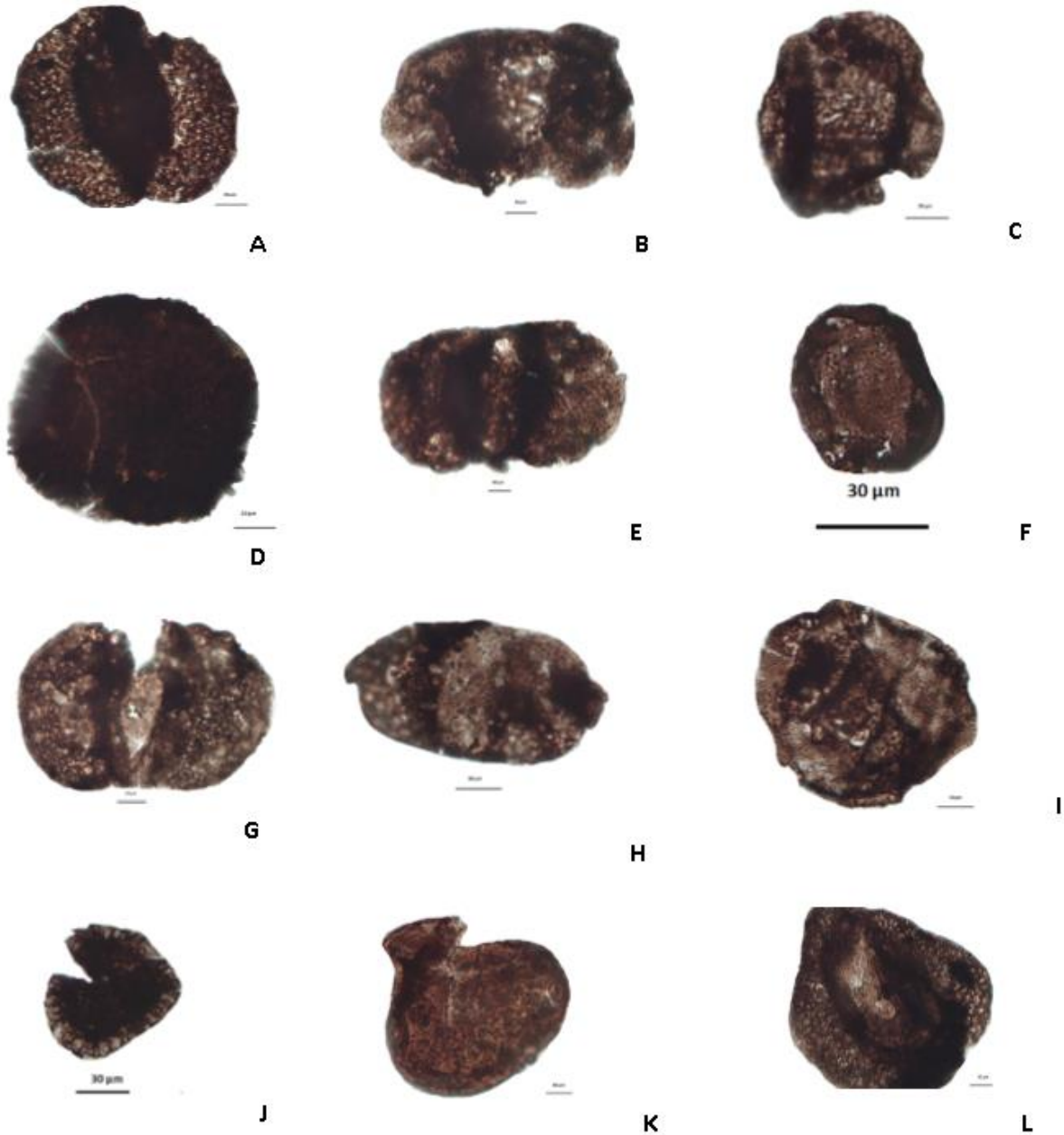
Plate 16 **Sample 18-12-15_C21** *A: Alisporites splendens (AH41-/3);* ***B:*** *Alisporites* spp. *(A-U34/3);* ***C:*** *Aberrant sporomorphs (A-W47/4);* ***D*** *sp. Ind. /(: B-R30);* ***E:*** *Alisporites* spp. *(B-S28);* ***F:*** *sp. Ind. (B-S28-1);* ***G:*** *Alisporites* spp. *(B-X27/2);* ***H:*** *Alisporites tenuicorpus (B-Y26);* ***I:*** *B2 sp. Ind;* ***J:*** *B3 Semiretisporis denmadii;* ***K:*** *B4 sp. Ind.;* ***L:*** *B5 Alisporites* spp..

3.2.5 Lashly Formation 5 (LF5)

Sample 18-12-15_C22 is composed by 40% inertinite, 22,2% vitrinite, 21,8% cutinite, 9% AOM and 7% sporomorphs (3,7% bisaccate), here among the sporomorphs is recognizable the *Classopollis meyerianus*.

The other uppermost samples of the Lashly Fm. Member Care sterile, or the sporomorphs are not recognizable due to the high level of thermal alteration due to the Jurassic sill intrusion. Of these, only sample 19-12-15_C12, are preserved impression and compression of leaves.

	Weller Coal Formations									Lashly Formations																		
	26-12-15_C21	26-12-15_C20	26-12-15_C18	26-12-15_C13	26-12-15_C11	26-12-15_C9	26-12-15_C8	28-1-15_C20	28-1-15_C26	20-12-15_C2	20-12-15_C3	20-12-15_C16	22-12-15_C9	31-1-15_C5B	31-1-15_C22	21-12-15_C6	22-12-15_C5	22-12-15_C6	21-12-15_C8	21-12-15_C9	18-12-15_C2	22-12-15_C22	21-12-15_C23	18-12-15_C17	18-12-15_C18	18-12-15_C19	18-12-15_C21	18-12-15_C22
Polycingulatisporites sp.	x																										x	x
Polycingulatisporites ?dejersii	x																											
Protohaploxypinus sp.	x	x	x	x		x		x									x			x								
Scheuringipollenites sp.	x		x					x									x											
Striatipodocarpites fusus	x						x																					
Cyclogranisporites sp.		x																										
Alisporites opii			x													x	x								x	x	x	
Cycadopites cimbatus			x			x		x						x	x	x	x	x									x	
Densoisporites sp.			x													x		x										
Lunatisporites sp.			x	x			x																					
Playfordiaspora sp.			x																									
Protohaploxypinus suchonensis			x																									
Punctatisporites sp.			x																									
Quadrisporites horridus			x								x																	
Reticulatisporites fabaginus			x																									
Striatipodocarpites sp.			x	x			x				x																	
Alisporites australis			x								A			x			x								x			x
Alisporites tenuicorpus			x																						x		x	x
Crucisaccites variosulcatus			x	x																								
Lunatisporites pellucidus			x			x																						
Striatopodocarpites cancellatus			x																									
Striatopodocarpites ovatus			x																									
Barakarites sp.					x																							
Barakarites rotatus					x	x																						
Cycadopites sp.					x		x										x								x	x		
Florinites sp.					x	x											x											
Alisporistes sp.					x				x		A				A		x			x								
Protohaploxypinus limpidus					x																							
Protohaploxypinus microcorpus					x	x																						
Taeniasporites noviaulensis					x													x										
Sulcatisporites ovatus					x																							
Osmundacidites sp.							x									x		x			x			x			x	
Alisporites nuthallensis											A			x		x							x					x
Alisporites splendens											x									x				x	x	x	x	
Aratisporites fischerii											x	x																
Bascanisporites undosus											x																	
Playfordiaspora crenulata											x							x									x	
Vesicaspora wilsonii											x																	
Aratisporites wollairiensis												x																
Algae/fungal spores													A															
Alisporites landianus														x										x				x
Deltoisporites Sp.														x														
Ephedripites sp.														x														
Guttatisporites sp.														x														
Kraeuselisporites apiculatus														A														
Lunbladispora sp.														x														
Sulcatisporites institatus														x														
Sulcunicysitis cuniculus														x														
Cycadopites follicularis															x													
Brevitrilestes sp.																x		x										
Falcisporites sp.																x		x										
Marsupipollenites sp.																x		x		x								
Marsupipollenites striatus																x				x								
Straurosaccites sp																x		x									x	
Alisporites indicus																x										x	x	
Alisporites ovatus																x											x	
Apiculatisporites sp.																x												
Pityosporites sp.																x												
Aratisporites sp.																		x						x				
Microblasculispora villosa																		x								x		
Horriditriletes sp																			x		x							
Leuckisporites sp																			x									
Scheuringipollenites ovatus																					x			x				
Distriatites sp																							x					
Protohaploxypinus noviaulensis																							x					
Marsupipollenites triradiatus																								x				
Vallatisporites arcuatus																								x			x	
Klassopollis meyeriana																											x	x

Figure 21 Distribution chart of the pollen taxa from determinable samples (x= presence of the sporomorph; A= abundance of the sporomorph)

4. Discussion

4.1 Palynofacies distribution

4.1.1 Weller Coal Measures Formation

In the Weller coal Formation four different palynofacies association could be recognized from bottom upwards: WC 1; WC2; WC3 and WC4.

WC1- It extends for most of the succession of the Weller Coal Measures, it includes some of the coal beds, with trunk remains and leaves impression/compression.

Definitively, this is the most representative portion of the Weller Coal Measures, both as thickness and floristic assemblages (preservation and representativeness). The stratigraphically lower palynofacies of the member C of the Weller Coal Measures Fm. here recorded, shows bisaccate pollen grains represent about 47% of the microflora. Accordingly, Kyle (1977) described a microfloristic assemblage for the Member C of the Weller Coal Measures Fm., where the bisaccate pollen represented a percentage of 47-55% and were prevalently striate ones.

The major component of the microflora is *Protohaploxypinus* spp. (sp., *P. suchonensis),* while *Cycadopites cimbatus, Striatopodocarpites* sp*., Scheuringipollenites* sp. were commonly present. Other forms as *Alisporites opii and Alisporites* spp*., Cyclogranisporites* sp*., Densoisporites sp., Lunatisporites* sp*., Playfordiaspora* sp*., Punctatisporites* sp*., Quadrisporites horridus, Reticutalisporites fabaginus* were also recovered.

WC2- This palynofacies marks the uppermost levels of coals with sandstone beds. It is mainly characterized by the occurrence of long-shape inertinite, while sporomorphs are totally lacking. On the base of the stratigraphic position, close to the PTB, and of the occurrence of long-shape inertinite, this palynofacies could be indicative of the event of paleofire, that some authors (Fielding et al., 2019; Vajda et al., 2020) recently assigned as EPE (end Permian extinction event). These authors described a similar association close to the PTB for the Sydney Basin, particularly involving the uppermost level of coal. The EPE revealed an abrupt change in floristic associations, just before the PTB (Permian Triassic Boundary).

WC3- This palynofacies placed just in the upper part of the Weller Coal Measures Fm. It represents a thin and top portion of the formation, just below the position of the inferred PTB. The palynofacies WC3, similar to the WC1, marks the reappearance of palynomorphs (65-68%), occurring as bisaccate pollen grains, of *taeniate* type, with on evidence the occurrence of *Protohaploxypinus* spp..   The main difference with the

palynofacies WC1 is the occurrence of *Protohaploxypinus microcorpus* instead lacking in WC1. This high amount of bisaccate pollens and the presence of *Protohaploxypinus microcorpus* allows tentatively to ascribe the palynofacies WC3 to the Lopingian Australian Stage 5, analogously to the upper part of the Buckley Formation in the Beardmore Glacier area and in the Central Transantatic Mountains (Kyle and Schopf, 1982). It is worth to note, as better deepened in the next paragraphs, that Kyle and Schopf (1982) ascribed this taxa marker to the Late Permian, while recentrecalibrations of the palynological biozones focused in the Sidney Basin, assign an early Triassic age for the *Protohaploxypinus microcorpus* Zone (Laurie et al., 2016; Fielding et al., 2019).

WC4 – This palynofacies is indicative of the top of the Weller Coal Measures Formation, probably including the PTB. It is totally lacking of sporomorphs and it is represented by inertinite only, to mark the potential PTB. These strata are coincident with a deep change in the fluvial style and a variation of the paleocurrent direction.

4.1.2 Feather Sandstone Fm.

The Feather Sandstone Fm., including its upper member, the Mt. Fleming Mb., is represented by an only palynofacies, characterized by inertinite only, lacking sporomorphs, or if present, in a very poor preservation state, to make them undetectable.

4.1.3 Lashly Formation

The Lashly Formation marks the reappearance of the microflora after the wide gap including the whole Feather Sandstone Fm., with the following palynofacies, from bottom upwards.

LF1- After the unfossiliferous Feather Sandstone Fm. including the Mt. Fleming Member, the first palynofacies recovered is located at the base of the Lashly Fm., in the lower and middle part of its Member A.

It is characterized by: *Alisporites* spp. *(A. australis, A. nuthallensis, A. splendens), Bascanisporites undosus, Quadrisporites* sp*., Playfordiaspora crenulata, Striatopodocarpites* sp*., Vesicaspora wilsonii.*

 Moreover, in these samples a great amount of cutinite fragments, sometimes well preserved, was also recovered, that could indicate a low level of sedimentary transport. These data, merged with the stratigraphic observations, that underline the presence of carbonaceous mudstone and coal, indicate the

presence of a stable depositional environment and low ratio of flux transport.

LF2- The second palynofacies association in the Lashly Fm. has been recognized in the upper part of the Member A. This palynofacies is represented from only two samples and highlights a more stable landscape with the presence of a developed soil. In these two samples: 22-12-15_C9 and 20-12-15_C16 have been recovered fungal spores, probably referred to hypogeum fungal forms.

LF3- From the upper part of the Member A of the Lashly Fm. and the whole Member B a different palynofacies has been recognized. Regarding the lithological features involving this palynofacies, the huge occurrence of sandstones and not frequent mudstones with the total lack of coal, make it not very significant for stratigraphic inferences. The stratigraphic portion relative to the palynofacies LF3 includes the horizons with the transported flow trunks, characterizing the   Allan Hills Fossil Forest, widely treated in next chapters.

 In this palynofacies, as in the palynofacies LF1, many of the pollen grains are composed by non-striate and non taeniate bisaccate forms, but the association is here characterized by high amount of *Alisporites* spp , that in some samples, it reaches the totality of all the sporomorphs. This assemblage is characterized by various species of *Alisporites* (*A. australis, A. indicus,* A. *landianus, A. nuthallensis, A. opii, A. ovatus*), moreover there are also *Densoisporites Sp., Ephedripites sp., Guttatisporites sp., Klausipollenites vestitus, Kraeuselisporites apiculatus, Lunatisporites noviaulensis, Lunblandispora brevicula, Lunblandispora sp., Sulcatisporites institatus, Sulcatisporites sp., Sulcunicysitis cuniculus.*

LF4-   The palynofacies LF 4 include the lower portion of the Member C. By a lithological point of view, this palynofacies is linked with the reappearance of mudstone deposits, and it is similar to LF1 and LF2, as confirmed also by the high presence and good preservation of cutinite fragments. In this assemblage, the major component is formed by non-taeniate, non-striate bisaccate pollen grains, often referred to *Alisporites* spp. (*A. australis, A. indicus, A. nuthallensis, A. opii, A. ovatus, A.* sp*.*) and other *taxa* as: *Apiculatisporites* sp*., Brevitriletes* sp*., Cycadopites cymbatus, Densoisporites* sp*., Falcisporites* sp*., Florinites* sp*., Marsupipollenites triradiatus, Miscroblasculispora villosa, Osmundacidites* sp*., Pityosporites* sp*., Playfordiaspora crenulate, Protohaploxypinus* sp*., Straurosaccites* sp*., Taeniatisporites noviaulensis,*

LF5- This palynofacies, and its sporomorphs content, constraining the upper part of the Member C. It is similar, in the percentage and in the presence of sporomorphs, to the LF4, but from the sample 18-12-15_C22 stratigraphically upwards, the *Classopollis meyerianus* has been recognized. The absolute age based on zircon (Liberato, unpublished PhD Thesis, 2020) constrains the age of this interval to Rhaetian which is concordant with the presence of *C. meyerianus.*

4.2 Bio-chronostratigraphic and paleoenvironmental insights based on palynofacies analysis

With a total of 95 samples analysed in the whole section of Allan Hills, it is possible to reconstruct a quite reliable interpretation of the paleoenvironment during the Permian and the Triassic time. Moreover, it is possible to add new insights about the transition of the flora between Permian and Triassic, overall across the dramatic change of the PTB.

Approaching to the lowest analysed lithostratigraphic unit, which is the Weller Coal Formation, through literature, we could affirm that during the late Permian the environmental conditions were humid and warm, lacking of any glaciers (or they were located just only very close to the pole), even if the Antarctica was in a very high latitude (the area of Allan Hills reached the 82° latitude during the late Permian, according to the model of (Torsvik e Cooks 2017). During this time, the *Glossopteris* flora grow up and it diversified in many different species and was formed by evergreen and deciduoness plants (Gulbranson et al., 2014). The landscape during this time evolved rapidly and the soil showed immature profile (with a maximum of a few hundred years) (Retallack et al., 1996; Gulbranson et al., 2020). In the Early Permian the *Glossopteris flora* were in the upper part of Gondwana and move to the extreme south part just in the Late Permian (reached c.a. 80° latitude).

The Weller Coal Measures Fm. in Southern Victoria Land, has been dated at the Early Permian or Early to earliest Middle Permian on the base of palynostratigraphy by Kyle (1977) and Kyle and Schopf (1982), which recognized the *Protohaploxypinus* zone of the Artinskian correlated with the upper part of the Australian Stage 4, differently by its equivalent in the Central Transantarctic Mountains (Fairchild Fm. and Buckley Fm.), where the Late Permian age has been recorded (Farabee et al., 1990). These data were supported by the recognition of a ferricrete level that Collinson et al. (1994) and Isbell and Cuneo (1996) interpreted, even in absence of a real unconformity, as the possible evidence of a gap with disconformity in the sedimentation involving the whole Late Permian.

Nevertheless, Askin (1995) though confirmed the late Early Permian (or Early to Middle Permian age based on recalibration by Laurie et al., 2016) for the Weller Coal Measures Fm. in SVL, based on the record of *Praecolpatites sinuosus* in the samples from the uppermost part of the formation at Mount Crean, suggests the possibility to have represented the *Praecolpatites* zone and consequently a Late Permian age for such top part of the formation. To follow, Awatar et al., (2014) revealed a sample from the Weller Coal Measures Fm. of Allan Hills, referable on the base of the palynomorph assemblage, to the *Densipollenites magnicorpus*

zone, suggesting a Late Permian (Lopingian) age. Similar data have been very recently obtained by Bomfleur et al., (2020) for the top of the Takrouna Fm. in Northern Victoria Land.

The data obtained in this thesis for the lower part of the studied section of Weller Coal Measures Fm., allow to strengthen this last dating, on the base of a much wider dataset. In fact, the palynomorph assemblage of the here recorded palynofacies WC1, in particular, due to the uncommon occurrence of *Protohaploxypinus microcorpus* and the great amount of bisaccate striate pollen grains, mainly represented by *Protohaploxypinus* spp., suggests a correlation with the APP 5 Zone, that Mantle et al., (2010) moved to the Wuchiapingian (early Lopingian), and then the radiometric recalibration moved again to the late Wuchiapingian-Changsingian (late Lopingian), marking the Late Permian (Laurie et al., 2016; Fielding et al., 2019).

This new data and recalibration, emphasize that the Upper Permian deposits occur also in the SVL, contrarily to whom previously stated, so to modify the paleogeographic and tectonic framework that previously suggested an important stratigraphic lacuna between the Weller Coal Measures Fm. and the above Triassic succession (Barrett, 1981; Barrett et al., 1991; Isbell and Cuneo, 1996). These new bio-chronostratigraphic data are on agree with geochemical, paleopedological, paleontological, sedimentological, physical architecture and bedding attitude emerged, in particular for the Allan Hills succession (Retallack et al., 1996; Retallack and Krull, 1999; Tewari et al., 2015; Liberato et al., 2017; Gulbranson et al., 2020). This necessarily should imply the occurrence of the PTB in the depositional record there, and relative continuity in the sedimentation across the PTB, compatibly with local and minor erosional phases also due to the fluvial depositional environments. Furthermore, the basinal subdivision of the Central TAM and of the Southern Victoria Land, as hypothesized by Collinson et al., (1994), should be reconsidered at the light of the new findings.

Particular focus has to be posed at the top of the Weller Coal Measures Formation, here probably due to the rising of the temperature or to other causes (as the volcanic eruption of the Siberian Traps) in the stratigraphic horizon corresponding to the WC2 palynofacies, a paleofire event could be hypothesized due to the high presence of long shape inertinite in the deposits. This event has been registered also in other areas of the Gondwana as in the Sydney Basin, using similar constraints (Mays et al., 2020; Vajda et al., 2020) and it's known as EPE (end-Permian Extinction event).

After this event the Permian flora changed (palynofacies WC3), but it is still present with many species of *Protohaploxypinus*, particularly with the recovering of abundant pollens assigned to *Protohaploxypinus microcorpus* and other typical Permian pollens and leaves.

The *Protohaploxypinus microcorpus* (APP6) Zone (Price, 1997; Mantle et al., 2010; Metcalfe et al., 2015) and referable informal zones, were for long time, assigned to late Permian age (Kyle, 1977) (Kyle et al., 1982) (Farabee, et al., 1990). But after the recalibration through radiometric methods of the palynostratigraphy by (Laurie et al., 2016), for this zone has been suggested an earliest Triassic age (early Induan) (Fig. 22). Other authors, in recent works (Mays et al., 2020) (Vajda et al., 2020) adopted this new palynostratigraphy zonation and assigned the *Protohaploxypinus microcorpus* Zone to the Early Triassic time and fixed the PTB in the uppermost part of the *Playfordiaspora crenulata* Zone, near the boundary with the *Protohaploxypinus microcorpus* Zone.
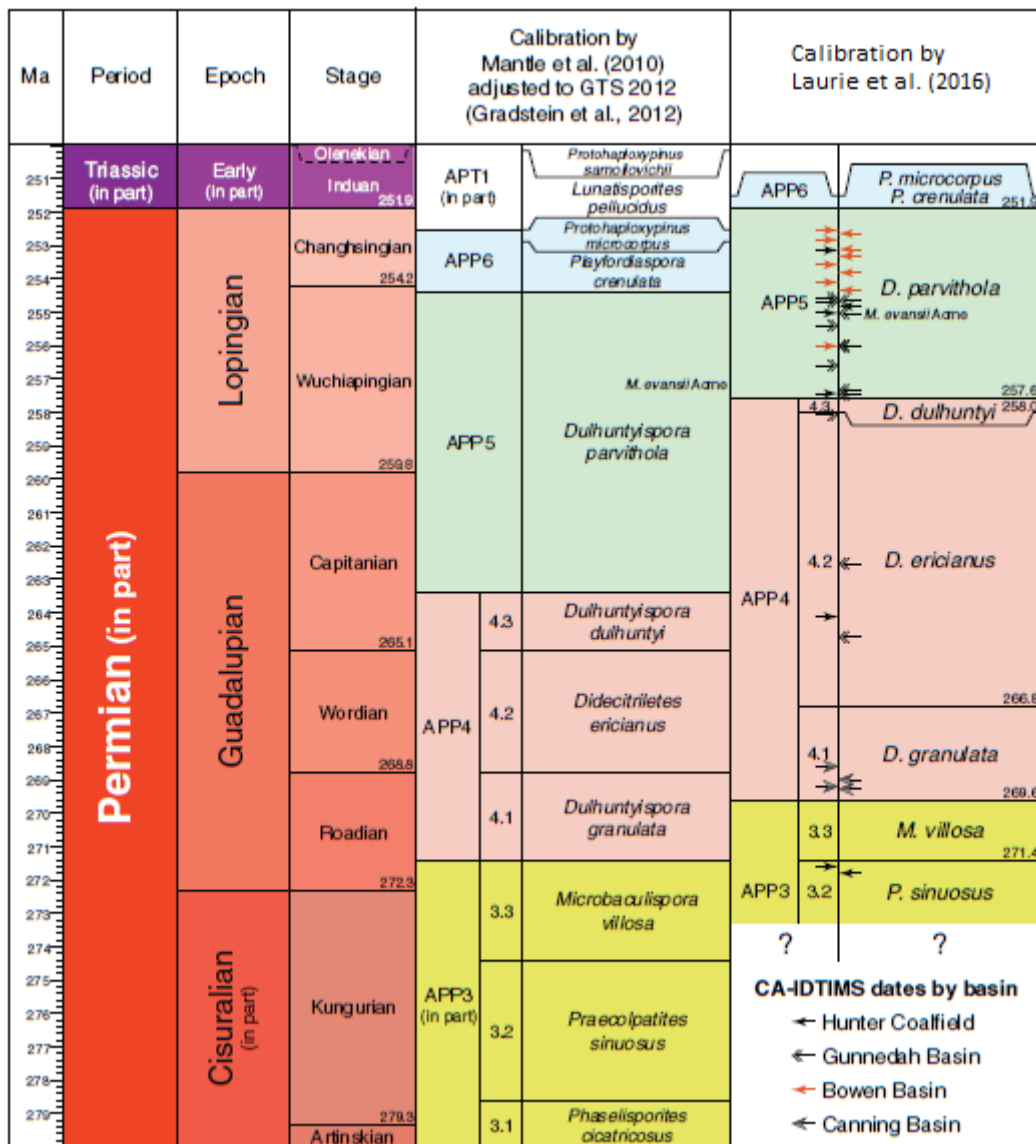

Figure 22 Palynostratigraphy zonation recalibrating by Laurie et al. (2016)

Comparing the palynostratigraphy with stratigraphic and sedimentological data, could be notable that, in Allan Hills, is noteworthy a deep change in fluvial style and mean paleocurrent direction between the Weller Coal Measures Formation and the Feather Sandstone Fm., and that the last recognizable palynozone along such portion of succession is the *Protohaploxypinus microcorpus* (in the uppermost part of the Weller Coal Measures Formation). Unfortunately, no more palynomorphs are present through the lower Triassic Feather Sandstone, also due to the absence of fine deposits. These informations and overall some critical issues emerged in the calibration of the biozones, and also keeping in mind the possibility of diachronicity of them (Barbolini et al., 2016; Gulbranson et al., 2020), lead us to keep a prudential line, so to formulate two possible hypotheses about the palynozonation of the PTB in South Victoria Land, in particular in the Allan Hills succession:

- Using the recent and calibrated palynostratigraphy zonation by Laurie et al. (2016) and Fielding et al. (2019) for the Australian basins, that assign the *Protohaploxypinus microcorpus* Zone at the Early Triassic. Therefore the palynofacies WC3 and WC4 should be placed in the earliest Triassic (early Induan) and the Permian-Triassic Boundary in Allan Hills should be positioned in the upper part of the Weller Coal Measures Formation, by the way disagree with the deep change in paleocurrent and fluvial style here reported (see in Liberato et al., 2017 and in Liberato, 2020).

- The second hypothesis is that the sensitive paleoenvironmental conditions developed in the time window between the EPE and the PTB, acted in different way due to the paleolatitude, causing a kind of local different response among different areas of the Gondwana. The provincialism, often recorded in Gondwana, could be accentuated by the stressful environmental condition, and it possibly led to a different palynostratigraphy zonation between the Sydney Basin and the Victoria Land Basin, as revealed by Barbolini et al. (2016) for the diachronic comparation between South Africa and Australia basins. In this case, in Allan Hills, the *Protohaploxypinus microcorpus* Zone could still indicate a latest Permian age, as well as for the palynofacies WC3 and WC4, while the PTB could be placed at the top of the palynofacies WC4, just at the transition between the Weller Coal Measures Fm. and the Feather Sandstone Fm., on agree with the deep change in fluvial style, in paleocurrents and in the features of the paleosols and landscapes, as for these last well documented by Retallack and Alonso-Zarza (1998), Retallack and Krull (1999) and by Retallack et al. (2005).

Taking into account these uncertainties and overall the sedimentological data (Liberato et al., 2016), as changes in facies, paleocurrent, fluvial style, sandstone provenance, and a possible diachronicity of the biozones, the second hypotheses has been considered more practicable for the present thesis, since it

satisfies many constraints. However, even the first hypothesis could be validated if new agreeing data will be revealed.

Figure 23 Palynostratigraphy zonation comparison focused on PTB

Moreover, among the other confident results, coming from these data there is that the *Protohaploxypinus microcorpus* Zone, as appear in this study, describes a transitional stage concerning the palynoassemblages, in which some species were extinguished or confined only in some areas, while other try to adapt themselves to the new environmental conditions, proved also by the presence of aberrant forms that indicate a stressful environment.

After the deposition of the portion of succession marked by the WC3, characterized by the abundance of *Protohaploxypinus microcorpus*, there was an abrupt change in the fluvial style, particularly increased above the WC4 across the PTB, and the deposits are mainly characterized by fine to coarse sandstones lacking of mudstones. For this reason, and for loss of the major part of the terrestrial plant ecosystem, a great number of samples where completely sterile or composed just whit AOM and inertinite. This absence well records the apocalyptic event of the PTB and of the following ecological crisis during the earliest Triassic, as revailed by the lack of significant plant remains within the Feather Sandstone Fm., until the Early to Middle Triassic

recovery phases during the deposition of the Lashly Fm. (Retallack et al., 1996; Fielding et al., 2019; Vajda et al., 2020).

After the ecologic collapse due to the Permo-Triassic mass extinction linked with the crisis of the EPE, in the Triassic Lashly Formation, were possible to note that the flora came back to be flourishing, even if with different genera and species (diagram 4).

During the Triassic, the Antarctica paleocontinent moved from south to a lower latitude, reaching a minimum of around 65° South during the Late Triassic (Torsvik and Cooks, 2017). During this time the landscape was much more stable than during Permian, this could be demonstrated by the high maturity of the soil that can reach thousands of years of stability.

The *Glossopteris* flora was replaced, through the PT boundary, by the *Dicroidium* and another genus. In the sporomorphs assemblages this is evident because a quite loss of striate bisaccate pollen grains (as *Protohaploxypinus* spp.) and the replacement of non-striate and non-taeniate pollen grains (i.e. *Alisporites* spp.).
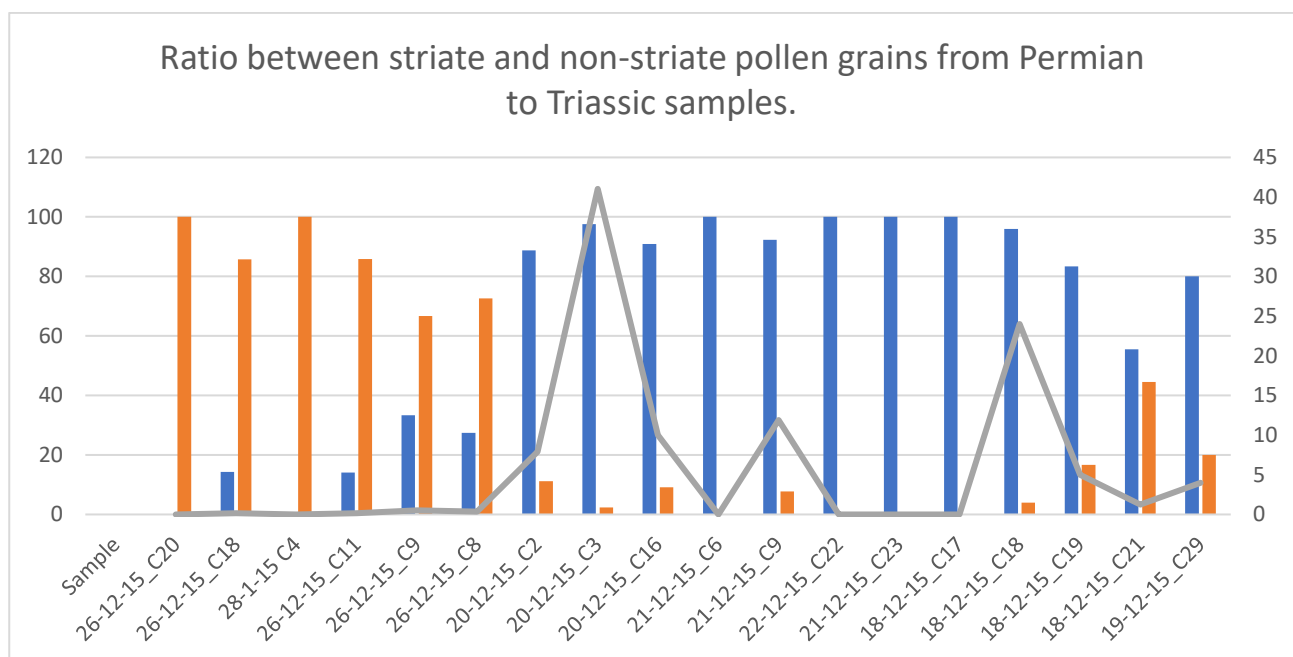

Diagram 3 Ratio between striate and non-striate pollen grains from Permian to Triassic samples: Microfloristic Turnover across PTB. Orange- Striate, taeniate bisaccate pollen grains; Blue: Non-striate, Non-taeniate pollen grains. Grey line: ratio between them. Th

From the Member A of the Lashly Formation upwards, different species of spores and pollen flourished, with the major components belonged to bisaccate, non- taeniate pollen grains. Even if the composition of the palynoasseblage, during all the Triassic, was mainly composed by *Alisporites* spp., it is possible to recognize diversified associations indicating more ages and more detailed within the Triassic and different depositional

environments; even if, furthers study based on the presence of the spores could provide a most detailed biostratigraphy and paleoenvironmental reconstruction.

With respect to the literature palynostratigraphic data for the Triassic in Allan Hills and in the whole Southern Victoria Land, the data obtained in this thesis allow to better refine the relative stratigraphy.

The previous stratigraphic data obtained through palynology show for the Lashly Fm. of Allan Hills, the correlation with the *Alisporites* zone, subdivided in four subzones, which are the subzone A of Early Triassic age, the subzone B of Middle Triassic age, the subzones C and D of Late Triassic age (Kyle, 1977; Kyle and Schopf, 1982).

Regarding the data obtained in this thesis, the palynofacies LF1 shows a very stable environment, with the deposition of thick levels of mudstone and coal and the high presence of cutinite in the sediments indicating the proximity of the depositional environment and a low level of transport. This paleoenvironmental conditions persisted up to the palynofacies LF2 where fungal spores occur, associated to hypogeum fungal, whose growth is strictly linked with a well-developed soil.

In this environment the association of sporomorphs, constituted by *Alisporites (A. australis, A. nuthallensis, A. splendens)*, *Bascanisporites undosus, Playfordiaspora crenulata, Quadrisporites sp., Striatopodocarpites sp.* and *Vesicaspora wilsonii,* indicates a correlation with the APT2 Zone of Price (1996), Early Triassic to earliest Middle Triassic (Olenekian to earliest Anisian) in age.

From the uppermost part of the member A of the Lashly Fm. and the entire Member B can be recognized the palynofacies LF3, that with the presence of various species of *Alisporites* (*A. australis, A. indicus, A. landianus, A. nuthallensis, A. opii, A. ovatus*) and *Densoisporites* sp*., Ephedripites* sp*., Guttatisporites* sp*., Klausipollenites vestitus, Kraeuselisporites apiculatus, Lunatisporites noviaulensis, Lunblandispora* sp*., Lunblandispora brevicula, Sulcatisporites* sp*., Sulcatisporites institatus, Sulcunicysitis cuniculus,* allows the correlation with the APT3 Zone of Price (1996). During the deposition of the deposits of the palynofacies LF3, the landscape was more instable, with a major flow index, as testified in the replacement of mudstone and coal by fine to coarse sandstone; in this environmental condition and stratigraphic position was also deposited the "Allan Hills Fossil Forest", transported and deposited by three different massive flow events (Liberato et al., 2017; Cornamusini et al., 2020). The APT3 Zone was assigned by Price (1997) and Mantle et al., (2010) to the Middle Triassic (Anisian to early Ladinian), then modified by some authors for the Australian basins (Bomfleur et al., 2014; Smith et al., 2015; Laurie et al., 2016) to a wider age interval (Anisian to middle Norian). Lately, Smith et al., (2016) recalibrated and reduced such time interval (Fig. 24) to the Anisian – earliest Norian (Middle-Late Triassic).

The palynofacies LF4, recovered in the lower part of the Member C of the Lashly Fm., is made of *Alisporites* spp. (*A. australis, A. indicus, A. nuthallensis, A. opii, A. ovatus, A.* sp.,), and *Apiculatisporites* sp*., Brevitrriletes* sp*., Cycadopites cymbatus, Densoisporites* sp*., Falcisporites* sp*., Florinites* sp*., Marupipollenites triradiatus, Miscroblasculispora villosa, Osmundacidites* sp*., Pityosporites* sp*., Playfordispora crenulate, Protohaploxypinus* sp*., Straurosaccites* sp*., Taeniatisporites noviaulensis;* and it could be correlated with the APT4 Zone of Price (1997), that following the recalibration of Smith et al., (2017), can be assigned to the Late Triassic (Norian). During the deposition of the deposits of the LF4, the paleoenvironmental reconstruction based on palynology and stratigraphy analyses, shows that the landscape came back to a more stable conditions, with a greater deposition of mudstone and coal and the high content of well-preserved cutinite fragments in the palynofacies association.
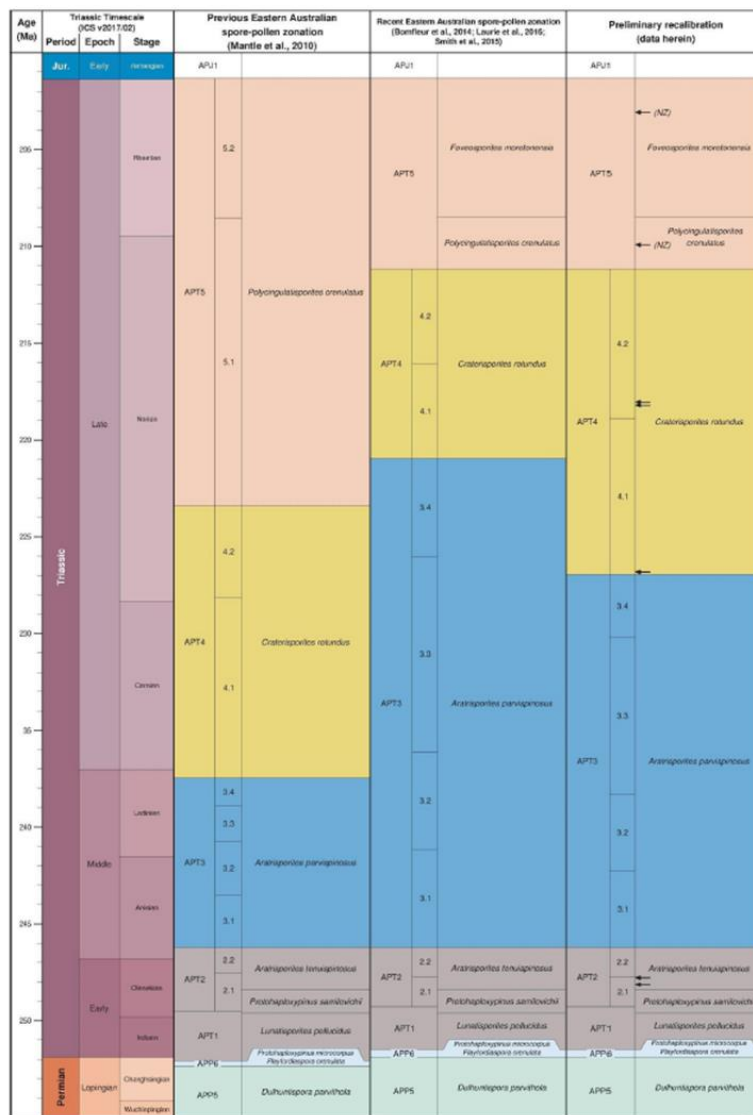

Figure 24 Recalibration of Triassic palynostratigraphy zonation by Smith et al. (2017)

The uppermost palynofacies (LF5) recognized in the Lashly Fm. is referred to the upper part of the Member C. Here the paleoenvironmental conditions and the sporomorph assemblage are similar to the those of the previous palynofacies, but in the LF5 differently by the LF4, *Classopollis meyerianus* and some other forms of *Polycingulatisporites* spp. are also present. This assemblage indicates an affinity with the APT5 Zone of Price (1997), that according to the most recent calibration of Smith et al. (2017), suggests a late Norian to Rhaetian age (Late Triassic).

Finally, the Triassic succession shows the Feather Sandstone Fm., directly above the Weller Coal Measures, totally barren of significant sporomorph, with the exception of its upper member of the Mt. Fleming, where some forms are present, but poorly preserved and not detectable. So, this formation can be only attributed to a time interval on the base of undirect data, analogously to the past literature, or to the Early Triassic, excluding the possibility advanced by some old authors of a Feather Sandstone Fm. of Late Permian age (Barrett, 1981).

The Lashly Fm. shows four lithostratigraphic members, that in the literature were ascribed by Kyle (1977) and Kyle and Schopf (1982), to the *Alisporites* zone, indicating a Triassic, more precisely, the Early Triassic subzone A for the Member A, up to the Middle Triassic subzone B for the Member B and to the Late Triassic subzones C and D for the members C and D.

The data here presented show a refinement of the dating of the Lashly Fm., using the Australian palynozonation of Price (1997), recalibrated by Smith et al., (2017). In general, the Lashly Fm. shows a substantial continuity in the deposition, where: the Member A assigned to the APT2 Zone, is referrable to the interval Early Triassic to earliest Middle Triassic (Olenekian to earliest Anisian); the Member B assigned to the APT3 Zone, is referrable to the Middle-Late Triassic (Anisian – earliest Norian); the lower part of the Member C assigned to the APT4 Zone, is referrable to the Late Triassic (Norian); the upper part of the Member C assigned to the APT5 Zone, is referrable to the Late Triassic (late Norian – Rhaetian).

Finally, the whole Permian-Triassic succession in Allan Hills records a probably continue stratigraphic succession, even if in consideration of its general fluvial/alluvial depositional environment, where minor, but not influencing the stratigraphic architecture, disconformities are possible (Fig.25). The Weller Coal Measures Fm. shows a Late Permian age for its middle-lower part in the studied section. Its upper part includes the catastrophic event of the so-called EPE (Fielding et al., 2019; Vajda et al., 2020), changing the main flora with the extinction of the *Glossopteris*, the atmosphere and the landscape, also with the development of extended wild paleofires. It also includes a short time of reappearance of plants, characterizing the latest Permian just before the Permian-Triassic Boundary, which is accompanied by the disappearance of flora again.

The above lying Feather Sandstone Fm., due to its totally lack of plant micro- and macroforms and to its dominance of coarse-grained deposits, signifies catastrophic changes in landscape and paleodrainage pattern (Retallack and Krull, 1999; Liberato et al., 2017) and a coal-gap phase (Retallack et al., 1996), anticipating the following plant and ecological recovery. This particular and possibly anomalous lithostratigraphic unit, within the context of the Victoria Group, can be tentatively, but with some certainty even if lack of fossils, ascribed to the Early Triassic, analogously to some literature (Collinson et al., 1994; Isbell and Cuneo, 1996; Retallack and Krull, 1999). This because this unit is totally constrained by data from the top of the Weller Coal Measures Fm. indicating the Changhsingian (late Lopingian), and from the bottom of the Lashly Fm. indicating the Olenekian (late Early Triassic), so to hypothesize an Induan age (early Early Triassic) for the Feather Sandstone Fm. Moreover, this implies, due the huge thickness of such formation (about 150-200 m) for a so short time interval (about 0.7 Ma), a high sedimentation rate, which is totally possible, due to the high-energy flow deposits, so testifying a great reset in the landscape and drainage pattern, probably due to climatic, but also tectonic processes (Liberato et al., 2017). The following younger Lashly Fm. testifies a full recovery of plant ecosystems and a re-stabilization of the landscape with the settling of low/middle-energy fluvial systems, happened starting from the late Early Triassic (Olenekian), until the Late Triassic.
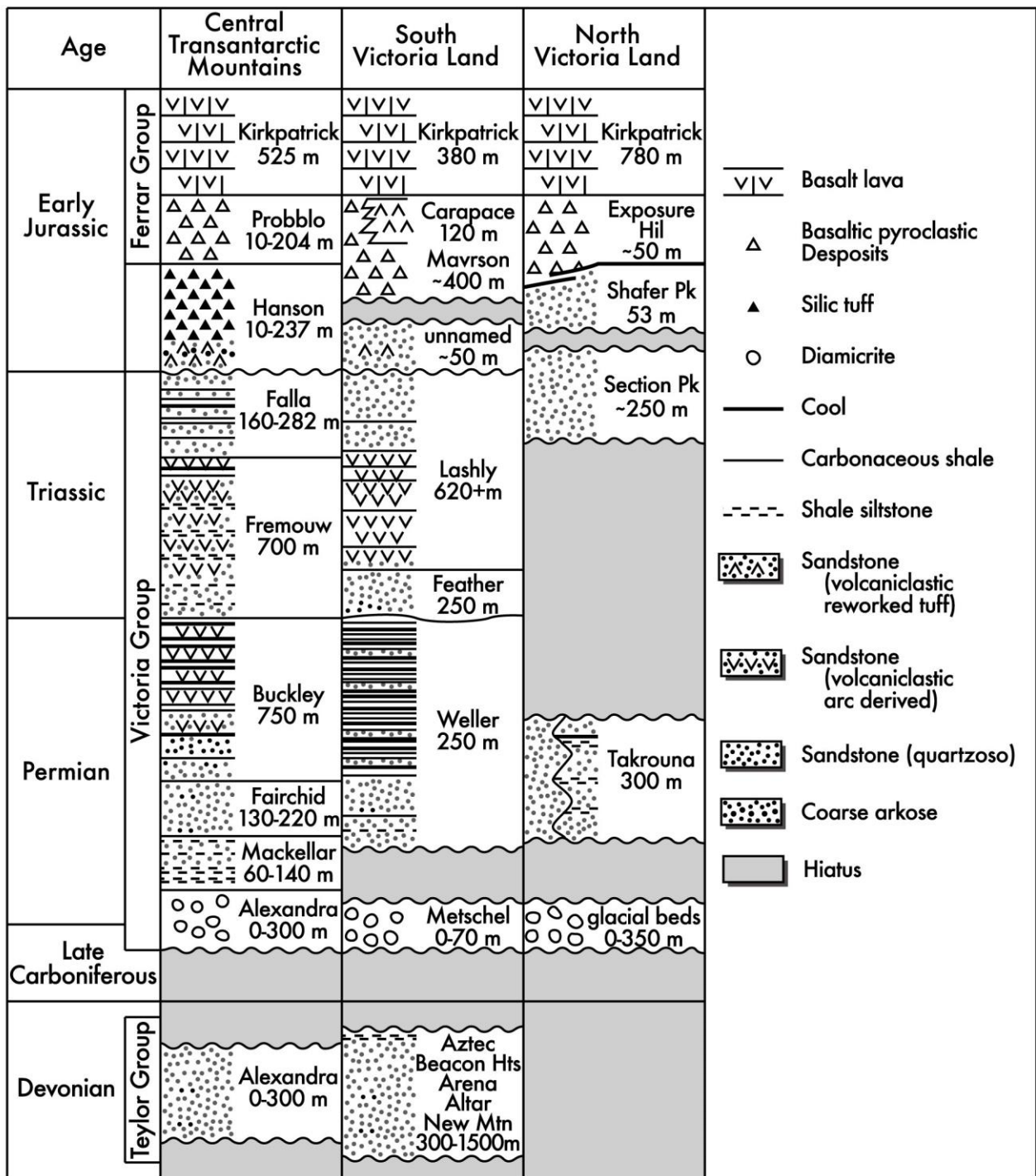
Figure 25 Stratigraphic succession of South Victoria Land whit the continuity of sedimentation between the Permian Weller Coal Measures Formation and the Triassic Feather Sandstone. Compared with CTM and NVL. Modified from Elliot et al. 2014

Part II: PALEOBOTANY

1.Introduction

The fossil history of the plant life is fundamental for the reconstruction of paleoenvironmental and paleoclimate evolution of Gondwana.

The history of the vegetation of Antarctica through the time is strictly linked to the geographical and climatic conditions and their mutual interaction. Due to the favourable nature of the sedimentary environments for the Permian-Triassic deposits occurring along the TAM, several traces of the past life were recovered. The first significant paleobotanical observation date back to 1901-1904 by the British Discovery Expedition, while the first paleobotany systematic sampling was done during the Scott Terra Nova Expedition in 1910-1913, where Glossopteris leaves fossils were consistently picked up from the Central Transantarctic Mountains.

Since then, numerous authors threated the Antarctic paleobotany remains (Rigby, 1985; Smoot et al., 1985; Gabites, 1985; Millay and Taylor, 1990; Archangelsky 1991; Yao et al., 1993; Taylor et al.,1994; Retallack et al., 1996; Yao et al., 1997; Axsmith et al., 2000; Phipps et al., 2000; Tayolr et al., 2006; Lindstrom and McLoughlin, 2007; Hermes et al., 2009; Bomfleur et al., 2011; Escapa et al., 2011; Cantrill and Poole 2012; Gulbranson et al., 2012; Gulbranson et al., 2014; Gulbranson et al., 2020), from systematic, paleoenvironmental and stratigraphic point of views, making clearer the paleobotany setting of Antarctica trough the time.

In this thesis, the paleoenvironmental conditions and the typology of fossilization of a fluvially drifted Triassic polar forest recovered in Allan Hills (SVL) were reconstructed. This reconstruction is based on a multidisciplinary approach joining classic, experimental and innovative frontier methodologies.

The main goals of this thesis are:

1- reconstruction of the paleoenvironmental condition during the Triassic time
2- to verify the occurrence of paleowildfires, as a presence of charcoal, suggested by particular features in the morphology of the fossil wood, based on different chemical composition between coal and charcoal
3- reconstruction the post-depositional events recorded on the multi-phase fossilization of the trunks.

1.1 Paleoflora reconstruction

The fossil history of the plant life is fundamental for the reconstruction of the paleoenvironmental and paleo climate of Antarctica and, most in general, of the entire world.

The history of the vegetation of Antarctica through the time is strictly linked to the geographic and climatic conditions and they are controlled and influenced one to each other.

Although the colonization of the land from the plants took place significantly since the Ordovician and rising during the Silurian, the first flora remains discovered in Antarctica are from the Devonian. This is due probably to double causes as a minor rate of plants during the first phases of colonization and due to the Ross orogen tectonism that delate the potential fossil material.

The first recovery flora in Antarctica was Devonian in age (Cantrill and Poole 2012) and particularly characterizing the Taylor Group of the Beacon Supergroup. This flora is mainly composed by *Lycophytes*, probably linked to a microflora composed prevalently by trilete spores. During this time appeared increasing its amount later, also the *Geminospora*, which indicates that progymnosperms such as *Archaeopteris* were also becoming an important component of the vegetation.

From the Middle Devonian, the plants were able to penetrate into the substrate stabilising stream banks and enhancing the formation of soil networks (Algeo and Schecker, 1998; Davies and Gibling, 2010). The roots systems were extensive (< 1 m in depth) and able to accelerate pedogenesis. This resulted in the generation of new terrestrial habitats were temperature, light and humidity became moderated, for part of the new year at least, and organic material was returned to the biosphere on an annual basis. (Cantrill and Poole, 2012)

The vegetation of the early Carboniferous, instead was characterized by a more articulated association, as the occurrence of Equisetales (e.g. Calamites), Sphenophyllales, Lycopodiales, Lepidodendrales, Filicales (ferns), Medullosales and the Cordaitales, and were joint in the late Carboniferous by other groups including the Voltziales, the Cycadophyta and Callystophytales. In the late Carboniferous pteridosperms along which Lycopsids, Cordaites and Ginkophytes prevailed, but since the Permian these florae become more diversified and characterised by Glossopteris with conifers and ferns, as well as Sphenopsids and Lycopsids. Even though each province was characterized by distinctly different flora, overlaps between these flora provinces are known from

several geographic areas and the provinces may have changed in composition over time (Cantrill and Poole, 2012).

The site of Allan Hills has been object of long time studies concerning macroflora assemblages focused on stratigraphy and paleobotany aims (i.e. Townrow, 1967; Taylor and Taylor, 1990; Chatterjee et al., 1983, 2013; Tewari et al., 2015), as well as other fossil sites of the TAM (Boucher et al., 1993).

1.1.1 Permian Macroflora

During the Permian, the *Glossopteris* flora (Figs. 26-27) dominated the Gondwana as recorded also for the Allan Hills samples here recovered. The *Glossopteris* are indeed the most widespread gymnosperms in Gondwana and judging from the variety if fructifications, they were probably quite diversified. (Archangelsky, 1991) This kind of flora was prevalently composed by *Glossopteris* but also from *Gangamopteris* and other species. This flora was particularly abundant in swamp environments around all the area. Remnants of fossil trunks, roots as *Vertebraria*, compression-impression of leaves of *Pteridospermophyta* were recovered not only in Antarctica but also in other regions of the Gondwana, as in Australia, in the Karoo Basin and in the Paranà Basin. For this group of pterodospermatophyta 8 orders were recognized: *Calamopityales* (Late Devonian- Early Carboniferous), *Lynginopteridales (*Carboniferous*), Medullosales* (Carboniferous - Permian), *Callystophytales* (Late Carboniferous), *Glosspteridales* (Late Carboniferous - Triassic), *Caytoniales* (Triassic - Cretaceous), *Corystospermales* (Triassic), *Peltaspermales* (Triassic). The *Glossopteris* is classified as a seed-fern, that is a plant producing seed but it's very similar to a fern. It's astonishing the rapid and widespread diversification of the *Glossopteris* during the Permian time. This kind of flora appeared after the ending of the early Permian glaciations. During the Permian, several orders were recovered:

PTERIDOPHYTE

- EQUISETALES: *Schizoneura, Phyllotheca, Stellotheca*
- SPHENOPHYLLALES: *Sphenophyllum, Raniganjia, Trizygia*
- LYCOPODIALES: *Cyclodendron*
- FLICALES: *Alethopteris, Gondwanium, Merianopteris, Pecopteris, Ptychocorpus, Sphenopteris, Angiopteridum, Cyathea, Callipteridium, Belemnopteris*

GIMNOSPHERMS

- GLOSSOPTERIDALES: *Gangamopteris, Glossopteris, Rubidgea, Rhabdotaenia, Taeniopteris, Macrotaeniopteris, Vertebraria, Cistella, Lancelatus, Dictyopteridium, Scutum, Ottokaria, Lidgettonia, Glossotheca*

- CYCADES: *Pseudoctenis*

- CORDAITALES: *Noeggerathiopsis, Euryphyllum, Cordiacorpus, Samaraopsis*

- GINKOALES: *Ginkgophyton, Psygmophyllum*

- CONIFERALES: *Buriadia, Walkomiella, Damudoxylon, Barakaria, Moranocladus, Indoxylon, Barakaroxylon, Dadoxylon, Kaokoxylun, Megaproxylum, Trigonomyelon, Prototaxopitys, Araucaroxylon, Agathoxylon, Prototaxoxylon.*

Trunk and leaves were recovered as impression-compression or petrification (in most of the cases as silification, but sometimes also as calcification). Even if the specie affinity in some cases is not still verified, the names of some part of the plants are here reported:

- ARAUCARIOXYLON KRAUS (Stems)
- VERTEBRARIA (roots of *Glossopteris*)
- GLOSSOPTERIS BROGNIART (Leaves)
- ARBERIELLA (Part of Nautiyal)
- GLOSSOTHECA (Male reproductive organ)
- ETRTMONIA (fructification of microsporangiums)
- SCUTUM (Seeds)
- OTTOKARIA (Female megasporangium's fructification)
- LANCELATUS (Female megasporangium's fructification)
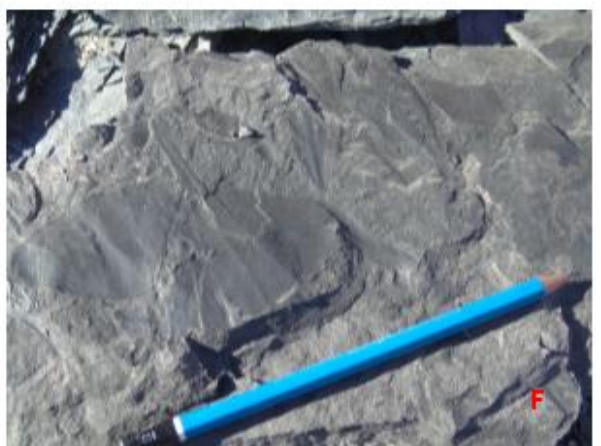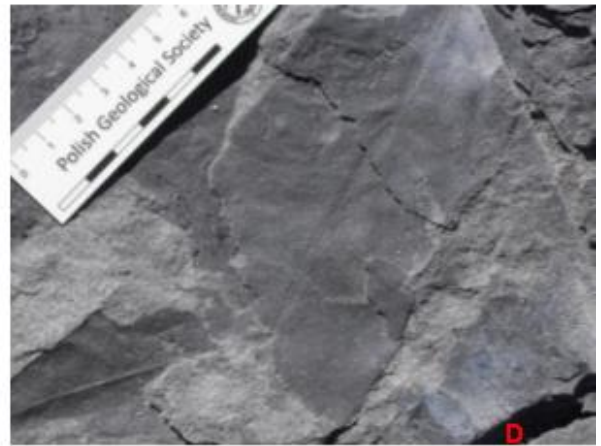- LIDGETTONIA (Female megasporangium's fructification).

Figure 26 Middle-Late Permian Glossopteris flora

The *Glossopteris* leaves show a marked central vein dividing in two symmetrical parts, also in the anatomized secondary veins. The various species of *Glossopteris* could be distinct on the base of the morphological aspect as the size, the ratio between long and short axes of the leaves and the venation. During the Permian, accompanying the evolution of the various species of *Glossopteris*, the central veins became time by time more evident.

The *Gangamopteris* are similar to the *Glossopteris* but they haven't the prominent central vein; in fact, the leaves of *Gangamopteris* are characterized by anatomized veins in a position of quite parallel one to each other. During the Permian, 12 species of *Gangamopteris* have been recovered, but the most common are the *G. angustifollia* and the *G. cyclopteroides.*
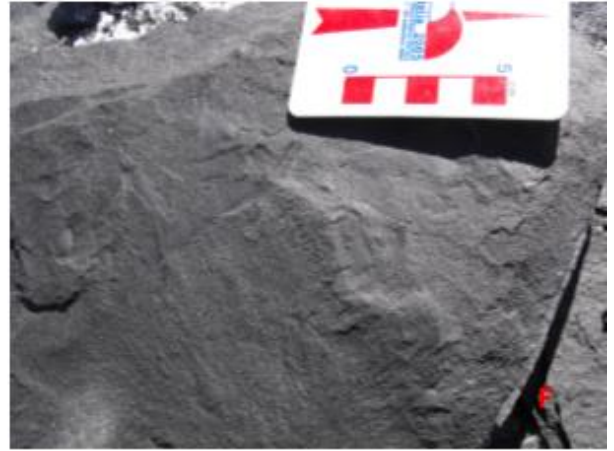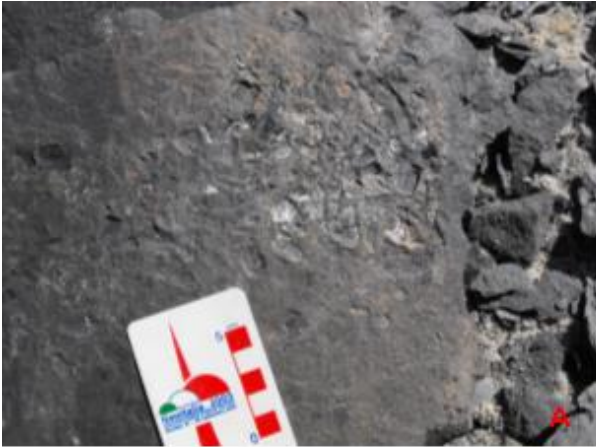
Figure 27 Presence of fossil leaf and roots (?) at the Permo-Triassic Boundary

1.1.2 Triassic Macroflora

Triassic fossil plants in Antarctica, and particularly in the Allan Hills, area of the major focusing of this thesis, show a remarkable increase in diversity in comparison with those of Permian for the same area. For example, the Lashly A Member revealed 3 species of *Dicroidium* (Escapa et al., 2011). Escapa et al. (2011) recorded a highly diversificated flora assemblage for the Member B of the Lashly Fm. w A brief summary of some of the arborescent morphogenera for this latter, is listed here: several species of Dicroidium, *Ginkgoales*, and conifers. The above lithostratigraphic unit, which is the Lashly C Member contains six species of *Dicroidium*, and *Heidiphyllum* (Escapa et al., 2011). Fossil woods in fragments or in trunks, have been revealed in several parts of Antarctica, particularly in Central Tam and in Victoria Land. Regarding this latter, at Roscolyn Tor in Allan Hills, an important fossil forest has been detected (Fig. 28) (Gulbranson et al., 2020).
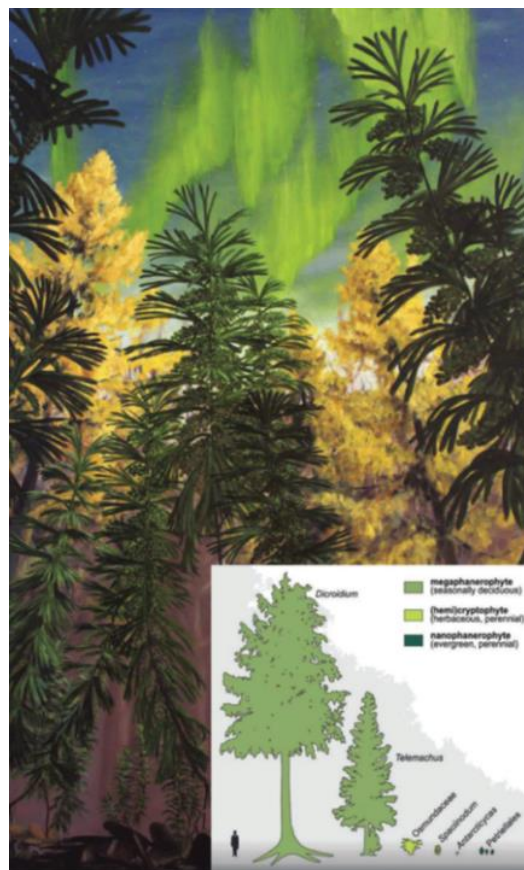

Figure 28 Reconstruction of a Triassic polar forest (from Bomfleur et al., 2014)

It is formed of in situ trunks associated with leaf mats of the coniferous *Heidiphyllum* morphogenera. Forest density of Triassic fossil forests ranges from 200 to 4000 trees ha−1 (Gulbranson et al., 2020). A further huge concentration of fossil trunks embedded within Triassic deposits, have been revealed and analysed in the Feather Plain in Allan Hills, and described in this thesis (see also in Gulbranson et al., 2020).

The most common groups for the Triassic flora are Lycopsids, Equisetaleans, Ferns, Seed Ferns, Ginkoaleans and conifers (Fig. 29-30-31). In this chapter the main features and the characterization of each group has been reported.

Lycopsids- *Lycopsids* spores were recovered in the Fremouw and Falla formations in the Beardmore and Shackleton glaciers in the CTM (*Aratisporites* spp*.* and *Uvaesporites verrucosus*); moreover, some *lycopsids* sporangia were recovered in Prince Charles Mountains.

Equisetales- The *equisetalean* diversity and distribution reaches a peak in the Late Paleozoic, while the diversity of this group decreased during the Mesozoic. The *Equisetales* occur in the Triassic deposits of Antarctica in the form of permineralization and compression. (Schewendemann, et al. 2010) described stems, leaves, buds and reproductive structures of *Spaciinodum collinsonii*. Other descriptions of *equisateles* are stems and leaves of *Neoclamites*. There are several morphology similarities between *Spaciinodum* and *Neoclamites* and they could be, in some way, related one to each other. Other leaves of equisetales were recovered in the Early Triassic of the Shackleton Glacier (in CTM) as poorly preserved leaves of *Phyllotheca brookvalensis*.

Figure 29 Presence of Dicroiidium leaf in the member A of Lashly Fm. A) B) C) form Allan Hills; D) E) F) from Ricker Hills– Morris Basin.

Ferns- The fern represents one of the most important components of the high latitude Triassic flora and it is widespread in various localities with several families; The ferns were recovered as impression-compression but also as permineralized remains.

- *Eusporangiate* ferns are represented by a single species, the *Scolecopteris antarctica*.
- *Leptosporangiate* ferns show high diversification and are abundant, with representatives of *Osmundaceae, Gleicheniaceae, Matoniaceae, Dipteridaceae and Cyatheaceae.*
    - The *Osmundaceae* are represented in the Middle Triassic of Antarctica with permineralized peat of *Ashicaulis beardmorensis*, stems and fronds of *A. woolfei* and compression-impression of *Osmunda claytonites*.
    - The *Gleicheniaceae* were recovered as permineralized sporangia of *Gleichenipteris antarcticus* in the Middle Triassic outcropping at Fremouw Peak;
    - The *Matoniaceae* (*Filicales*) were founded, as permineralized peat, with two species: the *Tomaniopteris kotonii* and the *Solopteris rupex*. Along the *Gleicheniaceae*, the *Matoniaceae* are considered one of the most ancient clades of *leptosporangiate* ferns.
    - The *Dipteridaceae* (*Filicales*) are represented by *Dictyophyllum*; this genus is really an important component of the Northern Hemisphere's Late Triassic flora, but in the Antarctica region, it was recognized only in the in the Upper Triassic Alfie's Elbow locality (Shackleton Glacier- CTM). This genus became more important, as record the Southern Hemisphere during the Early Jurassic age, here the proliferation of this species could significate a wet and warm climate condition.

Figure 30 Other Middle-Late Triassic flora present in Lashly Fm. Member C

Pteridosperms (Seed Ferns)- During the Triassic age the Seed Ferns plants were often one of the most important components of the flora.

They can be assigned to a variety of groups, but the major part of the *pteridosperms* fossil can be attributed to *Corystospermales*, a group that dominated the floras in the Gondwana during the Middle - Late Triassic.

One of the most common compression- impression genera of leaves in the Triassic of Antarctica was the *Dicroidium*.

The fronds of the *Dicroidium* are small to medium in size and characterized by an acute-angled bifurcation. The morphology of the *Dicroidium* leaves are very variable.

Corysptosperm pollen organs are assigned to genus *Pteruchus*; while the pollen grains are bisaccate, nontaeniate and have reticulate saccus ornamentation (*Alisporites, Falcisporites and Pteruchipollenites*).

Further seed-ferns groups are represented in Antarctica by sporadic occurrence. The *Petriellales* is a group that was recovered with permineralized fructification at Fremouw Peak. Other foliage of *Petriellales* also known in other regions of Gondwana, are *Rochipteris* (including *Kannaskoppifolia* and its ovulate organs *Kannaskoppia* and the pollen grains *Kannaskoppianthus*).

Cycadales- The *Cycadales* are represented, in the Triassic deposits of Antarctica just with a single plant, the *Antarcticas schopfii*, that occurs as permineralized peat at Fremouw Peak (CTM). There are also some compressions of *Taeniopteris*, that represents the only remains with possible *cycadalean* affinity.

Ginkgophyta-The *Ginkgophyta* was an important and abundant group during the Triassic of Gondwana. The most common leaf morphotaxa of this group are *Baiera, Sphenobaiera, Ginkophyllum* and *Ginko*. The only one that were present in the Triassic of Antarctica is the *Baiera*, that is present with three taxa.

There are several ginkgoalean-like leaves from different localities as the *Sphenobaiera schenkii* in the Upper Triassic of the Lashly Formation at Shapeless Mountains (SVL) and in the Falla Formation, here were also recovered a single specimen of the genus *Hamshawvia*, a reproductive organ.
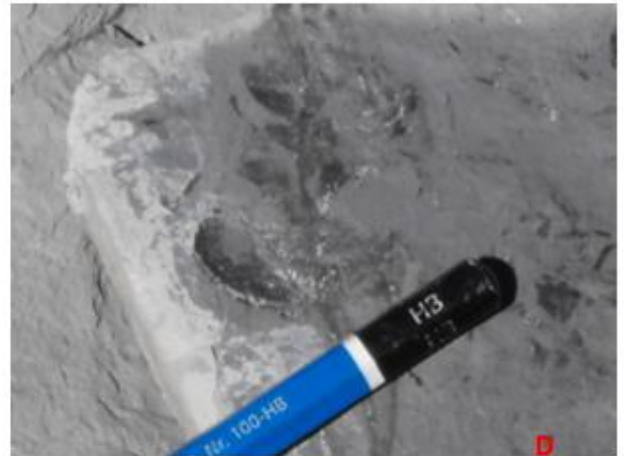
Figure 31 Middle-Late Triassic flora mainly composed from Dicroiidium and Hediphyllum elongatum

Conifers- The conifers, in the Southern Hemisphere, during the Triassic time were less abundant respect to the previous Permian.

Just such isolated organs as permineralized branches and leaves of *Notophytum*, compressed leaves and cuticles of *Heidiphyllum* (*H. elongatum*)(Fig.32), permineralized pollen cone *Leastrobus*, and permineralized seed cones assigned to *Parasciadopitys*, and compressed cones of *Telemachus*.

Gymnosperms- The *Gymnosperms*, in the Triassic of Gondwana are mainly represented by the fructification recovered in various areas of Antarctica and other lands. Species as *Protobolosperma antarcticum* and *Ignotospermum monilii* are isolated permineralized ovules recovered at Fremouw Peak. Other podophyllum have been recovered as the *Matatiella* and *Dordrechtittes* (this last one was previous assigned to another order). Moreover, also some leaves of *Gymnosperms* were collected as the leaf of *Dejerseya*, a possible seed fern, probably associated to the pollen cone *Switzianthus* and the ovuliferous organs *Matatiella*.
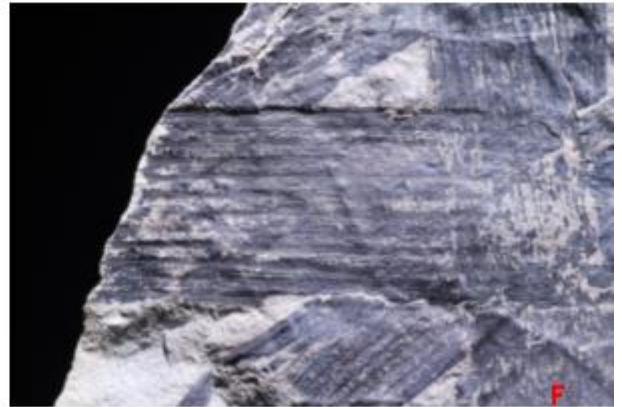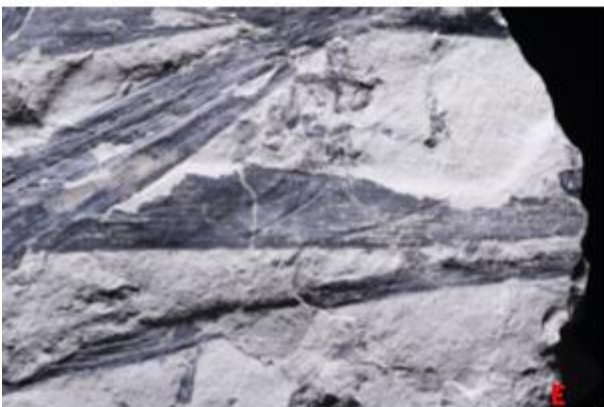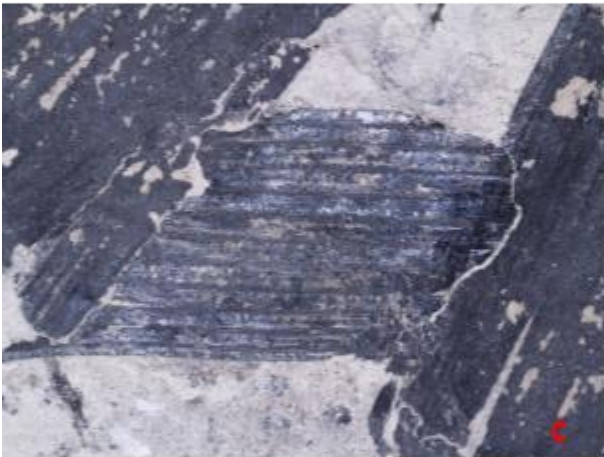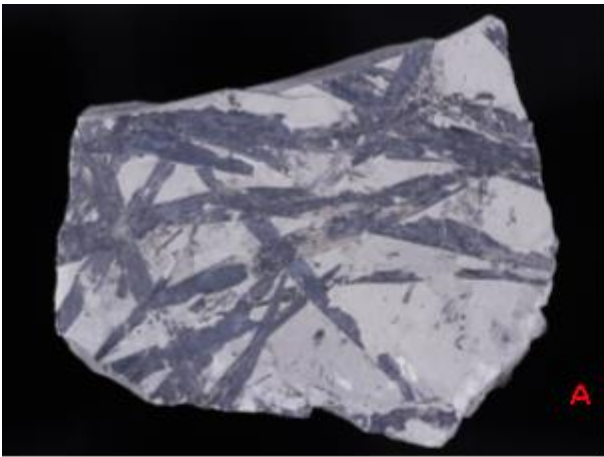
Figure 32 Hediphyllum elongatum

1.2 Allan Hills Fossil Forest

Across the TAM, in the Permo-Triassic formations the descriptions of macro-paleobotany remains, as leaves, cones, seeds and fossil trunks are numerous. Moreover, there are some localities where the fossil trunks (*in situ* or transported) are notably abundant. These concentrations of fossils within sandstones can be of in situ trunks, standing in growth position (Cuneo et al., 2003; Gulbranson et al., 2020), or in reworked position, forming the so-called log-jams of drifted fossil forests (Gulbranson et al., 2020). One of the best-preserved drifted fossil forest is located in Allan Hills (SVL) within the sandstone deposits of the Lashly Fm. Member B, object of this thesis.

The Allan Hills fossil forest is particular interesting both for the number of trunks and for the well-preserved conditions of them, and for the extension of the areas where the trunks were deposited with associated pieces of peat, with preserved peculiar sedimentary structures. The forest located in Allan Hills is for this reason defined a "drifted fossil forest", due to the transport of the logs (Liberato et al., 2017; Gulbranson et al. 2020).

This area was recognized and sampled with the support of a remote camp during the XXX and XXXI PNRA Italian Antarctic Expedition and were described over than 300 fossil trunks embedded in the sandstones of the Member B of Lashly Fm. These trunks, whose prevalent colour is grey, shift to a red/brow-red in the exposed part due to the weathering, or black when rich in carbon, and they reach 15 meters of length and maximum 60 cm in diameter, with occasionally preserved root system.

During the sampling was recorded the GPS position and orientation with respect to the North, of the trunks, and the major part of that results parallel or sub-parallel at the paleocurrent that point to N-NW with the roots system (when present) standing upstream; moreover there are a minor part of the trunks shift 90°, in a perpendicular way to the paleocurrent.

Raft of silicified peats were also recovered within sandstones, with relationships with sedimentary structures, suggesting an influence about their formation (see also in Gabites, 1985).
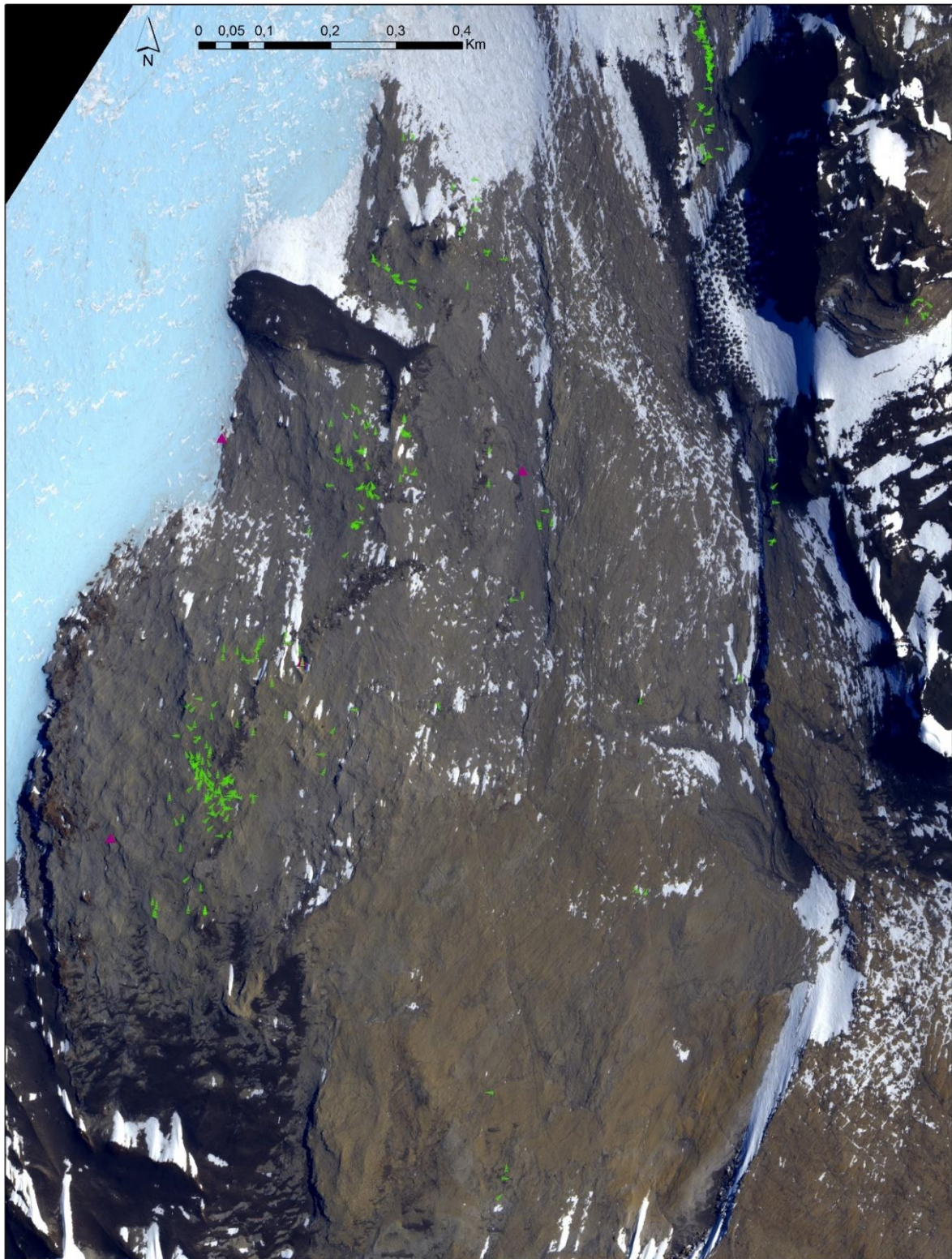
Figure 33 Localization and orientation of fossil trunks recovered in Allan Hills

The anatomic features of the fossil wood are well-preserved, with good growth rings, in some cases the rays are also recognizable, and the pith id preserved. Another peculiar feature is characterized by the occurrence of part or side of the logs with intense black colour, due to the great amount of carbon instead of silica.

Another feature of many trunks is the equatorial shape subcircular or ovoidal, due to the marked lithostatic compression.

The study of the "Allan Hills drifted fossil forest" is really complex and only with a multidisciplinary work has been possible to reconstruct, almost in part, the amazing history of this forest with paleoenvironmental reconstruction of the time-life and the depositional and post-depositional events.

The Allan Hills Fossil Forest is recovered in the Member B of the Lashly Formation, this member was analysed for the palynological content and a high percentage of non- taeniate bisaccate, with a good amount of various species of *Alisporites* made to attribute that to a middle-late Triassic age.

It's worth to note that the area surrounding Allan Hills deserves other fossil forest sites, as close to the Roscolyn Tor, south of the studied area, where an in situ fossil forest has been detected in the Triassic deposits (Gabites, 1985; Gulbranson et al., 2020).
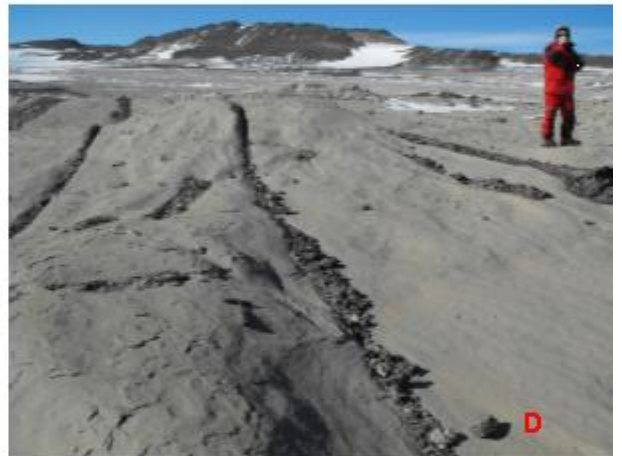
Figure 34 Allan Hills Fossil Forest

1.3   Paleowildfires in Gondwana, coal and charcoal

The paleowildfires have been described extensively for the Permian and Triassic time in various localities of Gondwana. Starting from the ending of the LPIA glaciation in the Artinskian, widespread wildfires have been signalled, thanks to the recovery of micro-charcoal (< 125µm), meso-charcoal (125 µm- 1 mm) and macro-charcoal (>1 mm), and they increase in number in Guadalupian and Lopingian time. Differently events of paleowildfires in the early Triassic time deposits, have been rarely recognized; lastly the number of paleowildfires back to increase during the middle Triassic.

This "charcoal-gap" is, almost in part, coincident with the "coal-gap" recorded for the early Triassic time, some authors (Retallack et al., 1996) (Veevers et al., 1994) refer this lack to taphonomy, atmospheric oxygen levels, lack of sediments suitable for the preservation of macroscopic charcoal, lack of fuel (Abu Hamad et al., 2012). The Figure 35 shows the distribution of the paleofires recorded in literature through Permian-Triassic. It is evident the different distribution of paleofires but also keeping in mind the different age span for each chronological unit (i.e. the Norian span about 18.500.000 years, lasted more than 25 times longer than the Induan, spanning about 700.000 years).
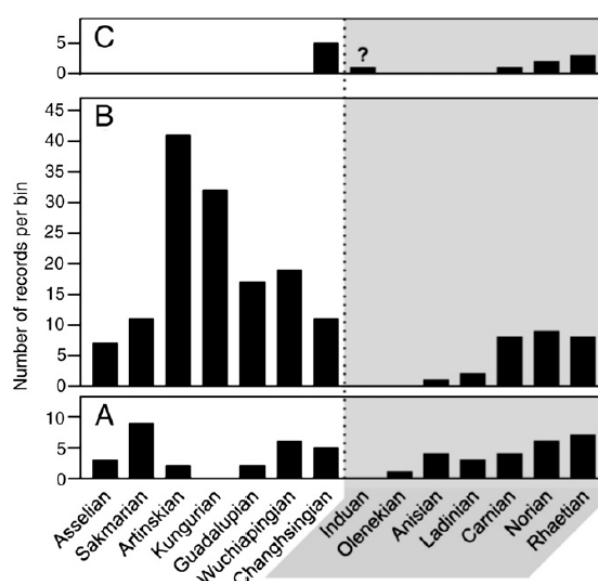

Figure 35 Overview of the number of published reports of fossil evidence for palaeowildfires during the Permian and Triassic [A–C: Triassic highlighted in light-gray. See Tables 1–3 and text for details; intertinite data were mainly taken from Diessel (2010), Glasspool and Scott (2010) and additional sources not cited in both works (cf. Table 2)]. A) Reported occurrences of macroscopic fossil charcoal, B) reported occurrences of inertinites/black carbon and C) reported occurrences of pyrogenic PAHs. The single occurrence in the Induan is questionable- From Amadh et al 2016

1.3.1 The combustion processes

The combustion (Fig. 36) is a rapid chemical oxidative reaction that generates heat, light and produces a range of chemical products. Plant combustion is usually produced by overheating and dry conditions, lightning or volcanic activity. Plants contain a range of organic compounds: the most common cellulose (a carbohydrate that is a linear polysaccharide polymer, usually found in the cell walls) but also lignin, hemicellulose, sporopollenin (in pollen) and cutin; during the combustion the initial high temperature causes a breakdown of the cellulose (and the other) molecule and produce a range of gaseous components: ammonia (NH_3), carbon dioxide (CO_2) and methane (CH_4), which mixed with the atmospheric oxygen promoting the rapid exothermic reaction.

When heated in absence of air the pyrolysis process results in the composition of the macromolecules to produce liquid and gaseous material. The resultant residue is termed charcoal, and this is highly aromatic, with an increased proportion of carbon over the starting material.

Temperature in the process are variable. Charcoalification starts at temperature generally of 275°C and higher temperatures promote the formation of a broad range of pyrolysis products that may be combusted.

Fire occurs where there is enough build-up of fuel dry enough to burn. Most often, a fire starts on surfaces where little fragments and duff and herbaceous plants and shrubs may occur. In a forest system, such surfaces fire may only burn the fuel on the forest floor. These fires tend to have a relatively low combustion temperature - often less than 400°C- (but, in some cases, can reach 900°C) and to be sometimes relatively slow. If a thick and sufficiently dry humic layer is present the fire can extend the combustion to this layer. In such case, with restricted oxygen supply, the fire may be then smouldered.

A significant build-up of surface fuel within a forest ecosystem can increase the fire temperature. In this case, the fire may spread out to the trunks of the tree into the crowns of the forest trees. Usually, after this kind of fire, leaves and other small parts of the tree don't survive and only trunks remain are left. Moreover, in the trunk often the outermost bark is the more compromised and sometimes it could be absent. This sort of fires has temperatures of 800-900 °C and in some cases, they can reach 1200°C.
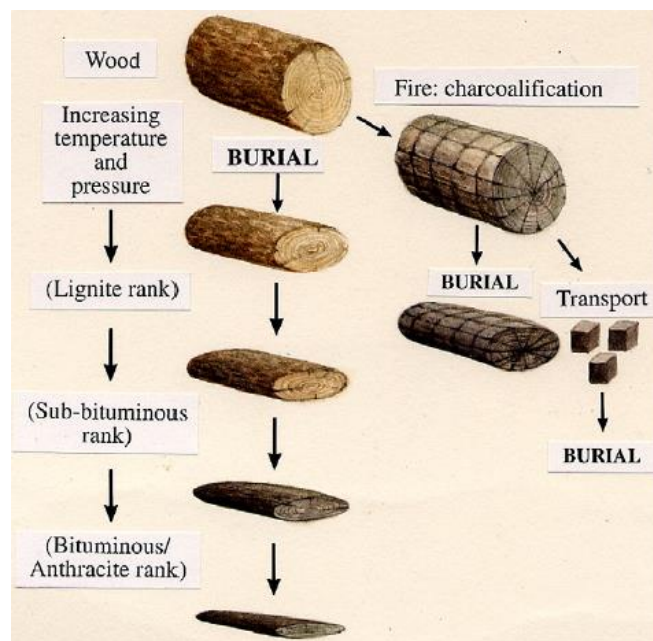
Figure 36 Coalification and Charcoalification, From Scott 2010

The pyrolysis and combustion process lead to the production of many materials and compounds. They could be divided in two categories: i) material that remains in place after the fire (mineral ash and charcoal) and ii) material that is transported away by smoke plume (water vapour, small charcoal particles, usually less than 125μm and sometimes also bigger, soot, volatile components and aerosols). Soot together with charcoal, is often referred to black carbon and it is formed by the recombination of vaporized organic molecules for forming new carbon material that is chemically similar to the pure carbon, but morphologically different. This material can be observed by SEM since it has a size less than 1 μm. Volatile gases and compounds include carbon dioxide (CO_2), carbon monoxide (CO) and oxides of nitrogen (NO_x), and important compounds consisting of complex organic molecules such as polycyclic aromatic hydrocarbon (PAHs). The PAHs may be produced in large quantities and their composition may depend on the type of burned vegetation and temperature involved. The higher temperature the larger the number of carbon rings found in the molecules. The most common of these molecules are cadinene and retene, including phenantrene, fluoranthene, chrysene, pyrene and coronene. These compounds may stay in the atmosphere for a considerable time and, consequently, they result in the prevention of rain formation, hence prolonging a wildfire event. Successively, these compounds may be washed out of the atmosphere and be incorporated in sediment (Scott, 2014). Levoglucosan derived from cellulose is widely used as a biomarker for vegetation fire.

1.3.2 Differentiation between coal and charcoal

Charcoal is often formed by the occurrence of paleo wildfires and can be observed as macro-meso and micro charcoal.

Charcoal typically has a well-preserved internal anatomy of wood and a high content of carbon. It can be recovered in both continental and costal-marine environments because trunk and fragments, affected by combustion, could be transported for long distances.

The process of charcoalification and the classification (Fig. 37) of charcoal is widely treated by Scoot (2010), that propose these scheme and definition for the identification of modern and fossil charcoal.
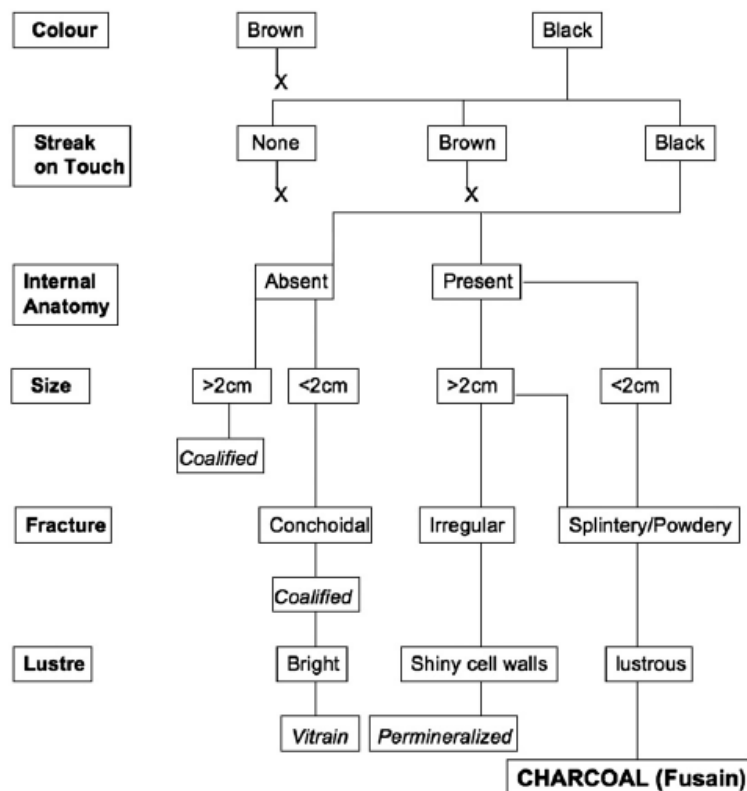

Figure 37 Scheme for the identification of modern and fossil charcoal Colour:

"The change in colour of plant material during charcoalification is from brown to black. Streak when rubbed: When rubbed with the finger charcoal easily soils the hands. It may be brittle and powdery and has a black streak. However, partially charred plants may have a dark brown streak. Internal anatomy: The charcoalification process preserves the anatomy of the plants. This may easily be seen with a hand lens in the field or under a binocular microscope in the

laboratory. With wood charcoal the elongate tracheid cells may be visible in longitudinal section and typical files of cells may be seen in transverse section. All organs of the plant may bepreserved as charcoal including leaves and flowers. Because of this, even small 1–2 mm pieces of charcoal may be worth collecting, not just large wood fragments that may be more obvious. Size: Large plant organs such as trunks and branches typically crack upon burning and the residue from charred wood usually comprises small, 1 cm cubes, together with smaller plant fragments. From wildfire any larger piece of plant will be only partially charred. From volcanic deposits, however, as there is no combustion, then larger trunks and branches may be charcoalified throughout if they have remained in hot ash or lava for a considerable time. Such material may be reworked into sedimentary rocks. Leaves and frondsmay also char and these may be flat structures and fragments may be rarely over 2 cm in maximum dimension. For very small fragments and organs (less than 2 mm) it may be necessary to first dissolve the rock matrix and examine under a binocular microscope. Fracture: Coalified plant material may show a conchoidal fracture and break into small equidimensional fragments. However, charcoal, depending on the original charring temperatures will be splintery or powdery. Higher temperature charcoals are more fragile than low temperature charcoals. Wood charcoals may splinter and break into elongate laths. Leaf charcoal may become powder when touched (in contrast coalified leaves will be more robust and will not crush upon touch). Lustre: Coalified wood fragments may have a very bright lustre and on vitrain fragments will show also conchoidal fracture and no anatomical preservation. However, in some cases, there may have been precipitation of mineral material by permineralization processes before compaction and coalification. In such cases the specimen will break in the same manner as a piece of rock. In contrast most charcoal has a silky lustre, which together with anatomical preservation, is diagnostic of charcoal (known also in the fossil record as fusain)." From Scott 2010.

2. Materials and Methods

The samples, collected during the XXXI Italian Antarctic expedition, are part of the collections kept by the Italian National Antarctic Museum in Siena. In this study, they have been processed with a variety of techniques following a multi-analytical approach that allowed to reconstruct the history, during the time-file and also after the deposition in the sediment, of the samples of wood, and, also, samples derived from pieces of peat and/or from paleosoils.

A list of all the employed techniques is here reported, whereas more detailed descriptions are in the following sections:

- Carbon Isotope analysis; for each sample analysed with this technique at least of 20 points (sub-samples) from the external to the internal part were analysed;
- Thin Section analyses through optical microscopy (this kind of analysis were only used as an auxiliary analysis for the dendrology calibration);
- Paleo-Dendrochronology, an experimentally approach for reconstructing the history during the life-time and the deposition of the trunks;
- PAHs analysis of little fragments of wood taken from the core and the rim of the samples;
- SEM analysis of thin sections or little pieces mounted in a stub with or without gold metallization;
- Reflectance Vitrinite imaging of two different samples (one sample was from coal, while the other one was from a fossil trunk).

2.1   Dendrochronology

Dendrochronology, or tree ring dating as it is often called, is defined as the study of the chronological sequence of annual growth rings in the trees. This subject was born in story and archaeological contest, and just recently it is developed in many other contests as ecology, hydrology and geomorphology. Thanks to this kind of study many objects are now dated (from a painting to a landslide!) but in the fossil field (PALEODENDROCHRONOLOGY) there are just few preliminary works (Gulbranson et al., 2020) and in this case this methodology is not used for dating but only for a better understanding of the environmental conditions at the time of the growth of the tree.

The dendrochronology is based on three principles:

- The trees that live in the areas where there is a net seasonal changed, produce a new tree ring each year, clearly visible in the transversal section
- The trees of the same species that live in the same area, in the same time produce similar tree rings series and the amplitude of the rings is influenced by the climatic and environmental conditions
- It Is possible to compare the tree ring series of trees that that live in the same area during the same time (Cross-Dating).

2.1.1 Dendrology vs Dendrochronology

The dendrology and dendrochronology are sometimes confused one to each other and in some cases the terms are used in an undistinguished way, but this is improperly. Even if the base of the two disciplines is the study of the growth rings, they have different goals.

The Dendrology (also called xylology) is the science and study of wooded plants (trees, shrubs, and lianas), specifically, their taxonomic classifications. There is no sharp boundary between plant taxonomy and dendrology; woody plants not only belong to many different plant families, but these families may be made up of both woody and non-woody members. Dendrology, as a discipline of industrial forestry, tends to focus on identification of economically useful woody plants and their taxonomic interrelationships. The paleo-dendrology is a discipline that had the main goal the reconstruction of paleoenvironmental condition that affected the growth rings in different and the taxonomic and taphonomy study of the fossil wood.

The Dendrochronology (or tree-ring dating) is the scientific method of dating tree rings (also called growth rings) to the exact year they were formed. As well as dating them this can give data for dendroclimatology, the study of climate and atmospheric conditions during different periods in history from wood. Dendrochronology is useful for determining the precise age of samples, especially those that are too recent

for radiocarbon dating, which always produces a range rather than an exact date. The paleo-dendrochronology is a totally new application of the technique utilized in dendrochronology analysis applied at paleobotany samples (fossil trunk). In particular, the area of this research has been carefully analysed for paleo-dendrology by Gabites (1985), but the paleo-dendrochronology methods has been applied in this thesis for the first time ever.

2.1.2 Botanical knowledge

Some botanical knowledges are necessary in order to help understanding the dendrochronology method.

The plants are divided in two fundamental subgroups: the gymnosperm (plant that produce cones) and the angiosperm (plants that produce flowers). There are a lot of differences between these two subgroups, but there are in total six main organs, so divided:

- Vegetative organs (roots, trunk and leaf)
- Reproductive organs (flowers, fruits and seeds)

The trunk could be sectioned in three different planes (usually for the dendrochronology analysis is more useful the transversal plane but there are some exception)
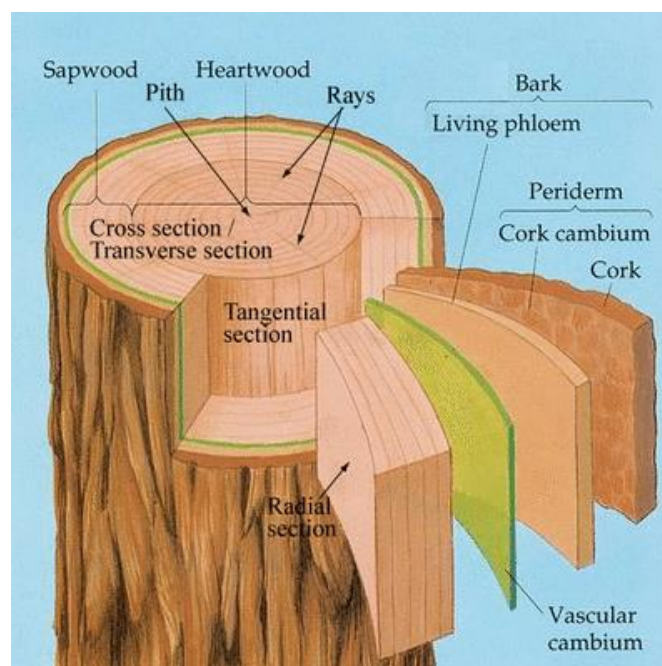
Figure 38 Nomenclature of the major features of a wood in tangential, radial and transverse sections.

In the Fig. 38 is possible to see the different organs that form the trunks. Starting from the external part thy include:

-BARK that is the parenchymatic tissue with the function to protect the phloem and the other parts of the plants from an excess loss of humidity and from an eventual fungal attach;

-PHLOEM is a complex system of tissues whit three functions (transport, reserve and support). The main function transport the sap (water based solution rich is sugar made by photosynthesis) from the non-photosynthetic part of the plant, such as the roots, or into storage structures, such as tubers or bulbs. The cellular of phloem, unlike those of the xylem, are alive even if some organelles are absent (as the core). The wall of these cells is not lignified and is porous;

- VASCULAR CAMBRIUM is a meristematic tissue that have the function to generate two different kind of cellules; the cellules generated in the external part there will be part of the phloem, whereas those generate in the internal part will be part of the xylem;

-XYLEM is a tissue whose main function is to transport the sap from the roots to the upper part of the plant. The xylemic cells are dead cells oriented vertically and hollow inside, they have lignified wall which has the task of supporting the plant. The size of these cells changes during the different seasons and this is the cause of the rings. In the xylem there are also the rays (fibres transversal orientated to the rings);

-PITH is a parenchyma tissues, sometimes these tissues could be absent and leave a cavity on the trunk.

2.1.3 Tree rings

Growth rings result from new growth in the vascular cambium and they are visible due to the change in growth speed through the seasons of the year. It is possible to divide each tree rings into two part:

-EARLYWOOD or SPRING WOOD, which is produced earlier in the growing season. The cells of the earlywood are larger and have thinner walls than those produced later in the grooving season (for this reason this have a lighter colour);

-LATEWOOD or SUMMER WOOD, which is produced later during the growing season. The cells are smaller and have a thicker walls respect those in the earlywood (for this reason this have a darkener colour).

The transition between the earlywood and the latewood is very abrupt and this is the cause of the tree rings (SEM image in Fig. 38).
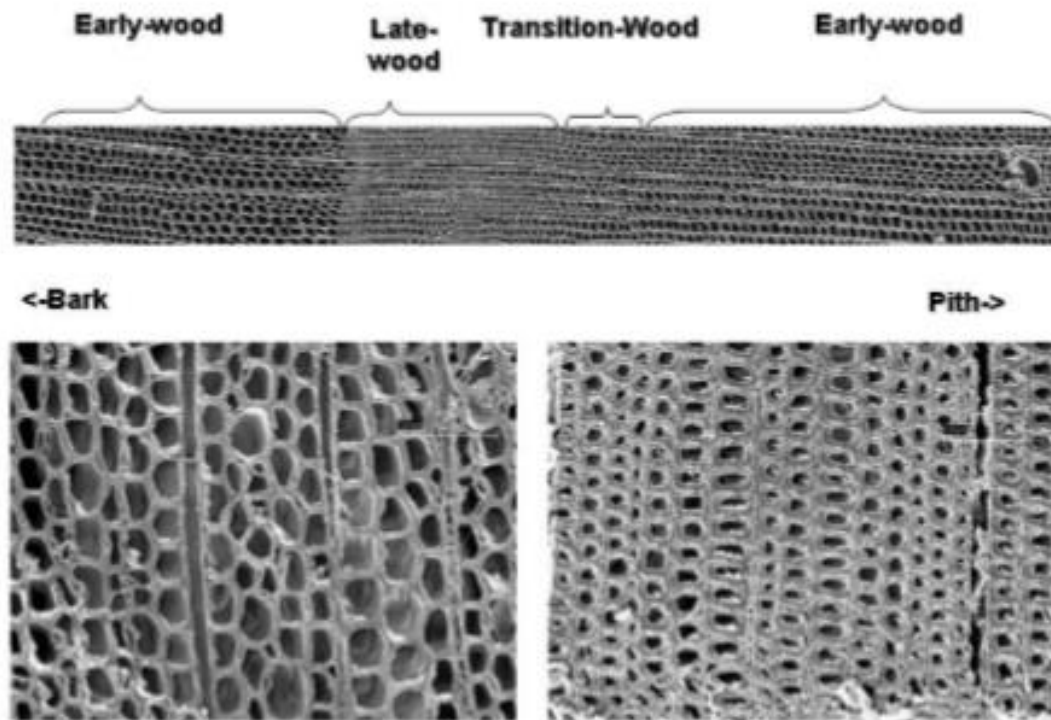
Figure 39 SEM image with the alternance of early-wood and the late-wood

In a transverse section, the younger tree rings are those near the pith, while the oldest tree rings are located near the bark.

At the same climatic condition, during a growth season, the vascular cambium produce the same quantity of xylem, for this reason the rings near the pith are bigger than the others (Fig. 39-40).
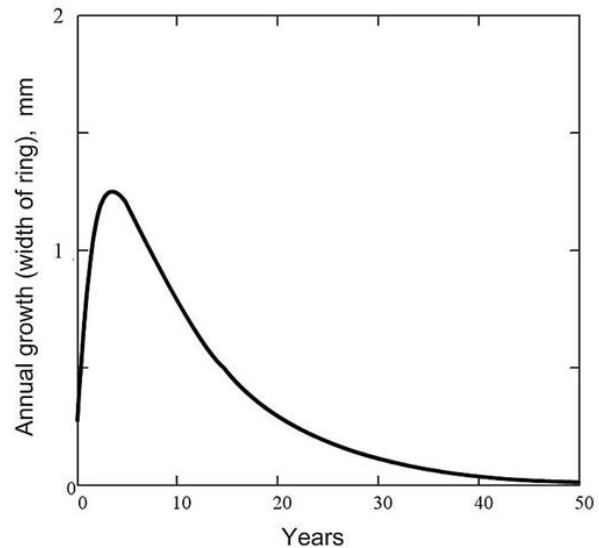
Figure 40 Different growing between the internal and the external part of the wood

This trend is well visible on the graph of amplitude of the tree rings. To understand the difference of amplitude due to the external factors (as climatic change) this exponential trend due to the normal growth must be detrend from the function.

### 2.1.3.1   Factors that influence the tree rings growth

The link between the past climate and the ring width occurs because plant growth is affected by certain conditions in the environment. A large number of these environmental conditions vary throughout the life of a plant, and at times they may limit and affect the form of many plant structures. (Fritts 1976)

The growing of the tree rings is influenced by many factors, which could be divided in:

EXTERNAL FACTOR (precipitation, temperature, light, CO2, O2)

INTERNAL FACTOR (availability of water in the soil, mineral, enzymes).
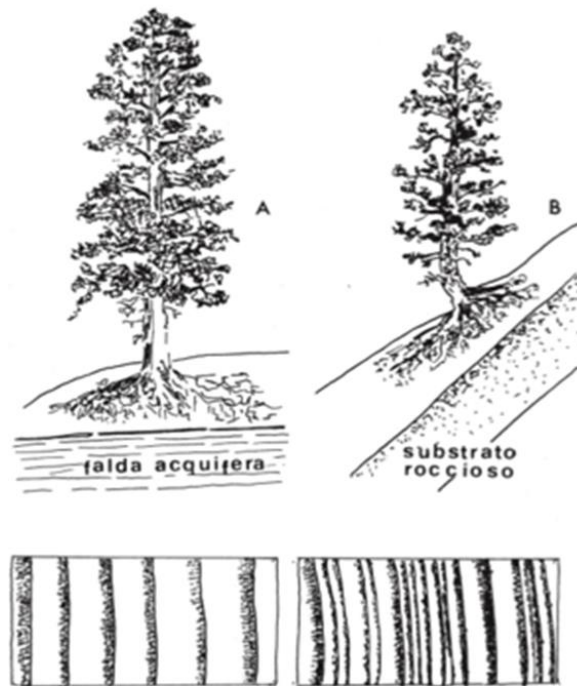
Figure 41 Different growing of the tree-rings due to the geomorphology factors

Obviously much of these factors are closely related one to each other; complex interactions occur between external and internal factors, physiological processes, and growth, but few of these interactions have been studied adequately. There is a lack of understanding, especially of the relationship between large trees and their environment. Moreover, the causes could be related also to the geomorphology of the landscape, as show in Fig. 41.

However, not all rings show distinct annual increments of growth. Sometimes when factor is highly limiting, growth cannot be possible, and no rings is produced. At other times, a stress period occurring in the middle of the growing season may cause two or more growth layers to form within a particular year. Moreover, there are some species that don't produce tree rings for anatomical features, for example the palm trees haven't the growing rings because their trunk is formed by the same structural part of the roots.

Another limit could be linked to the geographical areas, indeed many wood species, such as those growing in the tropics or semi tropics, can produce several growth layers per year (Fritts 1976).

2.1.4 Samples preparation: Polished blocks for reflected light microscopy

For analysing fossil trunks by means of reflected light microscopy, the samples must be cut (as show in Fig. 42). The fossil material, if necessary, could be embedded (allow a few days after the resin has hardened before starting the polishing).
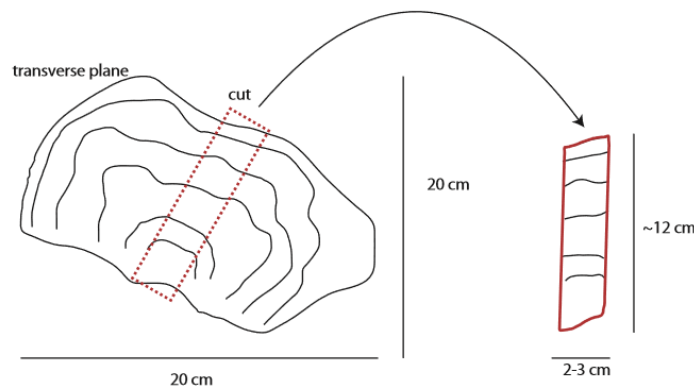

Figure 42 Cutting of samples

The polishing processes involves several stages, with each stage using a progressively finer abrasive powder. The first stage entails using a diamond lap to grind down to just above the final polished surface.

This should be followed by a grit such as 400 μm silicon carbide and water on a glass plate. Using moderate downwards pressures, moved the block through the paste. After 2-3 minutes polishing the surface under the water and check that in the face there are not scratches remaining from the diamond lap. In case, do again this step.

The other two stage are even mechanical polishing (Fig. 43A), whit the same method but with finest abrasive past, the first whit a 220 μm aluminium oxide and then with 0,05 μm aluminium oxide for the final stage.

The final polishing block needs to meet the following criteria:

- The surface must be flat and substantially free of relief
- The surface should be substantially free of pitting

- The surface should be substantially free from scratching.

When the surface respect these criteria, dry the samples (just with normal air for one night)

For show off the tree rings and all the other features of the samples put on the polished surfaces a bit chalk (Fig. 43B).

The samples are now ready for the tree rings analysis.
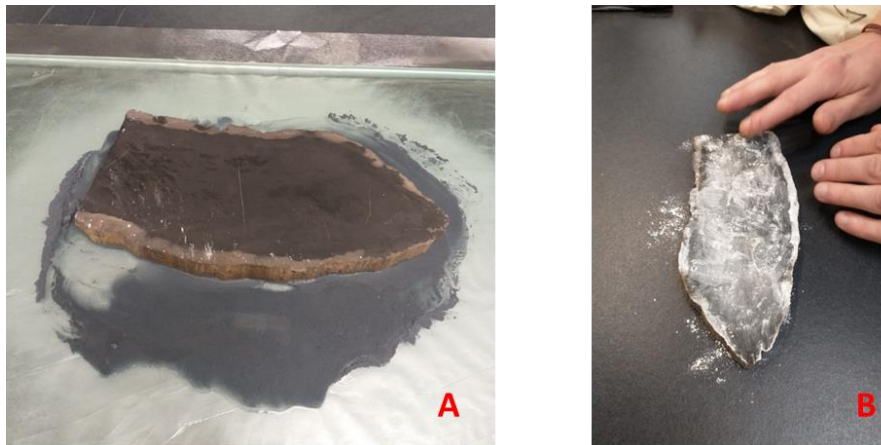
Figure 43: A) Polishing sample; B) Sample with layer of gypsum

2.1.5 Tree rings analysis

Dendrochronology is a statistical comparison of tree growth rings, where the goal is to provide an absolute match of a growth rings produced in the same time interval between two or more trees. Whereas contemporary dendrochronology seeks to provide absolute chronologies with annual precision, the extreme antiquity of the fossils examined here means that fossil wood specimens can only be cross-dated, or not. Thus, cross-dating of ancient fossil wood can only provide a relative dating of wood growth. The potential advantage of this technique is that multiple decades or potentially centuries of continuous wood growth for a given study area can be reconstructed, providing unparalleled time-resolution to study paleoclimate or paleoecologic processes.

Fossil wood was prepared for dendrochronological measurements of ring widths by first creating thin sections of a given sample to identify ring boundaries as the transition of latewood to earlywood cells, where latewood cells are identified as having thicker tracheid cell walls and smaller diameter cell lumen than earlywood cells. The thin section determined ring boundaries were compared to the expression of these ring boundaries in hand sample in order to validate the ring width

measurements to the anatomically defined wood growth increment. This technique was done to avoid erroneous ring boundary determination in hand sample as weathering and secondary mineralization can create features that resemble wood growth rings but have no connection to the anatomical transition from latewood to earlywood (Garland et al., 2007).

Ring width measurements were made at the University of Wisconsin-Milwaukee using a LINTAB™ linear table (Rinntech®, Heidelberg, Germany) with attached Leica microscope. Measurements were made at 1/1000 mm resolution using TSAP-Win™ software. For a given sample, at least four radial transects were measured (see cross matching below). Specimens with>20 growth rings were selected for dendrochronological analysis in order to produce statistically significant ring width series for a t-distribution.

2.1.6 Cross-matching fossil wood

Cross-matching of the fossil wood specimens consists of two phases:

1) internal cross-matching of the four-radial ring-width transects for an individual sample,

2) cross-matching of different samples based on the average ring widths of internally-cross matched samples.

The overall aim of these two phases of analysis is to statistically assess the replication of trends in ring width variation within an individual sample for quality control of ring width data; and replication of ring width variation is assessed between multiple samples in order to produce a statistically significant cross match. Cross-matching statistical analyses were performed using Past5™ software. We use the following statistical metrics to assess the quality and confidence of cross matches: correlation coefficient, gleichlaufigkeit (percent parallel covariation), and the Student's t-statistic following ring width normalization of Baillie and Pilcher (1973).
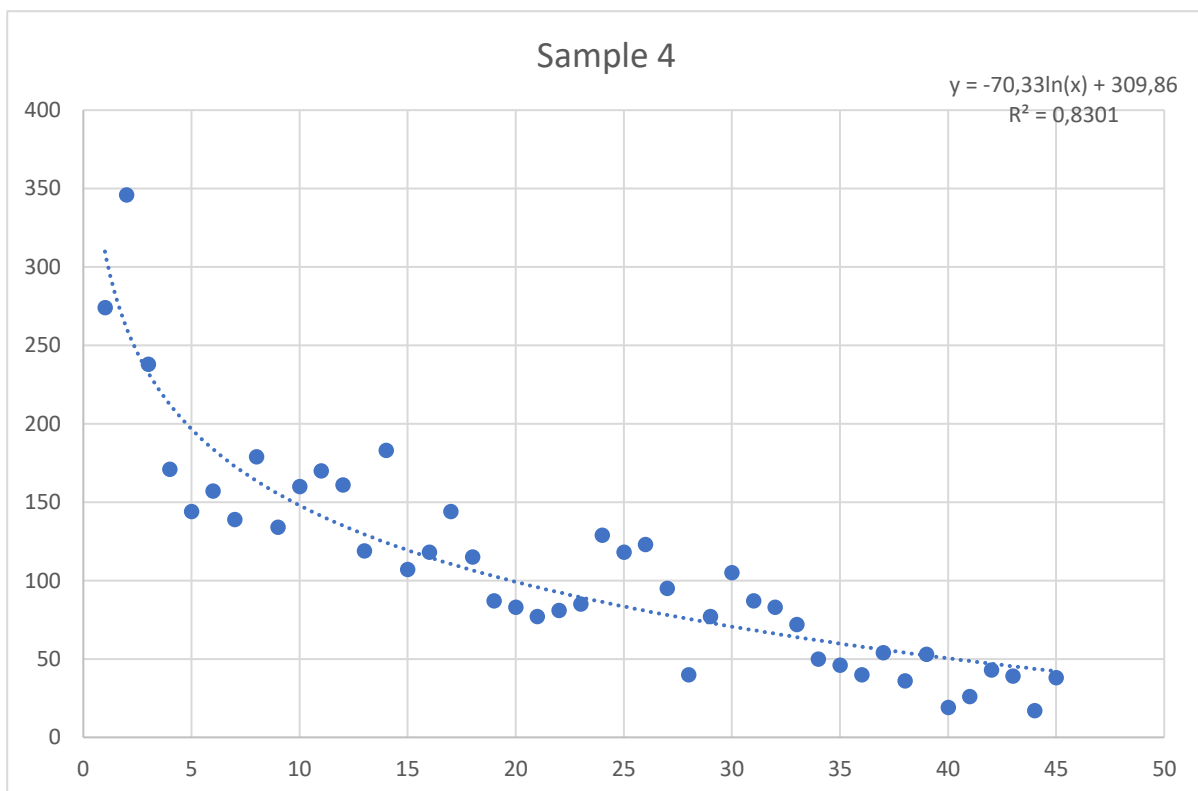

Figure 44Graph of amphlitude of the rings with the linear equation of the trending

After internal cross-matching was performed on an individual sample, and that the cross-match was successful, an average of the four radial transects was made and it is the average radial ring width transect that was used to cross match different samples.

2.1.7 Detrending and analysis

Growth related trends occur in all living trees. Given adequate preservation of growth rings in fossils, these growth-related trends should also be apparent in fossil wood material. Therefore, the average (of n = 4 radial transects) ring width measurements for a given specimen were detrended, after cross-matching, using a smoothing spline, where each spline was created for the measured time series of a given specimen. The resulting mathematical expression of the spline is used to compute the Ring Width Index (RWI), which is a time series of the observed growth (actual ring width measurement) divided by the expected growth (computed from the spline equation). As an index, there are three possible outcomes: 1) an RWI value of 1 indicates the measured ring width is equivalent to the predicted ring width for that year; 2) an RWI value > 1 indicates that the measured ring width exceeded the predicted ring width for that year; and 3) an RWI value less than indicates that the measured ring width was less than predicted for that year. RWI is a useful technique in evaluating growth trends over multiple individuals, given the potential for state factor changes in the paleo landscape that could limit or enhance plant growth, which would result in some trees showing wider/narrower rings than others due to differing growth rates. The ring width measurements and RWI are recorded for each studied specimen and are presented as the master chronology. The RWI curves are used in subsequent analysis and interpretation.

2.2 Carbon Isotope

The Carbon Isotope ratio between ^{12}C and ^{13}C and its relationship whit the growth rings, is a widely diffused technique that allowed to investigate in the environmental factors that affect the growing and the response of the plants (Helle and Schleser 2004; Wilson and Grinsted 1978; Mazany et al., 1980; Stuiver and Branzianus 1987; Leavit and Long 1991; Lipp and Trimbron 1991; Leavitt, 1992; Yakkir, et al. 1994; Panek, 1995;Panek and Warring 1997; Edwards, et al. 2000). The application of the stable carbon isotope analysis related to the growth rings of the trees allowed to reconstruct some environmental variables as temperature, precipitation and humidity. Other studies point to correlate the relationships between the $^{12}C/$ ^{13}C and the soil water content (Dupouey , et al. 1993) (Walcroft, et al. 1997) (Panker e Goldstein 2001). The studies on $^{12}C/$ ^{13}C and growth rings were done, during the time, both in actual samples (for a calibration) and in fossil samples, for the reconstruction of the paleoenvironmental factors that affected the growth of the plants.

Being that the stable carbon isotope analysis is becoming, with the modern technique, increasingly important other studies were done whit the aim of a correlative relationship between $^{12}C/$ ^{13}C in growth rings and the atmospheric concentration of $^{12}C/$ ^{13}C in the CO_2, (Farquhar et al., 1982) (Francey and Farquhar, 1982) (Farquhar et al., 1989) with the final focus to correlate directly whit the CO_2 atmospheric concentration and the intrinsic water-use efficiency (iWUE) (Rezaie et al., 2018).

Analysing the Carbon isotope ratio is useful not only for the paleoenvironmental reconstruction like atmospheric concentration, seasonality, water availability, but also because the trend of this ratio across the growth rings is a signature of the classification of wood.

Different kind of plants provided the $\delta^{13}C$ signature produced during primary CO_2 fixation is transferred to the constant developing tissues of the tree rings and it influenced the stomatal reaction and activities.

Instead of the final storage of $\delta^{13}C$ in wood and the photosynthate production had a difficult correlation because of the tree ring material is influenced by a partly of starch accumulated in parenchymal tissues during
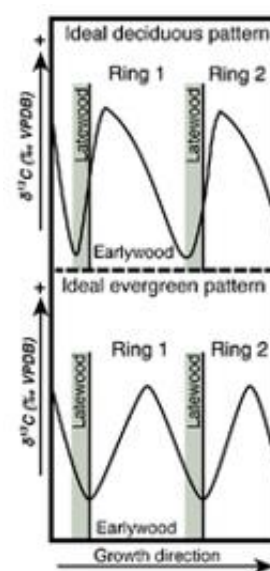

Figure 45 Different distribution of δ13C in deciduous and everegreen pattern. From Gulbranson et al. 2014

the previous year (Helle e Schleser 2004), the intra-annual values follow different trends between the evergreen and deciduous trees (Gulbranson et al., 2014).

Evergreen trees produce a quite symmetrical pattern in $\delta^{13}C$ values during the growth direction of the rings, whit a similar level at the beginning and at the ending of the growth season and a peak of the level in the middle. Different hypothesis are done about the symmetry of the $\delta^{13}C$ level in the growth rings from many authors: (Francey and Farquhar, 1982) attribute the symmetry to the low rates of photosynthetic CO_2 assimilation early in the growing season and a consequent negative values $\delta^{13}C$ in earlywood; Keeling (1960, 1961) suggests that positive values of $\delta^{13}C$ during the middle growing season could be associated to decreasing of atmospheric concentration CO_2 during the peak of photosynthetic rate; lastly (Davies and McCree, 1978; Rawson and Constable, 1980) affirmed that the negative $\delta^{13}C$ values of the latewood is due to the increasing intercellular CO_2 concentration from the time between the peak photosynthetic and the non-growing season.

Obviously, the symmetrical pattern is often affected by sifting due to external causes as meteorological factors, humidity and other; this can produce a double peak or an asymmetrical distribution in the $\delta^{13}C$/tree rings.

Deciduous trees produce indeed a different distribution of $\delta^{13}C$ values in the growth rings, in particular with an high resolution sampling, useful for an intra-annual deviation, is possible to recognize three different phases in the distribution curve (Helle and Schleser 2004):

1- $\delta^{13}C$ enrichment during the early vegetation period.
2- $\delta^{13}C$ decline during the main vegetation period
3- $\delta^{13}C$ increase at the very end of the vegetation period

The asymmetrical curve product from these three different trends is due to the storage of carbohydrates and the use of sorted carbohydrates, in the form of starch in parenchymatic tissue of the sapwood, as a carbon source.

Sample preparation: For each sample was grinder the whole surface of the ring, starting from the external part and, ring-to-ring, going to the pith (or where this is absent, to the internal part).

For each ring take 1 to 3 tin capsules with around 28 mg of sample, take notes about the exact weight and the position in the box where this is place.

Figure 46 Carbon isotope analysis: A) Box of capsule ready for the analysis; B) Magnification of a box whit dust of sample; C) Sample, grinded and dust of the sample

Carbon isotope are measured from permineralized wood at 1-2 mm interval, in the direction of growth, for a detailed concentration rings by rings, to infer the annual or seasonal uptake of CO_2 from the Middle Triassic atmosphere.

Sample of the tree rings were cut and drilled from the permineralized wood in a laboratory at the University of Wisconsin-Milwaukee. The powders generated from drilling the wood were homogenized and encapsulated in tin. Encapsulated samples were introduced to an elemental analyzer (Elementar Vario Micro) interfaced to a gas-source stable isotope ratio mass spectrometer operating in continuous flow mode (Elementar VisION) at the University of California Davis. Secondary reference materials were introduced in the sample queue at the beginning, intermediate positions, and at the end of the sample queue in order to monitor and assess quality control and quality assurance of stable isotope data and elemental abundance data. The quality control reference used for this analysis (March 2019) was bovine liver with an expected $\delta^{13}C$ value of -21.69‰ (VPDB) and a measured average value of -21.75‰ (±0.07‰, VPDB). Other references analysed for this sample set include: alfalfa flour, isotopically enriched alanine, and nylon. The performance of these quality assurance references results in a standard deviation of ±0.09‰ for replicate analyses of the references, and a mean absolute accuracy of ±0.05‰. The performance of these references provides explicit information for the accuracy and precision of the results of isotopic analysis of the fossil wood samples.

2.3   PAHs analysis

The Polycyclic Aromatic Hydrocarbons (PAH) are organic compounds characterized, from the structural point of view, by the presence of two or more aromatic rings (such as benzene) condensed in a single structure with angular and / or planar arrangement.

The simplest of PAHs is naphthalene ($C_{10}H_8$) which derives from the condensation of two benzene molecules.

PAHs with several rings varying from 2 to 7 are known which, according to the position in which the condensation took place, occur in the form of different isomers.

They are usually subdivided according to the molecular weight and the number of atoms that include light PAHs (2-3 condensed rings) and heavy PAHs (4-6 rings). In particular, the name PAH identifies those compounds containing only carbon and hydrogen atoms (that is to say the unsubstituted PAHs and their substituted alkyl derivatives), while the more general name of "aromatic polycyclic compounds" means also functional derivatives (eg nitro-PAH) and heterocyclic analogues (eg aza- irane).

The extreme heterogeneity of this class of compounds is further increased by the possible presence of pentaromatic rings, which, including planarity variations, can reach the three-dimensional systems of fullerens.

 PAHs can be formed during slow thermal maturation of organic matter (petrogenetic origin) or during incomplete combustion or pyrolysis of organic materials (pyrogenic origin).

PAHs of diagenetic origin imply formation temperatures between 100-150 ° C and formation times on a geological scale.

PAHs of pyrogenic origin are instead formed by incomplete combustion or pyrolysis of organic substance. The formation mechanisms are still under study, but it can be hypothesized that, when the pyrolysis occurs at high temperatures (650-900 ° C) and in lack of oxygen, the formation of PAHs is favored (with decreasing oxygen ratio).

In general, pyrogenetic materials contain more abundantly PAH at 4-5-6 rings due to their formation temperature (Hossain 2013), while in those of diagenetic origin, PAHs of 2-3-4 rings are prevalent.

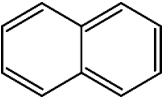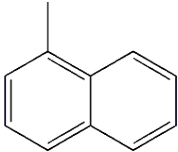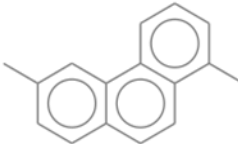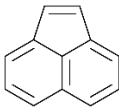### 2.3.1 General characteristics and structure of PAHs

Polycyclic aromatic hydrocarbons constitute a wide class of organic compounds that are formed during incomplete combustion and pyrolysis of organic materials. PAHs are characterized, from the structural point of view, by the presence of aromatic and non-aromatic rings containing 5 or 6 carbon atoms, condensed in a single structure with angular and / or linear arrangement. The simplest is naphthalene ($C_{10}H_8$) which can be considered as deriving from the fusion of two benzene molecules.

Theoretically the number of PAHs is enormous; for example, the different compounds with five benzene rings, in various combinations, can be twenty-two. It is possible to obtain 88, 333 and 1448 compounds, using six, seven and eight rings respectively. Furthermore, many polybenzenoid hydrocarbons are known as benzo derivatives, in which the fusion position is identified by a letter in brackets.
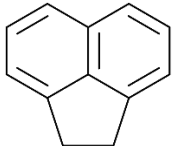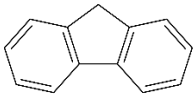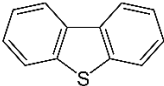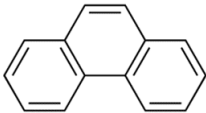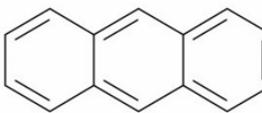
The extreme heterogeneity of this class of compounds is further increased by the possible presence of pentatomic rings, which inducing variations in planarity can lead to the three-dimensional systems of fullerenes. This heterogeneity makes the study of the whole class in environmental matrices very difficult, in fact in the literature the monitoring studies often refer to a limited number of PAHs. The United States Environment Protection Agency (EPA) and the World Health Organization (WHO) have identified 16 compounds defined as "priority pollutants " within the aforementioned class, from naphthalene to compounds containing up to six fused rings, as reference series and set representative of aromatic polycyclic contaminants (table 1.3). This is a coherent list of PAHs found together in the air, soil and water. The different type of PAHs are related to the origin (emission of diesel or petrol engines, cigarettes, incinerators) and the physical state (gas phase or particle phase). The different PAHs can be identified as markers characterizing an event or a site. Cosiderable attention is paid to the development of methods for their identification and subsequent quantification of PAHs in various environmental matrices mainly due to the fact that they represent a vast class of carcinogenic compounds and mutagenic pollutants.
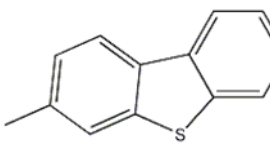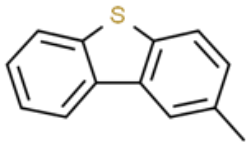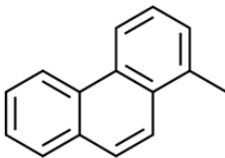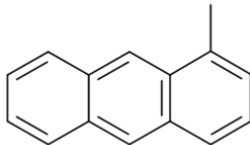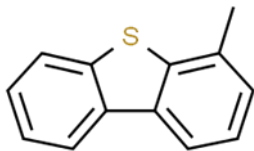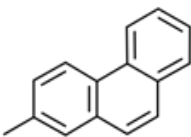
2.3.1.1   *Physico-chemical properties of PAHs*
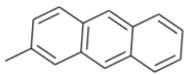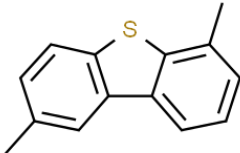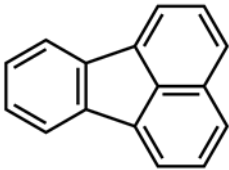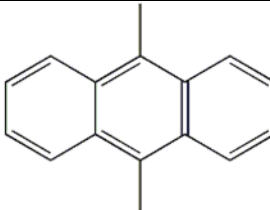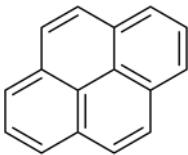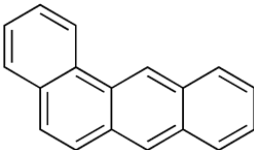
The chemical and physical properties are extremely important because they give information about the distribution and reactivity of a substance in the environment. PAHs are solid at room temperature and have high melting and boiling points. Their vapor pressure is generally low and is inversely proportional to the number of rings. For this reason, PAHs in the atmosphere are often associated with particulate matter. Moreover, it can be observed how, with decreasing temperature, the PAHs having a higher molecular weight (more than 4 rings), characterized by a low vapor tension, tend to rapidly condense and be adsorbed on the surface of the soot and ash particles, while those with lower molecular weight (3 rings), having higher vapor pressure, remain partially in the vapor phase. Therefore, in the air high molecular weight PAHs are found exclusively linked to particulate matter, while those with low molecular weight can also be in the gas phase (Ohkouchi et al., 1999). In general, PAHs, for their chemical and physical characteristics, have a rather low solubility in water that tends to decrease with the increase of the molecular weight. Consequently, PAHs with more than four rings are always linked to particulate substances while the ones with low molecular weight (2 or 3 rings) can also found in aqueous systems. PAHs adsorbed in soils or sediments, once "blocked ", are more resistant to degradation processes by bacteria and / or those due to exposure to atmospheric agents and light (PM Gewend et al., 1981).
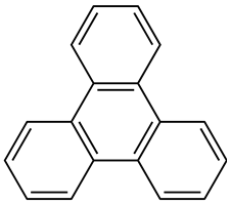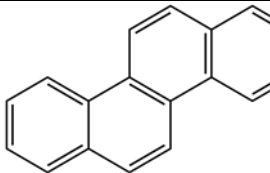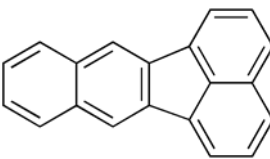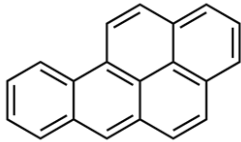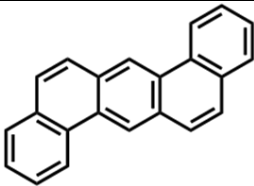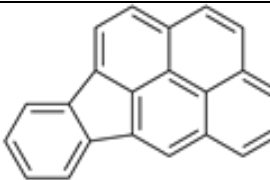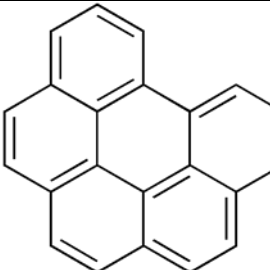
NAME	CHEMICAL COMPO-SITION	CHEMICAL RAPRESENTATION	MOLAR MASS	MELT-ING POINT	SOLU-BILITY IN WATER
NAPHTALENE	$C_{10}H_8$		128.174 g·mol^{-1}	-78.2 °C (172.8 °F ; 351.3 K) -80.26 °C (176.47 °F; 353.41 K) at 760 mmHg	19 mg/L (10 °C) 31.6 mg/L (25 °C) 43.9 mg/L (34.5 °C) 80.9 mg/L (50 °C) 238.1 mg/L (73.4 °C)
1-METHYLNAPHTHALENE	$C_{11}H_{10}$		142.20 g/mol	−22 °C (−8 °F; 251 K)	
1,6-DIMETHYLPHENANTHRENE	$C_{16}H_{14}$		206.28 g/mol		
ACENAPHTHYLENE	$C_{12}H_8$		152.196 g·mol^{-1}	91.8 °C (197.2 °F ; 364.9 K)	Insoluble

ACENAPHTHENE	$C_{12}H_{10}$		154.212 g·mol^{-1}	93.4 °C (200.1 °F ; 366.5 K)	0.4 mg/100 ml
FLUORENE	$C_{13}H_{10}$		166.223 g·mol^{-1}	116 to 117 °C (241 to 243 °F; 389 to 390 K)	1.992 mg/L
DIBENZOTHIOPHENE	$C_{12}H_8S$		184.26 g/mol	97 to 100 °C (207 to 212 °F; 370 to 373 K) (lit.)	insol.
PHENANTHRENE	$C_{14}H_{10}$		178.234 g·mol^{-1}	101 °C (214 °F; 374 K)	1.6 mg/L
ANTHRACENE	$C_{14}H_{10}$		178.234 g·mol^{-1}	216 °C (421 °F; 489 K) at 760 mm Hg	0.022 mg/L (0 °C) 0.044 mg/L (25 °C) 0.29 mg/L (50 °C) 0.00045 % w/w (100 °C,

					3.9 MPa)
3- METHYLDIBENZOTHIOPHE NE	C$_{13}$H$_{10}$S		198.29 g/mol		
2- METHYLDIBENZOTHIOPHE NE	C$_{13}$H$_{10}$S		198.29 g/mol		
METIL PHENANTRENE 1	C$_{15}$H$_{12}$		192.25 g/mol		
METHYLANTHRACENE-1	C$_{15}$H$_{12}$		192.25 g/mol		
4- METHYLDIBENZOTHIOPHE NE	C$_{13}$H$_{10}$S		198.29 g/mol		
2-METHYLPHENANTHRENE	C$_{15}$H$_{12}$		192.25 g/mol		

Name	Formula	Structure	Molar mass		
2-METHYLANTHRACENE	$C_{15}H_{12}$		192.25 g/mol		
DIMETHYLDIBENZOTHIOPHENE	$C_{14}H_{12}S$		212.31 g/mol		
FLUORANTHENE	$C_{16}H_{10}$		202.256 g·mol^{-1}	110.8 °C (231.4 °F; 383.9 K)	265 µg/l (25 °C)
9,10-DIMETHYLANTHRACENE	$C_{16}H_{14}$		206.28 g/mol		
PYRENE	$C_{16}H_{10}$		202.256 g·mol^{-1}	145 to 148 °C (293 to 298 °F; 418 to 421 K)	0.135 mg/L
BENZ[*A*]ANTHRACENE	$C_{18}H_{12}$		228.294 g·mol^{-1}	158 °C (316 °F; 431 K)	

TRIPHENYLENE	C_{18}H_{12}		228.294 g·mol^{-1}	198 °C; 388 °F; 471 K	
CHRYSENE	C_{18}H_{12}		228.294 g·mol^{-1}	254 °C (489 °F; 527 K)	Insoluble
BENZO[*K*]FLUORANTHENE	C_{20}H_{12}		252.316 g·mol^{-1}	217 °C (423 °F; 490 K)	
BENZO[*A*]PYRENE	C_{20}H_{12}		252.316 g·mol^{-1}	179 °C (354 °F; 452 K)	0.2 to 6.2 µg/L
DIBENZ[*A,H*]ANTHRACENE	C_{22}H_{14}		278.3466	262 °C (504 °F; 535 K)	
INDENO(1,2,3-CD)PIRENE	C_{22}H_{12}		276.3	164°C	Insoluble
BENZO[*GHI*]PERYLENE	C_{22}H_{12}		276.3307	278 °C (532 °F; 551 K)	

2.3.1.2   Sources and mechanisms of formation

PAHs can be formed during the slow maturation of organic matter (petrogenic origin) and during incomplete combustion or pyrolysis of organic materials (pyrogenic origin) (Soclo, Garrigues e Ewald 2000). PAHs of petrogenic origin represent a variable fraction of the chemical composition of fossil fuels. This type of origin implies a diagenetic formation characterized by relatively low temperatures (100-150 ° C) and formation times on a geological scale (millions of years).

The PAHs of pyrogenic origin are, instead, generated by the incomplete combustion or pyrolysis of organic substances. The formation mechanisms are not yet clear, but it can be hypothesized that, when pyrolysis occurs at high temperatures (650-900 °C) and in lack of oxygen, the formation of PAHs is favored; in fact, generally, as the oxygen-fuel ratio decreases, their formation speed increases. In general, a radical type mechanism has been proposed by various authors (Simoneit BRT, 1998; Andelman JB et al., 1970):

Initially there is a repolymerization in oxygen deficiency of the hydrocarbon fragments that form during the cracking process, a term which indicates the demolition process of the highest boiling fractions in more volatile fractions. During this process, the molecules rearrange into smaller molecules, and initially the prevalence of fragments containing only two carbon atoms is observed. These two free radicals carbon atoms react with an acetylene molecule (C_2H_2) leading to formation of another radical with four carbon atoms, that, in turn, can add another acetylene molecule forming a ring with six carbon atoms. At this point, the hydrogen atom, bound to the carbon of CH_2, can detach, giving rise to a molecule of benzene or adding other acetylene molecules for building chains that form further condensed benzene rings.

The PAH emissions can have natural or anthropogenic sources. The ones of natural origin are due to volcanic eruptions or forest fires; while the other ones are due to:

- burning of fossil products such as coke;

- combustion of organic substances such as wood, cellulose and tobacco;

- incineration of solid urban waste;

- exhaust fumes from internal combustion engines, especially those from diesel engines;

- electricity production plants;

2.3.2 Procedure for the PAHs analysis

The PAHs analysis were carried out on two samples of coal deposit, one from Permian and the other one from Triassic and two sample of fossil trunk, from Allan Hills Fossil Forest (Fig. 47). In the sample of fossil trunk, for each sample, were taken two sub micro-sample, one from the grey part and other one from the black part.

Each lyophilized specimen was crushed into small pieces with a hammer (e.g. 1-2 cm wide) and grounded by using an agate mortar (100 mm diameter) until to a fine powder was obtained. An aliquot of 5 g was sieved at 0.2 mm, and a sub-aliquot of 1 g was used for the PAHs extraction.

All the specimens were supplemented with 500 ng of deuterated PAHs mixture as internal standards (LGC- PAH-Mix 9 deuterated 10 µg/mL in Cyclohexane) and extracted according to the method described by Marynowsky et al. (2014). Briefly, the powdered samples were extracted at 75 °C by a micro-Soxhlet for 72 h with a dichloromethane:methanol (80:20, v/v) solution. The extracts were then transferred in 10 ml glass vials, sonicated for 1 min and centrifuged to deposit any eventually occurring solid phase. Thus, the supernatant liquid phase (i.e., solvent of extraction) was separated from the solid slurry and evaporated to a final a volume of about 1 ml. At this point, the liquid phase was placed on silica gel cartridges (Bond Elut Si, 1ml, Agilent Technologies), previously activated with 0.5 ml of $CHCl_3$, and sequentially eluted with solvents at different polarity to recover three fractions: aliphatic fraction using n-pentane eluting solvent, aromatic fraction using n-pentane:dichloromethane solution (in a 7:3 ratio, respectively), and finally, polar fraction using dichloromethane-methanol solution (1:1) (Marynowsky et al., 2014). The fractions were evaporated to small volume (10-200 µl) transferred in 250 50 µl insert vials and analyzed by GC-MS/MS.

The chromatographic analyses were performed on a fraction obtained with an Agilent 7890 gas chromatograph equipped with an agilent 7000 release D- Triple Quadrupole Mass spectrometer operating in Multiple reaction monitoring (MRM) mode. The column used for the separation was a Rxi-PAH 40m x 180 m x 0.1 m operating at a flow rate of 1.2 mL and the GC oven program was: from 40 °C to 150 °C at 20 °C/min and then from 150 °C to 340 °C at 10°C /min and the final temperature was held for 10 min for a total run time of 35.5 min. MS/MS conditions were set according to Andrianova and Quimbi (2019) A standard PAH mix (EPA 610 Polycyclic Aromatic Hydrocarbons Mixture by Supelco) was used to obtained a 5 points calibration curve (5, 10, 50, 100, 500 ppb

respectively for each analyte) by diluting the supelco standard in in dichloromethane. Each calibration level contained the same amount of internal standard as for the specimens before extraction. Finally, the data were analyzed by Agilent Mass Hunter software and the PAHs were identified by comparison of their retention times and spectral characteristics with the standards and the literature.
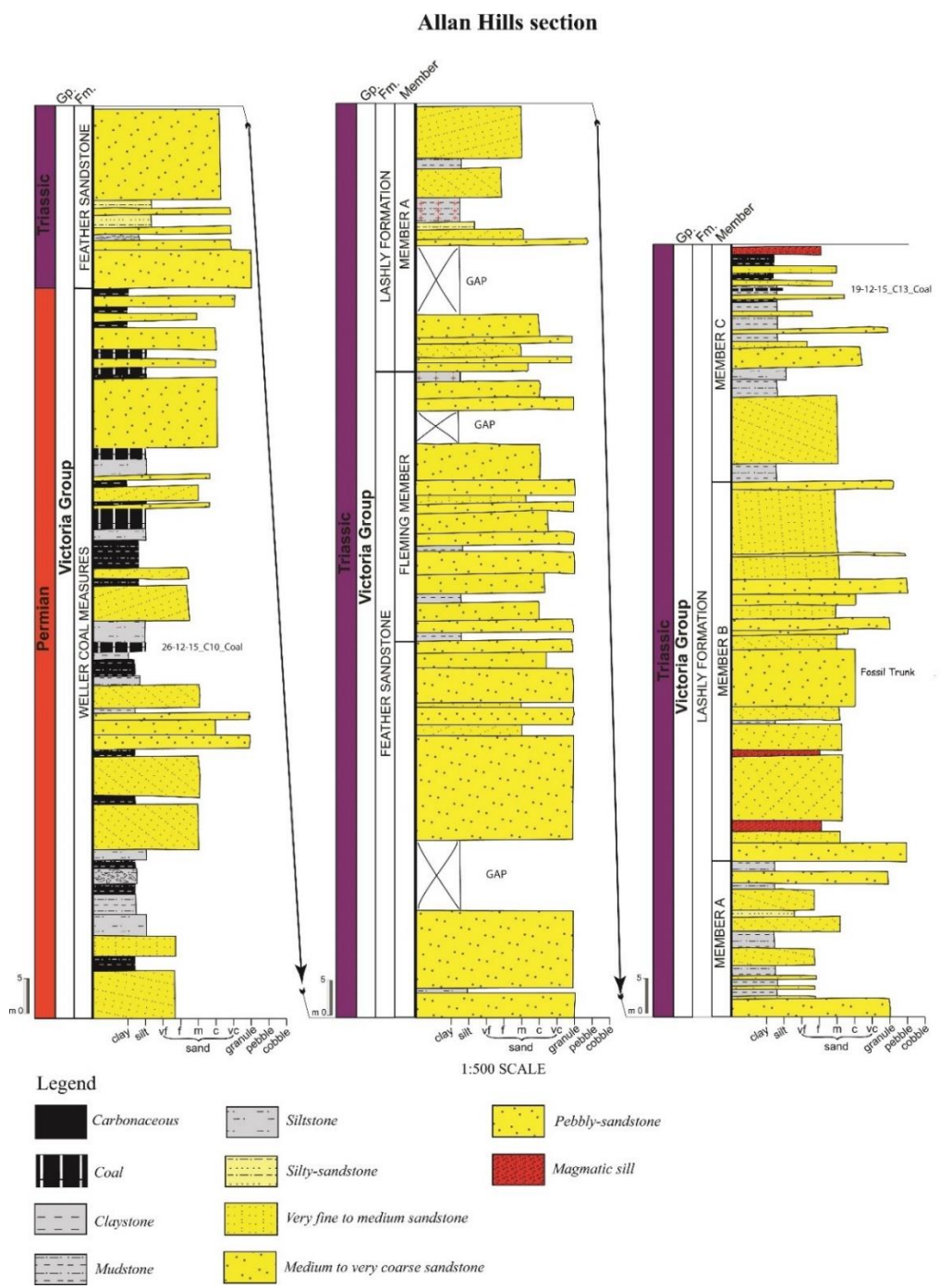
Figure 47 Stratigraphy position of samples utilized for PAHs analysis

2.4   Reflectance analysis

The reflectance analysis of vitrinite is a widely diffused technique for the reconstruction the paleotemperature history of the sedimentary rocks united to other geochemical and petrographic methods. The organic matter is, in the sedimentary rocks, the most temperature-sensitive constituent, for this reason the reflectance analysis is applied to vitrinite, pollen, spores and other organic components.

This method is used for estimating the maturity of the sediments and is often applied in the oil-reservoir reconstruction for establish the hydrocarbon maturity stages.

The irreversible changes undergone by the organic material are proportional to the increasing of the temperature during the diagenetic process. The temperature-related changes can be measured using a variety of optical and chemical maturity parameters. Maturation is a term commonly used in sedimentary basin studies to address thermally induced changes in nature of organic matter (Hartkopf-Froder et al., 2015).

Based on the organic maturation could be provided the temperature history or the maximum temperature reached from the sedimentary rocks.

Among optical maturity parameters, vitrinite and huminite reflectance are most used. However, optical and chemical properties of other macerals, palynomorphs and macrofossil with organic compounds or molecular composition of bitumen also serve as parameters of maturation (Hartkopf-Froder, et al. 2015).

In that case the reflectance analysis has been done on two different kind or coal: one piece of Permian coal from the deposit of the Weller Coal Formation, while the other one is a part of the fossil trunk.

The analysis, done in collaboration with UFRG- laboratory, had the purpose to reconstruct the different coalification/charcoalification process and, in addition aimed to highlight the diverse diagenetic process that affect the two samples, due to the nearness of the sill intrusion and a strongly diversification of the processes.

The reflectance measurement was made on the polished thin sections with a Leica MPV3 microphotometer. Polarized reflected light was used to measure reflectance in oil (with a reflective index of 1.515 at 26 _C).

2.5 SEM

In this study the sample, previously mapped and metallized, were observed using a scanning electron microscope (SEM -EDS).

The SEM- EDS is a microscope that uses a beam of focused primary electrons that hit the sample at a given point. Depending on the mineral present at that point we would have a different response, with the emission of various particles, including secondary electrons, backscattered electrons and x-ray emissions. These last emitted from the specimen are captured by a detector that transforms the signal into an electrical pulse which allows to follow the results on a monitor in real time, which are displayed in a graph with the various elements present on the abscissa. After the irradiation, the final data is automatically returned as a percentage of oxides.

Moving within the sample and applying this methodology at various points in the section we can have a picture of the chemical composition of the sample.

The samples analyzed were fragments of the fossil trunk and leaves, they have been posed on the stub and analyzed with gold metallization or without metallization.

Some of the fragments until be mounted on the stub were treated with HF and/or HCl for removing the inorganic material (mineralogic part) and make the anatomical features of the wood more visible.

3. Results

3.1 Dendrochronology results

In this project were analysed for the dendrochronology 13 samples (but here are reported just 11 of them because the other two don't cross match to the other). The minimum number of rings counting in the samples is 19 for the sample 9, while the maximum number of the rings is 147 in sample number 13. As regards the mean of the amplitude of the rings of each sample the minimum is 0,54 mm but this was counted in a sample that show features of roots; for the other samples the minimum recovered is in the sample 2 where the mean of amplitude is 0,82 mm. The maximum amplitude where instead found in sample number 17 where the mean is 2,89 mm. In the graphs below is reported the amplitude of the rings of each sample.

Sample 1 — $y = -13,29\ln(x) + 153,5$, $R^2 = 0,1154$

Sample 27 — $y = -20,16\ln(x) + 204,08$, $R^2 = 0,1484$

Sample 5

$y = 18,074\ln(x) + 95,927$
$R^2 = 0,0866$

Sample 6B

$y = -6,223\ln(x) + 71,04$
$R^2 = 0,0531$

Sample 23

$y = 4,4051\ln(x) + 213,41$
$R^2 = 0,0038$

Sample 13

y = -32,22ln(x) + 209,36
R² = 0,372

Sample 2

y = 14,913ln(x) + 43,615
R² = 0,1386

Sample 17

y = -96,87ln(x) + 514,63
R² = 0,5529

Sample 4

y = -70,33ln(x) + 309,86
R² = 0,8301

Sample 9

y = -11,14ln(x) + 246,19
R² = 0,0285

Sample 12

y = -11,94ln(x) + 123,16
R² = 0,0405
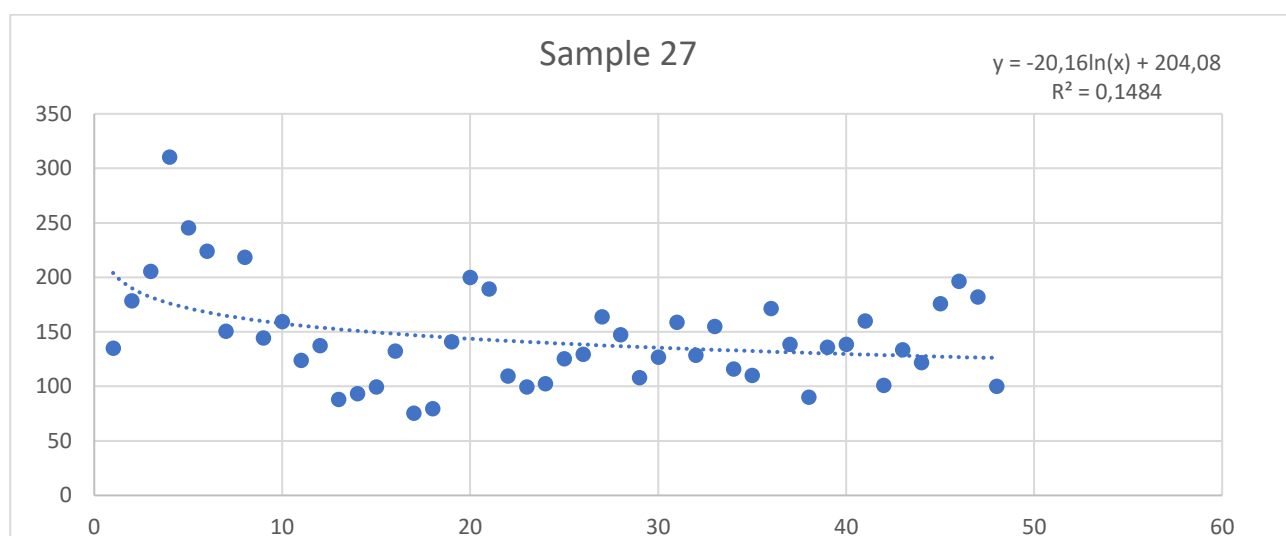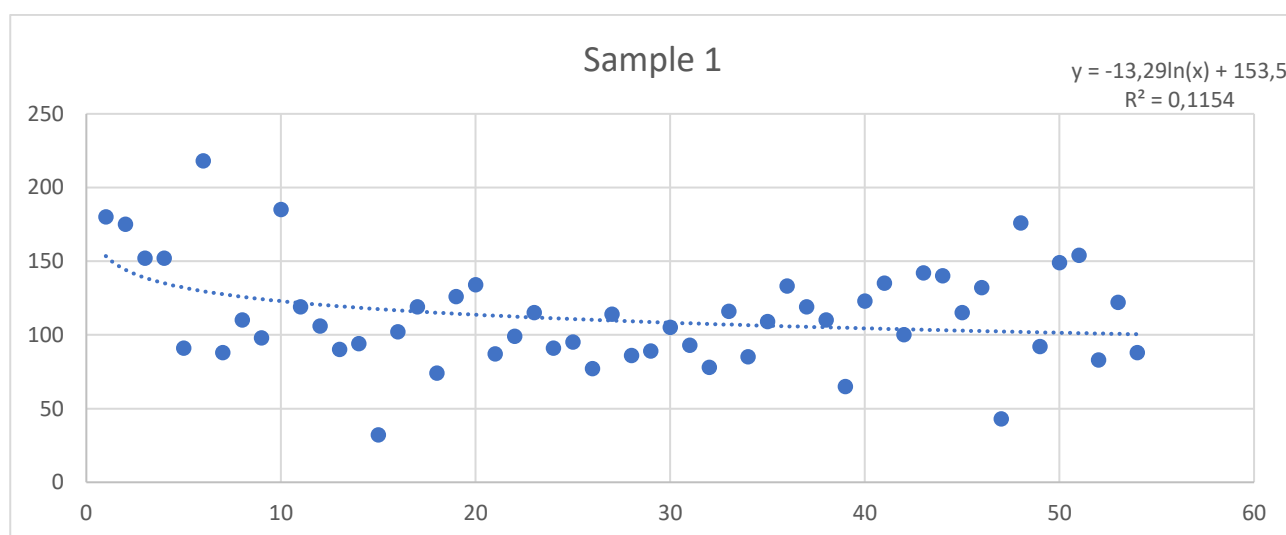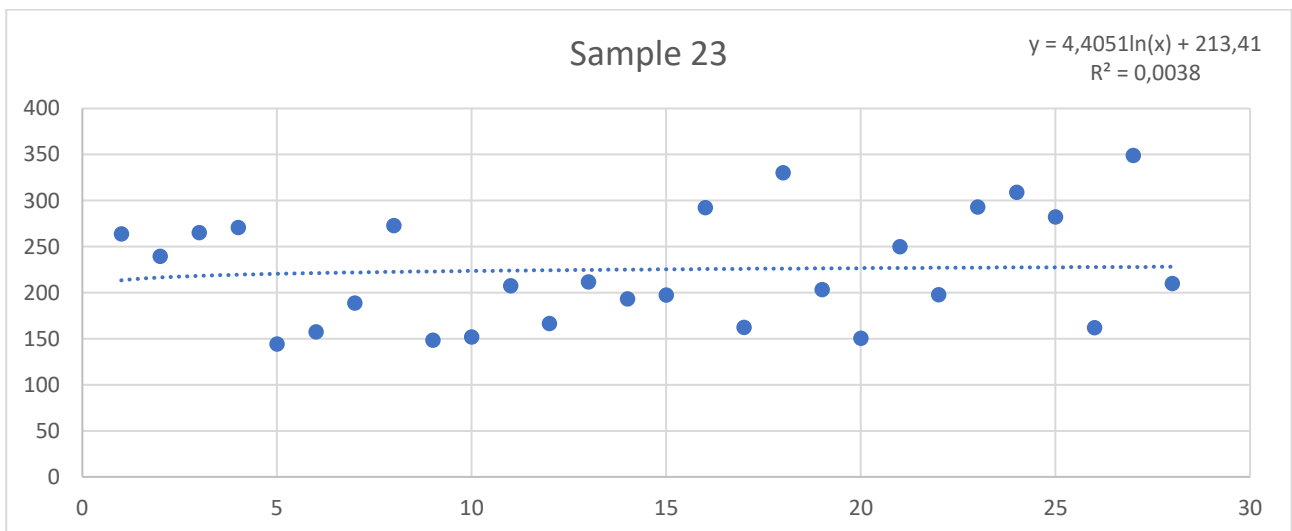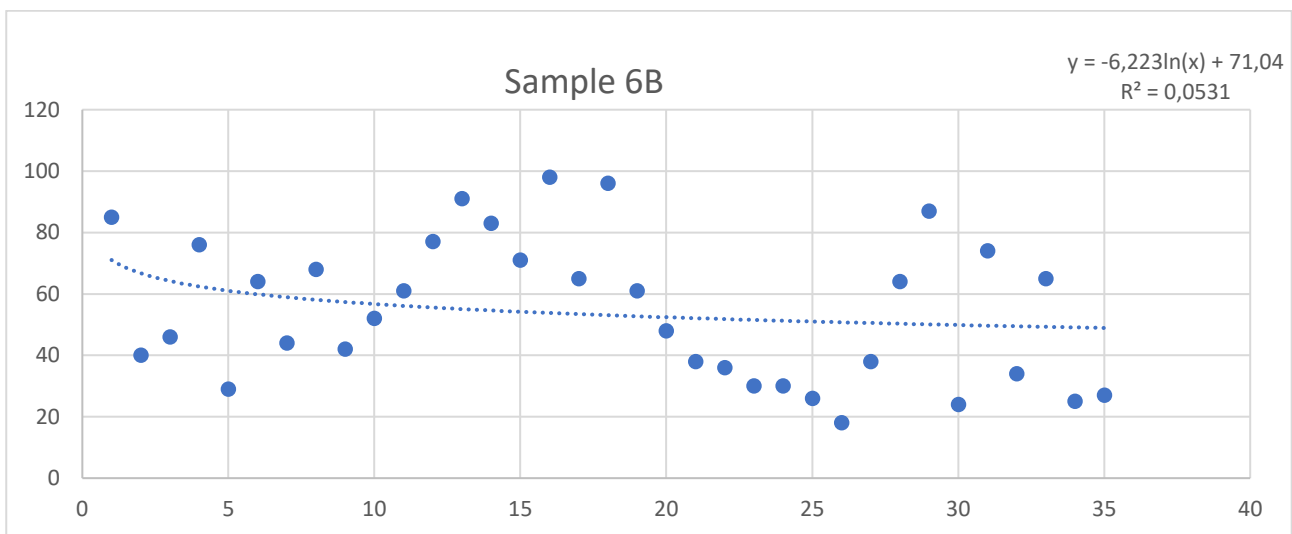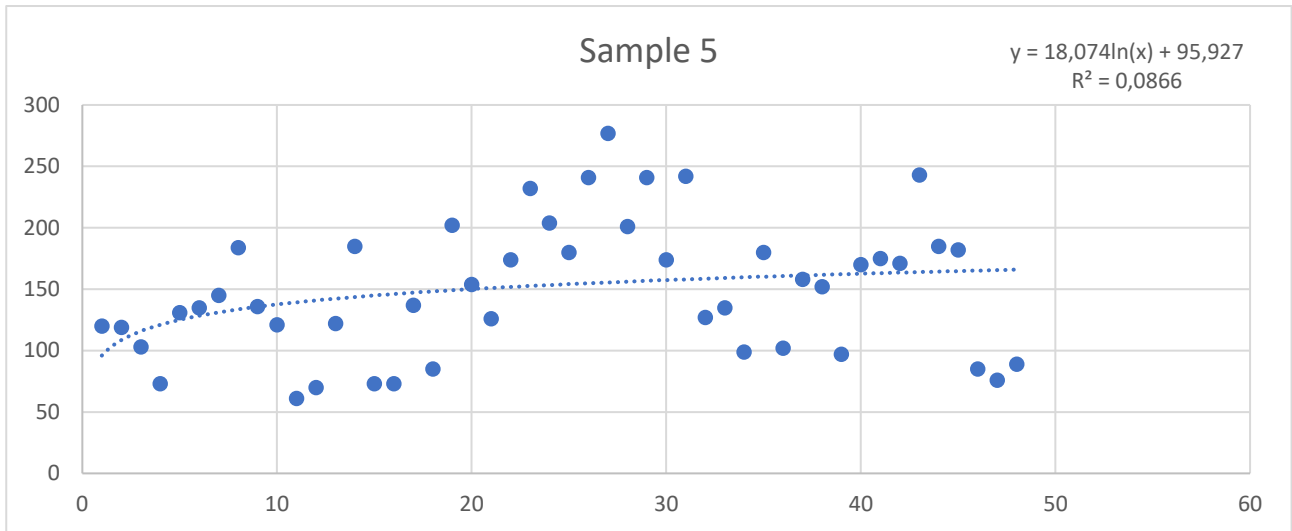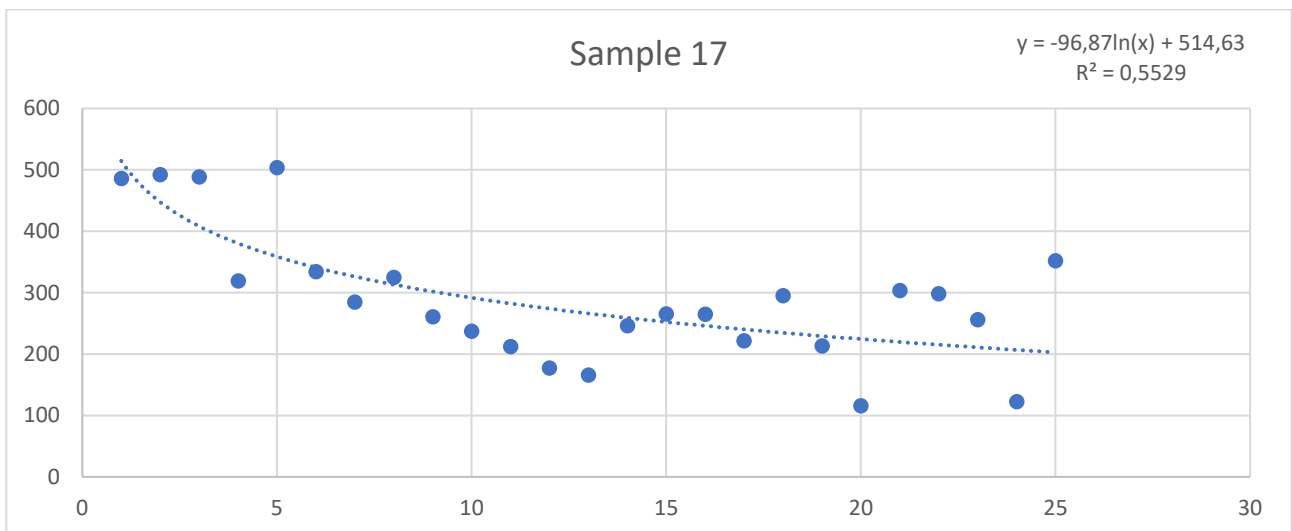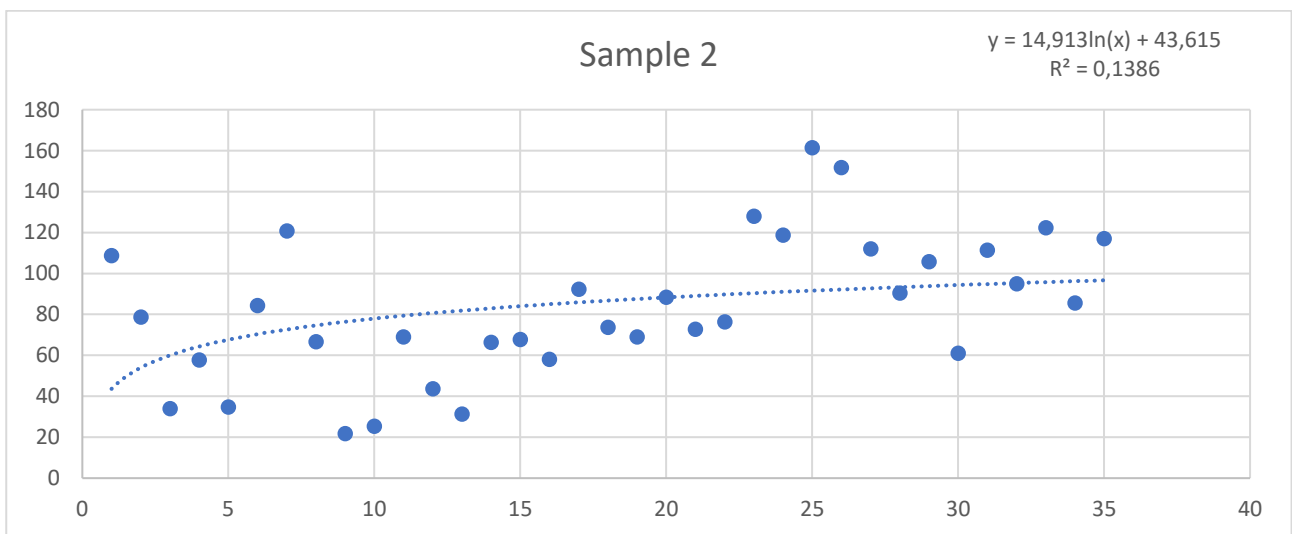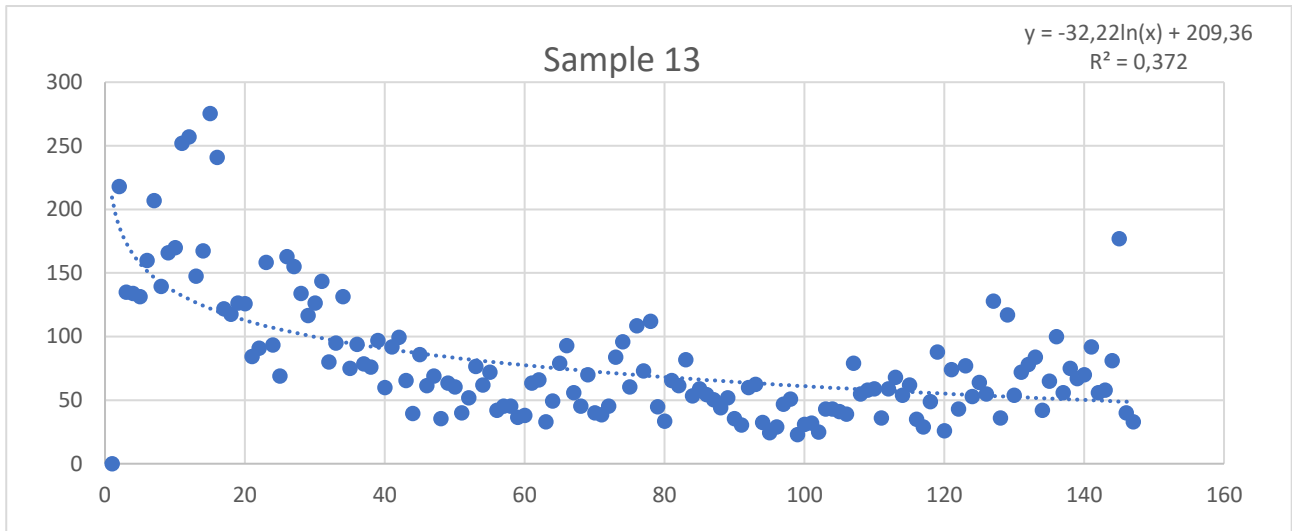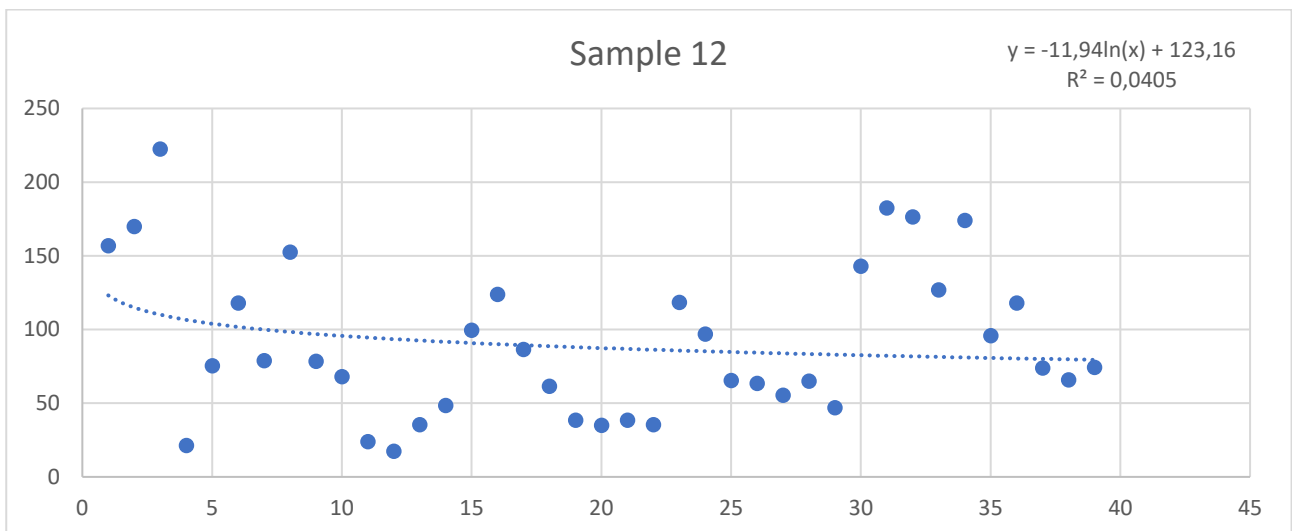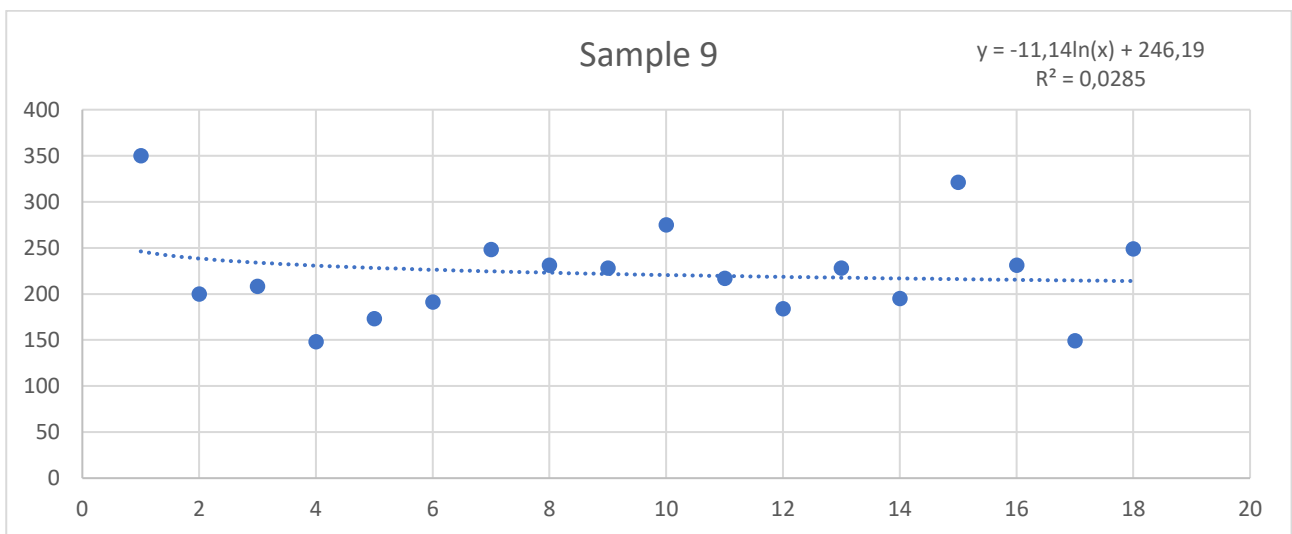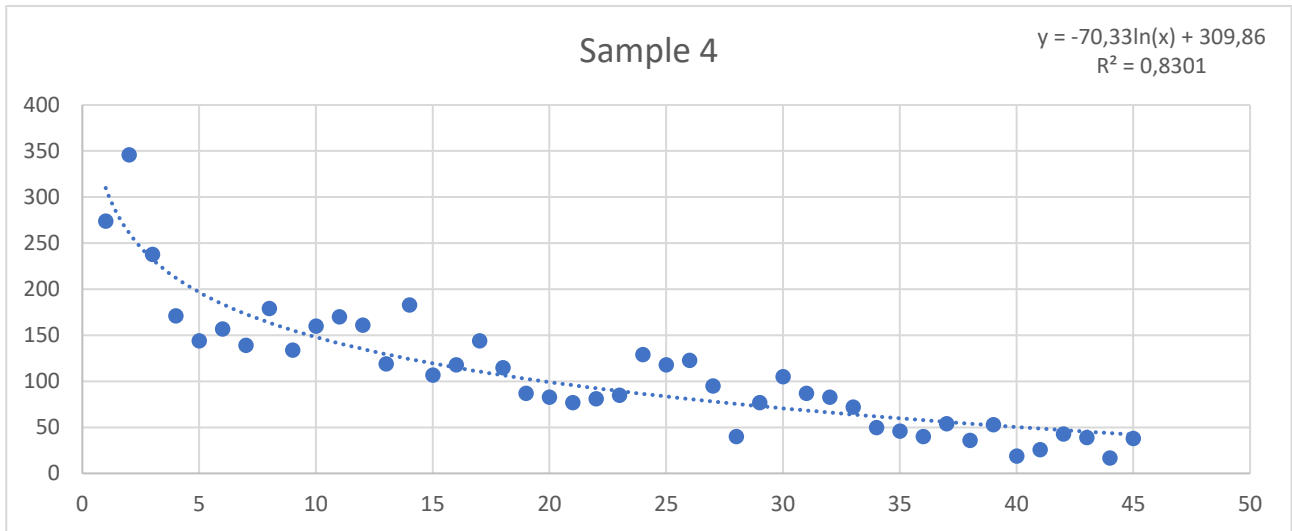
Ring #	Sample 1	Sample 27	Sample 5	Sample 6B	Sample 23	Sample 2	Sample 17	Sample 4	Sample 9	Sample 12
1	1,17	0,66	1,25	1,20	1,24	2,49	0,95	0,88	1,42	1,27
2	1,21	0,94	1,10	0,60	1,11	1,46	1,10	1,33	0,84	1,48
3	1,09	1,13	0,89	0,72	1,22	0,57	1,20	1,02	0,89	2,02
4	1,13	1,76	0,60	1,22	1,23	0,90	0,84	0,81	0,64	0,20
5	0,69	1,43	1,05	0,48	0,66	0,51	1,40	0,73	0,76	0,73
6	1,68	1,34	1,05	1,07	0,71	1,20	0,98	0,85	0,84	1,16
7	0,69	0,91	1,11	0,75	0,85	1,66	0,87	0,80	1,10	0,79
8	0,87	1,35	1,38	1,17	1,23	0,89	1,04	1,09	1,04	1,55
9	0,79	0,91	1,00	0,73	0,67	0,28	0,86	0,86	1,03	0,81
10	1,51	1,01	0,88	0,92	0,68	0,32	0,81	1,08	1,25	0,71
11	0,98	0,80	0,44	1,09	0,93	0,87	0,75	1,20	0,99	0,25
12	0,88	0,89	0,50	1,39	0,74	0,54	0,65	1,19	0,84	0,19
13	0,75	0,58	0,86	1,65	0,94	0,38	0,62	0,92	1,05	0,38
14	0,79	0,62	1,29	1,52	0,86	0,80	0,95	1,47	0,90	0,53
15	0,27	0,67	0,50	1,31	0,88	0,81	1,05	0,90	1,49	1,10
16	0,87	0,90	0,50	1,82	1,30	0,68	1,08	1,03	1,07	1,38
17	1,03	0,51	0,93	1,22	0,72	1,08	0,92	1,30	0,69	0,97
18	0,64	0,55	0,57	1,81	1,46	0,85	1,26	1,08	1,16	0,69
19	1,10	0,98	1,35	1,16	0,90	0,79	0,93	0,85		0,44
20	1,18	1,39	1,03	0,92	0,66	1,00	0,52	0,84		0,40
21	0,77	1,33	0,83	0,73	1,10	0,82	1,38	0,80		0,44
22	0,88	0,77	1,15	0,69	0,87	0,85	1,39	0,88		0,41
23	1,03	0,71	1,52	0,58	1,29	1,42	1,21	0,95		1,38
24	0,82	0,73	1,33	0,59	1,36	1,30	0,59	1,49		1,14
25	0,86	0,90	1,17	0,51	1,24	1,76	1,74	1,41		0,77
26	0,70	0,94	1,56	0,35	0,71	1,64		1,52		0,75
27	1,04	1,19	1,78	0,75	1,53	1,21		1,22		0,66
28	0,79	1,08	1,29	1,27	0,92	0,97		0,53		0,78
29	0,82	0,79	1,54	1,74		1,13		1,05		0,57
30	0,97	0,94	1,11	0,48		0,65		1,49		1,73
31	0,86	1,18	1,53	1,49		1,17		1,27		2,22
32	0,73	0,96	0,80	0,69		1,00		1,26		2,16
33	1,08	1,16	0,85	1,32		1,28		1,13		1,56
34	0,80	0,87	0,62	0,51		0,89		0,81		2,15
35	1,03	0,83	1,12	0,55		1,21		0,77		1,19
36	1,26	1,30	0,63					0,69		1,47
37	1,13	1,06	0,98					0,97		0,92
38	1,05	0,69	0,94					0,67		0,83
39	0,62	1,05	0,60					1,02		0,94
40	1,18	1,07	1,05					0,38		
41	1,30	1,24	1,07					0,53		
42	0,96	0,79	1,05					0,92		
43	1,37	1,04	1,48					0,86		
44	1,36	0,96	1,13					0,39		
45	1,12	1,39	1,10					0,90		
46	1,29	1,55	0,51							
47	0,42	1,44	0,46							
48	1,72	0,80	0,54							
49	0,90									
50	1,47									
51	1,52									
52	0,82									
53	1,21									
54	0,88									

Table 1 Amplitude of rings

Ring #	Sample 13	Ring #	Sample 13	Ring #	Sample 13
1	1,72	50	0,69	99	0,41
2	0,92	51	0,46	100	0,56
3	0,62	52	0,60	101	0,58
4	0,65	53	0,90	102	0,46
5	0,67	54	0,74	103	0,79
6	0,86	55	0,86	104	0,80
7	1,15	56	0,51	105	0,77
8	0,81	57	0,56	106	0,74
9	0,99	58	0,56	107	1,50
10	1,04	59	0,46	108	1,06
11	1,59	60	0,48	109	1,12
12	1,67	61	0,81	110	1,15
13	0,98	62	0,85	111	0,71
14	1,14	63	0,43	112	1,17
15	1,91	64	0,65	113	1,36
16	1,71	65	1,04	114	1,09
17	0,88	66	1,24	115	1,26
18	0,87	67	0,75	116	0,72
19	0,95	68	0,62	117	0,60
20	0,97	69	0,96	118	1,02
21	0,66	70	0,55	119	1,85
22	0,72	71	0,54	120	0,55
23	1,28	72	0,64	121	1,58
24	0,77	73	1,19	122	0,93
25	0,57	74	1,38	123	1,67
26	1,38	75	0,88	124	1,16
27	1,33	76	1,59	125	1,41
28	1,17	77	1,08	126	1,22
29	1,03	78	1,67	127	2,87
30	1,13	79	0,68	128	0,81
31	1,30	80	0,51	129	2,67
32	0,74	81	1,00	130	1,24
33	0,89	82	0,95	131	1,67
34	1,24	83	1,27	132	1,82
35	0,72	84	0,84	133	1,98
36	0,91	85	0,93	134	1,00
37	0,77	86	0,87	135	1,56
38	0,75	87	0,81	136	2,42
39	0,98	88	0,71	137	1,37
40	0,61	89	0,85	138	1,84
41	0,95	90	0,59	139	1,66
42	1,04	91	0,51	140	1,75
43	0,69	92	1,01	141	2,32
44	0,42	93	1,06	142	1,42
45	0,93	94	0,56	143	1,49
46	0,67	95	0,42	144	2,09
47	0,76	96	0,50	145	4,61
48	0,40	97	0,82	146	1,05
49	0,71	98	0,90	147	0,87

In the table 3, for each sample, are report the number of rings and the mean of the amplitude of the rings.

Sample	# Rings	Mean
Sample 1	54	113,06
Sample 27	49	144,99
Sample 5	49	148,90
Sample 6B	35	54,66
Sample 23	28	224,09
Sample 13	147	83,19
Sample 2	35	82,87
Sample 17	25	289,88
Sample4	45	108,04
Sample 9	19	223,67
Sample 12	40	90,53

Table 2 Total numbers of the Rings and Means samples-by-samples

The amplitude of the rings are now detrending with the linear equation for delete the component due to normal factor of growing. With this procedure the shifting of the amplitude of rings remain due just to the external causes.

The ring width variation in this master chronology is supported by an averaging of between two or four specimens per growth increment, indicating the extent of replication of these ring width signals in the population of fossil wood. An ensemble of Gleilaughikeit (Gl) (percent parallel co-variation in ring widths between two samples), the correlation coefficient (cc), and t-statistics (Tho = t-statistic with a Hollstein method of ring width normalization, TBP = t-statistic with the Baillie/Pilcher ring width normalization, after (Baillie 1973) are used to assess quality of the cross-match (Table 4).

SAMPLE	TBP	THO	CC	GL	OVERLAP
27-1	0	0	-0,187	62,5	44
1-5-	3,14	2,48	-0,04	70,8	48
1-6B	1,72	1,13	0,27	67,6	17
27-5-	2,39	2,5	0,26	64,7	34
27-6B	1,32	1,8	0,23	69	21
5-6B	1,95	1,84	0,55	64,3	35
5-23-	2,9	2,2	0,83	35,7	7
13-23-	1,25	1,43	0,06	72,2	27
23-2-	0,87	0,4	0,15	69,6	28
2-13-	2,19	2,5	0,29	78,6	35
17-13-	2,7	2,46	0,51	70	25
4-13-	2,1	2,58	-0,34	64,4	45
9-13-	0,98	1,02	0,15	83,3	9
9-12-	2,42	2,3	0,57	75	18
13-12-	1,2	1,93	0,19	79,4	17
12-4-	0	0	0,65	70	5

Table 3 Statistic values of the matching samples

In the samples here analysed Gl is comprised between 62,5 and 83,3, with an exception of 35,7 between sample 5 and 23 (Gl has values from 0 to 100, where 100 is perfect covariation in ring width trends), correlation coefficient (cc) ranged from -0,34 to 0.83, Tho ranged from 0 to 2,48, and TBP ranged from 0 to 3,14.

The maximum overlap is between sample 1 and 5 with a total of 48 rings.

The graphical data show in the previous chapter are now detrending from the exponential growth function for focus the difference of amplitude of the rings on the external causes.

In the graph is reported the amplitude of the rings of all the samples and the dark line is the mean
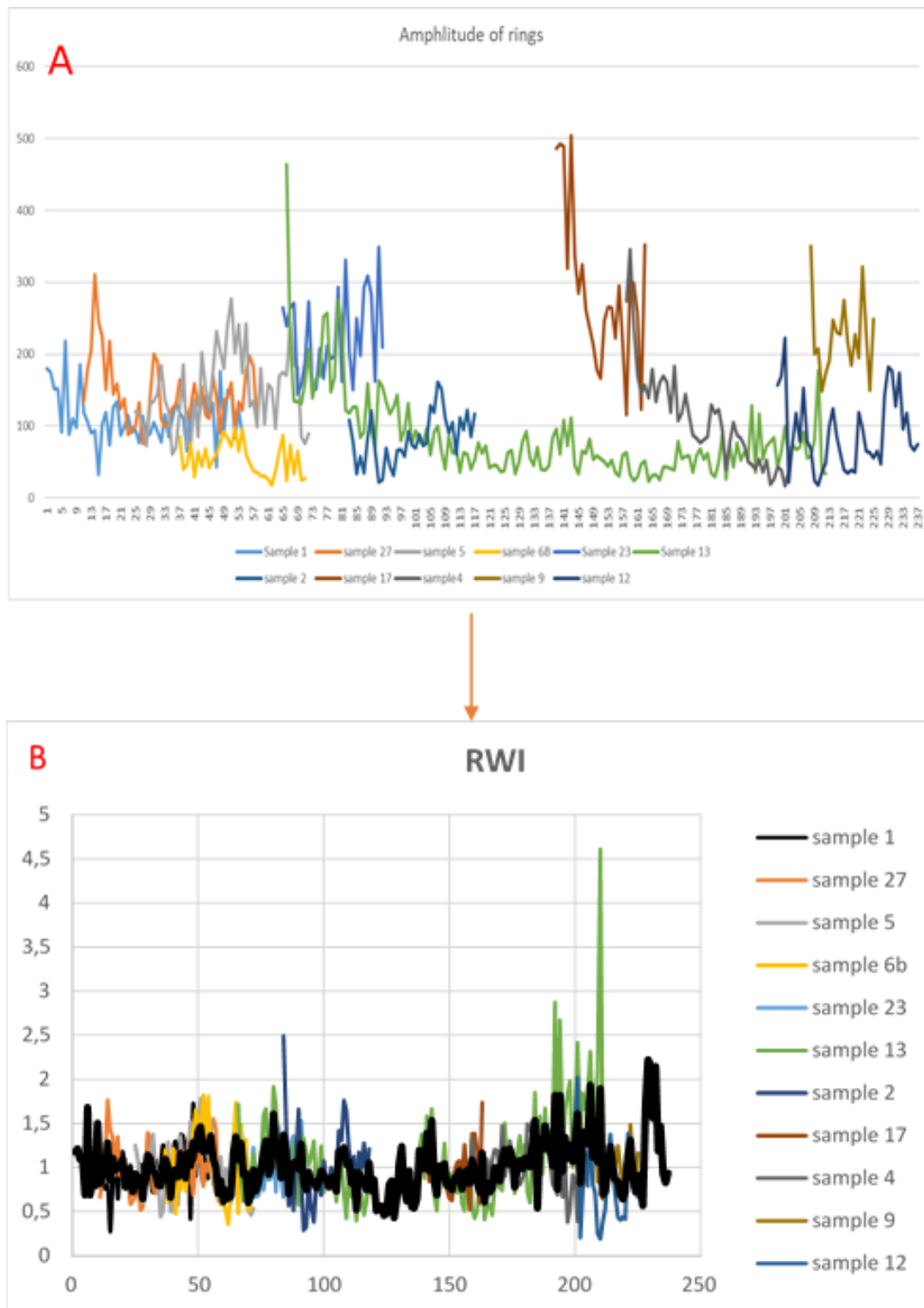
Figure 48 Cross-Matching of Samples

The cross match of this samples shows a climatic history of 237 years, this is the longer data existent about the dendrochronology of fossil samples. Moreover, this is a very strong data because in the crossmatch often fit together 3 or 4 samples (Fig. 48).

3.2 Carbon Isotope results

 Carbon isotope ratios in tree rings of evergreen trees display symmetrical variation while deciduous trees display pronounced asymmetrical carbon isotope ratio variation within tree rings. These distinct patterns open the possibility that high-resolution carbon isotope analysis of fossil wood can determine a deciduous or evergreen habit for fossil trees.

The Carbon Isotope pattern in the growth rings are distinct between evergreen and deciduous trees, the ratio between ^{12}C and ^{13}C follow two different trends.

In the table 5 are reported the $\delta^{13}C$ in each point analysis (calculate as a medium from the $\delta^{13}C$ in the microsamples) in the four analysed samples.

Sample	#	δ13CVPDB (‰)	Sample	#	δ13CVPDB (‰)
1	1	-23,05	12	1	-24,32
	2	-24,39		2	-24,28
	3	-24,15		3	-24,16
	4	-24,44		4	-24,32
	5	-24,31		5	-24,42
	6	-24,33		6	-24,15
	7	-24,42		7	-24,39
	8	-24,02		8	-24,38
	9	-23,84		9	-24,32
	10	-24,08		10	-24,26
2	1	-23,84		11	-24,35
	2	-24,20		12	-24,32
	3	-24,46		13	-24,21
	4	-24,52		14	-24,18
	5	-24,64		15	-24,17
	6	-24,87		16	-24,32
	7	-24,66		17	-24,44
	8	-24,81		18	-24,27
	9	-24,95		19	-24,32
	10	-24,95		20	-24,28
	11	-24,97	13	1	-23,79
	12	-24,92		2	-23,97
				3	-24,31
				4	-24,15
				5	-24,27
				6	-24,05
				7	-24,37
				8	-24,31
				9	-24,32

Table 4 Carbon isotope results ring by ring in 4 different samples
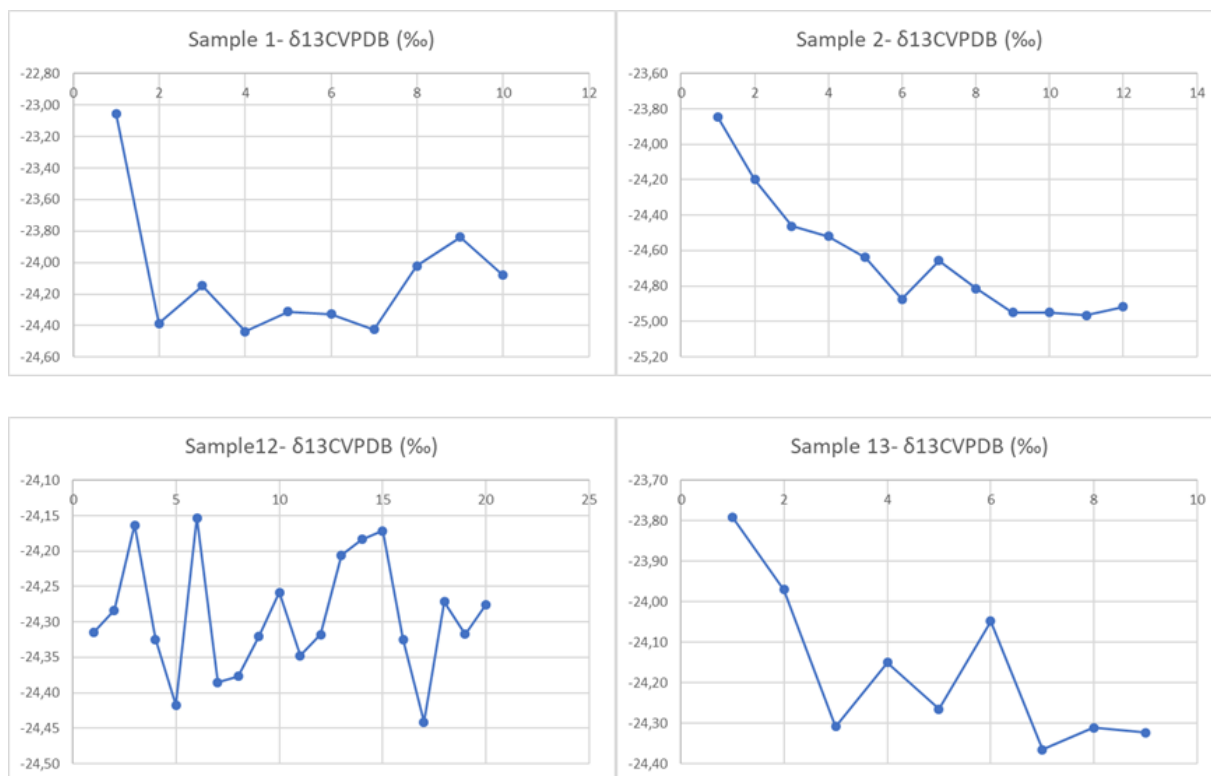
Table 5b: Carbon isotope results ring by ring in 4 different samples, graphical rapresentation

A total of 157 microsamples of 52 growth rings from 4 fossil trunks were analysed. Microsamples were collected in a number of 5-10 for each growth rings, based on the amplitude of rings, from 10 to 20-point analysis.

Sample 1- 20 microsamples were analysed (medium weight 28,23 mg) from 10point analysis from different growth rings and from the pith of the sample. The average values of $\delta^{13}C$ is -24,10‰(± 0,42).

Sample 2- 35 microsamples (medium weight 28,11 mg) from 12point analysis. The average values of $\delta^{13}C$ is -24,65‰(±0,35)

Sample 12- 62 microsamples (medium weight 27,98 mg) from 20 point analysis. The average values of $\delta^{13}C$ is -24,29‰(±0,08)

Sample 13- 31 microsamples (medium weight 28,35 mg) from 11 point analysis, the last two point analysis were situated 1 cm below the previous microsample for assessing a possible shifting of $\delta^{13}C$ from the external to the internal tissues of the plants. The average values of $\delta^{13}C$ is -24,17‰(±0,20).

The total of the samples presents an average δ^{13}C of -24,32‰ (± 0,32) and are represent together in the Fig. 49.
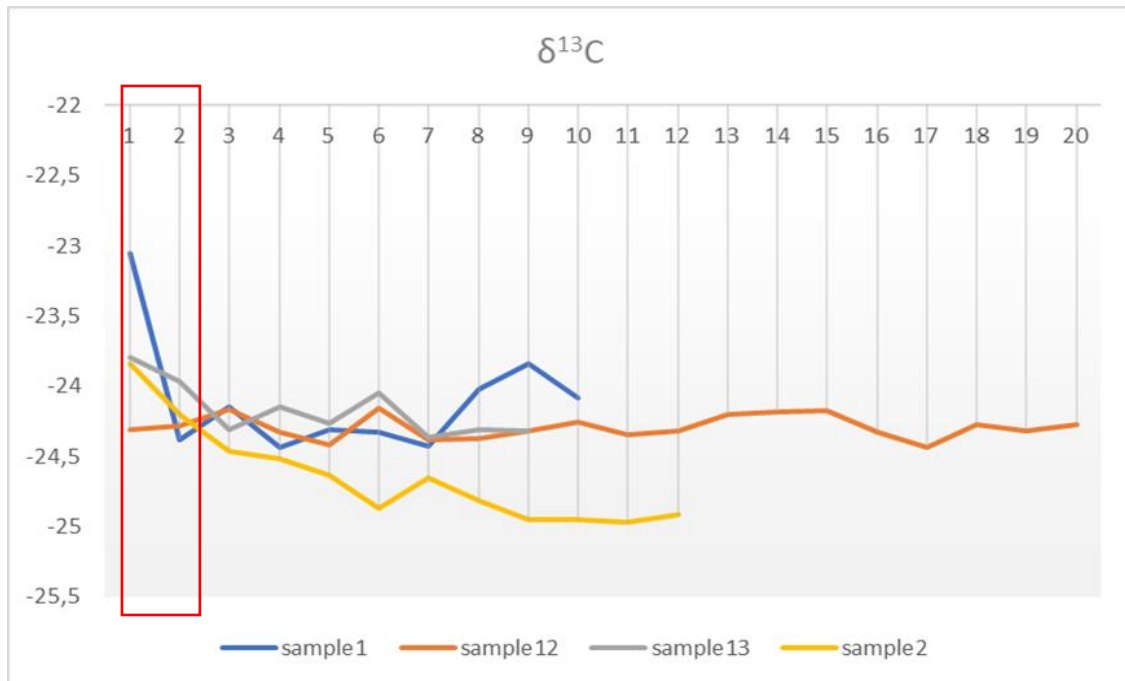
Figure 49 Carbon Isotope ratio for each sample, from the external part in measure 1 to the internal

From the graph is clear that 3 of the 4 samples suffer of an abrupt shifting of δ^{13}C in the first 2-3 analysis point, corresponding to the first growth rings. Only the samples that present the standard deviation 0,08, less than the standard deviation in the totally of the sample (0,32) not present an initially shifting (sample12). This shift could be attributed to an external factor that affect the major part of the samples, but not the totally.

Expect for the first anomalous growth rings, in the more internal part of the samples could be not possible to individuate different trends of δ^{13}C.

3.3 PAHs results

The PAHs analysis were carried out on two different samples of coal, one from Permian and the other one from Triassic, and from a fossil trunks of Allan Hills fossil forest. The Permian sample has been collected in the upper part of the Weller Coal Formation, from a level of coal (C10); while the Triassic one from a level of Coal of Lashly Formation (Member C) (C13). From the fossil trunks two subsamples on the basis of black or grey colour were differentiated (Table 6).

	Grey log	Black log	Charcoal 13	Charcoal 10
Naphthalene	4,5	0,6	0,4	0,1
methylnaphthalene	12,7	2,3	0,3	0,4
1,6-DimethylNaphthalene	0,5	0,0	0,0	0,0
Acenaphthylene	11,4	1,0	0,9	0,3
Acenaphthene	5,9	0,5	0,5	0,1
Fluorene	1,2	0,1	0,1	0,0
Dibenzothiophene	13,9	52,4	57,7	90,9
Phenantrene	1,0	2,3	13,6	2,5
Anthracene	1,5	0,3	1,6	0,3
3-MethylDibenzothiophene	3,3	2,6	0,9	0,5
MethylPhenanthrene	3,0	1,8	2,8	0,2
MethylAnthracene	3,8	2,6	4,3	0,4
4,6-DimethylDibenzothiophene	4,6	0,6	0,4	0,1
Fluoranthene	2,5	1,7	2,3	0,2
9,10-DimethylAnthracene	1,0	0,1	0,1	0,0
Pyrene	2,5	6,7	3,1	0,2
Benzo[a]anthracene	1,3	0,5	0,5	0,3
Tryphenylene	0,9	1,6	0,8	0,1
Chrysene	1,8	3,6	2,2	1,0
Benzo[b]fluoranthene	4,9	5,1	1,0	0,5
Benzo[k]fluoranthene	2,3	0,9	0,7	0,2
Benzo[a]pyrene	2,6	8,5	4,1	0,8
Dibenzo[a,h]anthracene	6,5	1,2	0,6	0,3
Indeno[1,2,3-CD]pyrene	3,0	1,1	0,3	0,2
Benzo[g,h,i]perylene	3,6	1,9	0,7	0,3

Table 6 PAHs composition on Carbon weight of samples; Red petrogenic PAHs, Green pyrogenic PAHs

The PAHs formed during high temperature incomplete combustion of biomass and/or fossil fuel (Alves, et al. 2009) and their characteristic distribution can survive for hundreds of millions of years

in sedimentary rocks and can used as indicators of paleowildfires and, in some exceptional cases, of other pyrolytic processes (Marynowski, et al. 2014).

Usually the distribution of PAHs in sedimentary organic matter is dominated by 3 and 4 ringed polynuclear aromatic hydrocarbons (Shen, et al. 2011), and the PAHs >4 ringed polynuclear aromatic hydrocarbons are predominantly attributed to pyrogenetic materials, for their temperature of formation (Hossain et al., 2013), (Stogiannidis and Laane 2015).
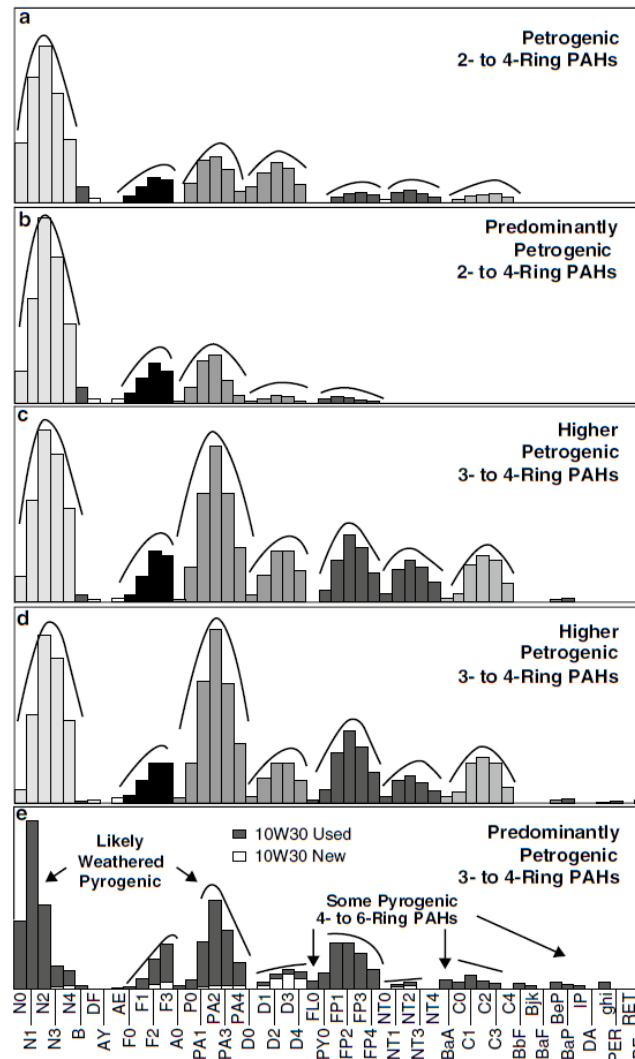
Figure 50 Source profiles/fingerprints of characteristic petrogenic PAHs. (a) crude oil, (b) fuel oil #2,

(c) fuel oil #4, (d) fuel oil #6, (e) new and used lubricating oils. Stoginnidis and Laane 2015

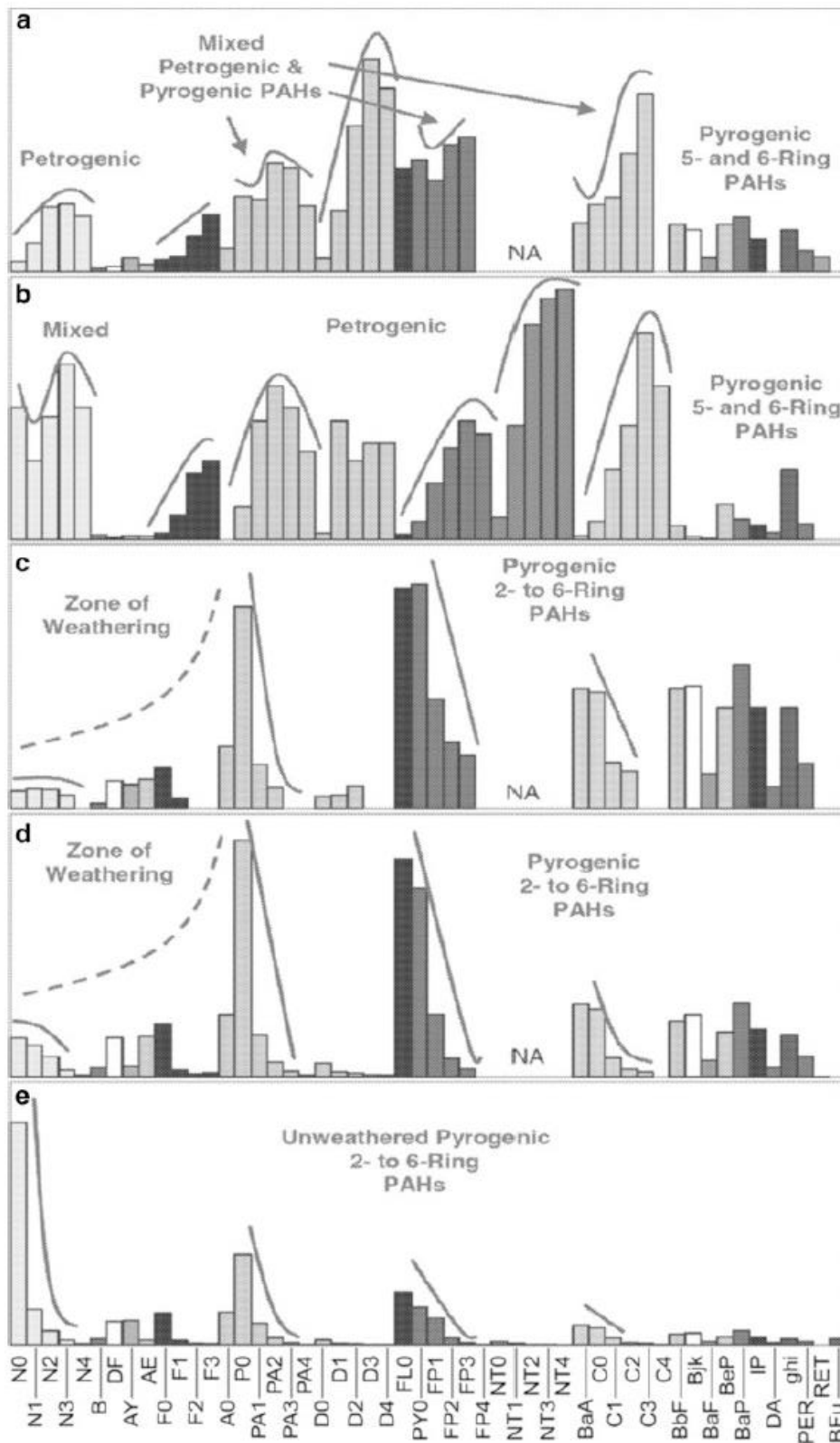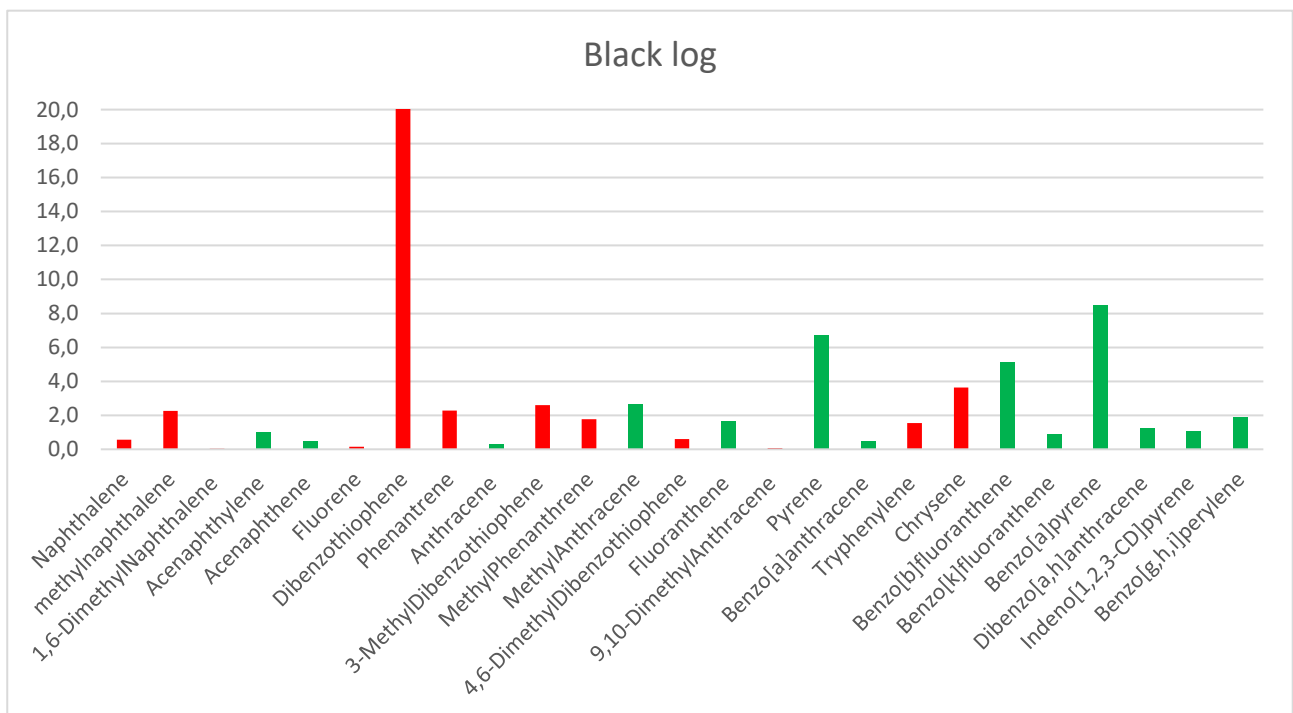*Figure 51Mixed PAH profiles. (a) hot patch (paving material), (b) modern (2005) roadway paving,*

(c, d) older types of roadway paving, (e) coal tar oil. NA: not analysed. *Stoginnidis and Laane 2015*

Grey log

Black log

Charcoal 13

Charcoal 10
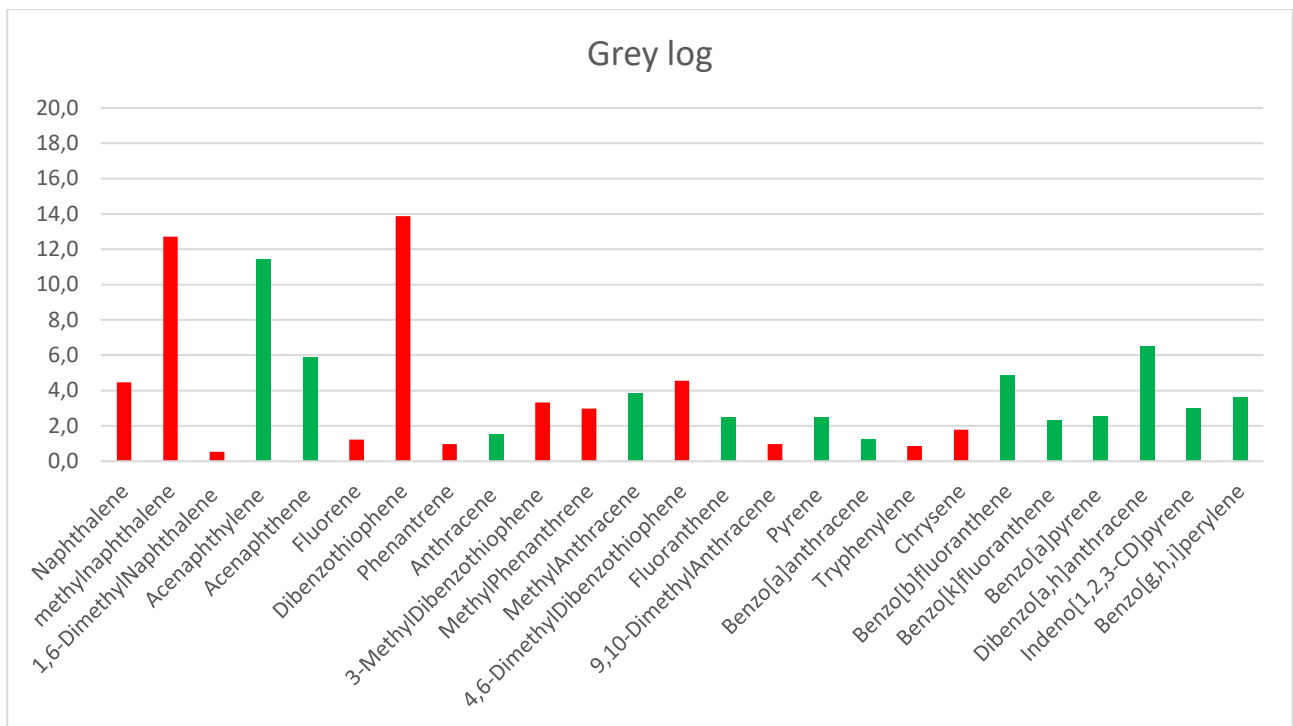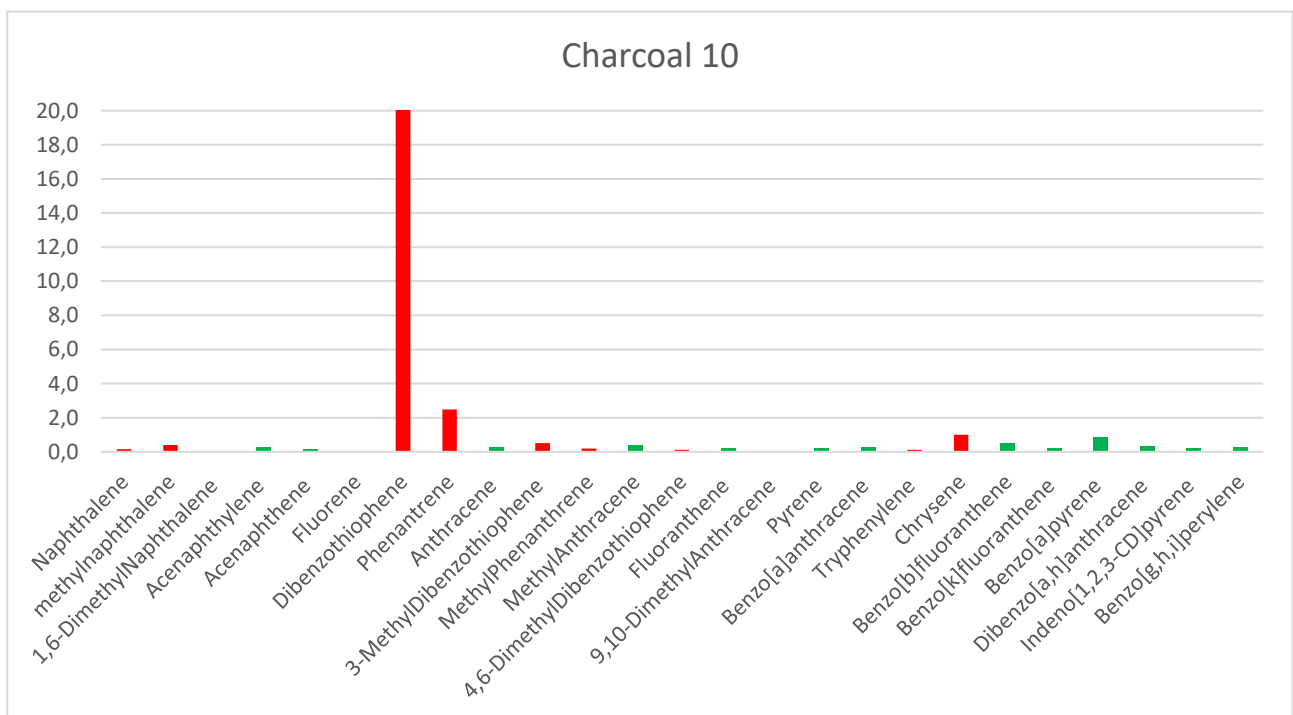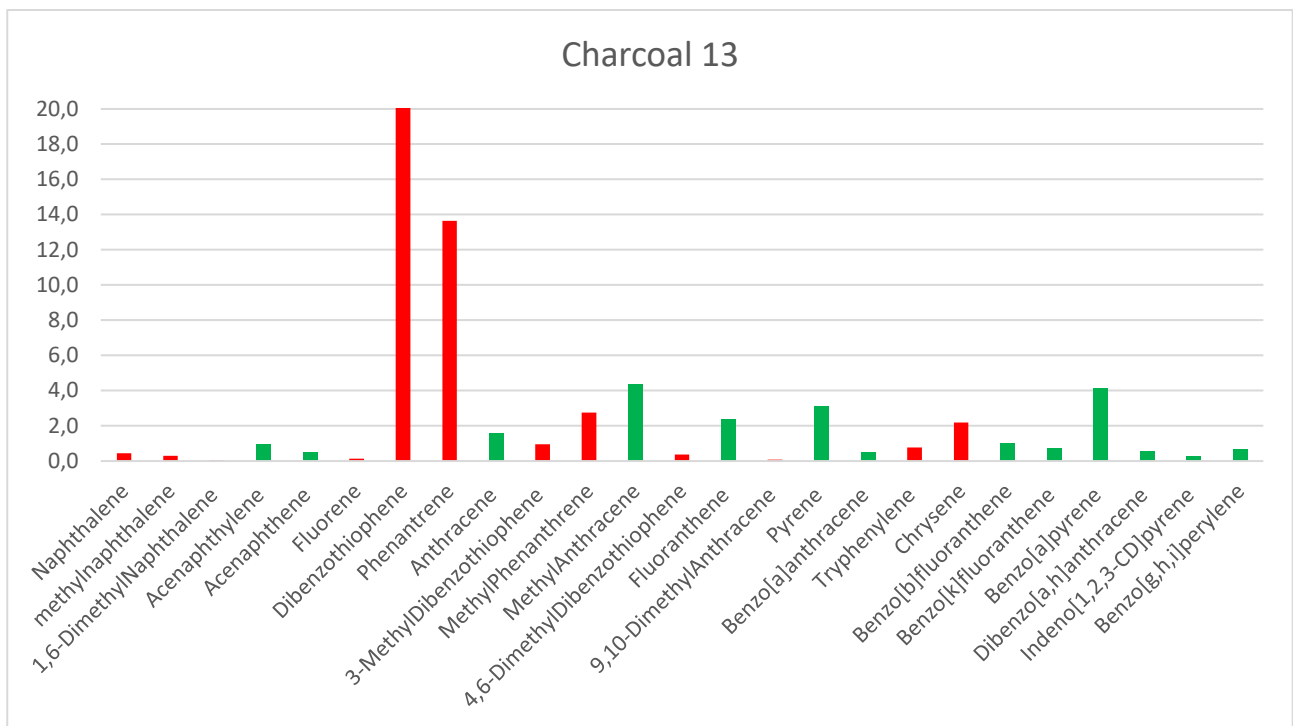
The nature of PAHs has been widely used to have information on the origin of materials and processes that have constituted not only as single component of PAHs but also as a ratio between them producing characteristics patterns. For an identification of the origin of the materials, among different types of relationships used:

- Methylphenantrene/Phenanthrene (MP/P) this ratio used to differentiate diagenetically derived PAHs from combustion/pyrogenic derived PAHs (Yunker, 2002); this is also used to distinguish the oxidation of organic matter, if caused to a hydrothermal or only diagenetic input. (Prahl and Carpenter 1983) suggest that values <1 indicate combustion, while MP/P> 2 indicates a diagenetic source

- Fluorantene/ Pyrene (Fla/Py) this ratio was firstly proposed by (Sicre, Marty e Saliot 1987) and confirmed by (Baumard et al., 1998) could be also used as a combustion parameters; Fla/Py>1 indicate a pyrolytic origins, while Fla/Py<1 are associated to petroleum source PAHs.

- BaAn / 228 (BaA / BaA + Ch)> 0.5 indicates combustion, while> 0.5 indicates a diagenetic formation source (even if the limit at 0.5 is sometimes "moved") (Yunker, 2002).

Despite of numerous studies based on the ratio of PAHs utilized to understand the source of the material, we didn't find examples of ratios calibrated for studying on petrified fossil trunk. For this reason, in many cases it could be inappropriate to base our results on the ordinary ratios therefore we have mainly considered for this study the prevalence PAHs-petrogenic source and PAHs-pyrolytic source and relative pattern. However, if we consider the molecular weight of PAHs, the rate of low versus high molecular weight parent PAHs (De Luca et al., 2004) could confirm the findings found by considering the PAH patterns. Values <1 indicate pyrogenic and values >1 indicate petrogenic origin.

L/H = PA0 + FP0/ BaA+C0+BkF+BaP+IP+DA+gh

Sample	L/H
Grey log	0,35
Black log	0,62
Charcoal 13	2,30
Charcoal 10	1,03

In the two samples analysed from fossil trunks is clear that an high number of pyrolytic-source PAHs are present in high quantity as: *Acenaphthylene, Acenaphtene, Anthracene, methyl antracene1, methyl anthracene 2, Fluoranthene, Pyrene, Benzo*[a]*anthracene, Benzo*[b]*fluoranthene, Benzo*[k]*fluoranthene, Benzo*[a]*pyrene, Dibenzo*[a,h]*anthracene, Indeno*[1,2,3-CD]*pyrene, Benzo*[g,h,i]*perylene;* that suggest a pyrolytic event for the origin of this PAHs, as the presence of a paleofire. Moreover, the graphs show a shifting of the PAH compounds distribution between the grey and the black log (the internal and external part), this could be due to post-depositional circulation of fluid rich of silica gel that having a strong affinity with PAHs moved inside the organic material and concentrate the PAHs.

As above mentioned, the two samples of coal came from two different formations: sample C10 from Permian (Weller Coal Formation) and sample C13 from Triassic (Lashly Formation-Member C).

The PAHs analysis on these two samples clearly show their different origin. The sample C13 has a mixed pattern where are present mainly petrogenic-source PAHs and pyrogenic-source PAHs like the black log samples but to a lesser extent. The sample C10 displays a PAHs composition completely different, in which most of PAHs have a petrogenic-source as *Fluorene, dibenzothiophene, Phenanthrene, 3-methyldibenzothiophene, methylphenanthrene, methyldibenzothiophene, 4,6-dimethyldibenzothiophene, , 9,10-dimethyl anthracene and Crysene,* and the pyrogenic- source PAHs are almost absent. The genesis of coal C13 could has been affected by further paleowildfire or maybe by PAHs contaminations of pyrolytic-source due to the heating of the material during the post-depositional event of sill intrusion.
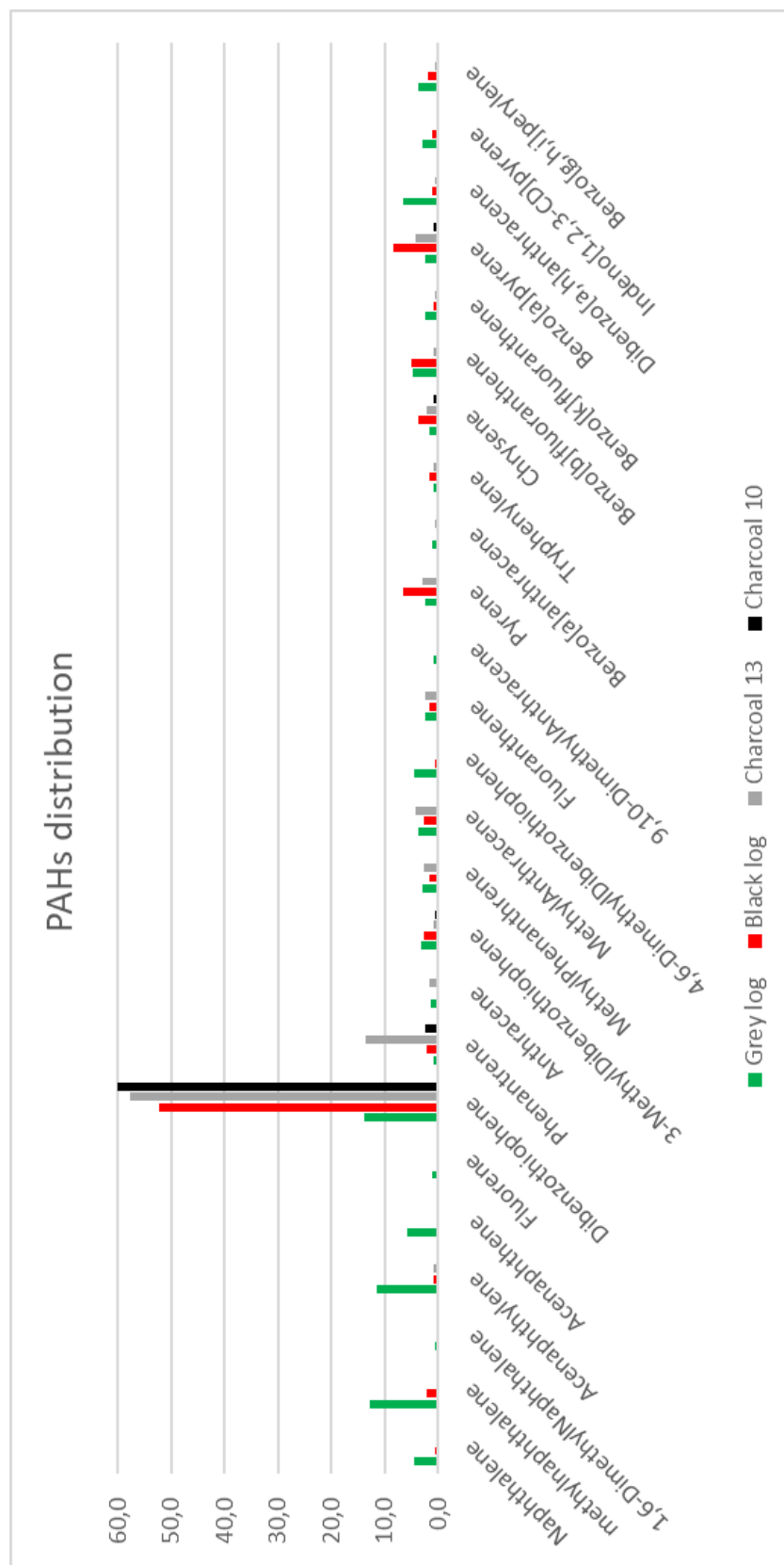
Figure 52 Total PAHs composition

3.4   Reflectance analysis

The reflectance analysis is very useful for identify the presence of vitrinite and inertinite in the sediment, moreover here has been utilized for to emphasize the difference between samples with high/low level of silicification. Tree samples are analysed with this kind of analysis:

- FR2
- C10
- C12

These fragments are the same that was utilized for PAHs and Carbon Isotope. In this image is usually possible to recognize the vitrinite and the inertinite. In our case, this is a bit more difficult to recognized that due to the high level of petrification. Here are reported the image from the samples (Fig. 53-54).
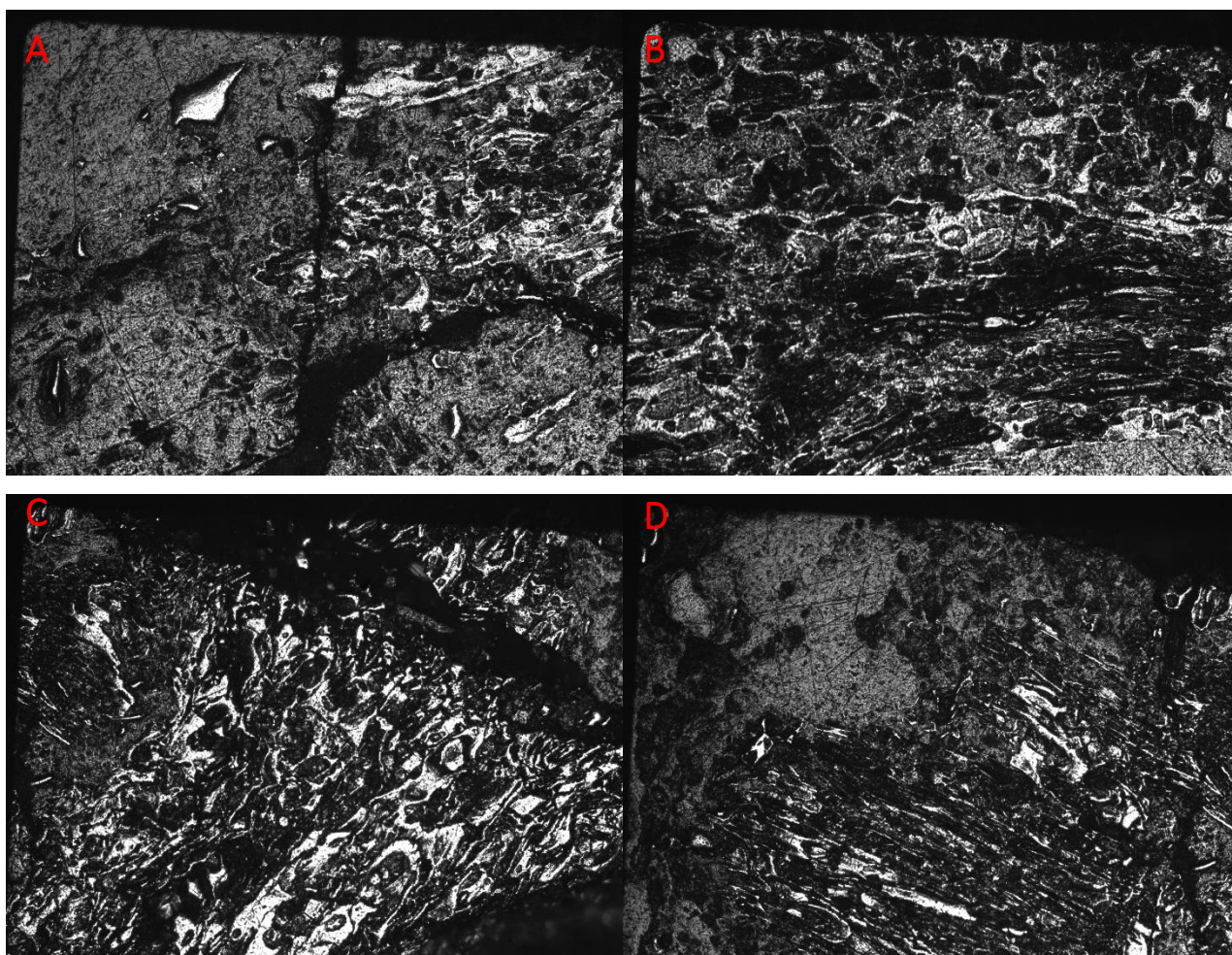
Figure 53 Reflectance image from sample C10
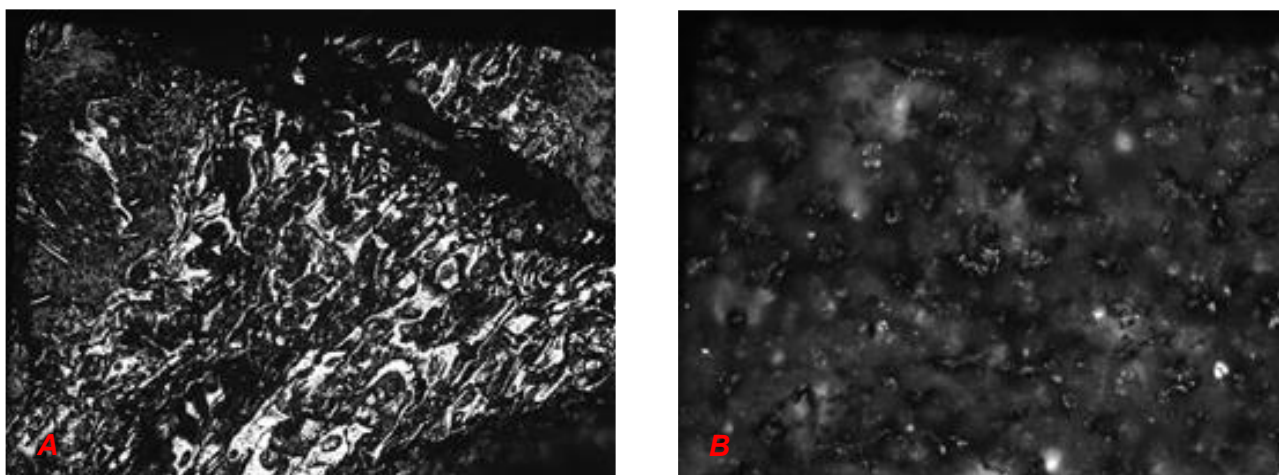
Figure 54- Reflectance Image: A. : Reflectance image of a piece of level of coal of the upper Permian formation; in "normal" preserved coal or charcoal is possible to distinguish vitrinite (light part) and inertinite (dark part); B image of a piece of fossil trunk, the high level of massive petrification delete every kid of vitrinite-inertinite structure

In this study the reflectance was utilized for understand the differentiation between a coal of Permian Weller Coal Formation and a piece of fossil trunk from the Triassic Lashly Formation.

With the occurrence of a paleofire could be preserved in the organic part of the sediment some characteristic features, these include a weight loss, increase in carbon content and an increase in reflectance, as measured in reflected light on polished blocks under oil. Although reflectance may also increase at a given temperature with time.

In the picture is possible to observe a clear distribution of vitrinite and inertinite for the sample of coal, while this is impossible to recognized for the fossil trunk samples.

The reasons of this deep different features could be linked not from the coalification/charcoalification of the samples because in both cases will be produced vitrinite and inertinite, when if in different percentage. This is probably linked to a massive silicification process that occurred in the fossil trunk sample. For this reason, is also impossible to reconstruct the combustion temperature of the wildfires.

3.5 SEM

Two samples of the fossil trunks were observed and analysed at SEM (samples #5 and #13). Several fragments of different sizes were mounted on the stub.

In some samples the anatomical features of the wood were completely loss and any kind of typical structures were not recognizable as show in Fig.55.
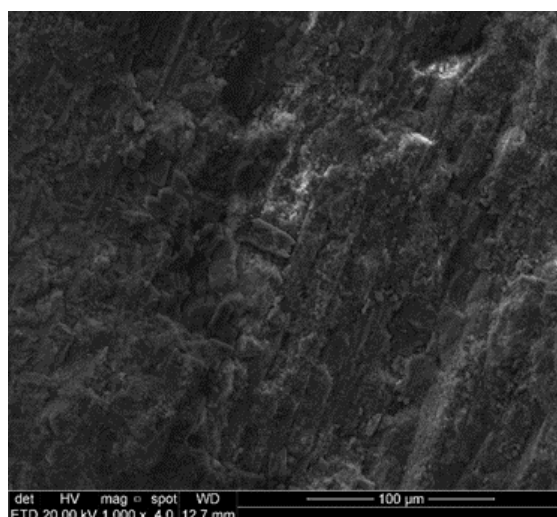
Figure 55 SEM image of sample n. 5

The analysis from EDS evidenced that in both samples the major chemical component was Si that substituted the major part of C in a massive way. For these reasons the kind of fossilization would be interpretable as a petrification and not a permineralization: is very probably that big molecules of mineral material had pervading the wood destroying the previous geometry of the anatomical features.

Instead the major part of mineral is represented by Silica, in a point of analysis was founded also Ca.

After that analysis was clear that could be impossible to see the anatomical features of the wood this this high-level of silica-petrification.

For this reason, some fragment of the samples n° 1 and n°13 were previously treated with HF for removing the mineral silica part before SEM analysis.

- **SAMPLE n°1**

Spectrum 2
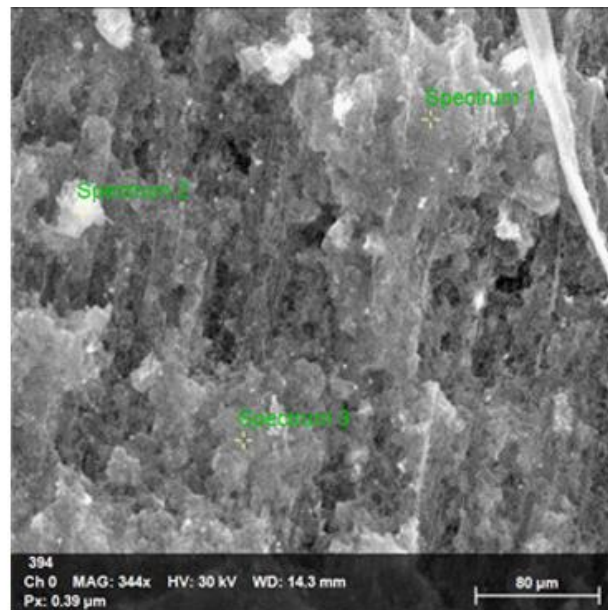
Element	At. No.	Netto	Mass [%]	Mass Norm. [%]	Atom [%]	abs. error [%] (1 sigma)	rel. error [%] (1 sigma)
Carbon	6	9358	87.19	87.19	90.55	12.35	14.16
Oxygen	8	367	11.42	11.42	8.90	3.55	31.11
Calcium	20	544	0.50	0.50	0.16	0.05	10.62
Sodium	11	75	0.39	0.39	0.21	0.09	23.01
Silicon	14	87	0.15	0.15	0.07	0.05	29.91
Magnesium	12	42	0.13	0.13	0.07	0.05	38.93
Zirconium	40	6	0.13	0.13	0.02	0.08	59.75
Aluminium	13	30	0.07	0.07	0.03	0.04	59.01
Chlorine	17	26	0.01	0.01	0.00	0.00	21.29
Nickel	28	3	0.01	0.01	0.00	0.01	57.09
Potassium	19	9	0.01	0.01	0.00	0.00	34.74
Iron	26	0	0.00	0.00	0.00	0.00	0.52
Titanium	22	0	0.00	0.00	0.00	0.00	0.73
Manganese	25	0	0.00	0.00	0.00	0.00	0.56
Chromium	24	0	0.00	0.00	0.00	0.00	0.60
Cobalt	27	0	0.00	0.00	0.00	0.00	0.49
Copper	29	0	0.00	0.00	0.00	0.00	0.45
		Sum	100.00	100.00	100.00		

Spectrum 1

Element	At. No.	Netto	Mass [%]	Mass Norm. [%]	Atom [%]	abs. error [%] (1 sigma)	rel. error [%] (1 sigma)
Carbon	6	3043	86.38	86.38	91.20	14.93	17.28
Oxygen	8	97	9.12	9.12	7.23	4.64	50.90
Calcium	20	1062	3.21	3.21	1.01	0.17	5.37
Silicon	14	113	0.50	0.50	0.23	0.09	17.04
Magnesium	12	34	0.26	0.26	0.14	0.08	30.71
Aluminium	13	27	0.15	0.15	0.07	0.06	39.32
Iron	26	15	0.13	0.13	0.03	0.06	45.27
Chlorine	17	63	0.10	0.10	0.04	0.04	38.02
Sodium	11	6	0.08	0.08	0.05	0.06	75.54
Copper	29	4	0.04	0.04	0.01	0.02	53.44
Potassium	19	9	0.02	0.02	0.01	0.01	34.76
Titanium	22	0	0.00	0.00	0.00	0.00	0.73
Manganese	25	0	0.00	0.00	0.00	0.00	0.56
Chromium	24	0	0.00	0.00	0.00	0.00	0.60
Cobalt	27	0	0.00	0.00	0.00	0.00	0.49
Nickel	28	0	0.00	0.00	0.00	0.00	0.46
Zirconium	40	0	0.00	0.00	0.00	0.00	0.57
		Sum	100.00	100.00	100.00		

Spectrum 3

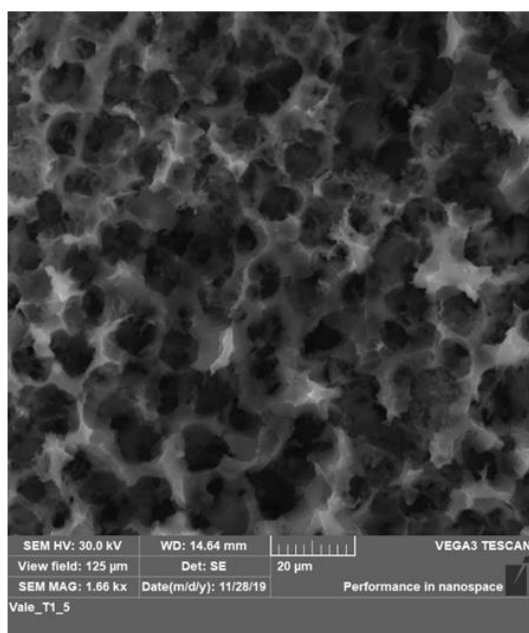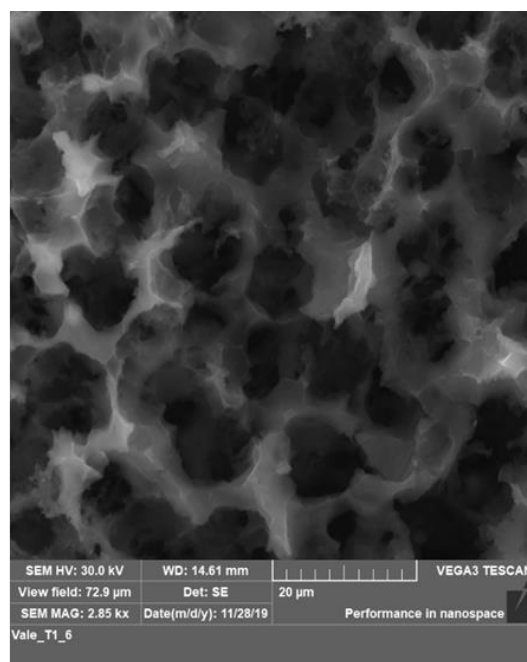| Element	At. No.	Netto	Mass [%]	Mass Norm. [%]	Atom [%]	abs. error [%] (1 sigma)	rel. error [%] (1 sigma)
Carbon	6	3888	88.18	88.18	91.86	14.50	16.44
Oxygen	8	119	9.25	9.25	7.24	4.34	46.90
Calcium	20	568	1.25	1.25	0.39	0.09	7.58
Silicon	14	109	0.39	0.39	0.18	0.07	18.59
Aluminium	13	59	0.27	0.27	0.12	0.07	25.48
Titanium	22	60	0.25	0.25	0.07	0.06	23.70
Magnesium	12	29	0.18	0.18	0.09	0.06	36.66
Chromium	24	23	0.13	0.13	0.03	0.05	40.88
Cobalt	27	7	0.05	0.05	0.01	0.02	38.16
Chlorine	17	33	0.04	0.04	0.01	0.01	18.99
Potassium	19	7	0.01	0.01	0.00	0.00	39.93
Zirconium	40	0	0.00	0.00	0.00	0.01	595.75
Iron	26	0	0.00	0.00	0.00	0.00	0.52
Sodium	11	0	0.00	0.00	0.00	0.00	4.81
Manganese	25	0	0.00	0.00	0.00	0.00	0.56
Nickel	28	0	0.00	0.00	0.00	0.00	0.46
Copper	29	0	0.00	0.00	0.00	0.00	0.45
		Sum	100.00	100.00	100.00		

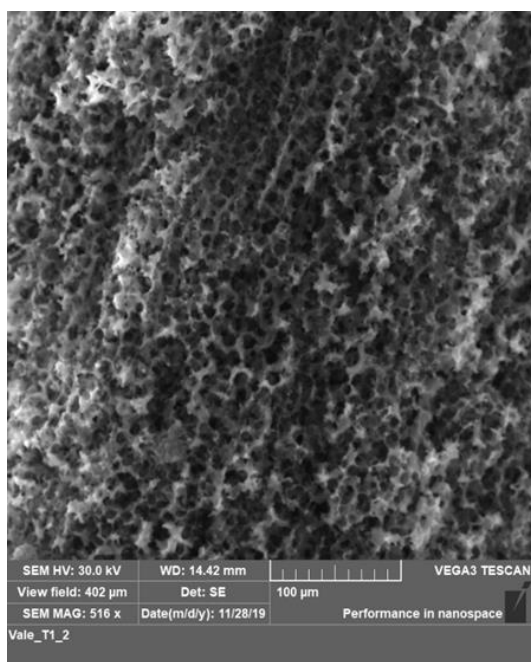*Figure 56 SEM analysis of Fossil wood- Sample 1*

Figure 57 SEM image with different magnification of a pice of fossil wood- Sample 1
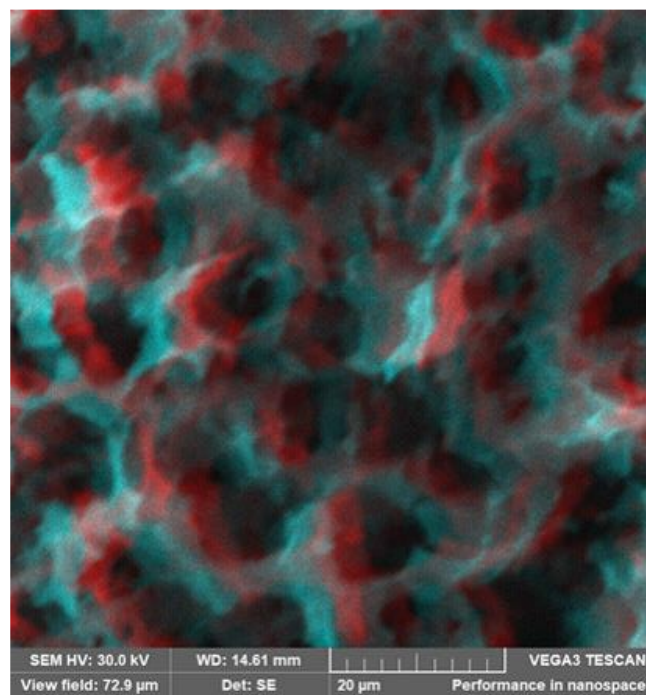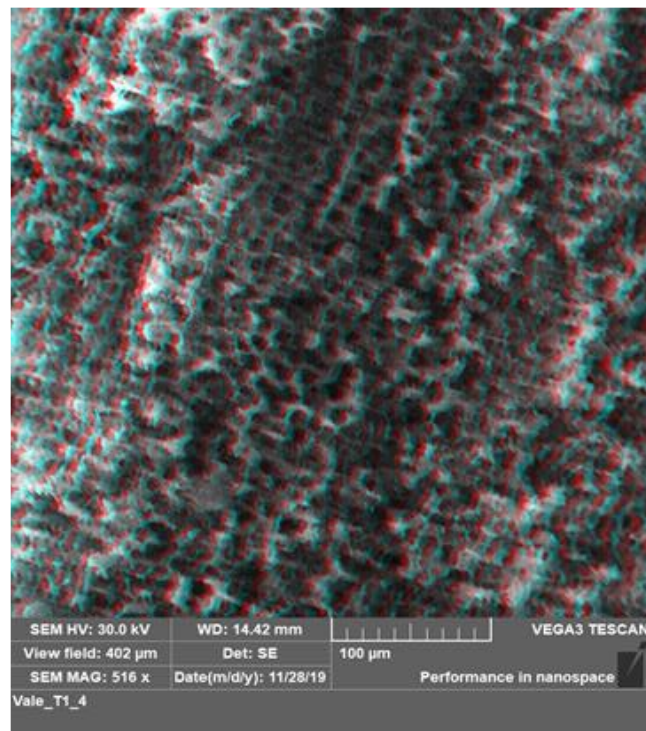
3D Image

Figure 58In this image is represented the same area of the previous image, but this is a 3D image, could be visible just with the 3D glass.

- **SAMPLE 13**

Spectrum 1

Element	At. No.	Netto	Mass [%]	Mass Norm. [%]	Atom [%]	abs. error [%] (1 sigma)	rel. error [%] (1 sigma)
Carbon	6	3681	74.51	81.43	90.01	12.39	16.63
Calcium	20	3630	7.32	8.00	2.65	0.28	3.87
Oxygen	8	115	6.66	7.28	6.04	3.17	47.66
Magnesium	12	349	1.11	1.21	0.66	0.13	11.73
Zirconium	40	9	0.70	0.77	0.11	0.26	37.46
Silicon	14	204	0.38	0.42	0.20	0.06	16.30
Aluminium	13	86	0.20	0.22	0.11	0.05	26.30
Copper	29	29	0.19	0.21	0.04	0.06	32.42
Sodium	11	31	0.17	0.19	0.11	0.06	37.42
Cobalt	27	14	0.08	0.09	0.02	0.05	57.71
Chlorine	17	56	0.06	0.07	0.03	0.03	54.71
Iron	26	12	0.06	0.07	0.02	0.04	69.71
Nickel	28	6	0.03	0.04	0.01	0.01	40.89
Chromium	24	2	0.01	0.01	0.00	0.01	70.23
Manganese	25	1	0.01	0.01	0.00	0.01	92.38
Potassium	19	0	0.00	0.00	0.00	0.00	1.06
Titanium	22	0	0.00	0.00	0.00	0.00	0.73
		Sum	91.49	100.00	100.00		

Spectrum 2

Element	At. No.	Netto	Mass [%]	Mass Norm. [%]	Atom [%]	abs. error [%] (1 sigma)	rel. error [%] (1 sigma)
Carbon	6	3233	66.02	81.11	89.67	11.27	17.07
Calcium	20	3573	6.83	8.39	2.78	0.27	3.90
Oxygen	8	92	5.74	7.05	5.85	3.00	52.24
Magnesium	12	307	1.56	1.91	1.05	0.18	11.42
Silicon	14	141	0.43	0.52	0.25	0.07	16.95
Sodium	11	28	0.25	0.30	0.17	0.08	33.88
Aluminium	13	48	0.18	0.23	0.11	0.06	31.22
Iron	26	23	0.14	0.17	0.04	0.05	40.11
Copper	29	11	0.09	0.11	0.02	0.05	58.46
Chromium	24	13	0.06	0.08	0.02	0.04	66.82
Chlorine	17	34	0.04	0.04	0.02	0.01	18.67
Manganese	25	6	0.03	0.04	0.01	0.01	41.65
Potassium	19	11	0.02	0.02	0.01	0.00	30.86
Cobalt	27	2	0.01	0.01	0.00	0.01	77.38
Titanium	22	3	0.01	0.01	0.00	0.01	61.27
Nickel	28	0	0.00	0.00	0.00	0.00	0.46
Zirconium	40	0	0.00	0.00	0.00	0.00	0.57
		Sum	81.39	100.00	100.00		

Spectrum 3

Element	At. No.	Netto	Mass [%]	Mass Norm. [%]	Atom [%]	abs. error [%] (1 sigma)	rel. error [%] (1 sigma)
Carbon	6	3520	84.18	84.18	91.35	14.12	16.77
Calcium	20	2971	6.61	6.61	2.15	0.27	4.02
Oxygen	8	77	5.96	5.96	4.85	3.34	56.05
Magnesium	12	266	1.81	1.81	0.97	0.21	11.59
Silicon	14	136	0.56	0.56	0.26	0.09	15.76
Sodium	11	39	0.45	0.45	0.26	0.12	26.49
Aluminium	13	42	0.22	0.22	0.10	0.07	30.11
Chromium	24	15	0.08	0.08	0.02	0.05	57.49
Nickel	28	9	0.07	0.07	0.02	0.05	69.05
Titanium	22	10	0.04	0.04	0.01	0.01	32.88
Chlorine	17	17	0.02	0.02	0.01	0.01	26.00
Iron	26	0	0.00	0.00	0.00	0.00	0.52
Potassium	19	0	0.00	0.00	0.00	0.00	1.06
Manganese	25	0	0.00	0.00	0.00	0.00	0.56
Cobalt	27	0	0.00	0.00	0.00	0.00	0.49
Copper	29	0	0.00	0.00	0.00	0.00	0.45
Zirconium	40	0	0.00	0.00	0.00	0.00	0.57
		Sum	100.00	100.00	100.00		

Spectrum 4

Element	At. No.	Netto	Mass [%]	Mass Norm. [%]	Atom [%]	abs. error [%] (1 sigma)	rel. error [%] (1 sigma)
Carbon	6	3460	85.74	85.74	92.24	14.43	16.83
Oxygen	8	75	6.09	6.09	4.92	3.44	56.52
Calcium	20	2281	5.87	5.87	1.89	0.25	4.25
Magnesium	12	141	0.86	0.86	0.46	0.13	15.34
Zirconium	40	5	0.43	0.43	0.06	0.23	52.74
Silicon	14	110	0.39	0.39	0.18	0.07	18.54
Aluminium	13	44	0.20	0.20	0.10	0.06	30.69
Sodium	11	15	0.16	0.16	0.09	0.07	46.17
Copper	29	12	0.11	0.11	0.02	0.06	52.19
Chlorine	17	49	0.07	0.07	0.03	0.04	51.27
Nickel	28	5	0.04	0.04	0.01	0.02	44.36
Iron	26	4	0.03	0.03	0.01	0.01	52.29
Potassium	19	3	0.00	0.00	0.00	0.00	62.57
Titanium	22	0	0.00	0.00	0.00	0.00	0.73
Manganese	25	0	0.00	0.00	0.00	0.00	0.56
Chromium	24	0	0.00	0.00	0.00	0.00	0.60
Cobalt	27	0	0.00	0.00	0.00	0.00	0.49
		Sum	100.00	100.00	100.00		

Spectrum 5

Element	At. No.	Netto	Mass [%]	Mass Norm. [%]	Atom [%]	abs. error [%] (1 sigma)	rel. error [%] (1 sigma)
Carbon	6	3511	85.19	85.19	90.55	14.29	16.78
Oxygen	8	118	9.36	9.36	7.47	4.41	47.08
Calcium	20	1454	3.48	3.48	1.11	0.17	4.95
Magnesium	12	87	0.65	0.65	0.34	0.12	18.52
Silicon	14	84	0.36	0.36	0.17	0.07	20.39
Sodium	11	20	0.25	0.25	0.14	0.09	37.59
Aluminium	13	45	0.25	0.25	0.12	0.07	28.22
Iron	26	22	0.14	0.14	0.03	0.06	39.97
Copper	29	14	0.10	0.10	0.02	0.05	51.39
Nickel	28	14	0.09	0.09	0.02	0.05	56.75
Titanium	22	13	0.06	0.06	0.02	0.04	71.18
Potassium	19	23	0.04	0.04	0.01	0.01	21.85
Chlorine	17	25	0.03	0.03	0.01	0.01	21.55
Chromium	24	3	0.02	0.02	0.00	0.01	57.11
Manganese	25	0	0.00	0.00	0.00	0.00	0.56
Cobalt	27	0	0.00	0.00	0.00	0.00	0.49
Zirconium	40	0	0.00	0.00	0.00	0.00	0.57
		Sum	100.00	100.00	100.00		

Spectrum 6

| Element	At. No.	Netto	Mass [%]	Mass Norm. [%]	Atom [%]	abs. error [%] (1 sigma)	rel. error [%] (1 sigma)
Carbon	6	3177	88.07	88.07	92.45	15.08	17.12
Oxygen	8	81	7.68	7.68	6.05	4.21	54.88
Calcium	20	997	2.83	2.83	0.89	0.16	5.56
Magnesium	12	43	0.46	0.46	0.24	0.11	24.54
Silicon	14	59	0.37	0.37	0.17	0.08	22.38
Sodium	11	12	0.22	0.22	0.12	0.10	44.72
Zirconium	40	2	0.16	0.16	0.02	0.14	88.63
Iron	26	12	0.10	0.10	0.02	0.06	53.52
Chlorine	17	51	0.08	0.08	0.03	0.04	47.76
Titanium	22	4	0.02	0.02	0.01	0.01	49.74
Aluminium	13	2	0.02	0.02	0.01	0.01	70.99
Potassium	19	0	0.00	0.00	0.00	0.00	1.06
Manganese	25	0	0.00	0.00	0.00	0.00	0.56
Chromium	24	0	0.00	0.00	0.00	0.00	0.60
Cobalt	27	0	0.00	0.00	0.00	0.00	0.49
Nickel	28	0	0.00	0.00	0.00	0.00	0.46
Copper	29	0	0.00	0.00	0.00	0.00	0.45
		Sum	100.00	100.00	100.00		

Figure 59: SEM results of fossilized wood
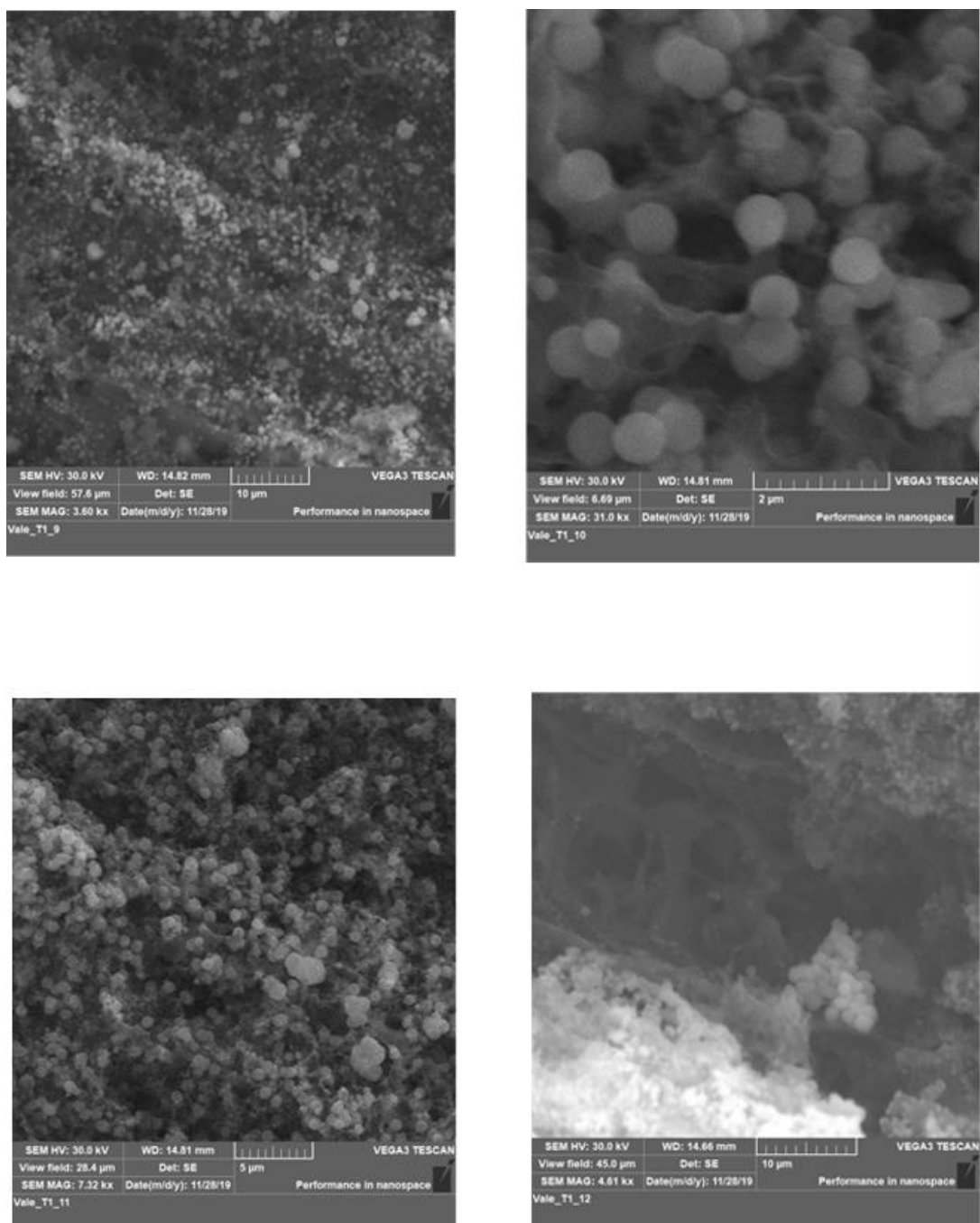
Figure 60 Spherules chemically composed by calcite

The presence of sub-micrometric (0,3-0,5 µm) spherules observed in Figure 61 were chemically composed by calcite. The well-define shapes indicate that these spherules were formed in a different time of the silica intrusion, because they have had the possibility of growing in their own shapes.

4. Discussion

4.1 Paleoenvironmental reconstruction based on paleo-dendrochronology and carbon isotope data

The carbon isotope analysis points out two differ trends of the values correlated with an external cause as the occurrence of a paleofire that enrich the external part of some of the wood in $\delta^{13}C$.

These two diverse distributions of $\delta^{13}C$ suggest that the Allan Hills Forest, recovery in three different stratigraphy level, was partially destroyed by a paleofire, while other trunk doesn't show the evidence of fire.

The Triassic environment of polar forest was so dominated from evergreen and deciduous trees that could reach meters length and an age, revelated from the dendrochronology analysis, of 147 years. Moreover, with the cross-match of the samples emerge a dendrochronology history of 237 yr.
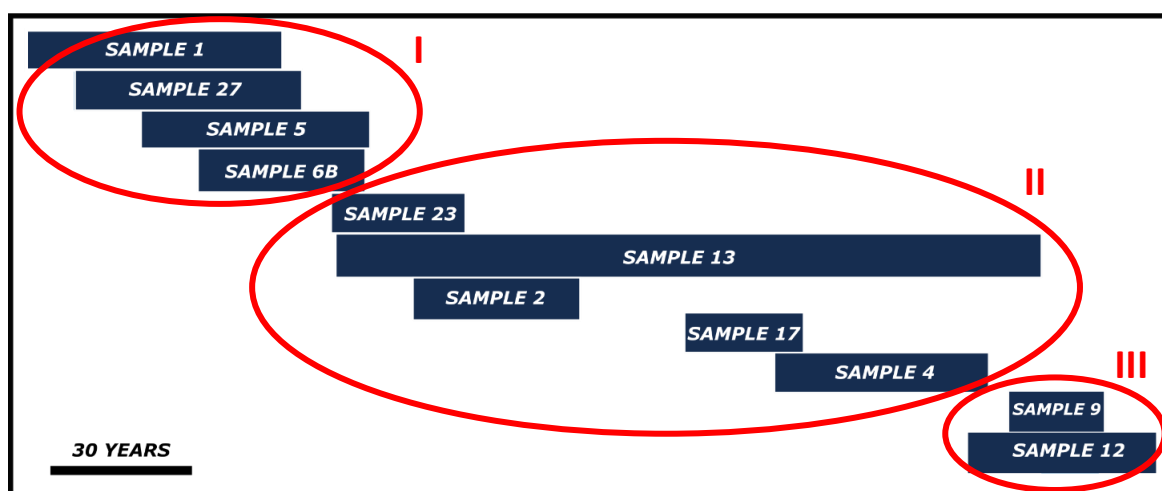

Figure 62 Reconstruction of the history and the position of the fossil trunk in the cross-match

The datum that emerge from the cross-match of this samples had important paleoenvironment implication because from the image is possible to note three different group of samples, it means that the massive flows that destroyed this forest occurred at least three times during 237 yr (Fig.62).

During this massive event the landscape doesn't complete destroyed, but only in a side, leading intact the contemporaneous plants on the other side.

Moreover, in the three distinct groups of wood have to be noted that in group I and II there are evidence of a paleofire (from the anatomic features, enrichment of $\delta^{13}C$ in the external part and abundance of pyrolytic origin PAHs), while in group III the paleofire are not register (sample 12 is the only one doesn't enrichen in $\delta^{13}C$ and both don't present anatomic feature linked to fire). This can suggest that the trunks, accumulated in the same areas, came at least, from two different source areas, that was affected from two different paleofires and a total of three massive flood events.

Other paleoecologically reconstruction could be done based on another paleo-dendrochronological datum, the Ring Width Index (RWI). The RWI is an index that show external factors that had influenced the growth of the threes, when RWI value is 1 indicates that the measured ring width is equivalent to the predicted ring width for that year; when RWI value > 1 indicates that the measured ring width exceeded the predicted ring width for that year; and when RWI value is less than 1 indicates that the measured ring width was less than predicted for that year.
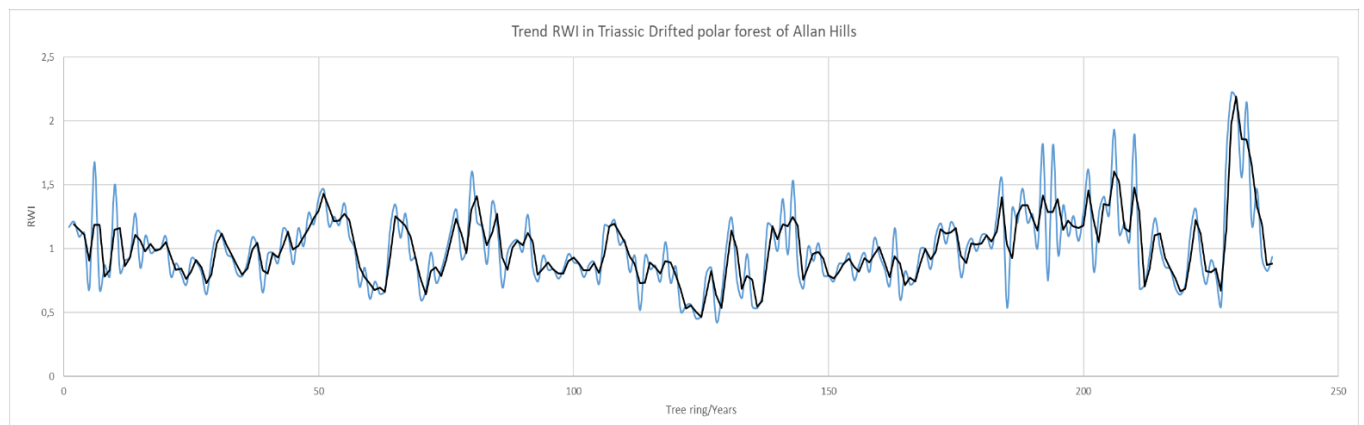

Figure 63 RWI Index from the Triassic Polar forest of Allan Hills: blue line the RWI expressed for each ring, black line the statistical trend

The data of RWI obtained show a growth trend of about 25 years (Fig. 63), this data was compared to the data obtained from (Gulbranson et al., 2020), here the RWI were measured on samples from

a Permian Polar Forest, and other Triassic samples of the Lashly Fm. (but in that case the samples are collected in member A of the formation, not in the B member as these samples).
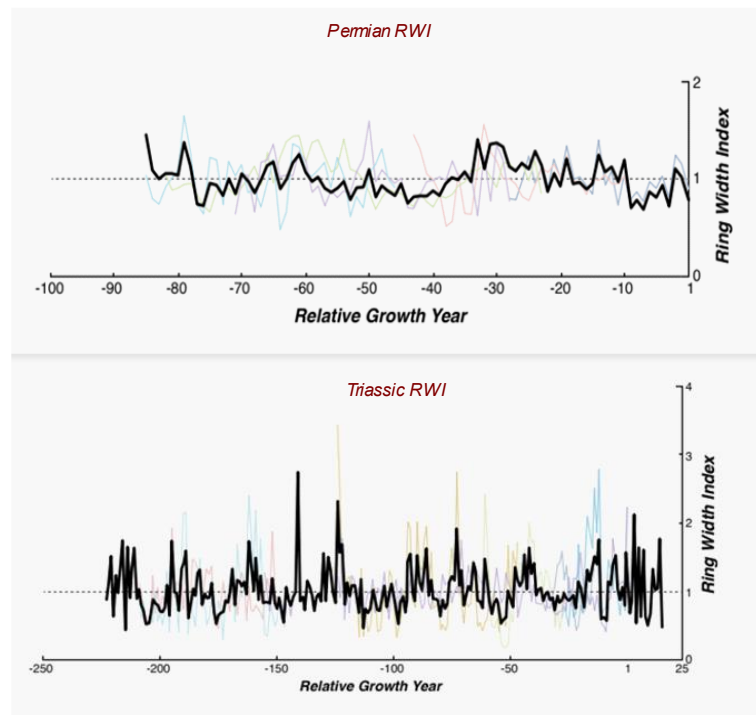

Figure 64 RWI in Permian and Triassic environment

Permian trees show remarkably lower frequency intervals of above average growth, and display longer period fluctuations in growing conditions, with a period of about 50 years (Fig. 64.

Triassic trees, in contrast, display much higher frequency and occurrence of above average growth and shorter-term 20-year period fluctuations in growing conditions.

The causes of these change of the trend are still not well known but is sure that the different paleoenvironments, with consequent different of the stability of landscape, meteorology conditions and different forms of flora, between the Permian and the Triassic time played a fundamental role. Another important role is linked to the different paleo-latitude of the Antarctica continent during the Permian and Triassic time.
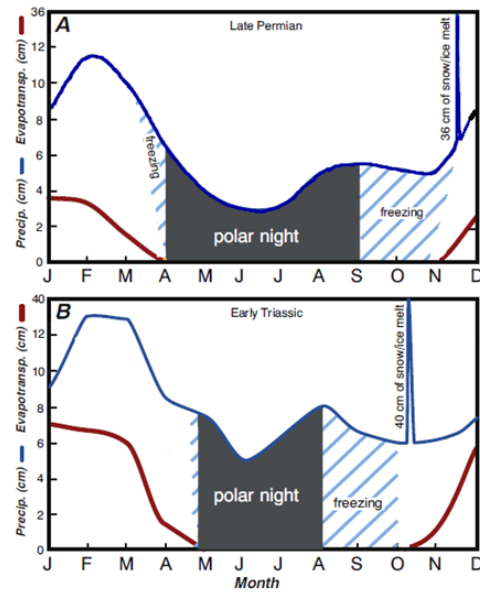
Figure 65 Distribution of sunlight and precipitation during the year, in Permian and Triassic Time, from Gulbranson et al. 2012

Paleogeographic reconstruction affirmed that during the Permian age the Victoria Land was situated at 75-80° latitude, during the Triassic time the continent was moved to north, reaching a maximum of 60° latitude in Upper Jurassic/Lower Triassic Time, during the deposition of Laslhy Fm member C (Gabites, 1985).

The diverse paleolatitude implies obviously different climatic condition, but the more important characteristic linked to the growth of the annual rings in the diverse concentration of the light-hours distributed during the years.

During the Permian time the polar night occurred for almost 6 moths, and a freezing condition of the soil persist for other 3 months. In this paleoenvironmental condition only 3 months could be suitable from the plants for their growth, otherwise the quite totally of the light-hours available during the year are concentrated during the growing season (Fig.65).

In the Triassic time the polar night was reduced to 3-4 months ant it's a partial polar night, the freezing conditions occurred for only two months, than the months available for the growing of plants are almost six, but in this case the light-hours available during the year were not concentrated during the growing season and some of that are lost during the non-growing season(Fig.65).

4.2 Fossilization of the samples: paleowildfire and multiple petrification/mineralization

A multidisciplinary approach was utilized for better understand the kind of fossilization of the wood of the fossil forest recovered in Allan Hills, because fossil charcoal, inertinites, and pyrogenic polycyclic aromatic hydrocarbons (PAHs) represent the only direct evidence for the occurrence of such paleowildfires and for characterized the wood.

PAHs-The partially combustion in some of the samples were firstly observed from the PAHs analysis, where the ratio between PAHs composed with different number of aromatics rings, show a pyrolysis diagenesis of the coal. The PAHs analysis by GC-MS on methanol- dichlorometane extracts of log specimens revealed the presence of a larger number of PAHs from pyrogenic origin indicating that the carbonized logs were of wildfire origin. However, a similar trend, albeit to lesser extent, it occurred also in the gray portions. This would indicate a migration of pyrogenic PAHs from the black burned zone probably occurring during the petrification process. In fact, the amorphous silica that initially permeated wood through fluid flow, due to its strong affinity with PAHs, would has adsorbed them and easily transported inside to the trunk during the silicification process.

Carbon Isotope- As regard the Carbon Isotope analysis, this show two different trends as regards the kind of plants, some of that are in fact deciduous, while some other were evergreen. Another fundamental data was possible to read in the graphs of Carbon Isotope results: in some sample is possible to seen a shifting of the curve in the first two-tree rings, this is due to a partially external combustion that have enriched that part of the wood in δ^{13}C.

Reflectance and SEM- For the reconstruction of the post-depositional history and the kind of fossilization were used SEM analysis, coupled with reflectance analysis.

From the SEM images, EDS and reflectance analysis it was possible to establish that fossilized samples were mainly composed by silica in a massive forms with some of the samples with little (on the order of microns) spherules of calcite that probably occurred in a different phase.

5. Conclusions

Palynology - Through the complete Permo-Triassic succession exposed in Allan Hills it has been possible to reconstruct, with a continuity of sedimentation, the palynostratigraphy associations that characterized the Weller Coal Measures Formation, the Feather Sandstone Fm. and the Lashly Formation.

One of the first results of this work is the substantial stratigraphic continuity between the Weller Coal Measures Formation and the Feather Sandstone Fm., even if with deep change in the paleoenvironmental conditions, registered on the base of fluvial style and paleocurrents. Based on an integrated approach of palynology and stratigraphy, the deep change of the paleoenvironmental condition across the end-Permian mass extinction event has been recorded also in Antarctica for the first time.

In the Weller Coal Measures Formation have been noted the occurrence of the EPE, to date recovered only in the Sydney Basin (Eastern Australia) , and the successive *Protohaploxypinus microcorpus* zone, this transition zone could be assigned to the Late Permian (due to the provincialism) or to the Early Triassic (as in Sydney Basin with the recent calibration).

Through the sporomorphs assemblage, supported also by the paleobotany remains, a deep change affecting the flora between the Permian and Triassic time has been observed. The floristic turnover, also noted in many areas of Gondwana, is strictly linked to the deep change of paleoenvironmental conditions between the Permian and Triassic widespread all over the world due to a general greenhouse.

Following a non-fossiliferous sandstone succession deposited during Induan and Olenekian time interval, the flora returned flourishing in the Middle Triassic in the member A of Lashly Fm. From this detailed palynostratigraphy reconstruction has been also possible to reveal that, at high latitude, the paleoenvironmental recovery taken place in at least 3 Ma, with a progressive recovered event during the Late Olenekian.

From the succession deposited in the Middle Triassic, five different associations of palynomorphs were recovered and has been possible to establish the different environmental conditions that affected the sedimentary sequence, with an alternation of stable and instable landscapes. The stable landscape, that dominated during the deposition of members A and C, was characterized by developed soil, testified by the presence of hypogeum fungal spores; while the instable landscape dominated during the deposition of member B of Lashly Fm., highly characterized by coarse sandstones linked with massive fluvial flows that caused also the transport and deposition of the "*Allan Hills Fossil Forest*".

The Triassic succession reaches, in the highest part of member C, the Rhaetian age.
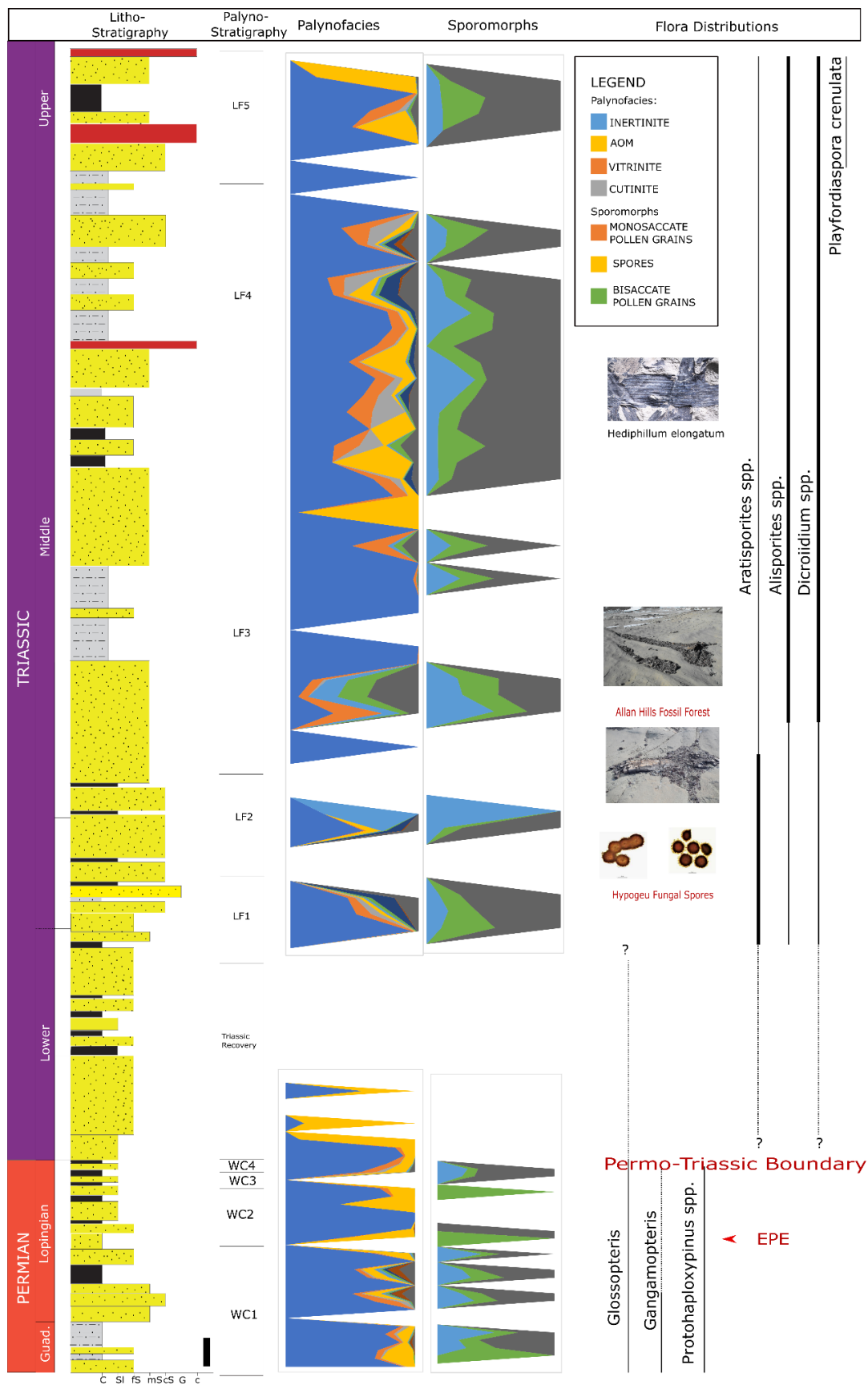
Figure 66 Stratigraphy Log with palynofacies, pollen and plants remains distribution

Paleobotany- The main goals of the paleobotany research were:

1- reconstruction of the paleoenvironmental conditions during the Triassic time;

2- to verify the occurrence of paleowildfires, as a presence of charcoal, suggested by particular features in the morphology of the fossil wood, based on different chemical composition between coal and charcoal;

3- reconstruction the post-depositional events recorded on the multi-phase fossilization of the trunks.

With a multidisciplinary approach and a variety of techniques it has been possible to accomplish the prefixed objectives, even if in some areas further study could be relevant.

1) Reconstruction of the paleoenvironmental conditions during the Triassic time

- The dendrochronology analysis of the Triassic fossil trunks confirmed the data of Gulbranson et al. (2020) and showed a different trend of flora from the Permian to the Triassic

- The fossil trunks reconstructed a climatic history of 237 years

- The samples probably were not destroyed together in a catastrophic event but in different times. This is a hypothesis (the uncertain is due to the absence of the bark in the samples), carbon isotope analysis could confirm or refused this point.

- 6 of 11 samples have pith and their position in the chronology show that they were born in different times (so there were three different catastrophic events)

- The RWI shows a trend of 20-25 years as a periodical fluctuation in growing conditions:

During the Triassic the Antarctica continent moved from the south to a low latitude, reaching a minimum of around 65° South during the Late Triassic.

The *Glossopteris flora* was replaced, after the PT boundary, from the *Dicroidium* and other orders. During these times the landscape were much more stable than in Permian Age, this could be demonstrated by the high maturity of the soils that can reach thousands of years.

The tree rings of the samples measured in the Lashly Fm show that RWI can have very high variation of amplitude, especially during the change of cycling that during about 25 years.

As concerned the anatomically characteristic the Triassic tree rings are very thinner than the Permian one.

This could be related to the migration at different latitude, during the Permian (at around 80°South) there was a net seasonal change and the annual sunlight hours was concentrated in

the growth season. During the Triassic, instead, the continent was moved to the north (since 65°C) so, despite there was a big difference between the ratio of sunlight between the season, there was anyway a part of sunlight that was lost during the non-growing season.

2) To verify the occurrence of paleowildfires, as a presence of charcoal, suggested by particular features in the morphology of the fossil wood, based on different chemical composition between coal and charcoal

The different kinds of methodology converge to the occurrence of a paleo-wildfire.

After a paleofire could be preserved, in the organic part of the sediment, some characteristic features as a weight loss, increase in carbon content and increase in reflectance and increase in the ratio between light and heavy PHAs. In the samples the distribution of PAHs is dominated PAHs >4 ringed polynuclear aromatic hydrocarbons that are typical attribute to pyrogenetic materials, due to their formation temperature (Hossain, Sampei e Roser 2013). Also, the $\delta^{13}C$ suggests a partial combustion of the wood, with a shifting of the $\delta^{13}C$ distribution in the first two-tree growth rings.

All these techniques are used for reconstruction the history of the fossil forest; mainly on the differentiation between coal and charcoal.

Figure 67 Paleo-landscape reconstruction; from bottom to top: I) Stable environment; II) First event of paleofire; III) Second event of paleofire; IV) event of massive flood

The occurrence of fossil charcoal within some of the fossil logs implies a paleoenvironmental scenery during the Middle Triassic, where possibly dramatic wildfires affected riparian forests or part of them. Then the burned trees would have been transported by floods and accumulated within the fluvial sand bars.
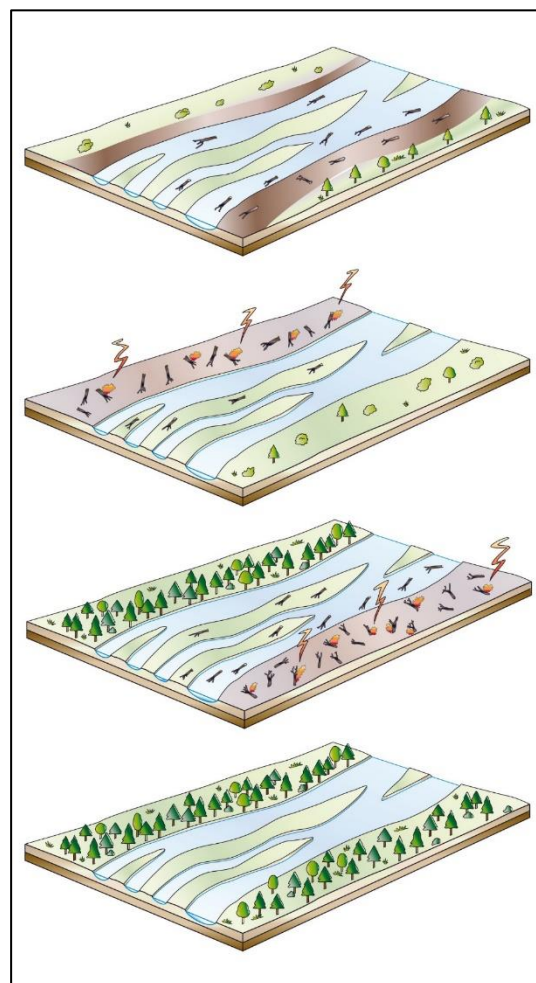
3) Reconstruction the post-depositional events recorded on the multi-phase fossilization of the trunks.

After the paleo-wildfire that caused the partial combustion of the trees, they were transported by an extraordinary massive flows together with pieces of peat, in some cases directly associated to the root system of the trees. The stumps were then deposited in this a massive sandstone.

Another notable feature of the fossil trunks is the compression axes that affect all the samples, this indicate a high lithostatic compression after the deposition.

The second step of history of the samples is the fossilization; we made use of SEM analysis, adding with reflectance analysis to understand the kind of fossilization that affected the sample.

Figure 68 A) Partially charcoalification; B) Burial and lithostatic compression; C) Coalification of the samples; D) Massive petrification

The samples result strongly petrified with a massive process, where the silica didn't replace totally the carbon and when this process was in act the silica partially destroyed the primary structure of the wood, usually preserved in coal and charcoal - *Partially Chalcedony Petrification,* probably occurred during the Jurassic sill intrusion. Moreover, were recovered spherules of calcite which overlain the silica intrusion, lighting a deposition during a second   phase.
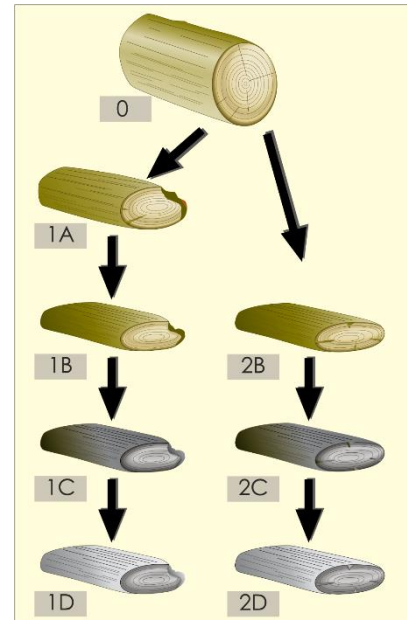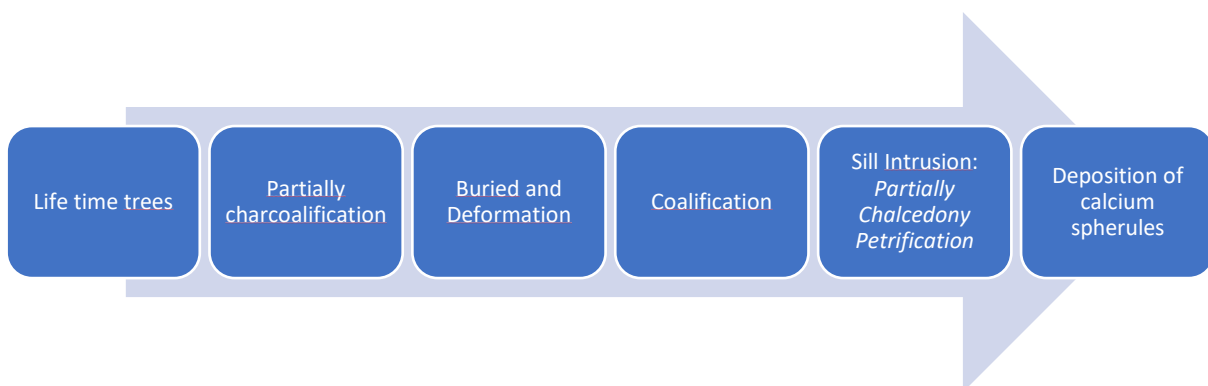
Figure 69 Reconstruction of the history of the fossil trunks of "Allan Hills Fossil Forest"

Acknowledgments

First and foremost, I'd like to thank my supervisors Prof. Franco Maria Talarico and Prof. Gianluca Cornamusini giving me the opportunity to undertake the PhD project and all the formative experiences.

I wish to thank Prof. Amalia Spina to adopt me as a PhD student and for all the teachings of these years. Without you my project would not have been the same!

I'd also like to extend my thank to Prof. Erik Gulbranson for hosting me at the University of Wisconsin-Milwaukee (UWM). My greetings also go to Prof. Paulo Alvez DeSouza and all the staff at the Universitade Federal Do Rio Grande Do Soul (UFRGS).

Moreover, I'd like to thank Prof. Simonetta Cirilli and Prof. Benjamin Bomfleur for their precious comment about the thesis.

Reference

Abu Hamad, A.M.B. , A. Jasper, and D. Uhl. "The record of Triassic charcoal and other evidence for palaeo-wildfires: Signal for atmospheric oxygen levels, taphonomic biases or lack of fuel?" *International Journal of Coal Geology*, 2012: 96-97, 60–71.

Algeo , T.J., and S.E. Schecker. "Terrestrial-marine teleconnections in the Devonian links between the evolution of land plants, weathering processes and marine anoxic events." *Philosophical Trasactions of the Royal Society of London- Series B 353*, 1998: 113-130.

Allibone, AH., and RJ. Norris. "Migmatite development in Koettlitz Group metasediment, Taylor Valley, Antarctica." *Jounral of Metamorphic Geology* , 1992: 10: 589-600.

Alves, CA, et al. "Characterisation of hydrocarbons in atmospheric aeresols from differernt European sites." *World Acad Sci Tech*, 2009: v. 33; p. 236-242.

Archangelsky, Sergio. "Plant Distribution in Gondwana During the Late Paleozoic." In *Anterctic Paleobiology- Its role in the Reconstruction of Gondwana*, by Thomas N. Taylor and Edith L. Taylor. 1991.

Askin , R.A. "The Antarctic region: Geological evolution and processes." *In Proceedings of the 7th International Symposium on Antarctic Earth Sciences*, 1997: 993-996.

Askin, R.A. "Permian palynomorphs from southern Victoria Land, Antarctica." *Antarctic Journal of the United States, 30,* , 1995: 47-47.

Axsmith, B.J., E.L. Taylor, T.N. Taylor, and N.R. Cuneo. "New perspectives on the Mesozoic seed ferns order Corystospermales based on attache organs from the Triassic of Antarctica ." *America Journal of Paleobotany*, 2000: v. 87, p. 757-768.

Baillie, M.G.L., Pilcher, J.R.,. "A simple cross-dating program for tree-ring research." *Tree-Ring Bull. 33,*, 1973: 7–14.

Ballance, P.F. "The Beacon Supergroup in the Allan Hills, central Victoria Land, Antarctica." *New Zealand journal of geology and geophysics 20,* , 1977: 1003-1116.

Barrett , P.J, and P.N. Webb . "Stratigraphic sections of the Beacon Supergroup (Devonian and older (?) to Jurassic) in South Victoria Land." *Publication of the Geology Department, Victoria University of Wellington, Antarctic Data Series 3,* , 1973: 1-165.

Barrett P.J. "The Devonian to Triassic Beacon Supergroup of the Trensantartic Mountains and correlatives in other parts of Antarctica ." *The Geology of Antarctica- Oxford Monographs on Geology and Geophysics*, 1991: 120-152.

Baumard, P., H. Budzinski, and P. Garrigues. "Plycyclic aromatic hydrocarbon in sediments and mussels of the western Mediterrenean Sea." *Environmental Toxicology ans Chemistry*, 1998: v.17; p. 765-776.

Bomfleur, B., E.L. Taylor, T.N. Taylor, R. Serbet, M. Krings, and H. Kerp. "Systematics and paleoecology of a new peltaspermalean seed fern from the Triassic polar vegetation of Gondwana." *Internationa Journal of Plant Science*, 2011: v. 172, p. 807-835.

Bradshaw, M.A. "Paleoenvironmental interpretations and systematics of Devonian trace fossils from the Taylor Group (lower Beacon Supergroup), Antarctica." *New Zealand Journal of Geology and Geophysics, 24(5-6)*, 1981: 615-652.

Cantrill, David J., and Imogen Poole. *The vegetetion of Antarctica through geological time.* Cambridge Univeristy Press, 2012.

CHATTERJEE, S., BORNS JR, H. W., & HOTTON III, N. I. C. H. O. L. A. S. "Gondwana rocks of the Allan Hills." *Geophysics, 20,* , 1983: 1003-1016.

Chatterjee, S., Tewari, R., & Agnihotri, D. "A Dicroidium flora from the Triassic of Allan Hills, South Victoria Land, Transantarctic Mountains, Antarctica. ." *Icheringa: An Australasian Journal of Palaeontology, 37(2),* , 2013: 209-221.

Collinson J.W., Isbell J.L., Elliot D.H., Miller M.F., Miller J.M., Veevers J.J.,. "Permian Triassic Transantarctic basin." *Geological Society of America MEmoris 184*, 1994: 173-222.

Collinson J.W., Pennington D.C., Kemp N.R. "Stratigraphy and petrology of Permian and Triassic fluvial deposits in northern Victoria Land, Antarctica- Geological investigations in Northern Victoria Lad." *Antarctic Research Series- American Geophysical Union*, 1986: 211-242.

Cook , YA. "Precambrian rift-related magmatism and sedimentation, South Victoria Land, Antarctica." *Antarctic Science* , 2007: 19(4): 471.

Cook, YA., and D. Craw. "Amalgamation of disparate crustal fragmentsin the Walcott Bay-Foster Glacier area, South Victoria Land, Antarctica." *Antarctic Science 19(4)*, 2001: 403-416.

—. "Neoproterozoic structural slices in the Ross Orogen, Skelton Glacier area, South Victoria Land, Antarctica." 2002.

Cornamusini G., Talarico F.M., Cirilli S., Spina A., Olivetti V., Woo J.,. "Upper Paleozoic glacigenic deposits of Gondawana: stratigraphy and pealeoenvironmental significance of a tillite succession in the North Victoria Land (Antarctica)." *Sedimentary Geology 358*, 2017: 51-69.

Cornamusini, G., V. Olivetti, and F.M. Talarico. "Overview on the stratigraphic and sedimentological features of the Permian-Mesozoic continental successions in Northern Victoria Land (Transantarctic Mountains, Antarctica). ." *Abstract of the 31st I.A.S. Meeting,.* Manchester,, September 2013.

Cox S.C., Turnbull I.M., Isaac M.J., Townend D.B., Smith Little B. *Geology of Southern Victoria Land, Antarctica 1:250000 geological map 22.* Institute of Geological & Nuclear Scinences , 2012.

Cuneo, N.R., J. Isbell, E.L. Taylor, and T.N. Taylor. "The Glossopteris flora from Antarctica: taphonomy and paleoecology." *In Comptes Rendus XII International Congress for the Carboniferous and Permian, Buenos Aires (Vol. 2, pp. 13-40).*, 1993.

Davies, N.S., and M.R. Gibling. "Cambrian to Devonian evolution of alluvial sysems: the sedimentological impact of the erliest land plants." *Earth-Science Reviews* , 2010: 171-200.

Davies, S.D., and K.J. McCree. "Photosyntetic rate and diffusion conduttance as a function of algae in leaves of bean plants." *Journal of Crop Science*, 1978: v. 18, p. 280-282.

Dupouey , J.L., S.W. Leavitt, E. Choisnel, and S. Jourdain. "Modeling carbon-isotope fractionation in tree rings based on effective evapotranspiration and soil water status." *Plant, Cell and Environment*, 1993: V. 16, P. 939-947.

Edwards, T.W.D., W. Graf, P. Trimbron, W. Stichler, J. Lipp, and B. Frenzel. "13C response surface resolves humidity and temperature signals in trre." *Geochimica et Cosmochimica Acta*, 2000: v. 64, p. 161-167.

Elliot D. H. "The geological and tectonic evolution of the Transantartic Mountains: a review." *Geological Society of London- Special Pubblication*, 2014: 7-35.

Erwin, D.H. "The end-Permian mass extinction." *Annu. Rev. Ecol. Syst.* , 1990: 21:69–91.

Escapa, Ignacio H., Benjamin Bomfleur, Edith Taylor, and Rudolph Serbet. "Triassic flora of Antarctica: Plant diversity and distribution in high paleolatitude communities." *Palaios 26(9)*, 2011: 522-544.

Farquhar, G.D., J.R. Ehleringer, and K.T. Hubick. "Carbon isotope discrimination and photosyntesis." *Annual review of Plant Physiology and Plant Molecular Biology*, 1989: v. 40, p. 503-437.

Farquhar, G.D., M.H. O'Leary, and J.A. Berry. "On the relationship between carbon isotope discrimination and the intercellular carbon dioxide condentration in leaves." *Australian Journal of Plant Physiology*, 1982: v. 9, p. 121-137.

Faure, G., and T.M. Mensing. *The transantartic Mountains: Rocks, Ice, Meteorites and water.* Springer science+Buisness Media, 2010.

Francey, R.J., and J.D. Farquhar. "An explenation of 13C/12C variation in tree rengs." *Nature*, 1982: v. 297, p.28-31.

Fritts, H.C. *Tree Rings and Climate.* The Blackburn Press, 1976.

Gabites, H.I. "Triassic Paleoecology of the Lashly Formation, Transantarctic Mountains, Antarctica ." *Unpublished M.Sc. thesis, Victoria University of Wellington, Wellington, New Zeland*, 1985: p. 148.

Ghezzo, C., et al. "Granitoid from the David Glacier Aviator Glacier segment of the Transantartic Mountains, Victoria Land, Antartica." *Mere. Soc.Gol.Ital., 33,* , 1987: 143-159.

Goodge, JW., IS. Williams, and P. Myrow. "Provenance of Neoproterozoic and lower Paleozoic siliciclastic rocks of the central Ross orogen, Antarctica: detrital record of rift-, passive- and active-margin sedimentation." *Geological Society of America Bullettin 116 (9/10)*, 2004: 1253-1279.

Goodge, JW., Walker NW., and VL. Hasen . "Neoproterozoic-Cambrian basement-involved orogenesis within the Antarctic margin of Gondwana." *Geology 21*, 1993: 37-40.

Grindley , GW, and G. Warren. "Stratigraphic nomenclatureand correlation in the western Ross Sea region." *Adie RJ ed. Antarctic Geology, Amsterdam, North HollandPublishing Company*, 1964: 314-333.

Gulbranson, E.L., J.L. Isbell, E.L. Taylor, P.E. Ryberg, T.N. Taylor, and P.P. Flaig. "Permian polar forest: deciduousness and enviormental variation." 2012.

Gulbranson, E.L., P.E. Ryberg, A-L. Decombeix, E.L. Taylor, T.N. Taylor, and J.L. Isbell. "Leaf habit of Late Permian Glossopteris trees from high-paleolatitude forest." *Journal of the Geological Society, London*, 2014: v. 171, p. 493-507.

Gulbranson, Erik L., Gianluca Cornamusini, Patricia E. Rybergc, and Valentina Corti. "When does large woody debris influence ancient rivers? Dendrochronology." *Palaeogeography, Palaeoclimatology, Palaeoecology*, 2020.

Gulbranson, Erik L., Gianluca Cornamusini, Patricia E. Rybergc, and Valentina Cortib. "When does large woody debris influence ancient rivers? Dendrochronology." *Palaeogeography, Palaeoclimatology, Palaeoecology*, 2020.

Gunn BM., Warren G.,. "Geology of Victoria Land between the Mawson and Mulock Glaciers, Antarctica." *New Zeland Geological Survey Bullettin 71, Wellington, Department of Scientific and Industrial Research*, 1962: 157.

Hartkopf-Froder, C., P. Konigshof, R. Littke, and J. Schwarzbauer. "Optical thermal maturityparameters and organic geochemical alteration at low grade diagenesis to anchimetamorphism: A review." *International Journal of Coal Geology*, 2015: 150-151, p. 74-119.

Helle, G., and G.H. Schleser. "Beyond CO2-fixation by Rubisco- an interpretation of 13C/12C variation in tree ringrs from novel intra-seasonal studies on broad-leaf trees." *Plant, Cell and Environment*, 2004: v. 27, p. 367-380.

Hermes, E.J., E.L. Taylor, and T.N. Taylor. "Morphology and ecology of the Antarcticycas plant." *Review of Paleobotany and Palynology*, 2009: v. 153, p. 108-123.

Hossain, H.M., Y. Sampei, and B.P. Roser. "Plycyclic aromatic hydrocarbons (PAHs) in late Eocene to early Pleistocene mudstone of the Sylhet succession, NE Bengal Basin, Bangladesh: Implication for source and paleoclimate conditions during Himalayan uplift." *Organic Geochemistry*, 2013: v. 56; p. 25-39.

Hudson, Benton M.J. Thames &. "When life nearly died: the greatest mass extinction of all time." London, UK, 2003.

Isbell J.L., Askin R.A.,. "Search for evidence of impact at the Permian-Triassic boundary in Antarctica and Australia:Comment." *Geology 27:859*, 1999.

Jhon. *Sedimentology and composition of the Takrouna Formation, norther Victoria Land, Antartica.* 2014.

Keeling, C.D. "The concentration and isopotic abondancues of carbon dioxide in rural and marine air." *Geochimica et Cosmochimica Acta*, 1961: v.24, p. 277-298.

Keeling, C.D. "The concentration and isotopic aboundances of carbon dioxide in the atmosphere." *Tellus*, 1960: v. 12, p, 200-203.

Kumar, K., S. Chatterjee, R. Tewari, N.C. Mehrotra, and G.K. Singh. "Petrographic evidence as an indicator of volcanic forest fire from the Triassic of Allan Hills, South Victoria Land, Antarctica"." *Current Science 104.4*, 2013: 422-424.

Kumar, M., R. Tewari, S. Chatterjee, and N.C. Mehrotra. "Charcoalified plant remains from the LashlyFormation of Allan Hills, Antarctica: Evidence of forest fire during the Triassic Period." *Episodes-Newsmagazine of the InternationalUnion of Geological Sciences, 34(2)*, 2011: p.109-118.

Kyle. "Palynostratigraphy of the Victoria Group of South Victoria Land, Antarctica." *New Zealand Journal of Geology and Geophysics*, 1977: 1081-102.

Kyle R.A., Schopf J.M.,. "Permian and Triassic palynostratigraphy of the Victoria Group, Transantartic Mountain." 649-659. Madison, University of Wisconsin: Craddock . ed. Antartic Geoscience, 1982.

Laird, MB. "Lower Paleozoic rocks of Antarctica. In Holland CH (ed) Lower Paleozoic of the Middle East, Eastern and Southern Africa and Antarctica." Wiley, London,: pp 257-314, 1981.

Leavit, S.W., and A. Long. "Seasonal stable-carbon isotope variability in tree rings: possible paleoenvironmental signals." *Chemical Geology (Isotope Geoscience Section)*, 1991: v. 87, p. 59-70.

Leavitt, S.W. "Seasonal 13C/12C changes in tree rings: species and site coherence, and possible drought influence." *Canadian Journal of Forest Research*, 1992: v. 23, p. 210-218.

Lindstrom, S., and S. McLoughlin. *Synchrounous palynofloristic extinction and recovery after the end-Permian event in the Prince Charles Mountains, Antarctica: Implication for palynofloristic turnover across Gondwana.* Review of Paleobotany and Palynology, 2007.

Lipp, J., and P. Trimbron. "Long-term records and basic principles of tree ring isotope data with emphasis on local environental conditions." *European Paleoclimate and Man*, 1991: v.1, p. 105-117.

Marynowski, Leszek, Rafal Kubik, Dieter Uhl, and Bernd R.T. Simoneit. "Molecular coposition of fossil charcoal and relationship with incolpete combustion of wood." *Organic geochemestry*, 2014: 22-31.

Mazany, T., J.C. Lerman, and A. Long. "Carbon-13 in tree ring cellulose as indicator of past climates." *Nature*, 1980: v. 287, p. 432-435.

Millay, M.A., and T.N. Taylor. "New ferns stems from the Triassic of Antarctica." *1990*, Review of Paleobotany and Palynology: v. 62, p.41-64.

Panek, J.A. "A stable carbon Isotope approach to Distinguish Climate stress from other Imposed Stresses in Coniferous Forest." *Disertation, Oregon State University Corvallis, OR., USA*, 1995.

Panek, J.A., and R.H. Warring. "Stable carbon isotopes as indicators of limitations to forest growth imposed by climate stress." *Ecological Application*, 1997: v.7, p. 854-863.

Panker, J.A., and A.H. Goldstein. "Responce of stomatal conduttance to drought in ponderosa pine: implication for carbon and ozone uptake." *Tree Physiology*, 2001: v. 21, p. 337-344.

Pertusati , P.C., C Ribeccacci , R Carosi, and M Meccheri. "Early Jurassic Age for Youngest Beacon Supergroup Strata Based on Palynomorphs from Section Peak, Norther Victoria Land, Antartica." *Terra Antartica Rep* , 2006: 99-104.

Phipps, C.J., B. Axsmith, T.N. Taylor, and E.L. Taylor. "Gleichenipteris antarcticus gen. et sp. nov. from the Triassic of Antarctica." *Review of Palebotany and Palynology*, 2000: v. 108, p. 75-83.

Prahl, F.G., and R. Carpenter. "Plyciclic aromatic hydrocarbon (PAH)-phase association in Washington coastal sediment." *Geochimica at Cosmochimica Acta*, 1983: v. 47; p. 1013-1023.

Rawson, H.M., and G.A. Constable. "Carbon production of sunflouers cultivars in fiel and controlled environments. I. Photosyntesis and traspiration of leaves, stems and heads." *Australian Journal of Plant Physiology*, 1980: v.7, p. 555-573.

Retallack G.J. "Search for evidence of impact at the Permian Triassic boundary in Antarctica and Australia:Reply." *Geology 27:860*, 1999.

Retallack G.J., Metzger C.A., Greaver T., Jahren A.J., Smith R.M.H., Sheldon ND.,. "Late Permian mass extintion on land." *Geological Society of America Bulletin 118*, 2006: 1398-1411.

Retallack G.L., Jahren A.J., Sheldon N.D., Chakrabarti R., Metzger C.A., SmithR.M.H.,. "The Permian-Triassic Boundary in Antarctica ." *Antarctic Scince 17*, 2005: 241-258.

Retallack, G.J., A. Seyedolali, E.S. Krull, W.T. Holser, C.P. ambers, and F.T. Kyte. "Search for evidence of impact at the Permian-Triassic boundary in Antartica and Australia." *Geology* , 1998: 979-982.

Retallack, G.J., J.J. Veevers, and R. Morante. "Global coal gap between Permian-Triassic extinction and Middle Triassic recovery of peat-forming plants." *Geological Society of America Bullettin*, 1996: v. 108, p.195-207.

Rezaie, N., E. D'Andrea, A. Brauning, G. Matteucci, P. Bombi, and M. Lautieri. "Do atmospheric CO2 concentration increase, climate and forest management affect iWUE of common beech? Evidences from carbon isotope analyses in tree rings." *Tree Physiology*, 2018: v. 38, p.1110–1126.

Rigby, J.F. "Some Triassic (Middle Gondwana) floras from South Victoria Land, Antarctica." *in Cooper, R., eds. Hornibrook Symposium: Extende Abstracts: NEw Zeland Geologycal Survey Record*, 1985: v.9, p.78-79.

Rigby, J.F., and J.M. Schopf. "Stratigraphic implications of Antarctic paleobotanical studies." *Gondwana stratigraphy, 2,*, 1969: 91-106.

Roland, N.W., A.L. Laufer, and F. Rossetti. "Revision of the Terrane model of Northern Victoria Lanta (Antartica) 11,1." *Terra Antartica*, 2004: 55-65.

Rowell, AJ., MN. Rees, EM. Duebendorfer, ET. Wallin, WR. VanSchumus, and EI. Smith . "An active Neoproterozoic margin: Evidence from the Skelton Glacier area, Trasnatarctic Mountains." *J. Geol Soc. London* 150 (1993): 677-682.

Schewendemann, A.B., T.N. Taylor, E.L. Taylor, M. Krings, and J.M. Osborn. "Modern traits in early Mesozoic sphenophytes: The equisetum-like cones of Spaciinodum collinsonii with in situ spores elates from the Middle Triassic of Antarctica." *Plant in Mesozoic Time: Morphological Innovation, Phylogeny, Ecosystems: Indiana Univeristy Press, Bloomingoton, Indiana*, 2010: 15-34.

Scott A.C., Bowman D.M.J.S, Bond W.J., Pyne S.J., Alexander M.E.,. *Fire on earth- An introduction.* wiley Blackwell, 2014.

Shen, W., Y. Sun, Y. Lin, D. Liu, and P. Chai. "Evidence for wildfire in the Meishan section and implications for Permian–Triassic events." *Geochimica et Cosmochimica acta*, 2011: v.75, p.1992–2006.

Sicre, M.A., J.C. Marty, and A. Saliot. "Aliphatic and aromatic hydrocarbons in different sized aeresols over the Mediterranean Sea: occurrence and origin." *Atmospheric Environment* , 1987: v. 21, p. 2247-2259.

Skinner, DNB. "Stratigraphy and structure of low-grade metasedimentary rocks of the Skelton Group, southern Victoria Land; Does the Teall graywacke really exist?" *Craddock (ed) Antarctic Geoscience. Univeristy of Wisconsin Press, Madison, WI*, 1982: 555-563.

Smoot, E.L., T.N. Taylor, and T. Delevoryas. "Structurslly preserved fossil plant from Antarctica. I.Antarcticycas, gen. nov., a Triassic cycad stem from Beardmore Glacier area." *American Journal of Botany*, 1985: v. 72, p. 1410-1423.

Soclo, H.H., P.H. Garrigues, and M. Ewald. "Origin of polycyclic aromatic hydrocarbons (PAHs) in coastal marine sediments: case studies in Cotonou (Benin) and Aquuitaine (France) areas." *Mar Pollut Bull*, 2000: v. 40; p. 387-396.

Stogiannidis, E., and R. Laane. "Source Characterization of Polycyclic Aromatic Hydrocarbons by Using Their Molecular Indices: An Overview of Possibilities." *Reviews of Environmental Contamination and Toxicology* , 2015: v. 234, p.49-133.

Stuiver, M., and T.F. Branzianus. "Tree cellulose 13C/12C isotope ratios and climatic change." *Nature*, 1987: v. 328, p. 58-60.

Stump , E. "The ross orogen of the Transantartic Mountains." *Cambridge University Press* (1995), 1995: 284.

Talarico , FM., RH. Findlay, and N. Rastelli. "Metamorphic evolution of the Koettlitz Group in the Koettlitz-Ferrar Glacier Region (Southern Victoria Land, Antarctica)." *Terra Antartica*, 2005: 12(1): 3-23.

Taylor, T.N., G. Del Fueyo, and E.L. Taylor. "Permineralized seed ferns cupules from the Triassic of Antarctica: Implication for cuoule and carpel evolution." *American Journal of Botany*, 1994: v. 81, p. 666-677.

Tayolr, E.L., T.N. Taylor, H. Kerp, and E. Hermsen. "Mesozoic seed ferns: Old paradigms, new discoveries." *Journal of the Torrey Botanical Society* , 2006: v. 133, p.62-82.

Torsvik, T.H., and L.R.M. Cooks. "Earth History and Paleogeography." *Cambridge University Press*, 2017.

Veevers, J.J., C.M.A. Powell, J.W. Collinson, and O.R. Lopez-Gamundi. "Permian-Triassic Pangean Basins and Foldbelts along the Panthalassan Margin of Gondwanaland." *Geological Sociery of America Memoir*, 1994: v.184, p. 331-353.

Walcroft, A.S., W.B. Silvester, D. Whitehead, and F.M. Kelliher. "Seasonal changes in stable carbon isotope ratios within annual rings of Pinus radiata reflect environmental regulation of growth processes." *Australian Journal of Plant Physiology*, 1997: v.24, p. 57-68.

Wilson, A.T., and M.J. Grinsted. "The possibilities of deriving past climate information from stable isotope studies on tree rings." *New Zeland Department of Scientific and Industrial Research Bulletin*, 1978: v. 220, p. 61-66.

Wysoczanski, RJ., and AH. Allibone. "Age, correlation and provenance of the Neoproterozoic Skelton Gruop, Antarctica: Grenville ag detritus on the margin of EastAntarctica. ." *Journal of Geology*, 2004: 401-416.

Yakkir, D., A. Issar, J.R. Gat, E. Adar, P. Trimbron, and J. Lipp. "C-13 and O-18 of wood from Roman siege rampart in Masada, Israel (AD70-73)- Evidence for less arid climate for the region." *Geochimica et Cosmochimica Acta*, 1994: v. 58, p. 3535-3539.

Yao, X., T.N. Taylor, and E.L. Taylor. "A taxodiaceous seed cone from the Triassic of Antarctica." *AMerican Journal of Botany*, 1997: v. 84, p. 343-354.

Yao, X., T.N. Taylor, and E.L. Taylor. "The Triassic seed cone Telemachus from Antarctica." *Review of Paleobotany and Palynology*, 1993: v.78, p. 269-276.

Yunker. "PAHs in the Farser River Basin: a critical appraisal of PAHs ratio as indicator of PAHs source and composition." *Organic Geochemestry* , 2002: 489-515.

Appendix I: Paleobotanical Samples

Sample n 1- Faint rings, <1mm up to 2mm widths, features suggestive of wood rot in pith area. Likely an aboveground stem. Heartwood appears to be preserved based on parting of the fossil near the center of the stem. Partially charcoalified, probably less than 2% organic carbon by weight per cent.
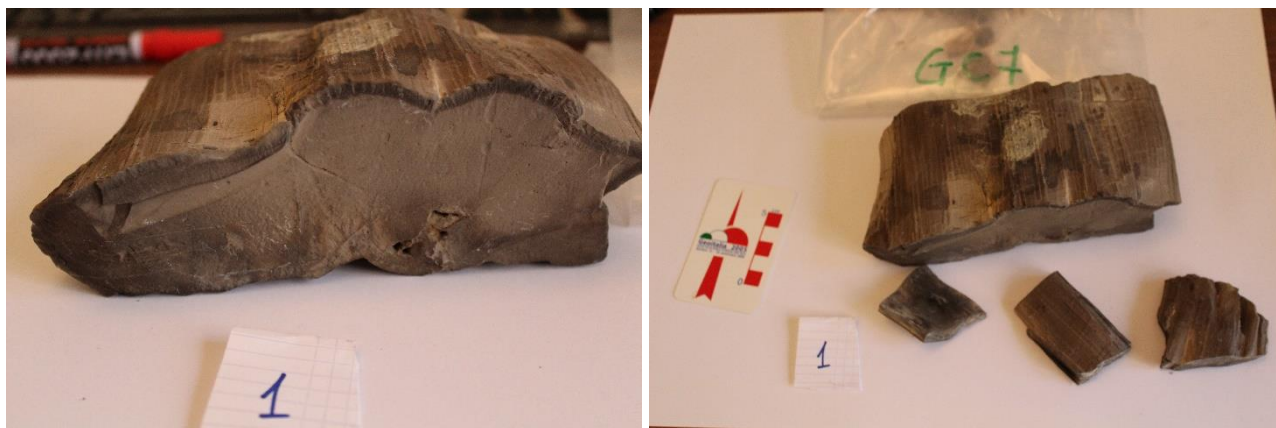
Sample n 2- Good organic carbon preservation, probably 2% organic carbon by weight. No evidence of rot. Good ultra structure preservation on oblique cut of tangential and radial planes (IMG 4535). Difficult to tell if pith is preserved or center of wood is preserved. Appears to have at least 20 rings. This may polish well, consider cutting the radial plane (oblique to the geometry of the sample).

Sample n3- Long stem appears to have reaction wood with at least 20 rings. Similar ring and organic carbon preservation as sample 1. No evidence of rot.

Sample n4- Two samples. The first (IMG 4570) appears to have too few rings. Ventifact surface doesn't reveal the organic carbon or ultrastructure preservation. The second sample (IMG 4581) displays good ring and organic carbon preservation with at least 20 rings. No evidence of rot.

Sample n 5- Excellent ultrastructure preservation, appears to be a branch with few lateral shoots and center of wood is intact. At least 20 rings. Not lobate, no evidence of rot. Transverse plane is the best, retain weathered surface.

Sample n 6- Probably root-stem transition, charcoalified (partially by paleo-fire?). At least 20 rings. Good organic carbon preservation.

Sample n 7- Excellent preservation of ring structures. Some organic carbon preservation, similar to sample 1. Center of wood is preserved. Appears to be a stem, no pith. No rot.

Sample n 8- Root-stem transition, possibly lobate. Could attempt cross matching on different lobes within this sample. Different lobes could help to cross match the specimen as well as delineate phases of lobed growth relative to other lobes.

Excellent ring and organic carbon preservation. Evidence of rot.

Sample n 9- May contain pith. Numerous radial shoots, stem wood. At least 20 rings. No evidence of rot.

Sample n 10- At least 20 rings. Preservation may be poor, appears grainy in appearance perhaps from zeolite formation. May polish in transverse plane. Definitely thin section to check if rings are preserved, secondary mineral formation could produce ring-like features.

Sample n 11- Fragment- Preservation is difficult to describe.
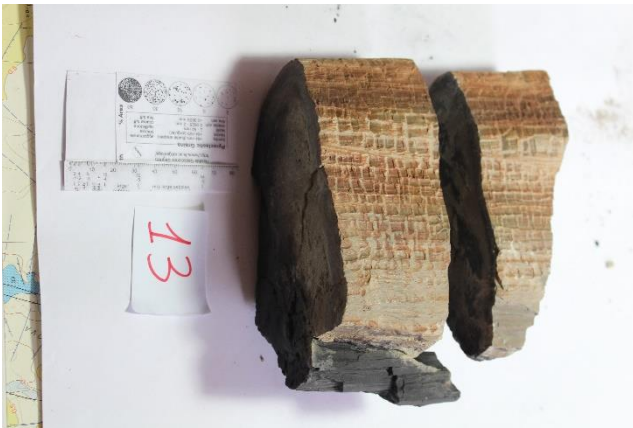

Sample n 12- Lobate (shrub habit) with overgrowth on separate axes. Good ring preservation. Probably stem(s) wood near the root-stem transition. No evidence of rot.

Sample n 13- Lobate fragment (shrub habit?). Numerous rings and good organic carbon preservation. Likely stem wood of single lobe. No rot.

Sample n 14- Numerous rings, <1mm up to 2mm in width. Similar preservation to sample 1, but w/ some remineralization possible. Stem fragment, no center preserved, no rot.

Sample n 15- Charcoalified with sulphur residue. Catabolism may smear organic matter across the anatomy making ring boundaries indistinct in thin section. Indistinct ring boundaries in macroscale.

Sample n 16- Same as sample 15, yet faint rings are seen. Stem wood.

Sample n 17- Numerous rings on radial plane, decent organic carbon preservation.

Sample n 18- Good ring preservation and moderate organic carbon preservation. Fragment of stem wood. Transverse plane in the middle of specimen may work as the sample appears highly friable elsewhere.

Sample n 19- Wonderful organic carbon and ring preservation. Charcoalification is also abundant. Good ultrastructure on radial plane. Center (pith?) is present. Lobate with overgrowth on numerous radial shoots (shrub habit? Not clear). Good ring preservation, preserve weathered face on transverse plane for dendrochronology.

Sample n 20- Good ring appearance on weathered surface, but interior suggests organic matter is smeared across the anatomy.
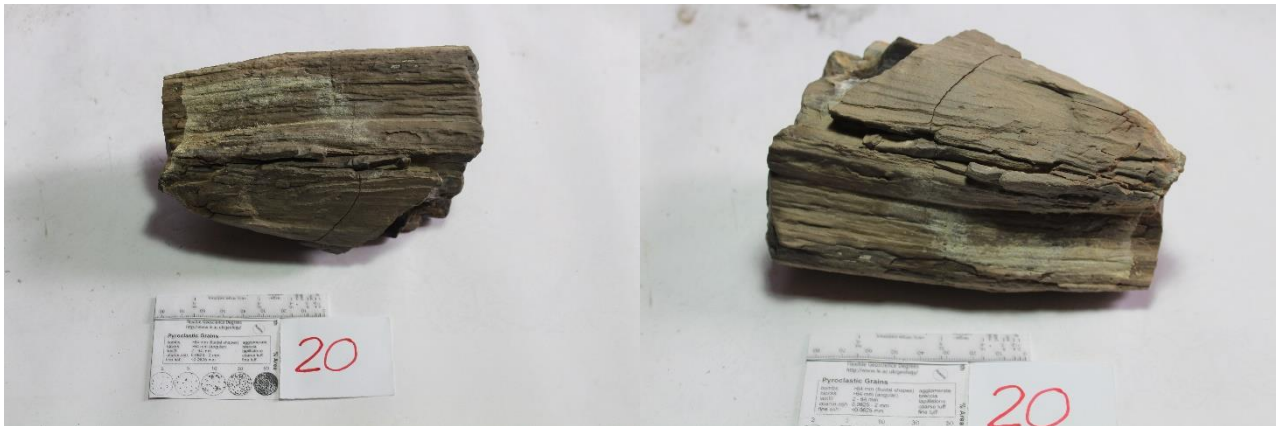
Sample n 21- Fragment of stem. Faint rings on transverse plane. Preserved weathered surface.

Sample n 22- Stem with pith preserved. Few radial shoots, some terminating after 20 rings or so. Lower portion of transverse plane contains solid blocks of rings connected to the center of the stem.

Sample n 23- Highly charcoalified stem fragment. Up to 20 distinct rings, but outside edge area is indistinct.

Sample n 24- Charcoalified stem. Transverse plane shows indistinct rings, radial plane have better preservation.
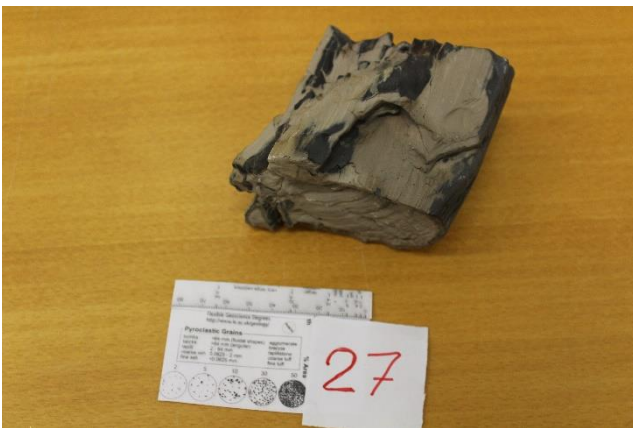

Sample n 25- Like sample 24 charcoalified stem. Transverse plane shows indistinct rings.

Sample n 26- Composed by different fragment with highly charcoalified with indistinct rings.

Sample n 27- Excellent structure in transverse plane and good organic carbon preservation. Numerous radial shoots. Stem fragment.

Sample n 28- Large burrow or rot feature obscures pith area. Stem fragment with good ring preservation and organic carbon preservation. Numerous thin rings.
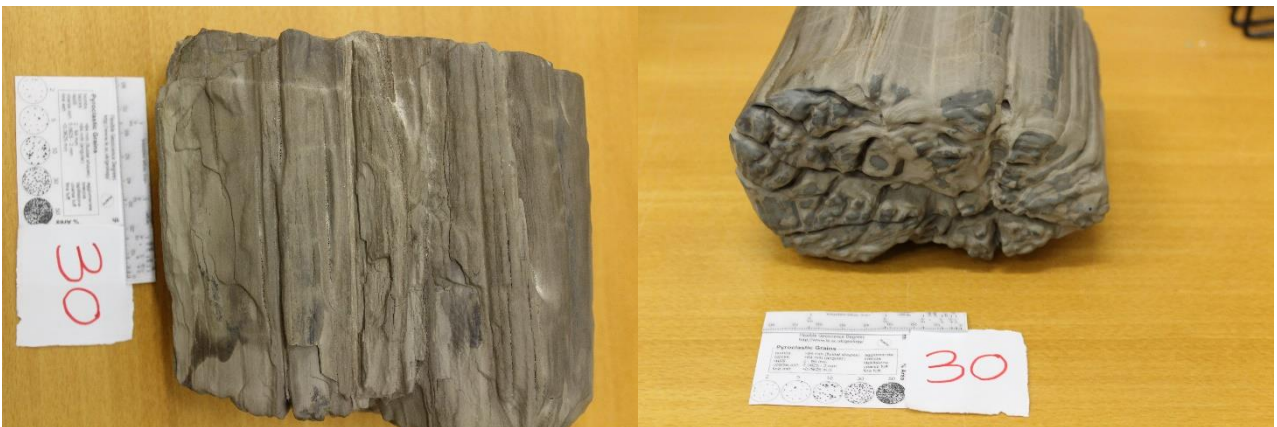
Sample n 29- Same as sample 28, stem fragment with good ring preservation and organic carbon preservation.

Sample n 30- Lobate stem with overgrowth, near root-stem transition. Excellent ring and organic carbon preservation.

Sample n 31- Stem fragment with pith preserved. Excellent ring preservation and numerous radial shoots.

Sample n 32 and 33- *Museum exposed samples-* Stem fragment with few widely spaced radial shoots. Good organic carbon and ring preservation.